Structural Basis for Ligand-Receptor Interactions at the P2X7 Receptor

Emily Alice Caseley

Submitted in accordance with the requirements for the degree of Doctor of Philosophy

The University of Leeds

Faculty of Biological Sciences

September, 2016

The candidate confirms that the work submitted is her own, except where work which has formed part of jointly authored publications has been included. The contribution of the candidate and the other authors to this work has been explicitly indicated below. The candidate confirms that appropriate credit has been given within the thesis where reference has been made to the work of others.

Chapter 1: General Introduction contains work from the following publication:

Caseley, E.A., Muench, S.P., Roger, S., Mao, H.-J., Baldwin, S.A. and Jiang, L.-H. 2014. Non-synonymous single nucleotide polymorphisms in the P2X receptor genes: association with diseases, impact on receptor functions and potential use as diagnosis biomarkers. International journal of molecular sciences. 15(8), pp.13344-13371.

This is a review paper written by the candidate, with some sections written by Lin-Hua Jiang and edited by Stephen Muench, Sebastien Roger, Hong-Ju Mao and Stephen Baldwin.

Chapter 3: Homology Modelling of P2X7 Receptors contains work from the following publication: Caseley, E.A., Muench, S.P., Baldwin, S.A., Simmons, K., Fishwick, C.W. and Jiang, L.-H. 2015. Docking of competitive inhibitors to the P2X7 receptor family reveals key differences responsible for changes in response between rat and human. Bioorganic & medicinal chemistry letters. 25(16), pp.3164-3167.

The research in this paper was carried out by the candidate with guidance from Katie Simmons. The text was primarily written by the candidate, with editing by Lin-Hua Jiang and Stephen Muench.

Chapter 4: Identification of Novel Human P2X7 Receptor Inhibitors Using a Structure-Based Approach contains work from the following publication: Caseley, E.A., Muench, S.P., Fishwick, C.W. and Jiang, L.-H. 2016. Structure-based identification and

characterisation of structurally novel human P2X7 receptor antagonists. Biochemical Pharmacology. 116, pp.130-139.

The research in this paper is directly attributable to the candidate, who carried out all the experiments with guidance from the supervisory team. The text was primarily written by the candidate, with some sections of text and editing being contributed by Lin-Hua Jiang and Stephen Muench. Colin Fishwick provided intellectual inputs for the original design of the experiments in this paper.

Acknowledgements

I would like to thank my supervisors Dr. Lin-Hua Jiang, Dr. Stephen Muench and Prof. Colin Fishwick, whose expertise and guidance have been invaluable throughout the course of my project. I would also like to show appreciation for Prof. Stephen Baldwin, a great scientist and a truly wonderful person.

My thanks also go to the Jiang, Muench and Fishwick research groups for their assistance in teaching me new techniques, especially Dr. Katie Simmons and Dr. Martin McPhillie for their help in guiding me through the confusing world of molecular docking.

I will be forever grateful to the family and friends who have helped me over the past four years. I would like to thank my Mum and Dad, who are thoroughly brilliant and couldn't have been more supportive if they tried. I am also thankful for Megan, my favourite sister, for reminding me that just because we are little doesn't mean we aren't strong. I am grateful for Aunty Ann, who has been an inspiration to me with her hilarious, if occasionally horrifying, sense of humour through difficult experiences. I am also thankful for my friends who have tolerated my constant complaining, Ruthy for being the most kind-hearted best friend I could ask for, Kenny for much-needed injections of Northern wisdom and Tom for being so passionate about the world that it occasionally rubs off on me. Last but not least thank you to Sam for having confidence in my intelligence even when I haven't, and making sure I didn't contract scurvy by cooking tasty treats. I couldn't have done this without you and I love you all very much.

Abstract

P2X7 receptors (P2X7Rs) belong to the P2X receptor family of ligand-gated ion channels activated by extracellular ATP. The human P2X7R (hP2X7R) is implicated in numerous debilitating disease conditions and thus represents a promising therapeutic target. However, P2X7R structure-function relationships remain less well understood. The study presented in this thesis used electrophysiology in conjunction with structural modelling, molecular docking and site-directed mutagenesis to better understand the structural basis for ligand-receptor interactions at P2X7Rs and used such structural information to identify novel hP2X7R antagonists.

Initially, P2X7R homology models were produced based on the crystal structures of the zebrafish P2X4R (zfP2X4R) in closed and ATP-bound states and validated through docking and biochemical approaches. First of all, molecular docking showed that ATP binds to the zfP2X4R and hP2X7R in a strikingly similar configuration to the crystal structure. Secondly, docking of the antagonists AZ11645373, KN62 and SB203580 revealed a specific interaction with Phe95 in the hP2X7R that is absent in the rat P2X7R (rP2X7R), providing structural insight into their preferential hP2X7R antagonism. Thirdly, replacing Asp48 and Ile331 with cysteine resulted in disulfide bonding that impaired hP2X7R-mediated currents, which was reversibly restored by dithiothreitol. These results are consistent with the transmembrane domains moving substantially apart, as predicted by the closed and open state models. Overall, these experiments show that homology models can yield meaningful structural information in terms of P2X7R interactions with ATP, antagonists and receptor activation.

The second part of the study searched for P2X7R antagonists using a structure-based approach. Virtual screening of ~100,000 compounds in the ZINC library against the ATP-binding pocket in the hP2X7R model identified C23, C40 and C60 as structurally novel antagonists of the hP2X7R but not the rP2X7R. These compounds inhibited the agonist-evoked increase in intracellular Ca^{2+} concentration ($[Ca^{2+}]_i$) with IC_{50} values in the

micromolar range. C23 and C40 also inhibited agonist-induced currents with similar potency, but C60 did not. All three compounds suppressed large pore formation with micromolar potency. While C23 inhibited agonist-induced $[Ca^{2+}]_i$ increase mediated by the hP2X4R and rP2X3R, C40 and C60 were more selective towards the hP2X7R. In conclusion, these results show C23, C40 and C60 as novel hP2X7R antagonists. Such structure-based approaches should aid novel P2XR antagonist identification.

Finally, the models were used in combination with site-directed mutagenesis to investigate residues influencing hP2X7R-agonist interactions. The first set of experiments examined four residues implicated in interactions with ATP, and only the mutation of Tyr288 to various residues significantly affected agonist sensitivity. This Tyr288 mutation abolished receptor function, which was mainly due to impairment in protein surface expression as shown by immunofluorescent imaging. The second set of experiments examined several residues for their contribution in the difference in functional expression and agonist sensitivity. Substitution of Val87 in the hP2X7R for Ile in the rP2X7R increased the maximal agonist-induced currents.

Overall, the present study provides structural insights into ligand-receptor interactions at the P2X7Rs. It demonstrates that structure-based approaches are feasible in identifying novel antagonists, and this has wider implications for the P2XR family and membrane proteins as a whole.

Table of Contents

List of Tables

List of Figures

List of Abbreviations

AD	Anxiety disorder
ADP	Adenosine diphosphate
ANOVA	Analysis of variance
APS	Ammonium persulfate
ATP	Adenosine triphosphate
BSA	Bovine serum albumin
BBG	Coomassie Brilliant Blue G
BD	Bipolar disorder
BzATP	2′(3′)-O-4-benzoylbenzoyl-ATP
cAMP	Cyclic adenosine monophosphate
CNS	Central nervous system
DMEM	Dulbecco’s modified Eagle’s medium
DMEM/F12	Dulbecco’s modified Eagle’s medium-F12
DMSO	Dimethylsulfoxide
DNA	Deoxyribonucleic acid
dNTP	Deoxy-(adenosine/guanine/thiamine/cytosine)-triphosphate
DR	Dose-response
DRG	Dorsal root ganglion
EC_{50}	Half maximal effective concentration
EDTA	Ethylenediaminetetraacetic acid
EGTA	Ethylene glycol tetraacetic acid
EPSC	Excitatory postsynaptic current
EtBr	Ethidium bromide
FBS	Foetal bovine serum
eGFP	Enhanced green fluorescent protein
GPCR	G-protein coupled receptor

GΩ	Giga ohm
HEK293 cell	Human embryonic kidney 293 cell
HEPES	4-(2-hydroxyethyl)-1-piperazineethanesulfonic acid
I	Current
IBD	Inflammatory bowel disease
IC_{50}	Concentration for half maximal inhibition
IL-1β	Interleukin-1 beta
kDa	Kilodalton
LPS	Lipopolysaccharide
LTP	Long-term potentiation
MDD	Major depressive disorder
mM	Millimolar
mRNA	Messenger RNA
mV	Millivolts
MW	Molecular weight
nA	Nanoamp
NEB	New England Biolabs
ng	Nanogram
nM	Nanomolar
NMDG	N-methyl-D-glucamine
NS-SNP	Non-synonymous single nucleotide polymorphism
p	T-test critical significance level
PAGE	Polyacrylamide gel electrophoresis
Panx1	Pannexin-1
PBS	Phosphate buffered saline
PCR	Polymerase chain reaction
PI	Propidium iodide

PLC	Phospholipase C
P1R	P1 receptor
P2R	P2 receptor
P2XR	P2X receptor
P2YR	P2Y receptor
rpm	Rotations per minute
RNA	Ribonucleic acid
ROS	Reactive oxygen species
RT	Room temperature
RT-PCR	Reverse transcription polymerase chain reaction
SBS	Standard bath solution
SDS	Sodium dodecylsulfate
SDS-PAGE	SDS-polyacrylamide gel electrophoresis
SEM	Standard error of the mean
TBS	Tris buffered saline
TBST	Tris-buffered saline tween-20
TEMED	N,N,N',N'-Tetramethylethylenediamine
TM	Transmembrane
V	Voltage
WT	Wild-type
zfP2X4R	Zebrafish P2X4 receptor
µg	Microgram
µl	Microlitre
µM	Micromolar
µm	Micrometer

Amino Acid Abbreviations

A	Alanine	Ala
C	Cysteine	Cys
D	Aspartic acid	Asp
E	Glutamic acid	Glu
F	Phenylalanine	Phe
G	Glycine	Gly
H	Histidine	His
I	Isoleucine	Ile
K	Lysine	Lys
L	Leucine	Leu
M	Methionine	Met
N	Asparagine	Asp
P	Proline	Pro
Q	Glutamine	Gln
R	Arginine	Arg
S	Serine	Ser
T	Threonine	Thr
V	Valine	Val
W	Tryptophan	Trp
Y	Tyrosine	Tyr

Chapter 1

General Introduction

1.1 General overview of purinergic signalling

Adenosine triphosphate (ATP) is a nucleoside triphosphate which is primarily recognised as an intracellular source of energy required for a vast number of processes inside cells. As such, it is widely referred to as the 'energy currency of the cell'. However, ATP also functions as a signalling molecule. This signalling role was initially identified in a study which demonstrated that ATP released from sensory nerves led to vasodilation (Holton and Holton, 1954). The theory of purinergic signalling was subsequently proposed by Geoffrey Burnstock (Burnstock, 1972), although this was highly contested until the 1990s when the genes encoding the receptors for extracellular ATP were cloned (Webb et al., 1993; Lustig et al., 1993; Valera et al., 1994; Brake et al., 1994). Since this discovery the field of purinergic signalling has grown, and as a result there is currently a wealth of knowledge regarding this signalling and the purinergic receptors which mediate its action.

1.1.1 Release and metabolism of ATP and nucleotides

Extracellular ATP release has been seen in most mammalian cell types including astrocytes (Anderson et al., 2004), macrophages (Riteau et al., 2012), neutrophils (Eltzschig et al., 2006), erythrocytes (Sikora et al., 2014), platelets (Hiasa et al., 2014), hepatocytes (Gonzales et al., 2010) and neurons (Zhang et al., 2007). ATP cannot diffuse directly through the plasma membrane and is therefore released through different pathways. These include vesicular exocytosis, a mechanism by which ATP is commonly released at nerve terminals (Sperlágh and Vizi, 1996) often alongside transmitters including noradrenaline and acetylcholine (Burnstock, 2014). Additionally, membrane-bound proteins such as connexins have also been implicated in ATP release. These proteins act as gap junctions and the subtype connexin 43 has been connected with ATP release from several endothelial cell lines (Leybaert et al., 2003). However, this is not a universal mechanism as cells including erythrocytes do not express this hemichannel

(Locovei et al., 2006). Pannexin channels, in particular pannexin 1 (Panx1), are also associated with ATP release. This transmembrane channel has been implicated in cell types including T cells (Schenk et al., 2008), erythrocytes (Sridharan et al., 2010), airway epithelial cells (Ransford et al., 2009) and multiple others (Dahl, 2015).

Following ATP release, its activity is limited by ectonucleotidases. Membrane-bound ectonucleotidases involved in the purinergic signalling cycle include those from the ecto-nucleotide pyrophosphatase/phosphodiesterase (E-NPP) family, the ecto-nucleoside triphosphate diphosphohydrolase (E-NTPDase) family and ecto-5'-nucleotidase (Yegutkin, 2008). These metabolise nucleotides as shown in Figure 1.1 in order to prevent perpetual purinergic signalling stimulated by these agonists.

1.1.2 Purinergic receptors

1.1.2.1 P1 receptors

P1 receptors (P1Rs) are a group of G-protein coupled receptors (GPCRs) with adenosine as their endogenous ligand. There are four known receptor subtypes in this family; A1, A2A, A2B and A3 (Burnstock, 2007). A1 receptors are coupled to $G_{i/o}$ proteins and their activation by adenosine or its derivatives inhibits adenylate cyclase (AC), which in turn leads to a reduction in the amount of the second messenger cyclic AMP (cAMP) in the cell. The A2 receptors were definitively determined to be two separate subtypes following their cloning and sequencing (Stehle et al., 1992). They are both mainly coupled to G_s proteins and their activation promotes AC activity, increasing cAMP levels. The A2B receptor is coupled to G_q, the activation of which stimulates phospholipase C (PLC) and leads to an increase in inositol triphosphate and subsequent mobilisation of calcium from intracellular stores. The A3 receptor also couples to this G_q protein, although it primarily interacts with $G_{i/o}$. These receptors, together, mediate a diversity of adenosine-stimulated functions in the mammalian body (Burnstock, 2007; Fredholm et al., 2000).

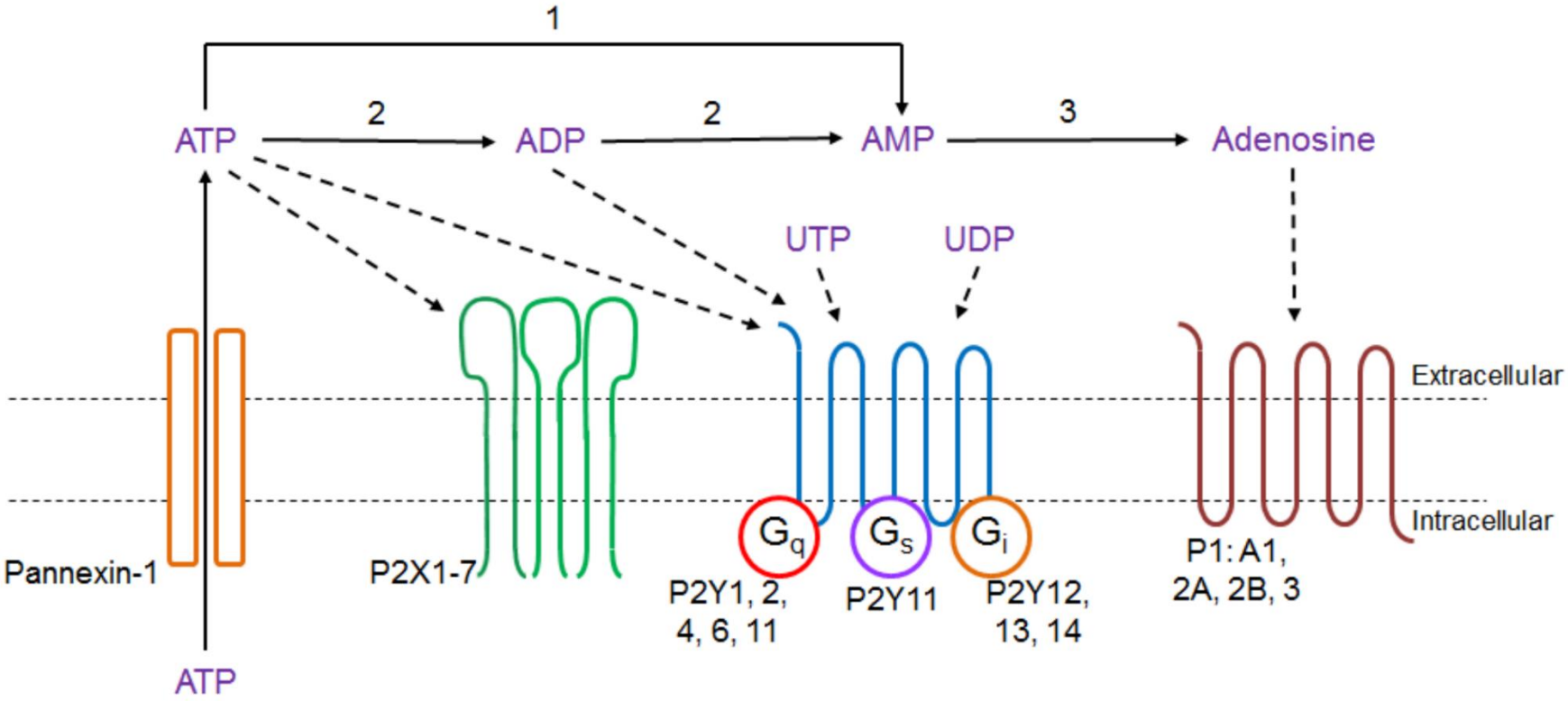

Figure 1.1 Overview of purinergic signalling

1 corresponds to ecto-nucleotide pyrophosphatase/phosphodiesterase, 2 to ecto-nucleoside triphosphate diphosphohydrolase and 3 to ecto-5'-nucleotidase.

1.1.2.2 P2 receptors

P2 receptors (P2Rs) are divided into two categories; P2Y receptors (P2YRs) and P2X receptors (P2XRs). P2YRs are GPCRs of which there are eight known subtypes, P2Y1, 2, 4, 6, 11-14 (von Kügelgen and Wetter, 2000; Burnstock, 2007). Similarly to P1Rs, P2YRs couple with G proteins (Figure 1.1) to help regulate most systems in the body including immune, cardiovascular and nervous systems (Abbracchio et al., 2006). Based on their coupling with second messengers and sequence homology, P2YRs are split into two subfamilies. The first comprises P2Y1, 2, 4, 6 and 11 which are coupled with G_q and stimulate PLC as described for P1Rs above. P2Y11Rs also couple to G_s, which promotes AC activity. The second subfamily (P2Y12-14) is coupled to G_i proteins but conversely acts by inhibiting AC. This interaction with second messengers is stimulated by various extracellular nucleotides. P2Y1, 12 and 13 are primarily activated by ADP, P2Y2 and 11 by ATP, P2Y6 and 14 by UDP, P2Y2 and 4 by UTP and P2Y14 by UDP-glucose (von Kügelgen and Hoffmann, 2016; Jacobson et al., 2015).

In contrast, P2XRs are ligand-gated ion channels. Mammalian cells express seven genes encoding different P2XR subunits, P2X1-P2X7 (North, 2002), which form trimeric homomeric and heteromeric receptors (Jiang, 2012). All seven subunits of the P2XR family can form functional homomeric receptors when studied in heterologous expression systems (Jones et al., 2004; North, 2002), although the ability of P2X6 to form trimers is extremely poor (Barrera et al., 2005; Aschrafi et al., 2004). In addition, seven heteromeric receptors have been characterised; P2X1/2, P2X1/4, P2X1/5, P2X2/3, P2X2/5, P2X2/6 and P2X4/6 (Torres et al., 1998b; Lê et al., 1998; Lê et al., 1999; Brown et al., 2002; Nicke et al., 2005; Compan et al., 2012). This family of receptors is expressed in various tissues and cells, where they mediate diverse physiological functions of ATP.

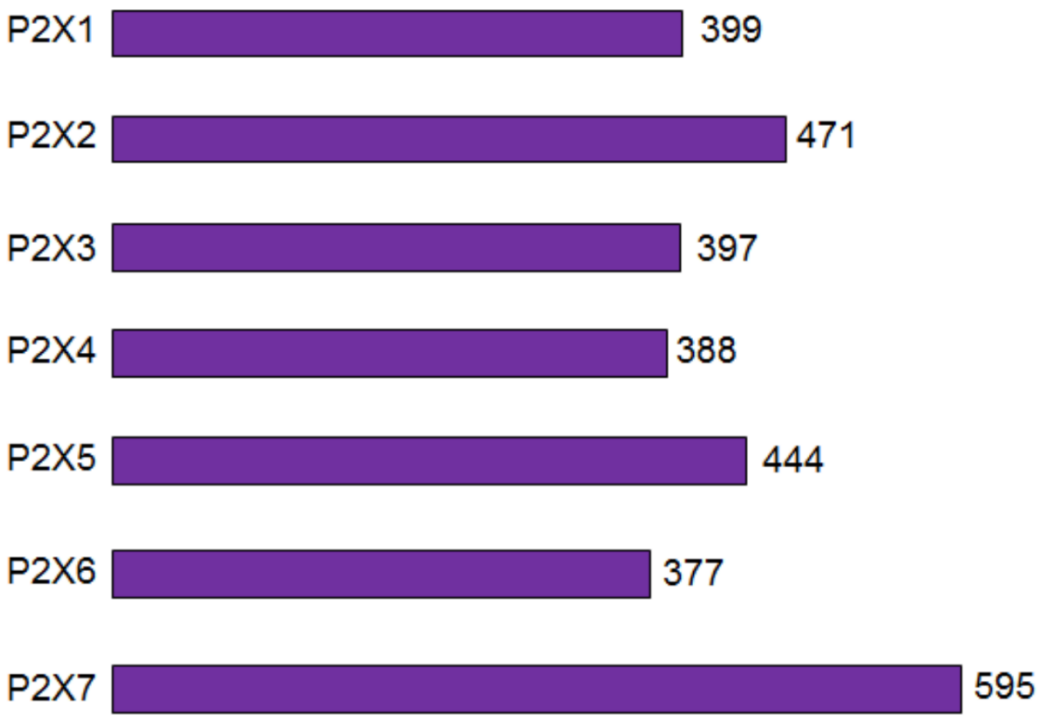

Figure 1.2 Length of P2XR subunits

The relative lengths of each receptor subtype subunit is shown as the number of amino acids.

1.2 The P2X family of receptors

1.2.1 P2X receptor structure

The seven human P2XR subunits vary in length from 377 (P2X6) to 595 (P2X7) amino acids (North, 2002) (Figure 1.2) but share the same membrane topology. Prior to the elucidation of the first P2XR structure, understanding of the structure of these proteins was largely speculative as their primary sequence lacks significant homology with other ATP-binding proteins or ligand-gated ion channels.

1.2.1.1 Crystallisation

A huge step forward came when the crystal structure of the zebrafish P2X4 receptor (zfP2X4R) was published in the closed, apo, state at a resolution of 3.1 Å (Kawate et al., 2009). This was followed by further crystal structures of the zfP2X4R produced in both the ATP-bound state (2.8 Å) and a higher resolution closed state structure (2.9 Å) (Hattori and Gouaux, 2012). This group screened zfP2X4R constructs for stability; the higher resolution structures were determined from a construct starting at Ser28 and ending at Lys365 (Figure 1.3), lacking the intracellular N- and C-termini (Figure 1.4), and containing four mutations (ΔN27/ΔC24/N78K/N187R). This construct had similar ATP-binding and gating activities to the wild-type (WT) receptor (Hattori and Gouaux, 2012).

More recently, this breakthrough has been supplemented by additional crystal structures. The first of these was of a P2XR from the Gulf Coast tick *Amblyomma maculatum*, which was published in the presence of both ATP and zinc ion at 2.9 Å. The construct that was crystallised to produce this structure lacked 23 residues from the N-terminus and 7 from the C-terminus, based on the deletions seen in the zfP2X4R structure, and contained N171Q and C374L mutations. Electrophysiological analysis showed this construct to behave in a similar manner to the WT receptor (Kasuya et al., 2016). In addition, a further publication outlined the first mammalian P2XR structure. This was of the human P2X3 receptor (hP2X3R) in the apo, ATP-bound/open pore, ATP-bound/desensitised and two antagonist-bound closed states at 2.8-3.6 Å. These structures, as well as providing

Figure 1.3 Sequence alignment of P2XR subunits

Sequences of the extracellular region of P2XR subunits. Core ATP binding residues are shown in magenta and conserved cysteines forming disulfide bonds are highlighted in yellow.

insights into states not seen before in crystal structures, were less truncated and therefore give an insight into N- and C-terminus structure (Mansoor et al., 2016).

1.2.1.2 P2X receptor architecture

P2XR subunits are largely extracellular, with two transmembrane (TM) domains and intracellular N- and C-termini (Hattori and Gouaux, 2012; Kawate et al., 2009; Mansoor et al., 2016). When the first crystal structure was published the subunit shape was likened to that of a dolphin leaping from the 'sea' of lipid bilayer, a comparison now entrenched in P2XR-related literature (Figure 1.4A). These subunits assemble into trimers, evidence for which was provided by blue native polyacrylamide gel electrophoresis (Nicke et al., 1998), atomic force microscopy (Barrera et al., 2005) and electron microscopy (Young et al., 2008) before confirmation by the zfP2X4R structure (Hattori and Gouaux, 2012; Kawate et al., 2009). These subunits intertwine to form chalice-shaped trimers (Figure 1.4B) which have extensive contact interfaces, the three major points of contact being body to body, head to body, and left flipper to dorsal fin. The subunits interlock in three-fold symmetry perpendicular to the cell membrane with each subunit wrapping around its neighbour with a right-handed twist, in contrast to the TM helices which twist in an anticlockwise direction (Hattori and Gouaux, 2012; Kawate et al., 2009; Mansoor et al., 2016). The extracellular domain is large and protrudes ~70 Å from the membrane. This domain is hydrophilic, glycosylated and cysteine-rich, with ten conserved cysteine residues (North, 2002) which are all involved in disulfide bonds. These bonds are formed between Cys117-Cys165, Cys126-Cys149, Cys132-Cys159, Cys217-Cys227, and Cys261-Cys270 (as in the P2X1R) (Figure 1.3), and are required for receptor trafficking to the cell membrane. Disruption of the Cys261-Cys270 or Cys117-Cys165 bond together with a mutation in another conserved cysteine (C126A, C149A, C159A, or C217A) has been shown to severely reduce trafficking (Ennion and Evans, 2002; Hattori and Gouaux, 2012; Kawate et al., 2009; Ennion and Evans, 2001).

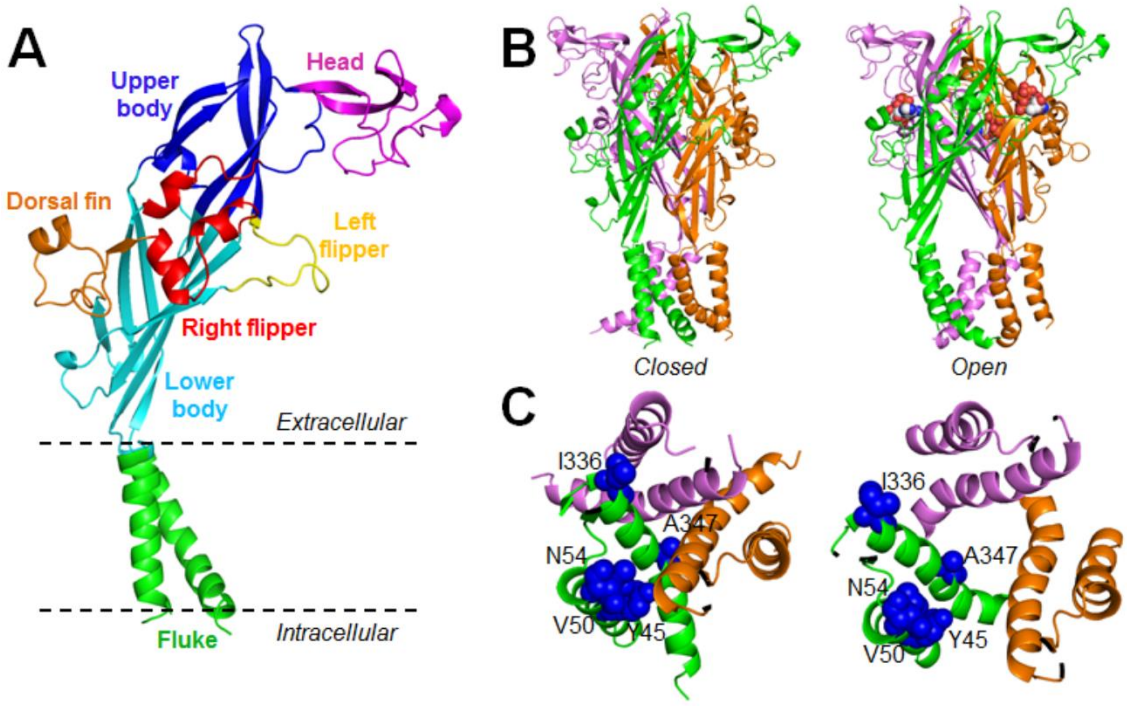

Figure 1.4 P2XR structure

(A) The zfP2X4R crystal structure, with sections coloured to indicate the dolphin nomenclature. (B) Structure of the zfP2X4R viewed parallel to the membrane with each of the three subunits in a different colour. (C) The transmembrane domains as viewed from the intracellular side. Residues involved in channel gating are shown as blue spheres.

1.2.1.3 Transmembrane domains

Each P2XR subunit has two TM domains, TM1 and TM2. These α-helical domains extend ~28 Å across the membrane and in the apo state are oriented approximately antiparallel to each other at an angle of around 45° from the membrane (Figure 1.4A). The TM domains form a central aqueous ion-conducting pathway. Channel opening is facilitated by the direct coupling of beta sheets in the lower body domain to TM1 and TM2, as their outward flexing causes TM1 and TM2 to expand outward and open the pore (Mansoor et al., 2016). TM2 is the innermost TM region and defines the closed state of the channel by forming a physical barrier to limit ion flow (Figure 1.4C). Studies have shown that mutating residues in TM2 affects the spontaneous gating, unitary conductance, and rectification characteristics of the P2X2R (Cao et al., 2009; Cao et al., 2007). Additionally, P2X2Rs can be optically activated by introducing light-activated azobenzene molecules into TM2 (Browne et al., 2014). The width of the ion conducting pathway is determined at its narrowest part at residue Ala347 (in the zfP2X4R) (Figure 1.4C), and in the open state the ion-conducting pathway width is delineated by residues with Cα atoms 6.4 Å from the central axis (Hattori and Gouaux, 2012).

In contrast, TM1 domains are located at the periphery and are less involved in forming the central pore. Studies have shown that mutating residues in TM1 to Cys and modifying them with methanethiosulfate (MTS) reagents does not have a significant effect, although it does at the TM2 domain (Li et al., 2008; Browne et al., 2010). Even though TM1 side chains are not directly involved in the ion permeation pathway (Li et al., 2010), residues Tyr43 and Gln52 in the P2X2R (Tyr45 and Asp54 in zfP2X4R) have been shown to influence calcium permeability (Samways et al., 2008; Samways and Egan, 2007) (Figure 1.4C). Furthermore, introducing cysteines at Val48 in TM1 and Ile328 in TM2 of the P2X2R (Val50 and Ile336 in zfP2X4R, Figure 1.4C) forms a disulfide bond which inhibits P2X2R-mediated current. This current is restored when the bond is reduced (Jiang et al., 2001). Together, this also illustrates a role for TM1 in P2XR gating.

1.2.1.4 Intracellular domains

Until very recently, understanding of the structure of the intracellular N- and C-termini in P2XRs has been speculative due to the truncated nature of the zfP2X4R crystal structures. However, the hP2X3R structure was solved with the majority of the intracellular domains intact. This is a very variable domain, the C-terminus in particular, accounting for much of the variation in subunit length (Figure 1.2). These regions form a domain named the 'cytoplasmic cap'. They anchor the TM domains in order to allow a change in the TM2 helical pitch upon receptor activation, as well as providing a lateral exit pathway for ions. It is suggested that the stability of the folding-unfolding transition of this cytoplasmic cap is directly linked to rate of desensitisation, and that P2XR subtypes that desensitise faster may have a less stable domain (Mansoor et al., 2016). Indeed, previous mutagenesis studies have shown the intracellular termini to largely determine P2XR deactivation kinetics (Boué-Grabot et al., 2000; Allsopp and Evans, 2011).

1.2.1.5 ATP binding site

The ATP-bound zfP2X4R structure verified early studies based on ATP dose-response (DR) curves which proposed that these channels open in response to ATP binding to three identical, non-interacting sites (Bean, 1990). Evidence shows that they can also activate with only two ATP molecules bound (Stelmashenko et al., 2012). Before the elucidation of this structure, the ATP binding site was not clear as P2XR protein sequences do not contain a typical ATP binding consensus sequence such as the Walker motif (Walker et al., 1982). However, the exact ATP binding site and the residues involved in binding were clarified in 2012 (Hattori and Gouaux, 2012) and corroborated in 2016 (Mansoor et al., 2016). The ATP binding pocket is located at the interface between two subunits, which was first suggested following disulfide cross-linking studies in the P2X1R (Marquez-Klaka et al., 2007), with the binding site at the top of this pocket (Figure 1.5A). Ten residues from two subunits are vital for ATP binding; four hydrophilic residues (Lys70, Lys72, Thr189, and Lys193) and three hydrophobic residues (Leu191,

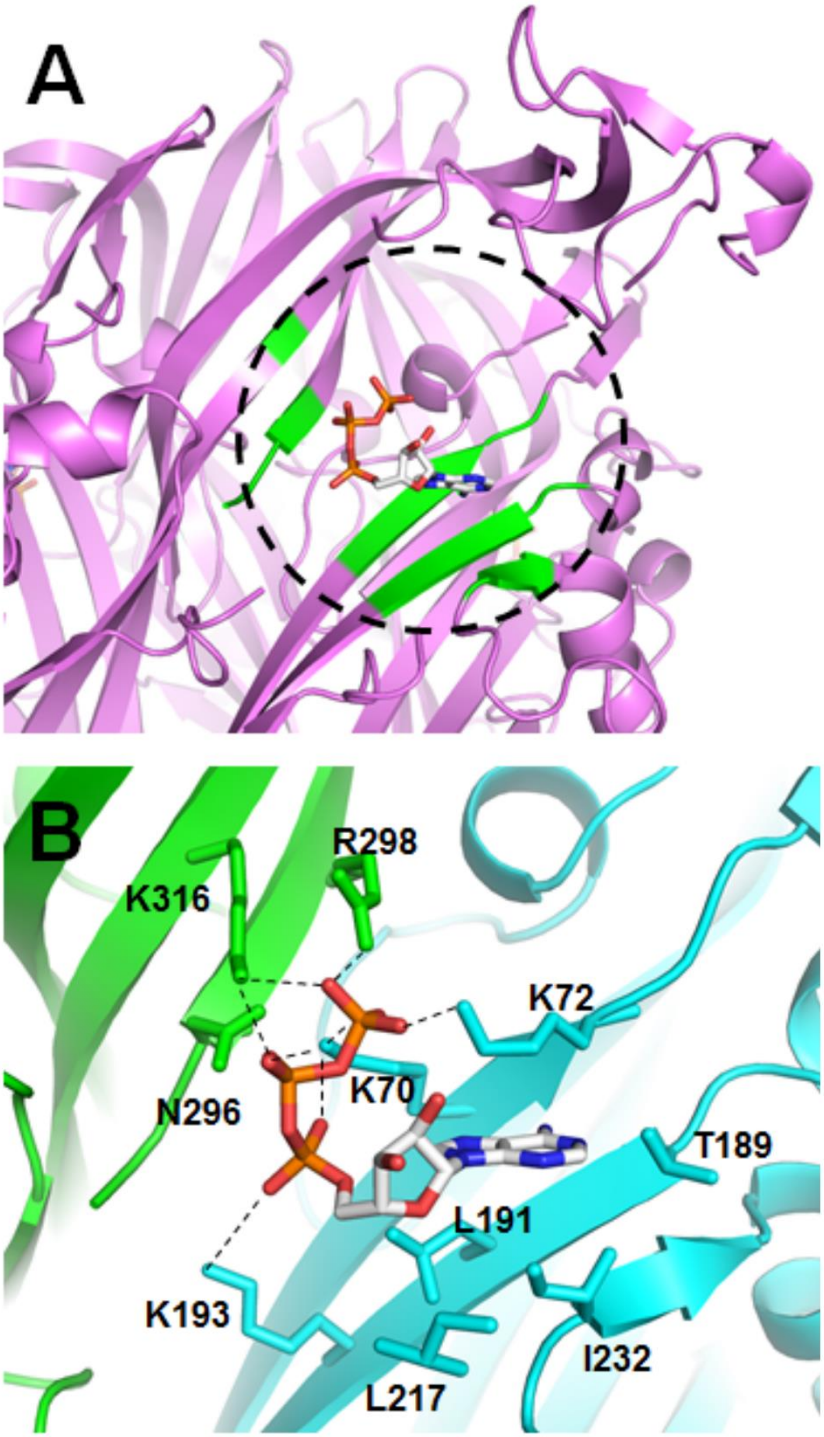

Figure 1.5 ATP binding in the zfP2X4R

(A) The inter-subunit ATP binding pocket in the zfP2X4R, highlighted in green. (B) Expanded view of the zfP2X4R ATP binding site with the amino acids involved in binding labelled. Residues contributed by different subunits are highlighted in different colours and hydrogen bonding interactions are shown as dashed lines.

Leu217, and Ile232) come from the first subunit, whilst three hydrophilic residues (Asn296, Arg298, and Lys316) come from the second (Hattori and Gouaux, 2012) (Figure 1.5B). Of these, the hydrophilic residues are conserved and are required for P2XR activation (Wilkinson et al., 2006; Worthington et al., 2002; Adriouch et al., 2008), whereas the three hydrophobic residues vary in their presence in the mammalian P2XRs. Interestingly, the P2X7R has no equivalent residue to Leu217 in the zfP2X4R (Figure 1.3).

It is fortunate that ATP-bound structures are available due to the unusual conformation that this ligand adopts in the binding site, with ATP bent in a tight U-shape and the β- and γ-phosphates folded towards the adenine ring. The negative charge of the phosphate groups appears important for hydrogen bonding interactions, for example mediating interactions between Lys70 and oxygen atoms on the α, β and γ phosphate groups, Lys316 and the β-phosphate and Lys72, Arg298 and Lys316 with the γ-phosphate (Figure 1.5B). The adenine of the ATP, in contrast, forms hydrogen bonds with Thr189, Lys70 and Thr189. The ribose ring also appears to interact via hydrophobic interactions with Leu217 in the dorsal fin.

1.2.2 Agonists

All P2XRs are activated by the physiological agonist ATP, which stimulates these receptors in a subtype-specific manner. ATP activates both homomeric and heteromeric P2XRs at concentrations ranging from nanomolar to micromolar, except for the P2X7R which is less sensitive and requires high micromolar to millimolar concentrations. Whilst there are currently no identified subtype-specific agonists, many ATP analogues activate particular P2XR subtypes with varying levels of specificity. One such analogue is 2′(3′)-O-4-benzoylbenzoyl-ATP (BzATP). This modified ribose derivative contains two additional benzoyl groups (Figure 1.6) and activates the P2X7R in the micromolar range (Surprenant et al., 1996; Young et al., 2007). BzATP can also activate the P2X1R and

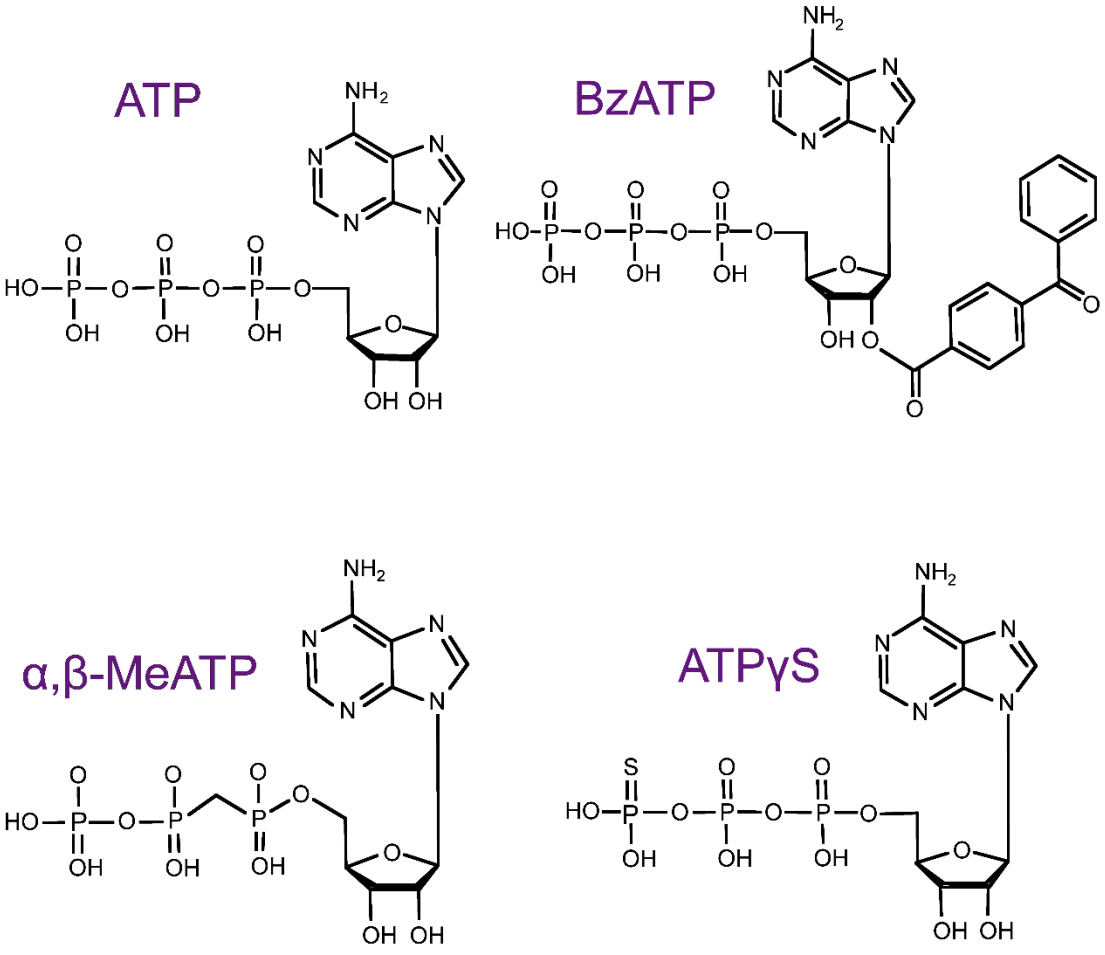

Figure 1.6 Common P2XR agonists

P2X2R (North and Surprenant, 2000). A second is α,β-methylene-ATP (αβ-MeATP) (Figure 1.6), which strongly activates P2X1Rs and P2X3Rs (Valera et al., 1994; Lewis et al., 1995; Bianchi et al., 1999) but is ineffective at the P2X2R, P2X5R, P2X6R, and P2X7R up to 100 μM (Collo et al., 1996; Brake et al., 1994; Surprenant et al., 1996). αβ-MeATP has varied effects at P2X4Rs from different species, acting as a partial agonist of the human and mouse isoforms but as an antagonist of the rat isoform (Jones et al., 2000; Wang et al., 1996). Furthermore ATPγS, which has one phosphate oxygen substituted for sulfur (Figure 1.6), activates all P2XRs except the P2X7R (Evans et al., 1995; Brake et al., 1994; Lewis et al., 1995; Collo et al., 1996).

1.2.3 Antagonists and inhibitors

The P2XR family, a widely expressed group of membrane proteins with ties to extensive diseases in humans (outlined in section 1.2.6), is a prime candidate for the development of subtype-specific inhibitors. Common P2XR antagonists are described below and their structures are shown in Figure 1.7.

1.2.3.1 Suramin and its analogues

Suramin, along with pyridoxalphosphate-6-azophenyl-2',4'-disulfonic acid tetrasodium salt (PPADS), was one of the first compounds to demonstrate P2XR antagonism (Dunn and Blakeley, 1988). It is nonselective and competitive, with varying efficacy across the P2XR subtypes (Table 1.1) as well as the P2YRs (Charlton et al., 1996). Suramin has been modified to produce antagonists with more favourable characteristics. The first of these was NF023, a competitive P2X1R antagonist which is less potent at the P2X2R, P2X3R and P2X4R (Lambrecht, 1996; Soto et al., 1999). Another analogue, NF110, is potent at the P2X1R but more effective at the P2X3R, inhibiting both in the nanomolar range (Hausmann et al., 2006). NF279 is a further inhibitor (Damer et al., 1998) with high affinity for the P2X1R, P2X2R and P2X3R but only mediates partial P2X4R inhibition (Rettinger et al., 2000; Klapperstück et al., 2000). NF449 is the most potent commercially

Table 1.1 Common P2XR antagonists

Receptor	Suramin	PPADS	TNP-ATP	IP_5I	PSB-1011	A-317491	5-BDBD	References
hP2X1	1-5, 0.9	1-5, 1.8	0.006			11		(Bianchi et al., 1999; Ennion et al., 2000; Baqi et al., 2011; Evans et al., 1995; King et al., 1999; Virginio et al., 1998)
rP2X1	<10	<30, 0.09, 0.1		0.003	0.4			
rP2X2	1-5, 33	1-5, 3.8	2		0.079	8 (human)		(Bianchi et al., 1999; Brake et al., 1994; Evans et al., 1995; Baqi et al., 2011; Virginio et al., 1998)
hP2X3	<100	5.1				0.097		(Baqi et al., 2011; Bianchi et al., 1999; Chen et al., 1995; King et al., 1999; Virginio et al., 1998)
rP2X3	0.8, 3	3.6, 1.5	0.0009	2.8	0.5			
rP2X2/3	0.8	1.3	0.007		1	0.016 (human)		(Baqi et al., 2011; Virginio et al., 1998)
hP2X4	<100	<100	1.5, 15			>100	0.5, 1.2	(Donnelly-Roberts and Jarvis, 2007; Balázs et al., 2013; Virginio et al., 1998; King et al., 1999; Baqi et al., 2011)
rP2X4	>100	<100	15	Potentiate	>10			
mP2X4	>100	10.5						
hP2X5	2.9	0.2						(Bo et al., 2003a; Collo et al., 1996)
rP2X5	4	2.6						
rP2X6	>100	>100						(Collo et al., 1996)
hP2X7	<100	4.6				>100		(Baqi et al., 2011; Virginio et al., 1998)
rP2X7			>30		>10			

The value for each compound is presented as the IC_{50} in μM.

available version of these analogues. It is a P2X1R-specific antagonist effective at nanomolar concentrations and can inhibit the P2X3R, but requires significantly higher concentrations to inhibit the P2X3R, P2X7R, P2Y1R and P2Y2R (Rettinger et al., 2005; Hülsmann et al., 2003). These analogues have been a valuable source of inhibitors.

1.2.3.2 PPADS and pyridoxal-based compounds

PPADS was an early nonselective P2R inhibitor which generally has similar or greater potency than suramin. It acts at the P2X1R, P2X2R, P2X3R, and P2X5R (Table 1.1), as well as the P2Y2R and P2Y4R (Lambrecht et al., 1992; Gever et al., 2006; McLaren et al., 1994). It is usually a non-competitive antagonist with slow onset and reversal of action (Lambrecht et al., 1992). PPADS is an imperfect inhibitor so, as with suramin, structural analogues have been generated to improve selectivity and potency. One such analogue, PPNDS, specifically inhibits P2X1Rs more effectively than PPADS, with an IC_{50} of 14 nM (Lambrecht et al., 2000). It can also inhibit the P2X7R at higher concentrations. Additionally, MRS2159 and MRS2220 represent two derivatives with P2X1R specificity. MRS2159 is a reversible antagonist with an IC_{50} of 9 nM at the P2X1R, which is less potent at the rP2X2R and rP2X3R with IC_{50}s of 11.9 and 0.14 µM, respectively (Kim et al., 2001b). MRS2220 similarly binds reversibly and surmountably, inhibiting the P2X1R with an IC_{50} of 10.2 µM. It also inhibits the rP2X3R but less effectively, with an IC_{50} of 58.3 µM. Despite being less potent, MRS220 shows greater subtype specificity than MRS2159, not inhibiting the P2Y1R, P2X2R, P2X4R or P2X6R (Jacobson et al., 1998).

1.2.3.3 TNP-ATP

A modified analogue of ATP, 2′,3′-O-(2,4,6-trinitrophenyl)ATP (TNP-ATP) has selectivity for the P2X1R, P2X2/3R and P2X3R (Virginio et al., 1998). This antagonist inhibits currents from cells expressing these receptors with IC_{50}s close to 1 nM, but is 1000-fold less effective at the P2X2R, P2X4R and P2X7R (Balázs et al., 2013; Virginio et al., 1998).

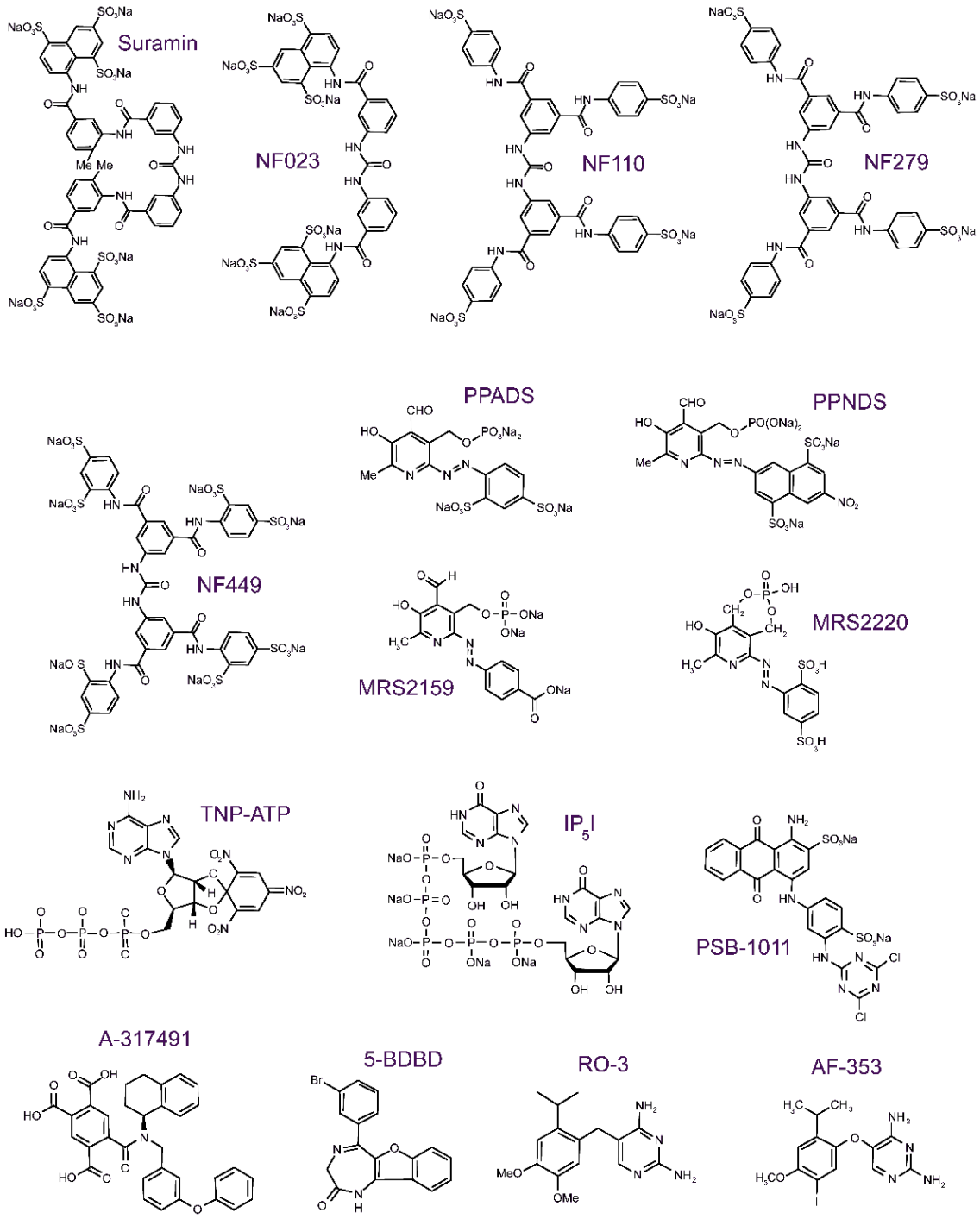

Figure 1.7 Common P2XR antagonists

It also only minimally inhibits hP2X5R-mediated currents (Bo et al., 2003a) (Table 1.1). An NMR study recently suggested TNP-ATP to block the channel by closing ion conductance pathways instead of stabilising the closed state of the channel (Minato et al., 2016). However, the recent hP2X3R structure showed it to bind deeply in the ATP binding site and prevent movement of the extracellular domain necessary for channel opening, therefore stabilising the receptor in the apo state (Mansoor et al., 2016).

1.2.3.4 IP_5I

P1,P5-bis(5′-inosyl) pentaphosphate (IP_5I) was initially identified as an inhibitor of P2XRs in synpatosomes of the rat cerebral cortex and the guinea-pig vas deferens (Pintor et al., 1999; Pintor et al., 1997; Hoyle et al., 1997). Further characterisation showed this compound to act primarily at the P2X1R, where it has an IC_{50} of 3 nM at the rat receptor. This compound also inhibits the rP2X3R, although 900-fold less potently with an IC_{50} of 2.8 µM. Interestingly it potentiates the rP2X4R (King et al., 1999) whilst being inactive at the P2X2/3R (Honore et al., 2002) (Table 1.1).

1.2.3.5 PSB-1011

A P2X2R-specific antagonist has only relatively recently been made available, when a study of structurally modified anthraquinone derivatives found a number of potent selective antagonists. The most effective was disodium 1-amino-4-[3-(4,6-dichloro[1,3,5]triazine-2-ylamino)-4-sulfophenylamino]-9,10-dioxo-9,10-dihydroanthracene-2-sulfonate (PSB-1011). PSB-1011 strongly inhibits the rP2X2R, but is 5-6 fold less effective at the P2X1R and P2X3R and inactive at the P2X4R and P2X7R. This inhibitor shows selectivity for the P2X2R over the P2X2/3R and, as such, is a useful tool to distinguish between the two (Baqi et al., 2011) (Table 1.1).

1.2.3.6 A-317491

A-317491 is a competitive P2XR antagonist which exhibits specificity for the P2X3R and P2X2/3R. This compound blocks hP2X3R- and hP2X2/3R-mediated currents at nanomolar concentrations and the application of 10 µM A-317491 causes complete and

reversible inhibition (Jarvis et al., 2002). Its action at other subtypes is variable, showing significantly less activity at the human P2X1R, P2X3R, P2X4R, P2X7R and P2Y2R (Table 1.1). Of these, it is most potent at the P2X1R where it acts with an IC_{50} of 11 μM (Jarvis et al., 2002). Similarly to TNP-ATP, an hP2X3R crystal structure showed A-317491 to act at the ATP binding pocket by preventing movement necessary for activation and thereby locking the receptor in the closed state. This compound has been shown to inhibit various pain states in *in vivo* tests (McGaraughty et al., 2003; Jarvis et al., 2002; Wu et al., 2004).

1.2.3.7 5-BDBD

Past studies of the P2X4R have encountered difficulties due to the lack of specific inhibitors and the insensitivity of this subtype to nonspecific antagonists such as PPADS and suramin (Garcia-Guzman et al., 1997; Jones et al., 2000). However, the benzodiazepine derivative 5-(3-Bromophenyl)-1,3-dihydro-2H-benzofuro[3,2-e]-1,4-diazepin-2-one (5-BDBD), which was developed to treat arteriosclerosis and restenosis via P2X4R antagonism (Fischer et al., 2004), effectively inhibits P2X4R-mediated currents (Donnelly-Roberts et al., 2008). This initial data was hidden by a patent, but fortunately a more recent study characterised this antagonist in depth. ATP-induced hP2X4R-mediated currents are blocked competitively by 5-BDBD (Balázs et al., 2013) with a similar potency to TNP-ATP at the human subtype, although investigation of different species is required. Functional studies suggest that this antagonist is also effective at P2X4Rs from different species, for example in the guinea pig cochlea (Wu et al., 2011) and mouse teratocarcinoma cells (Kwon, 2012), although further characterisation is required.

1.2.3.8 Trimethoprim derivatives

Two derivatives of the antibacterial agent trimethoprim have more recently been identified as having P2XR inhibitory activity. The first of these was RO-3, which inhibits the P2X3R and P2X2/3R at submicromolar concentrations and is selective for these

Table 1.2 P2XR expression

Receptor	Regions of expression	References
P2X1	Bladder, smooth muscle, small arteries, platelets, dorsal horn spinal neurons	(Burnstock, 2008; Elneil et al., 2001; Gachet, 2008; Inscho et al., 2003; Petruska et al., 2000; Vial and Evans, 2000)
P2X2	CNS, autonomic and sensory ganglia, retina, smooth muscle	(Greenwood et al., 1997; Hausmann and Schmalzing, 2012; Nori et al., 1998; Song et al., 2012; Vulchanova et al., 1997)
P2X3	Sensory neurons, spinal cord, cardiac muscle	(Kaan et al., 2010; North, 2002; Usoskin et al., 2015)
P2X4	CNS, endothelial cells, immune cells, cardiac muscle, brain	(Bo et al., 2003b; Boumechache et al., 2009; Inoue et al., 2004; Yamamoto et al., 2006)
P2X5	Spinal cord, sensory ganglia, bladder, gut, thymus	(Collo et al., 1996; Creed et al., 2010; Glass et al., 2000; Kobayashi et al., 2013)
P2X6	CNS, spinal cord, cardiac muscle, kidney distal convoluted tubule	(Banfi et al., 2005; Collo et al., 1996; de Baaij et al., 2014; Kobayashi et al., 2013)
P2X7	Immune cells, salivary glands, pancreas, osteoclasts, osteoblasts, CNS	(Grol et al., 2009; North, 2002; Novak et al., 2010; Sperlágh and Illes, 2014; Surprenant et al., 1996)

An outline of the main areas of expression of each receptor as determined by mRNA expression and/or functional properties of the receptors in cells and tissues. It is not an exhaustive list.

subtypes (Ford et al., 2006). The second is AF-353, a non-competitive antagonist with 300-fold specificity for the P2X3R which has been shown to inhibit receptor-mediated calcium influx and currents in the nanomolar range (Gever et al., 2010). This orally bioavailable compound has already proven effective in rat models of bone cancer pain (Kaan et al., 2010).

1.2.5 Physiological functions

P2XR function is widely varied and often linked to its expression. The expression of this receptor family has been documented in a variety of tissues and cells, as summarised in Table 1.2.

1.2.5.1 P2X1

The P2X1R is expressed in the urinary bladder (Longhurst et al., 1996; Valera et al., 1994). This directly links to functional studies which implicate this receptor as being important in bladder contractility. Inward currents and contractions were abolished in smooth muscle from the bladder of P2X1R knockout mice (Vial and Evans, 2000) and a ketamine-induced increase in P2X1R expression led to an increase in urination frequency (Meng et al., 2011). In addition, P2X1R influence on contractile responses in the vas deferens has been seen. It is expressed in the vas deferens (Valera et al., 1994), and P2X1R-null mice have ~90% reduction in male fertility. This is due to reduced contraction of the vas deferens in response to sympathetic nerve stimulation, causing less sperm to be propelled into the ejaculate (Mulryan et al., 2000). Reduced P2X1R expression has been shown to decrease male mouse fertility in further studies (Kauffenstein et al., 2014; White et al., 2013).

P2X1R mRNA has also been identified in the small muscle layers of small arteries and arterioles (Valera et al., 1994). Receptor knockout or inhibition has shown its importance in the autoregulation of blood flow in the kidney (Inscho et al., 2003; Osmond and Inscho,

2010). Furthermore, it has been implicated in thrombosis. P2X1R knockout mice exhibit reduced collaged-induced platelet aggregation and a lowered mortality rate compared to wild-type (WT) mice, who developed acute vascular occlusion (Hechler et al., 2003). Conversely, overexpression of P2X1Rs in mice enhanced platelet secretion and aggregation (Oury et al., 2003) and thrombosis in knockout mice was restored by the infusion of platelets and neutrophils from WT mice (Darbousset et al., 2014). The P2X1R is additionally implicated in promoting neutrophil chemotaxis. Neutrophils from knockout mice move more slowly (Lecut et al., 2009) as these receptors are involved in promoting neutrophil activation (Lecut et al., 2012). As such, the range of action of the P2X1R is clear.

1.2.5.2 P2X2

The P2X2R is involved in relatively few physiological functions. However, it is expressed throughout the CNS including parasympathetic, sensory, enteric and retinal neurons (Zhong et al., 1998; Thomas et al., 1998; Zhou and Galligan, 1996) and plays a role in chemosensory signalling. Cells expressing the P2X2R are excited by hypoxia and hypercapnia (Prasad et al., 2001). P2X2R knockout mice also have reduced ventilator responses to hypoxia; the conduction of arterial oxygen levels from cells of the carotid body to the brainstem was diminished due to impaired carotid sinus nerve function (Rong et al., 2003). This receptor is also involved in taste transduction, and P2X2R deficient mice cannot taste NaCl or the artificial sweetener SC45647 (Eddy et al., 2009). They also show reduced behavioural responses to sweeteners, glutamate and bitter substances, and these stimuli do not elicit a response from gustatory nerves (Finger et al., 2005). The P2X2R is additionally expressed in the ear, mainly in the cochlea and primary auditory neurons (Housley et al., 1999; Järlebark et al., 2000). This subtype is important in reducing hearing sensitivity in response to elevated sound levels (Housley et al., 2013) and has been implicated in contributing to the kinetics of purine-mediated sound transduction in the ear (Morton-Jones et al., 2015).

1.2.5.3 P2X3

The P2X3R has been strongly linked to neuropathic and inflammatory pain states, which is reflective of its expression in sensory neurons (Chen et al., 1995). P2X3R knockout in mice causes enhanced thermal hyperalgesia in chronic inflammation (Souslova et al., 2000), and its knockdown from the dorsal root ganglion (DRG) and dorsal horn of the spinal cord by siRNA diminished pain responses in rats in models of both agonist-evoked and chronic neuropathic pain (Dorn et al., 2004). Furthermore, downregulation of this receptor by antisense oligonucleotides in the rat lumbar DRG reduced pain-related behaviour in neuropathic and inflammatory pain models (Barclay et al., 2002).

The P2X3R is also involved in the urinary bladder reflex. Mice deficient in this receptor exhibited urinary bladder hyporeflexia, with decreased urination frequency and increased bladder capacity in addition to reduced pain-related behaviour in response to ATP and formalin injection (Cockayne et al., 2000). It is further suggested to influence peristalsis in the small intestine. Inhibited gastrointestinal transit in ileal segments from P2X3R-null mice has been demonstrated as a result of this receptor's participation in neural pathways mediating peristalsis (Bian et al., 2003). However, a further study found ATP-induced contractions in colon segments from P2X3R knockout mice to be similar to the WT (DeVries et al., 2010) and so further research is necessary to clarify this discrepancy.

1.2.5.4 P2X4

P2X4Rs are expressed on neurons (Burnstock, 2013; Ho et al., 2014) and have been implicated in neuropathic pain sensation. P2X4R expression in the spinal cord increases following nerve injury, and administration of either TNP-ATP or P2X4R antisense oligodeoxynucleotide inhibits tactile allodynia after nerve injury (Inoue et al., 2004; Tsuda et al., 2003). Additionally, a role in long-term potentiation (LTP) has been seen in the mouse hippocampus. P2X4R knockout mice have diminished LTP compared to the WT, and Ivermectin which selectively potentiates P2X4R currents was shown to increase LTP

(Sim et al., 2006). The ATP-induced LTP of C-fibre-evoked field potentials in the spinal dorsal horn has also been shown to involve this receptor (Gong et al., 2009).

The ability of blood vessels to adapt to environmental change relies on endothelial cells sensing and responding to blood flow. The P2X4R is key in vascular remodelling; knockout mice have abnormal endothelial cell responses to fluid shear stress, for example calcium influx, and suppressed vessel dilation in response to an acute increase in blood flow. Conversely, these mice showed no decrease in blood vessel size in response to a sudden decrease in blood flow (Yamamoto et al., 2006). Together, this indicates a role for the P2X4R regulating flow-sensitive mechanisms.

1.2.5.5 P2X5

The P2X5R is expressed in various regions, including satellite cells of the skeletal muscle (Ryten et al., 2002). There is evidence that this receptor is involved in the differentiation of satellite cells into mature multinucleated muscle fibres. P2X5R inhibition in satellite cells prevents proliferation, increases muscle cell differentiation and increases the rate of myotube formation, demonstrating its role in directing cell fate (Ryten et al., 2002).

1.2.5.6 P2X6

The P2X6R is the only subunit that is almost unable to form functioning homomeric receptors (Barrera et al., 2005). However, there is evidence that expression of the functional P2X6R is dependent on its glycosylation (Jones et al., 2004). Possibly due to this, evidence for physiological functions of this subtype is limited. Its expression in the distal convoluted tubule of the kidney led to its role in ATP-mediated signalling in the kidney being investigated. However, P2X6R knockout mice were found to have a normal phenotype compared to WT suggesting no role for the P2X6R in renal electrolyte transport (de Baaij et al., 2016). As such the physiological function for this homomer is still not known.

1.2.5.7 P2X7

The expression and physiological functions of the P2X7R are outlined in sections 1.3.4 and 1.3.5, respectively.

1.2.6 Diseases

1.2.6.1 P2X1

As discussed above, the P2X1R has a role in bladder contractility, male fertility, blood flow regulation and thrombosis. There is little evidence for the involvement of this receptor in disease states in humans, although it has been tentatively linked to cardiovascular disease. P2X1R mRNA is upregulated in the hearts of rats suffering congestive heart failure and in the atria of human patients suffering from dilated cardiomyopathy (Musa et al., 2009), but downregulated in rat mesenteric arteries (Malmsjö et al., 1999). However, this receptor has been suggested as a drug target for a nonhormonal, reversible male contraceptive due to the fact that the P2X1R inhibition causes 100% male infertility with no negative effects on sexual behaviour or sperm function (White et al., 2013).

1.2.6.2 P2X2

The P2X2R is involved in few disease states. Sensory nerve endings of inflamed skin have increased P2X2/3 heteromer expression (Hamilton et al., 2001) and P2X2/3R antagonists have been shown to reduce nocifensive behaviour in animal models of chronic pain (Gum et al., 2012; Hansen et al., 2012; Kaan et al., 2010). As such, this subunit has been suggested as a potential therapeutic target for pain treatment.

There is also strong evidence associating P2X2R malfunction with hearing loss. This receptor is expressed in the cochlea of the inner ear (Table 1.2), and sustained loud noise induces upregulated P2X2R expression (Wang et al., 2003). P2X2R knockout mice have progressive hearing loss (Housley et al., 2013; Yan et al., 2013). In humans,

genetic linkage studies have shown the 178G>T polymorphism causing the loss-of-function V60L mutation to be significantly connected with the DFNA41 form of deafness in two unrelated Chinese families. These families had greater high-frequency hearing loss after exposure to noise when young (Blanton et al., 2002). In addition, the 1057G>C polymorphism which causes the G353R mutation has been significantly associated with autosomal dominant hearing loss in an Italian family (Faletra et al., 2014).

1.2.6.3 P2X3

As introduced above, the P2X3R plays a role in pain sensory functions. In addition to physiological pain, its link with bone cancer pain has been widely explored. P2X3R expression is upregulated in DRG neurons in rats inflicted with a model of bone cancer, where the animals suffered cancer-related pain which was attenuated by the intrathecal or local injection of A-317491 (Wu et al., 2012). A-317491 was also shown to reduce nerve injury and chronic inflammatory nociception in rat models (Jarvis et al., 2002). Additionally, oral administration of AF-353 to rats inflicted with a model of bone cancer pain led to the prevention and reversal of bone cancer pain behaviour (Kaan et al., 2010). As with the P2X2/3R, P2X3R inhibitors have also shown to be effective in reducing pain from inflammatory skin conditions in rats (Hamilton et al., 2001).

The role of the P2X3R in visceral sensory function has also led this receptor to be implicated in inflammatory bowel disease (IBD). IBD is characterised by colorectal hypersensitivity, which is virtually absent in P2X3R knockout mice in a murine model of zymosan-induced hypersensitivity (Shinoda et al., 2009). P2X3R expression in DRG neurons was increased in a rat model of colitis (Wynn et al., 2004), and in colon extracts from human IBD patients (Yiangou et al., 2001). Furthermore, PPADS applied to mice infected with a model of postinfectious bowel disease inhibited afferent sensitivity to intestinal distention (Rong et al., 2009). Administration of A-317491 in rats suffering from a model of acute colitis also dose-dependently reversed visceral hypersensitivity, although not completely (Deiteren et al., 2015). Overall, whilst there is evidence for P2X3R involvement in IBD, more evidence for its role in human disease is desirable.

1.2.6.4 P2X4

The P2X4R is expressed in endothelial cells, and its activation in response to fluid shear stress ultimately results in vasodilation (Yamamoto et al., 2000). Knockout of this receptor in mice suppresses vessel dilation in response to acute increase in blood flow (Yamamoto et al., 2006). It thus has a connection to blood pressure regulation. The loss-of-function 1248A>G polymorphism in the P2X4R gene coding for the Y315C mutation is a potential risk factor for high pulse pressure, as determined in a genotyping study of two Australian cohorts consisting of 430 and 2874 subjects, respectively (Stokes et al., 2011).

This subtype has also been connected to age-related macular degeneration (AMD). Degeneration of the macula in the retina is a major cause of blindness in the elderly (Ting et al., 2009) and a study of Caucasian AMD patients found a strong association between the 1248A>G polymorphism and increased AMD risk (Gu et al., 2013). This is thought to be linked to P2X4R expression on macrophages, which clear debris in the retina. As mentioned above, the P2X4R is additionally implicated in chronic pain states, although evidence for the involvement of this receptor in human pain diseases is lacking.

1.2.6.5 P2X5 and P2X6

The P2X5 and P2X6 receptors are involved in few currently known physiological processes, in the case of the P2X6R due to largely not forming functioning homomers. As such these proteins have not been convincingly implicated in disease states.

1.2.6.6 P2X7

The P2X7R is the member of the P2XR family which is predominantly implicated in pathological conditions. Its role in disease is described in detail in 1.3.6.

1.3 The P2X7 receptor

Originally, the P2X7R was given its own separate classification as a P2Z receptor. This was after a receptor which was similar to, but distinct from, P2XRs and P2YRs was connected to ATP-induced membrane permeabilisation (Falzoni et al., 1995; Gordon, 1986). This matter was settled when the P2X7R was cloned from the rat brain and experiments showed it to cause ATP-dependent lysis of macrophages by large pore formation (Surprenant et al., 1996). To date P2X7Rs from several species have been cloned; the rat (Surprenant et al., 1996), human (Rassendren et al., 1997), mouse (Chessell et al., 1998), guinea pig (Fonfria et al., 2008) and dog (Roman et al., 2009) as well the non-mammalian bony fish seabream (López-Castejón et al., 2007) and *Xenopus laevis* (Paukert et al., 2002). Mammalian P2X7R subunits are 595 amino acids long, except for in the guinea pig which lacks one residue. These P2X7Rs, and others from species such as the rhesus macaque monkey (Bradley et al., 2011b), have also been characterised pharmacologically.

The P2X7R described in this chapter is focussed on the full length receptor. However, there are also several naturally occurring splice variants with structural differences. These are named P2X7A-K, P2X7A being the full length protein. One of the best characterised is P2X7B, which has a similar tissue distribution to P2X7A (Cheewatrakoolpong et al., 2005) but due to a premature stop codon lacks the last 171 amino acids and therefore has no C-terminus. Due to this truncation, P2X7B can form ion channels but does not have the large pore forming functionality described in section 1.3.1.2 (Adinolfi et al., 2010). Other splice variants are less well characterised. P2X7C-F lack various exons coding for sections of the extracellular domain and are non-functional. P2X7G and H are also non-functional but contain an additional exon which means they do not have a TM1 domain (Cheewatrakoolpong et al., 2005). In contrast, P2X7I contains the uncommon loss-of-function 1513A>C (E496A) mutation. This gives rise to a null allele which abolishes pore formation (Skarratt et al., 2005). A further splice variant, P2X7J, was originally identified in cervical cancer cells. This is a severely

truncated P2X7R 258 amino acids in length, missing the C-terminus, TM2, and the distal third of the extracellular loop. It is non-functional and does not bind ligands, although it does heteroligomerise with WT subunits. It has been suggested that this antagonises the apoptosis initiated by the full-length receptor in cancer cells (Feng et al., 2006). Finally, P2X7K is the most recently characterised splice variant which was identified in the rat gene (Nicke et al., 2009). Variations in both the N-terminus and TM1 domain give it a sensitivity to BzATP 8-fold higher than at P2X7A in addition to much slower deactivation kinetics, increased rates of dye uptake and membrane blebbing. This splice variant is not inactivated in GlaxoP2X7 -/- mice, which has caused some ambiguity in studies of the P2X7R as described in section 1.3.4 (Nicke et al., 2009). As of yet P2X7K has not been identified in humans.

1.3.1 Unique receptor properties of P2X7

Different P2XR subtypes have unique characteristics, for example the P2X5R which is an anomaly due to its significant permeability to chloride ions (Bo et al., 2003a). However, the P2X7 subtype is distinctive in numerous ways which distinguish it from the others in the family.

1.3.1.1 Agonist response

The first of these characteristics is its response to agonists. P2X1-6 are stimulated by submicromolar concentrations of ATP. In contrast, the P2X7R is significantly less sensitive to this native agonist and requires submillimolar to millimolar concentrations of ATP to activate it (North and Barnard, 1997) as further described in section 1.3.2.

1.3.1.2 Pore formation

During short-term activation (over seconds), the P2X7R acts as an ion channel which conducts cations such as calcium, sodium and potassium. However, prolonged activation over many seconds or minutes increases receptor permeability, allowing molecules up to 900 Daltons in size into the cell (Steinberg et al., 1987). Whilst this pore-

forming function is primarily attributed to the P2X7R, it also occurs in the P2X2R, P2X2/3R, P2X2/5R and P2X4R (Li et al., 2015). N-methyl-D-glucamine (NMDG) and fluorescent dyes such as YO-PRO-1, Lucifer yellow and ethidium can enter and are commonly used to study this receptor function (Wei et al., 2016). This fascinating functionality has been the subject of much investigation, and yet to date a mechanism that satisfactorily explains the current evidence has not been proposed. Two main methods are used to investigate pore formation, this first of which is to carry out patch clamp recording with sodium and NMDG as the intracellular and extracellular cations, respectively. Subsequently analysing the current reversal potential can give an indication of membrane permeability to the large molecule NMDG (Khakh et al., 1999). The second is to measure the intracellular accumulation of fluorescent dyes such as YO-PRO-1 or ethidium by fluorescence microscopy (Roger et al., 2010b).

There are two prominent theories concerning how the P2X7R forms this large pore (Alberto et al., 2013; North, 2002); either that the ion channel dilates to accommodate larger molecules or that a different protein is recruited to act as the pore. The ‘pore dilation’ hypothesis was devised as a result of the increase in permeability to NMDG and YO-PRO-1 of cells expressing the P2X7R (Virginio et al., 1999b). However, more recently a study has shown that prolonged stimulation of such cells can lead to an increase in permeability to YO-PRO-1 but not NMDG. This, in addition to evidence that deletion of a cysteine-rich microdomain in the C-terminus prevents the reversal potential shift (indicating NMDG permeability) but not YO-PRO-1 uptake, is an indication that separate pathways mediate the entry of NMDG and YO-PRO-1 into P2X7R-expressing cells (Jiang et al., 2005).

The theory that a separate protein is recruited to act as the large pore is largely centred on Panx1. This is a membrane channel (Dahl and Locovei, 2006) implicated in pore formation. It is highly expressed in human and mouse monocytes, macrophages and astrocytes and co-immunoprecipitates and interacts with the P2X7R. Furthermore, Panx1 siRNA or Panx1 inhibiting peptides block P2X7R-mediated dye uptake and IL-1β

processing. Because of this, there is plentiful evidence to implicate Panx1 (Pelegrin and Surprenant, 2006). However, this is refuted in studies which have shown the pore to be unaffected by Panx1 knockout (Alberto et al., 2013) or inhibition with carbenoxolone or inhibitory peptides (Bhaskaracharya et al., 2014). Additionally, recent evidence shows that the P2X7R ion channel can dilate to form the pore (Browne et al., 2013). Together, it appears that the pore dilation hypothesis is the more likely of the two most prominent theories proposed to date, although substantial further study is required before a concrete conclusion can be drawn.

1.3.1.3 Structure

The P2X7R has the same overall structure that is described in section 1.2.1. However, one notable difference is that its intracellular C-terminus is 200 amino acids longer than those of the other P2XRs (Surprenant et al., 1996). This domain interacts with different proteins (Gu et al., 2009; Kim et al., 2001a) and is required for the formation of the large pore (Surprenant et al., 1996), as is TM2 (Sun et al., 2013). Furthermore, whilst all P2XR subunits form homomeric receptors and P2X1-6 form heteromers, the P2X7R is believed to form homotrimers alone (Nicke, 2008; Boumechache et al., 2009). Whilst there is some evidence for structural and functional interaction between P2X7 and P2X4 subunits (Guo et al., 2007), whether these subunits form functional heterotrimers is yet to be determined.

The P2X7R also undergoes a number of post-translational modifications. The first of these is N-linked glycosylation, where sugar moieties are covalently attached to specific amino acids. There are several glycosylation sites in the P2X7R, consisting of Asn187, Asn202, Asn213, Asn241 and Asn284 in the human isoform (Lenertz et al., 2010). There is evidence that the C-terminus of the receptor is important for mediating the proper processing of N-linked glycosylation modifications. Mutating Arg578 within the trafficking domain of the C-terminus leads to defective P2X7R modification in the endoplasmic reticulum, causing reduced receptor activity and presence at the cell surface (Wickert et

al., 2013). This is an indication of the importance of these post-translational modifications in determining P2X7R function.

The P2X7R additionally undergoes palmitoylation, during which fatty acids such as palmitic acid are covalently attached to cysteines. This process is also mediated by the C-terminus. Mutation of intracellular cysteines abolishes P2X7R palmitoylation and leads to protein retention in the endoplasmic reticulum, resulting in a decrease in cell surface expression (Gonnord et al., 2009). This post-translational modification has also been shown to promote P2X7R association with lipid rafts (Robinson et al., 2014), which play an important role in the organisation of signalling pathways such as the P2X7R-mediated inflammatory response (Robinson and Murrell-Lagnado, 2013).

One further modification is ADP-ribosylation, whereby the ADP-ribosyltransferase (ART) ecto-enzyme ART2.2 covalently attaches ADP-ribose to the extracellular domain of the P2X7R. This attachment occurs at Arg125 in the ‘head’ region (Figure 1.4A) at the interface of two receptor subunits (Adriouch et al., 2008; Hattori and Gouaux, 2012). The effect of this modification is described in further detail in section 1.3.2.

1.3.1.4 Facilitation

The P2X7R displays current facilitation in response to repeated agonist application, which is unique in that the other P2XRs desensitise (North, 2002). The underlying mechanism has been shown to be a result of a distinct calcium- and calmodulin-dependent process (Roger et al., 2008). However, facilitation at the human receptor is 5-fold slower than at the rat receptor. Investigation of chimeric rat/human receptors has demonstrated that the hP2X7R shows only calcium-dependent facilitation due to it lacking the calmodulin binding domain present in the C-terminus of the rP2X7R (Roger et al., 2010a). The basis of this facilitation has been in part described by the mathematical modelling of ATP binding at the P2X7R and its kinetics. A sixteen-state Markov model developed by the Stojilkovic group suggested that P2X7Rs with one or two ATP molecules bound slowly transition to a desensitised state, whereas those with three ATP

binding sites occupied switch to a sensitised or dilated state (Khadra et al., 2013). Such modelling has been a useful tool in expanding our understanding of P2X7R function.

1.3.2 Agonists

Of the P2XRs, the P2X7R has a distinctive agonist profile. As mentioned above, all P2XRs are activated by ATP, but the P2X7Rs have 30-100 times lower sensitivity to ATP compared to the others and require submillimolar concentrations for activation. In contrast, BzATP is commonly used in studies as it stimulates the P2X7R with approximately 30-fold higher potency than ATP (Surprenant et al., 1996; Bianchi et al., 1999; Young et al., 2007). Interestingly, there is a difference in the sensitivity of the hP2X7R to these two agonists compared to other species. The EC_{50} of ATP at the hP2X7R was approximately 10-fold greater than at the rP2X7R and for BzATP this was 25-fold greater (Rassendren et al., 1997). Compared to this, the rhesus macaque monkey P2X7R (rmP2X7R) was approximately half as sensitive to both ATP and BzATP as the hP2X7R (Bradley et al., 2011b) and the mouse P2X7R has a similar sensitivity to ATP compared to the human receptor but requires almost double the concentration of BzATP (Chessell et al., 1998). Of the species that have been characterised pharmacologically, the dog receptor response most resembles that of the human (Roman et al., 2009). Studies have identified two residues, Asp284 and Lys127, that affect the species-dependent difference in agonist potency between rat and mouse. Asp284 alone fully accounted for the 10-fold difference in ATP sensitivity, whereas Asp284 and Lys127 together affected the 100-fold difference in BzATP sensitivity (Young et al., 2007).

The hP2X7R is also activated by ADP-ribosylation. This is an enzyme-catalysed post-translational modification which involves the covalent attachment of ADP-ribose from the coenzyme nicotinamide adenine dinucleotide (NAD) to Arg125. This process is catalysed by ADP-ribosyltransferases (ARTs), specifically the subtype ART2.2. The addition of the

bulky, negatively charged ADP-ribose usually inactivates proteins by sterically blocking their interactions with their targets. However, P2X7 is activated due to the fact that ADP-ribose shares a common adenine-ribonucleotide moiety with ATP. Attaching this moiety to Arg125 brings ADP-ribose into close proximity with the ATP binding site, thereby activating the channel (Adriouch et al., 2008; Hattori and Gouaux, 2012).

1.3.3 Antagonists

The structures of the P2X7R antagonists described here are shown in Figure 1.8.

1.3.3.1 Oxidised ATP

An early P2X7R antagonist was oxidised ATP (oATP), which irreversibly blocks the P2X7R at micromolar concentrations provided cells are incubated with it for at least two hours (Murgia et al., 1993; Surprenant et al., 1996). As such, oATP was used in early studies but has since been replaced with the more effective inhibitors described below.

1.3.3.2 AZ11645373

AZ11645373 is a non-competitive P2X7R antagonist identified through high throughput screening. It has slow onset of inhibition ranging up to several minutes for lower nanomolar concentrations. Inhibition is slowly reversible, with full recovery taking up to 30 minutes after washout of higher concentrations (Stokes et al., 2006; Michel et al., 2009). This antagonist can inhibit receptor functions including P2X7R-evoked membrane currents, large pore formation and IL-1β release (Stokes et al., 2006). AZ11645373 is species specific and inhibits the human (Stokes et al., 2006), rhesus monkey (Bradley et al., 2011b) and dog (Roman et al., 2009) P2X7Rs potently, the mouse and guinea-pig receptors weakly and does not inhibit the rat receptor (Michel et al., 2009). In the species in which this compound is most effective, AZ11645373 has potency in the low nanomolar range (Stokes et al., 2006).

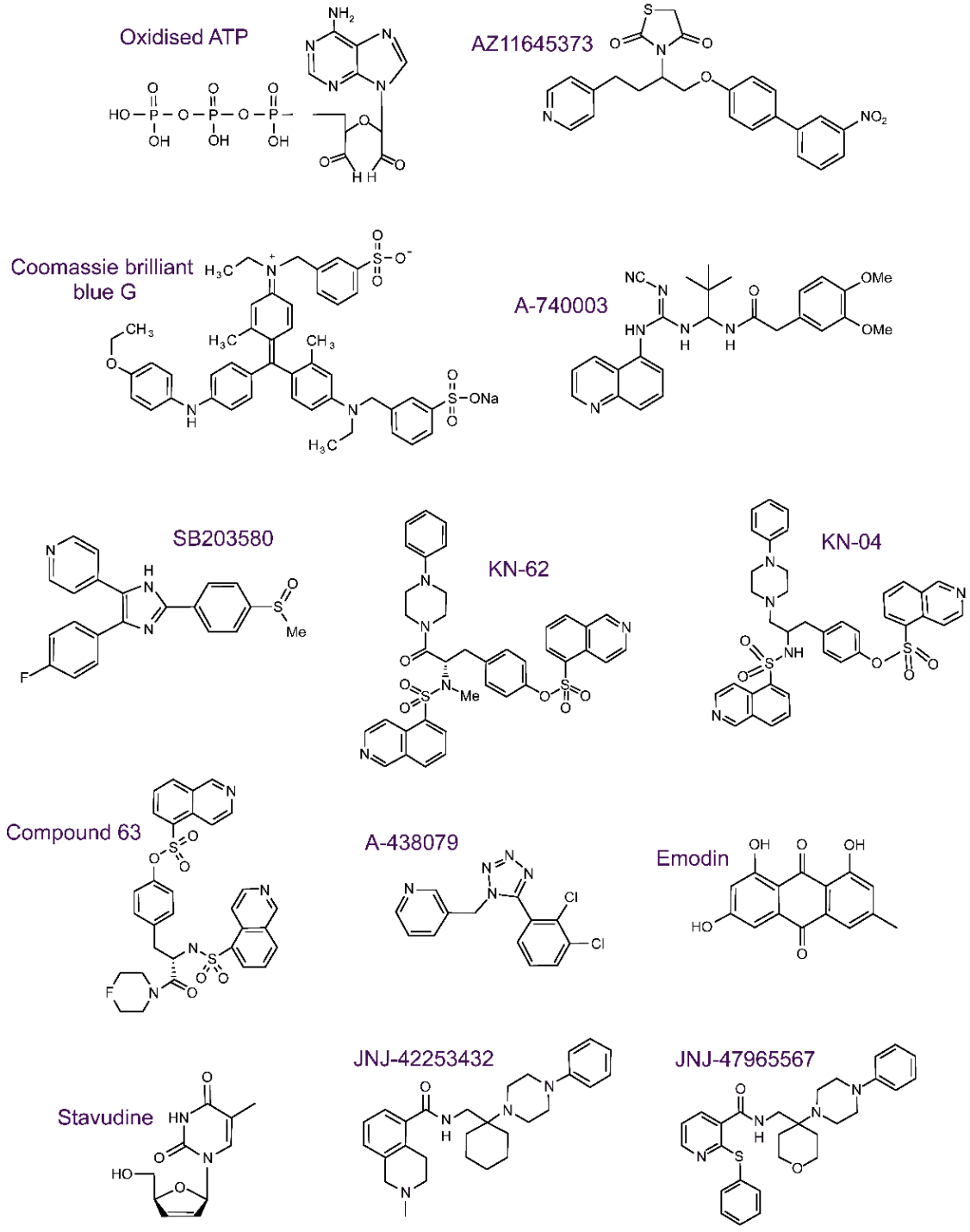

Figure 1.8 Common P2X7R antagonists

1.3.3.3 Coomassie brilliant blue G

Coomassie brilliant blue G (BBG) is a non-competitive inhibitor of P2X7Rs, acting with an EC_{50} of 10 and 200 nM at the rat and human receptors, respectively (Jiang et al., 2000a). This antagonist has also been shown to have an IC_{50} of 20 nM at the guinea pig receptor (Fonfria et al., 2008). BBG prevents membrane blebbing and large pore formation in rP2X7R-expressing cells and has been shown to be largely specific to the P2X7R, inhibiting the P2X2R with a lower efficacy (Jiang et al., 2000a). BBG is a structural analogue of a Food and Drug Administration-approved food dye and has been proposed in several studies as a potential basis for drug development.

1.3.3.4 A-740003

A-740003 is a highly selective P2X7R antagonist which acts competitively and reversibly. It is effective in blocking BzATP-evoked IL-1β release and large pore formation in human THP-1 cells (Honore et al., 2006) and its structural modification has been explored in attempts to produce a novel tracer of P2X7R-mediated neuroinflammation (Janssen et al., 2014). This is a further example of a P2X7R inhibitor which exhibits species specificity. It acts potently at the human and rat isoforms, being effective in the low nanomolar range, whilst in others such as the mouse it is slightly less effective (Donnelly-Roberts et al., 2009).

1.3.3.5 SB203580

SB203580 was initially identified as a mitogen activated protein kinase inhibitor. Further study showed that this compound is also a non-competitive hP2X7R antagonist which has no effect at the rat nor mouse P2X7Rs (Michel et al., 2006). However, it inhibits the hP2X7R fairly weakly with an IC_{50} of approximately 6 µM. Mutagenesis studies have identified an amino acid which determines the species specificity of this compound. The residue at position 95 is phenylalanine in the human receptor and leucine in the rat, and F95L mutation into the human receptor vastly reduced SB203580 inhibition (Michel et al., 2008). The importance of residue at this position in species difference of SB203580

Table 1.3 Common P2X7R antagonists

Species	oATP	AZ11645373	BBG	A-740003	SB203580	KN-62	A-438079	Emodin	References
Human		0.005-0.09, 0.034	0.2, 0.3	0.04	0.4-4, 6	0.013, 0.02	0.122	3	(Stokes et al., 2006; Michel et al., 2009; Jiang et al., 2000a; Honore et al., 2006; Donnelly-Roberts et al., 2009; Michel et al., 2006; Gargett and Wiley, 1997; Liu et al., 2010)
Rhesus monkey		0.023				0.086	0.297		(Bradley et al., 2011b)
Dog		0.039	0.05		Partial	0.01			(Michel et al., 2009; Roman et al., 2009)
Rat		>10	0.01	0.018	>10	>100	0.31, 0.32	0.2, 0.5, 3.4	(Stokes et al., 2006; Jiang et al., 2000a; Honore et al., 2006; Donnelly-Roberts et al., 2009; Michel et al., 2006; Humphreys et al., 1998; McGaraughty et al., 2007; Liu et al., 2010)
Mouse	30	1.45	<100	0.75, 1.73	>10	>100	0.79, 0.55		(Murgia et al., 1993; Michel et al., 2009; Donnelly-Roberts et al., 2009; Michel et al., 2006)
Guinea-pig		1.15	0.023			0.131			(Michel et al., 2009; Fonfria et al., 2008)

The value for each compound is presented as the IC_{50} in μM.

is shown in structural analysis of ligand-receptor interactions (see chapter 3).

1.3.3.6 KN-62

KN-62 was initially identified as a calcium/calmodulin-dependent protein kinase II (CaMKII) inhibitor (Tokumitsu et al., 1990; Hidaka and Yokokura, 1996) and was

subsequently shown to inhibit the P2X7R. KN-62 is potent at the human and mouse P2X7R where it completely inhibits function at 500 nM, but is ineffective at the rat orthologue (Gargett and Wiley, 1997; Humphreys et al., 1998). Inhibition has a slow onset, over a period of several minutes, and is only partially reversible upon washout (Gargett and Wiley, 1997). KN-62 potency increases markedly when the incubation period is prolonged (Donnelly-Roberts et al., 2009). This compound inhibits ATP-induced cation influx, large pore formation and phospholipase D activation (Gargett and Wiley, 1997). Interestingly, KN-62 completely inhibits both ATP and BzATP-mediated currents, but only partly inhibits ethidium uptake stimulated by BzATP whilst fully inhibiting that stimulated by ATP (Humphreys et al., 1998).

1.3.3.7 KN-62 derivatives

KN-62 was the first small molecule P2X7R antagonist that was identified, and as such has been modified in order to develop new inhibitors. KN-04 is a structural analogue of KN-62 which inhibits the P2X7R without affecting CaMKII (Humphreys et al., 1998). Further structural modification of KN-62 was carried out by Baraldi *et al*, who produced several inactive or weak antagonists (Baraldi et al., 2000; Baraldi et al., 2002) before introducing different phenyl-substituted piperazine moieties which resulted in a number of effective inhibitors. Compound 63, the most potent, had an IC_{50} of 1.3 nM (Baraldi et al., 2003).

In addition to these compounds, a frequently used KN-62 structural analogue is A-438079 (Nelson et al., 2006). This is a competitive antagonist capable of blocking calcium flux in human and rat recombinant P2X7 cell lines, large pore formation and IL-1β release in human THP-1 cells (Nelson et al., 2006) as well as BzATP-induced currents

in DRG cells and IL-1β release in macrophages (McGaraughty et al., 2007). A-438079 has an IC_{50} of 320 nM at the rat receptor but does not inhibit the P2X1, P2X2, P2X2/3, P2X4, P2Y1 and P2Y2 receptors as determined by a calcium influx assay (McGaraughty et al., 2007).

1.3.3.8 Emodin

A relatively recent P2X7R-specific antagonist is Emodin, an anthraquinone derivative extracted from *Rheum ofiicinale Baill* (Chinese rhubarb). This compound reduces ATP-induced death in rat macrophages with an IC_{50} of 0.2 μM, and strongly inhibits ATP-induced pore formation as well as BzATP-evoked currents in HEK293 cells transfected with the rP2X7R with an IC_{50} of 3.4 μM (Liu et al., 2010). This compound is effective in antagonising P2X7R physiological functions including IL-1β secretion, ROS production and phagocytosis in rat macrophages (Zhu et al., 2014) as well as inhibiting the invasiveness of human cancer cells (Jelassi et al., 2013) (Table 1.3).

1.3.3.9 Nucleoside reverse transcriptase inhibitors

Nucleoside reverse transcriptase inhibitors (NRTIs) are used to treat HIV. Recently, the NRTI stavudine has been demonstrated to have anti-inflammatory activity by blocking *Alu* RNA- or LPS/ATP-induced caspase-1 activation which leads to NLRP3 inflammasome activation (see section 1.3.5.1). This is independent of its reverse transcriptase inhibition and, interestingly, appears to preferentially (although not completely) block large pore formation by P2X7R whilst not affecting the ion channel (Fowler et al., 2014). Further pharmacological characterisation of the activity of this compound on the P2X7R is desirable but its efficacy in animal models of retinal pigment epithelium degeneration, graft-vs-host disease, liver inflammation and tumour angiogenesis is promising (Jiang, 2015; Fowler et al., 2014).

1.3.3.10 JNJ- compounds

Recently, a series of brain-penetrating P2X7R antagonists have been developed (Letavic et al., 2013). One of these is JNJ-42253432, which acts at the human, rat and

mouse P2X7Rs with IC_{50}s ranging from 3-78 nM in calcium flux, IL-1β release and electrophysiology assays. It also improves rat models of hyperactivity but not neuropathic pain or inflammatory pain (Lord et al., 2014). Additionally, the same study showed that JNJ-47965567 is highly selective and inhibits the human, macaque, dog, rat and mouse subtypes with IC_{50}s of 5-63 nM in the cell-based assays. It is also effective in animal models of CNS pathology (Bhattacharya et al., 2013) and as such has been utilised in studies of epilepsy (Jimenez-Pacheco et al., 2016; Jimenez-Mateos et al., 2015).

1.3.4 Expression

The P2X7R is widely expressed in mammals. It has been located by reverse transcription polymerase chain reaction (RT-PCR) and functional analysis in cells of hematopoietic origin such as B and T lymphocytes, microglia, macrophages, monocytes and mast cells (Coutinho-Silva et al., 1999; Greenberg et al., 1988; Hickman et al., 1994; Hughes et al., 2007). P2X7R expression has also been detected in salivary glands, the pancreas, pituitary glands, epithelia, osteoclasts and osteoblasts, liver, heart, thymus, vas deferens and DRG (Tenneti et al., 1998; Luo et al., 1999; Stojilkovic et al., 2010; Gröschel-Stewart et al., 1999; Grol et al., 2009; Rassendren et al., 1997; Queiroz et al., 2003; Chen et al., 2012b). This wide-ranging expression reflects the variety of physiological processes and diseases in which this receptor has been implicated (see sections 1.3.5 and 1.3.6).

Further to this, antibodies raised against amino acids 576-595 of the rat receptor subunit have been used to demonstrate P2X7R expression at presynaptic terminals in synapses of the peripheral and central nervous systems (Armstrong et al., 2002; Deuchars et al., 2001; Sperlágh et al., 2002). However, controversy has arisen with respect to the specificity of the antibodies used in these studies. A study investigating P2X7R expression in rodent brain neurons found that antibodies targeting different receptor epitopes could not detect similar expression patterns in various brain areas (Sim et al., 2004). Western blots from brain tissue from two P2X7R knockout mice, GlaxoP2X7 -/-

(Chessell et al., 2005) and Pfizer P2X7 -/- (Solle et al., 2001), showed P2X7R-sized bands (Sim et al., 2004). It has been suggested that these antibodies could detect splice variants which have escaped deletion in the knockout mice, for example the P2X7K splice variant which was not deleted in the GlaxoP2X7 -/- mouse (Nicke et al., 2009) and P2X7 C-terminal truncated variants, 13B and 13C, which were not deleted in the Pfizer P2X7 -/- mouse (Masin et al., 2012). This complicates studies into P2X7R expression, although a functional role for this receptor in neurons is clear (see section 1.3.5.4).

1.3.5 Physiological functions

1.3.5.1 Cytokine release

The P2X7R plays a pivotal role in the processing and release of interleukin-1β (IL-1β) (Ferrari et al., 2006), a pro-inflammatory cytokine which mediates host-defence responses to injury and infection (Netea et al., 2010). The NLRP3 inflammasome is a multiprotein complex vital for the processing and activation of IL-1β (Guo et al., 2015). Prior to activation, NLRP3 requires two separate steps. The first of these is for a stimulus such as lipopolysaccharide (LPS) binding to the toll-like receptor 4, which induces the expression of biologically inactive pro-IL-1β. The second is for a signal which can activate NLRP3 and cause formation of the inflammasome complex, such as a P2X7R-mediated drop in intracellular potassium (Karmakar et al., 2016; Franceschini et al., 2015). This allows caspase-1 to process the inactive precursor pro-IL-1β by proteolytic cleavage (Brough and Rothwell, 2007; Ferrari et al., 2006) and results in the secretion of biologically active or mature IL-1β. The absence of the P2X7R in knockout mice leads to a lack of post-translational processing of pro-IL-1β present in macrophages, which is not released in its mature form (Solle et al., 2001). In addition, LPS-dependent IL-1β release in microglial cells is inhibited by oATP (Ferrari et al., 1997). In human monocytes, the loss-of-function E496A mutation results in significantly impaired release of the proinflammatory cytokine IL-18 (Sluyter et al., 2004a) and a marked reduction in IL-1β

release (Sluyter et al., 2004b). In contrast, P2X7Rs containing the gain-of-function mutations Q460R and A348T correlate with increased IL-1β secretion from LPS-primed monocytes (Stokes et al., 2010).

1.3.5.2 Cell death

Sustained exposure of immune cells to high concentrations of extracellular ATP results in necrotic or apoptotic cell death dependent on P2X7R activity (North, 2002; Burnstock, 2002). Necrosis is the premature death of cells and is characterised by loss of cell membrane integrity, resulting in the leakage of intracellular materials into the extracellular milieu (Berghe et al., 2014). Apoptosis is a form of programmed cell death featuring specific changes within the cell including nuclear condensation and fragmentation, cell shrinkage and membrane blebbing (Ouyang et al., 2012). The intercalating agent propidium iodide (PI) has been used to stain dead cells to demonstrate ATP-induced cell death in murine thymocytes (Le Stunff et al., 2004) and Jurkat cells (Aguirre et al., 2013) as well as that stimulated by amyloid β peptide in glial cells (Wakx et al., 2016).

P2X7R activation also affects cell morphology. Large morphological changes and membrane blebbing in response to extracellular ATP have been observed in P2X7R-transfected HEK293 cells (Virginio et al., 1999a) as well as cells which endogenously express the P2X7R such as macrophages (Verhoef et al., 2003; Perregaux and Gabel, 1994) and dendritic cells (Ferrari et al., 2000). Membrane blebbing is one of the most prominent hallmarks of apoptosis (Mills et al., 1998; Coleman et al., 2001) and is thought to be a result of cytoskeletal rearrangement in which the P2X7R plays a role. Application of high-dose BzATP to P2X7R-expressing cells causes disassembly of focal adhesion complexes resulting from a loss of the membrane-cytoskeletal interactions, clustering of α-tubulin and the redistribution of F-actin (Mackenzie et al., 2005).

A further characteristic of apoptosis is DNA fragmentation (Gavrieli et al., 1992). ATP application causes DNA fragmentation in the mouse microglial cell line N13 but not when

lower concentrations of ATP or other nucleotides are applied (Ferrari et al., 1999). This phenomenon is also seen in mesangial cells, where it can be induced by BzATP and inhibited by oATP (Schulze-Lohoff et al., 1998), and in P2X7R-expressing cell lines including cervical epithelial cells (Wang et al., 2004a), gingival epithelial cells (Yilmaz et al., 2008) and thymocytes (Le Stunff et al., 2004). Overall, P2X7R involvement in cell death is one of its more interesting characteristics from a pharmaceutical perspective.

1.3.5.3 Cell proliferation

The P2X7R has also been shown to be involved in cell proliferation. Increased proliferation is seen in human T lymphocytes stimulated with BzATP or ATP (Baricordi et al., 1996). Cells transfected with P2X7R cDNA also proliferate in serum-free medium, whilst cells lacking this receptor do not. Similarly, incubation of P2X7R-expressing cells with oATP or the ATP hydrolysing enzyme apyrase abolishes any proliferation increase (Baricordi et al., 1999). The presence or absence of serum in the cell media appear to determine whether ATP causes P2X7R-mediated cell proliferation or death. Furthermore, microglial cell exposure to LPS prevents proliferation and causes differentiation. This correlates with reduced P2X7R expression. Similarly, P2X7R inhibition by oATP, KN62 and BBG or knockdown by siRNA decrease cell proliferation, demonstrating that reduced P2X7R activity is important in the antiproliferative effect of LPS in microglia (Bianco et al., 2006).

Mitochondria play a central role in cell proliferation (Antico Arciuch et al., 2012). P2X7R transfected cells exhibit physiological changes in their mitochondria including increased resting mitochondrial potential, increased basal mitochondrial calcium and increased cellular ATP content. P2X7R expression also confers the ability to grow in serum-free medium (Adinolfi et al., 2005). This depends on large pore formation, as proliferation is abolished in cells expressing the P2X7R missing the C-terminal tail (Smart et al., 2003). The group conducting this study theorised that tonic P2X7R activity causes a constant ‘leak’ of calcium across the mitochondrial membrane, increasing basal metabolic activity and stimulating ATP synthesis. This pathway may allow cell proliferation in the absence

of serum. The cell death induced by high concentrations of ATP could be due to increased calcium influx to the mitochondria leading to calcium overload, fragmentation of the mitochondrial network and apoptosis (Adinolfi et al., 2005).

1.3.5.4 Neuronal function

The P2X7R is present at presynaptic terminals in synapses of both the peripheral and central nervous systems (Armstrong et al., 2002; Deuchars et al., 2001; Sperlágh et al., 2002). Deuchars *et al* showed by whole-cell patch clamp of rat spinal cord slices that P2X7R activation caused excitation of CNS neurons through glutamate release. BzATP application also caused depolarisation of neurons which was inhibited by oATP and BBG (Deuchars et al., 2001). ATP also stimulates GABA and glutamate release in mouse hippocampal slices which can be prevented by PPADS and BBG, a phenomenon virtually absent in P2X7R-deficient mice (Papp et al., 2004). Additionally, exposure of mouse brainstem slices to BzATP elicits excitatory postsynaptic currents (EPSCs) in hypoglossal motor neurons which are prevented by BBG (Ireland et al., 2004). P2X7R expression in rat cerebrocortical glutamatergic nerve terminals is also important for calcium-dependent vesicle release which contributes to glutamate release (Marcoli et al., 2008). A further study found that P2X7Rs expressed on presynaptic terminals of mossy fibre synapses in the rat hippocampus mediated inhibition of neurotransmission when stimulated by BzATP, which was blocked by oATP (Armstrong et al., 2002). Similarly, BzATP application in mouse hippocampal mossy fibre CA3 synapses was shown to depress field potentials (Kukley et al., 2004). However, contradictorily, this depression was not altered by P2X7R knockout in mice but was blocked by the A1 receptor antagonist DPCPX (Kukley et al., 2004). As such the role of P2X7Rs in mossy-fibre CA3 synapses is a subject that would benefit from further investigation.

1.3.5.5 Neuron-glial interactions

The P2X7R is also implicated in the interaction between neurons and glial cells. One study found that the P2X7R provides a route for excitatory amino acid release from

astrocytes. L-glutamate and D-aspartate were released from astrocytes stimulated with BzATP more potently than ATP, which was amplified by low divalent cation medium and blocked by PPADS and oATP (Duan et al., 2003). Astrocytes also release neurotransmitters in a manner that is activated preferentially by BzATP over ATP, whilst being blocked by BBG and absent in P2X7R null mice (Suadicani et al., 2006). Additionally, ATP released after electrical stimulation of DRG activates P2X7Rs expressed on satellite cells wrapped around each DRG neuron, initiating communication between glial cells and the neuronal somata. P2X7R activation can also cause the emission of tumour necrosis factor α, which in turn affects P2X3R responses in order to increase the excitability of DRG neurons (Zhang et al., 2007). A further study showed that P2X7R activation in satellite cells causes ATP release, which in turn activates the P2Y1 receptor and down-regulates P2X3R expression in DRG neurons to mitigate P2X3R-mediated pain (Chen et al., 2008).

1.3.5.6 Bone homeostasis

The P2X7R is expressed on osteoclasts and osteoblasts (Table 1.2). P2X7R signalling is also required for calcium signalling between the two cell types and, therefore, also bone formation and remodelling (Jørgensen et al., 2002). A link between the P2X7R and osteoclasts is seen in functions including apoptosis (Ohlendorff et al., 2007), multinucleated cell formation (Gartland et al., 2003a) and NF-κB activation (Korcok et al., 2004). In osteoblasts the P2X7R activates downstream extracellular signal-regulated kinases which follow fluid flow to induce ATP and stimulate mineralisation (Panupinthu et al., 2007; Panupinthu et al., 2008; Li et al., 2005; Okumura et al., 2008).

Several studies have been carried out to examine the effect of P2X7R knockout in mice on bone homeostasis, although the results have often been contradictory due to their use of knockout mice that in fact still express various P2X7R variants. These animals have been shown to exhibit impaired periosteal bone formation and increased trabecular bone resorption (Ke et al., 2003). However, a subsequent study found no obvious skeletal phenotype (Gartland et al., 2003b). Syberg *et al* showed that mice with P2X7Rs

containing the loss-of-function P451L mutation had weaker femurs and lower levels of the bone resorption marker C-telopeptide collagen compared to WT, in addition to their macrophages having less large pore-forming activity in osteoclasts (Syberg et al., 2012b). The same group investigated several strains of P2X7R knockout mice and found that, overall, receptor knockout contrarily led to mice with higher bone mineral density and increased bone strength compared to WT mice (Syberg et al., 2012a; Orriss et al., 2011). Overall this implicates the P2X7R as being involved in bone metabolism in a multifaceted manner, although *in vivo* studies are differing and require further research.

1.3.6 P2X7 receptor in disease

The P2X7R is a desirable target for the development of therapeutic compounds due to its relation to various diseases. The characteristics of the P2X7R mean that if its activity is affected, either by alterations in its levels of expression or function, the downstream effects can trigger a variety of conditions. It must also be noted that non-synonymous single nucleotide polymorphisms (NS-SNPs) are an important factor in connecting this receptor to disease. The P2XR genes (the *P2RX* gene family) are highly polymorphic and the hP2X7R in particular contains a large number of NS-SNPs. These polymorphisms have been identified as a genetic factor which impacts the susceptibility of individuals to a series of conditions. NS-SNPs relevant to disease are summarised in Table 1.4.

1.3.6.1 Pain

Altered P2X7R function is linked to chronic pain conditions (Sorge et al., 2012; Donnelly-Roberts and Jarvis, 2007; Chessell et al., 2005). P2X7R-mediated IL-1β release mediates numerous downstream events related to pain (Ren and Torres, 2009), and P2X7 knockout in mice has been shown to interrupt cytokine signalling cascades and consequently diminish IL-1β processing (Labasi et al., 2002). As such, P2X7 null mice lack both inflammatory and neuropathic hypersensitivity in response to mechanical and

Table 1.4 Disease-associated NS-SNPs in the P2RX7 gene

Nucleotide change	Amino acid change	Implicated conditions	References
370T>V	A76V	Multiple sclerosis	(Oyanguren-Desez et al., 2011)
474G>A	G150R	Osteoporosis	(Husted et al., 2013; Wesselius et al., 2013)
489C>T	H155Y	Multiple sclerosis, chronic pain, severe sepsis, child febrile seizures	(Oyanguren-Desez et al., 2011; Sorge et al., 2012; Geistlinger et al., 2012; Emsley et al., 2014)
835G>A	R270H	Chronic pain	(Sorge et al., 2012)
946G>A	R307Q	Osteoporosis	(Gartland et al., 2012; Jørgensen et al., 2012)
1068G>A	A348T	Osteoporosis, anxiety disorder, toxoplasmosis	(Husted et al., 2013; Jørgensen et al., 2012; Wesselius et al., 2013; Erhardt et al., 2007; Jamieson et al., 2010)
1096C>G	T357S	Osteoporosis	(Gartland et al., 2012)
1405A>G	Q460R	Osteoporosis; severe sepsis, bipolar disorders and major depressive disorders*	(Husted et al., 2013; Jørgensen et al., 2012; Wesselius et al., 2013; Geistlinger et al., 2012; Barden et al., 2006; Lucae et al., 2006; McQuillin et al., 2008; Hejjas et al., 2009)
1513A>C	E496A	Osteoporosis, tuberculosis, cardiovascular risks	(Gartland et al., 2012; Husted et al., 2013; Jørgensen et al., 2012; Ohlendorff et al., 2007; Wesselius et al., 2013; Fernando et al., 2007; Niño-Moreno et al., 2007; Gidlöf et al., 2012)
1729T>A	I568N	Osteoporosis	(Gartland et al., 2012; Jørgensen et al., 2012; Ohlendorff et al., 2007)

Table adapted from (Caseley et al., 2014). *Association with bipolar disorders and major depressive disorders is refuted by the following studies: (Green et al., 2009; Grigoroiu-Serbanescu et al., 2009).

thermal stimuli, but have normal pain responses (Chessell et al., 2005).

P2X7R-specific antagonists are effective in *in vivo* pain models. oATP relieves inflammatory pain when applied locally to arthritic rat paws (Dell'Antonio et al., 2002), A740003 dose-dependently reduces neuropathic pain in rats in the spinal nerve ligationmodel, chronic constriction injury of the sciatic nerve and vincristine-induced neuropathy (Honore et al., 2006). Similarly, A438079 is anti-allodynic in these three rat models of neuropathic pain (McGaraughty et al., 2007). In addition to animal models, a large-scale genetic study in humans has identified the gain-of-function H155Y and loss-of-function R270H mutations to confer greater or reduced sensitivity to chronic pain, respectively (Sorge et al., 2012) (Table 1.4).

1.3.6.2 Affective mood disorders

Mood disorders encompass illnesses including major depressive disorder (MDD), bipolar disorder (BD) and anxiety disorder (AD). A large scale genetic study initially identified the *P2RX7* gene as a locus of interest with respect to mood disorders (Shink et al., 2005), and subsequent studies have been carried out with opposing results. The 1405A>G and 1068G>A polymorphisms, resulting in Q460R and A348T mutations respectively, have been implicated in the pathogenesis of BD (Barden et al., 2006; Lucae et al., 2006; McQuillin et al., 2008; Hejjas et al., 2009), MDD (Hejjas et al., 2009) and AD (Erhardt et al., 2007). However, other studies found no link (Green et al., 2009; Grigoroiu-Serbanescu et al., 2009; Sklar et al., 2008; Sklar et al., 2011). As such whilst there is evidence for a connection with affective mood disorders, much of this is contradictory.

A link between the P2X7R and mood disorders is possible due to its expression on astrocytes and microglia in the CNS (Rappold et al., 2006; Kukley et al., 2001; Sperlágh et al., 2006) in conjunction with its role in calcium signalling and neurotransmitter release (Wang et al., 2002; Sperlágh et al., 2002). Changes in intracellular calcium have been reported in patients suffering from mood disorders (Andreopoulos et al., 2004). However, there is contradictory evidence regarding the effects of the Q460R and A348T mutations

on receptor function, as they appear to cause no clear loss- or gain-of-function effects (Roger et al., 2010b; Cabrini et al., 2005; Bradley et al., 2011a).

1.3.6.3 Bone diseases

The P2X7R has been linked to osteoporosis and bone fracture risk. Osteoporosis causes a progressive loss of bone mineral density (BMD) and deterioration of the microarchitecture of bone, increasing fracture risk (Kanis et al., 1994). P2X7 knockout in mice reduces cortical bone content, periosteal bone formation and periosteal circumference in femurs (Ke et al., 2003), as well as diminishing the effect of mechanical loading on periosteal bone formation (Li et al., 2005). Furthermore, P2X7 knockout mice do not lose BMD in an inflammation-mediated osteoporosis model, whereas WT mice exhibit loss of BMD, bone strength and trabecular microarchitecture (Kvist et al., 2015).

Human genotyping studies have linked NS-SNPs in the *P2RX7* gene with bone disease. Generally, loss-of-function mutations correlate with lower BMD and increased fracture risk. The loss-of-function mutations 1513A>C (E496A) and 1729T>A (I568N) have been associated with increased vertebral fracture rate (Ohlendorff et al., 2007) and rate of bone loss (Jørgensen et al., 2012). 946G>A (R307Q) is linked to lower spine BMD (Gartland et al., 2012) and increased bone loss (Jørgensen et al., 2012). 474G>A (G150R) correlates with lower hip BMD in both men and women (Husted et al., 2013) and 1513A>C (E496A) leads to decreased BMD in the hip and lower lumbar spine in women and in the lower hip in men (Husted et al., 2013) (Table 1.4). Similarly, the loss-of-function P451L in mice increased susceptibility to osteoporosis (Syberg et al., 2012b). Conversely the gain-of-function mutations 1068G>A (A348T) and 1405A>G (Q460R) are associated with increased BMD and lower vertebral fracture incidence (Jørgensen et al., 2012; Husted et al., 2013; Wesselius et al., 2013). These effects seem to be mainly determined by 1068G>A in men and the 1405A>G and 1513A>C polymorphisms in women (Husted et al., 2013). It is apparent that the P2X7R has a complex but clear link to bone disease.

1.3.6.4 Neurodegenerative diseases

The P2X7R has been implicated in neurodegenerative (ND) diseases. This includes multiple sclerosis (MS), an ND disease of the CNS which causes inflammation, axonal degeneration and white matter lesions with demyelination (Sobel, 2015). In mice, sustained P2X7R activation induces MS-like lesions. Furthermore, treatment of mice inflicted with the chronic experimental autoimmune encephalomyelitis (EAE) model of MS with BBG or oATP diminished demyelination and reduced neurological symptoms (Matute et al., 2007). P2X7R null mice subjected to the EAE model also have a 4-fold reduced incidence rate of disease compared to WT mice (Sharp et al., 2008). However, in contrast a study using the EAE model showed that P2X7R-null mice were more susceptible to developing MS (Chen and Brosnan, 2006). In humans, the 370T>C and 489C>T NS-SNPs, corresponding to the gain-of-function A76V and H155Y mutations respectively, have been linked to increased MS susceptibility (Oyanguren-Desez et al., 2011). The 946G>A NS-SNP, which causes the R307Q loss-of-function mutation, has been linked with a protective effect against MS and the resulting neuroinflammation (Gu et al., 2015). As such the evidence available is in parts conflicting, but does suggest that this receptor plays a role in MS pathogenesis.

As well as MS, the P2X7R has been linked to Alzheimer's disease (AD). Animal studies have shown that the P2X7R is upregulated in models of this disease; this is seen in the Tg2576 transgenic mouse model carrying an APP(K670N,M671L) double mutation (Parvathenani et al., 2003) and the APPswe/PS1dE9 mouse model (Lee et al., 2011) as well as rats injected with amyloid peptide Aβ42 (McLarnon et al., 2006). Furthermore, P2X7 blockade *in vivo* in mouse models has been shown to be neuroprotective. BBG administration into the Aβ42-injected rat hippocampus attenuates gliosis as well as being neuroprotective (Ryu and McLarnon, 2008) and treatment of J20 hAPP transgenic mice with BBG reduced the incidence of amyloid plaques (Diaz-Hernandez et al., 2012).

Furthermore, the P2X7R has also been implicated in affecting patient recovery following spinal injury. Acute spinal cord injury (SCI) displays an immediate loss of tissue at the

site of injury and a subsequent second injury which causes further tissue damage. In rat models of SCI, oATP or PPADS application significantly improved their recovery (Wang et al., 2004b). A later study found that the BBG administration in a model of thoracic SCI in rats reduced damage to the spinal cord and improved motor recovery, implicating the P2X7R as a promising target for SCI treatment in humans (Peng et al., 2009). Relatedly, the P2X7R is also associated with the induction, but not maintenance, of morphine tolerance. Its protein levels are upregulated in the spine following chronic exposure to morphine. In rat models of morphine tolerance intrathecal administration of BBG reduced their tolerance and prevented P2X7R upregulation and microglial activation, as did siRNA knockdown of spinal cord P2X7R (Zhou et al., 2010). This is linked to a mechanism in the spine whereby chronic morphine application causes interaction between glia and neurons in the spine through a signalling pathway involving the P2X7R, IL-18, the *N*-methyl-D-aspartate receptor and protein kinase Cγ (Chen et al., 2012a).

1.3.6.5 Rheumatoid arthritis

Rheumatoid arthritis (RA) is a debilitating disorder characterised by chronic inflammation of the joints (Arnett et al., 1988). In an animal study of RA, mice were injected with a panel of four monoclonal antibodies generated against type II collagen, then injected with LPS to induce RA-like symptoms. WT mice displayed a severe arthritic phenotype within 7 days of LPS injection, with significant paw swelling and inflammation. In contrast, P2X7 knockout mice were much less likely to develop RA symptoms and when they did these symptoms were less severe and present in fewer limbs (Labasi et al., 2002). In addition in humans, the H155Y gain-of-function mutation has been identified as conferring enhanced function to P2X7Rs expressed on lymphocytes from patients with RA (Portales-Cervantes et al., 2012). Together this suggests a role for the P2X7R in RA.

1.3.6.6 Infection

The P2X7R is expressed on macrophages, where its activation causes the destruction of pathogens such as *Toxoplasma gondii (T. gondii)*, a protozoan parasite that can cause

toxoplasmosis (da Silva and Langoni, 2009). P2X7R activation in macrophages by ATP and BzATP prevents the increase of the *T. gondii* parasite load which is prevented by pre-treatment with BBG, and also induces reactive oxygen species (ROS) production which is part of the host defence mechanism (Corrêa et al., 2010). P2X7R knockout mice infected with this parasite were more susceptible to developing toxoplasmic ileitis (Miller et al., 2015). In humans, macrophages from patients expressing the loss-of-function E496A P2X7R were less capable of ATP-induced *T. gondii* removal (Lees et al., 2010), whereas patients with the 1068G>A SNP expressing the gain-of-function A348T mutation were less susceptible to congenital toxoplasmosis resulting from infection in utero (Jamieson et al., 2010).

The P2X7R also has connections to the removal of the tuberculosis-causing *Mycobacterium tuberculosis*. This predominantly replicates in macrophages, which can also kill the bacteria by producing ROS or reactive nitrogen species (Chan et al., 1992). Human macrophage exposure to ATP and BzATP initiated killing of intracellular bacteria which was prevented by oATP, suramin and KN62 (Lammas et al., 1997), and macrophages pre-incubated with oATP or in media containing elevated magnesium had an inhibited tuberculocidal effect (Kusner and Adams, 2000; Kusner and Barton, 2001). However, genetic association studies are contradictory; a link between E496A and tuberculosis susceptibility was seen in Southeast Asian (Fernando et al., 2007) and Mexican populations (Niño-Moreno et al., 2007) but not in Gambian (Li et al., 2002), Chinese (Xiao et al., 2009) and Asian Indian subjects (Sambasivan et al., 2010). However, meta-analysis has concluded that E496A is a significant factor in Asian populations (Wu et al., 2014).

1.3.6.7 Cancers

Increased P2X7R expression has been reported in cancers including thyroid papillary carcinoma (Solini et al., 2008), prostate cancer (Slater et al., 2004a), breast cancer (Slater et al., 2004b; Xia et al., 2015; Jelassi et al., 2013; Jelassi et al., 2011; Roger et

al., 2015), uterine epithelial cancers (Li et al., 2006), neuroblastoma (Raffaghello et al., 2006) and chronic lymphocytic leukaemia (CLL) (Adinolfi et al., 2002). However, the connection between CLL and the P2X7R has been the most widely investigated. CLL is the most common form of leukaemia in Western countries and is characterised by the proliferation and accumulation of neoplastic B lymphocytes in the blood, lymph nodes, bone marrow and spleen (Rozman and Montserrat, 1995). 'Indolent' CLL displays no disease progression, whereas 'evolutive' CLL requires cytotoxic therapy due to its rapid progression. A higher level of P2X7R expression in lymphocytes and increased calcium influx in response to ATP has been seen in patients suffering from evolutive CLL compared to the indolent variant (Adinolfi et al., 2002). There have also been investigations exploring the connection between the loss-of-function E496A polymorphism and CLL susceptibility. The prevalence of E496A in CLL patients was found to be three-fold greater than in lymphocytes from control patients (Wiley et al., 2002) and E496A-positive patients had a significantly longer CLL survival rate (Thunberg et al., 2002). However, this link has subsequently been refuted (Zhang et al., 2003; Starczynski et al., 2003; Nückel et al., 2004; Sellick et al., 2004). A further study suggested that this connection may be limited to Indian populations and that this polymorphism may affect the disease progression of familial rather than sporadic CLL (Dao-Ung et al., 2004). As such the connection with CLL may benefit from investigation accounting for nuance in populations with respect to patient background and form of CLL.

1.3.7 P2X7 ligands as potential therapeutics

The P2X7R is a desirable drug target due to its connection with multiple debilitating conditions as discussed above. As such, great efforts have been made to develop small molecules which can specifically target the P2X7R. hP2X7R-specific compounds have been developed by pharmaceutical companies to treat chronic conditions such as RA, osteoarthritis and chronic obstructive pulmonary disease (Arulkumaran et al., 2011; Bartlett et al., 2014). However, the progress of drugs developed to target this receptor

has been limited once they reach phase 1 and 2 clinical trials. These include CE-224535, developed by Pfizer to treat osteoarthritic pain of the knee (Pfizer, 2008) as well as RA (Stock et al., 2012), AZD9056 developed by AstraZeneca to treat the signs and symptoms of RA (Keystone et al., 2012) and GSK1482160 produced by GlaxoSmithKline as a treatment for chronic inflammatory pain (Ali et al., 2013). Trials testing these compounds for the treatment of arthritis have subsequently been discontinued due to their lack of efficacy compared to control groups rather than because of adverse effects caused by these compounds. However, there are more recent developments in this field which have proven to be more promising. The orally active P2X7R inhibitor AZD9056, which is indistinguishable from the placebo group in the treatment of RA, has been shown in a phase 2a clinical trial to be effective in the treatment of moderate to severe Crohn's disease (Eser et al., 2015). This progress is an indication that the P2X7R has promise as a therapeutic target and that efforts towards uncovering new inhibitors which act specifically at this receptor are worthwhile.

1.4 Aims of this study

The P2X7R exhibits many unique properties within the P2X family of receptors and many of these properties are inexorably linked to the interaction of this protein with its ligands. The conserved ATP binding residues have been identified, although residues outside of this central group have been explored to a lesser extent for their influence on ATP binding. Additionally the species-specific response to BzATP in P2X7Rs is much less understood and could hugely benefit from further in-depth investigation. As well as these factors regarding agonist interaction with the P2X7R, there are a number of P2X7R-specific antagonists available to us. However, as yet there are none which have been discovered using a directed structural approach and their sites of interaction with the receptor are often largely speculative. As such, the investigation discussed in this thesis aimed to investigate the structural basis of ligand-receptor interactions at the P2X7R and apply such information in search for new P2X7R antagonists.

The aims of this study were:

1. To generate structural models of P2X7Rs from different species based on the zfP2X4R crystal structures and to determine the validity of these models with further experiments.
2. Use a structural approach to carry out virtual screening experiments, followed by measurement of their effects on agonist-induced calcium responses, to identify novel antagonists of the P2X7R and to characterise the actions of identified antagonists on P2X7R function.
3. To investigate residues other than the conserved ATP binding residues in the interaction between agonists and the P2X7R.
4. To explore a select subset of residues for their contribution to the species-specific activity and agonist sensitivity of the human and rat P2X7Rs.

In order to achieve these aims, a multidisciplinary approach was adopted. This encompassed *in silico* techniques including homology modelling, molecular docking and virtual screening, which were followed by molecular biology techniques such as site-directed mutagenesis and heterologous expression of point mutant receptors, which subsequently paved the way for experiments including patch-clamp recording and calcium imaging.

Chapter 2

Materials and Methods

2.1 Chemicals, reagents and solutions

2.1.1 Chemicals and reagents

General chemicals or reagents were commercially obtained at the appropriate grade from Sigma, unless otherwise stated. The custom designed compounds EC-001, EC-002 and EC-003 were synthesised by Enamine.

2.1.2 Solutions

All solutions were prepared using Milli-Q deionised water (summarised in Table 2.1). All solutions involved in DNA and cell culture processes were sterilised by autoclaving or syringe filtering.

2.1.3 Enzymes and kits for nucleic acid preparations

DNA restriction and modification enzymes and DNA polymerases were purchased from New England Biolabs, Promega, Stratagene or QIAGEN. Plasmid DNA mini- and midi-preparation kits, gel DNA extraction kits and PCR purification kits were purchased from QIAGEN. All enzyme buffers were supplied with the enzymes as shown in Table 2.2.

2.1.4 Antibodies

Antibodies were sourced as indicated in Table 2.3.

2.1.5 E. coli strains and growth medium

Competent *E. coli* cells were purchased from Agilent or Bioline. XL10-Gold ultracompetent (Agilent) or α-select bronze efficiency (Bioline) cells were used to amplify plasmids for site-directed mutagenesis and XL1-Blue supercompetent cells (Agilent) were used for transformation of ligation products. Competent *E. coli* cells were prepared

as described in section 2.3. Powders for *E. coli* growth medium and agar plates were purchased from Sigma (see Table 2.1).

2.1.6 Cell culture media and transfection reagents

HEK293 cells and HEK293 cells stably expressing C-terminal EE-tagged hP2X7R (Rassendren et al., 1997) and rP2X7R (Surprenant et al., 1996), hP2X4R (Garcia-Guzman et al., 1997) and rP2X3R (Lewis et al., 1995) were provided by Dr Lin-Hua Jiang, University of Leeds. HEK293 cells stably expressing C-terminal His-tagged hP2X7R were produced during the present study. Dulbecco's Modified Eagle Medium (DMEM), DMEM/F12, foetal bovine serum (FBS), trpsin/EDTA, Optimedia and Lipfectamine2000® reagent were purchased from Invitrogen (Table 2.1).

2.1.7 Plasmids and oligonucleotides

cDNAs encoding the WT hP2X7 (Rassendren et al., 1997) and rP2X7 (Surprenant et al., 1996) subcloned in pcDNA3.1, were available in Dr Lin-Hua Jiang's lab. Oligonucleotides/primers were custom made by Sigma, Integrated DNA Technologies or Invitrogen. As specifically indicated, some plasmids encoding point mutations generated from previous lab members were used in this study.

2.2 Molecular simulation methods

2.2.1 Homology modelling of P2X receptors

Structural models of the P2XRs were produced based on the crystal structure of the zfP2X4R in the closed and ATP-bound open states (Protein Data Bank code 4DW0 and 4DW1, respectively) using Modeller version 9.12 (Eswar et al., 2006). One hundred models were generated for each model, and the five with the lowest energy were analysed using MolProbity (Davis et al., 2007). Those with the greatest percentage of

Table 2.1 Solutions and media used in the present study

	DNA preparation
10 mg/ml Ethidium bromide (EtBr)	Dissolved in 10 mM Tris pH 8.0, and 1 mM EDTA, pH 8.0
TAE buffer	40 mM Tris-acetate, 1 mM EDTA, pH 8.0
Buffer P1 (resuspension buffer)	50 M Tris-HCl, pH 8.0, 10 mM EDTA, 100 µg/ml RNase A, stored at 4°C
Buffer P2 (lysis buffer)	200 mM NaOH, 1% sodium dodecyl sulfate (SDS)
Buffer P3 (neutralisation buffer)	3 M potassium acetate, pH 5.5
Buffer QBT (equilibration buffer)	750 mM NaCl, 50 mM 3-(N-morpholino)propanesulfonic acid (MOPS), 15% isopropanol, 0.15% triton X-100, pH 7.0
Buffer QC (wash buffer)	1 M NaCl, 50 mM MOPS, 15% isopropanol, pH 7.0
Buffer QF (elution buffer)	1.25 M NaCl, 50 mM Tris-HCl, pH 8.5, 15% isopropanol
Buffer EB	10 mM Tris-HCl, pH 8.5
Buffer N3	4.2 M HCl, 0.9 M potassium acetate, pH 4.8
Buffer PE	10 mM Tris-HCl pH 7.5, 80% ethanol
Buffer PB	5 M Gu-HCl, 30% isopropanol
Buffer QG	5.5 M guanidine thiocyanate, 20 mM Tris-HCl, pH 6.6
NEBuffer1	10 mM Bis-Tris-Propane-HCl, 10 mM $MgCl_2$, 1mM dithiothreitol (DTT), pH 7.0
NEBuffer2	50 mM NaCl, 10 mM Tris-HCl, 10 mM $MgCl_2$, 1 mM DTT, pH 7.9
NEBuffer3	100 mM NaCl, 50 mM Tris-HCl, 10 mM $MgCl_2$, 1 mM DTT, pH 7.9

NEBuffer4	50 mM potassium acetate, 20 mM Tris-acetate, 10 mM magnesium acetate, 1 mM DTT, pH 7.9
NEBuffer *EcoRI*	100 mM Tris-HCl, 50 mM NaCl, 10 mM $MgCl_2$, 0.025% Triton X-100, pH 7.5
2X Quick ligase buffer	66 mM Tris-HCl, 10 mM $MgCl_2$, 1 mM DTT, 1 mM ATP, 7.5% polyethylene glycol, pH 7.6
1% DNA agarose gel	1% agarose (w:v) dissolved in TAE buffer
6x DNA gel loading buffer	2.5% Ficoll®-400, 11 mM EDTA, 3.3 mM Tris-HCl, 0.017% SDS, 0.015% bromophenol blue, pH 8.0
	DNA gel electrophoresis
EtBr	10 mg/ml EtBr dissolved in Milli-Q H_2O
TAE buffer	40 mM Tris-acetate, 1 mM EDTA, pH 8.0
1% agarose gel	1% agarose (w/v) dissolved in TAE buffer
6 x loading buffer	0.25% bromophenol blue (w/v), 40% sucrose (w/v)
	PCR
10x PfuUltra DNA polymerase buffer	200 mM Tris-HCl, pH 8.8, 100 mM $(NH_4)_2SO_4$, 100 mM KCl, 1% Triton X-100 (v/v), 1 mg/ml BSA
10 mM dNTP mix	Diluted 100 mM stock of dATP, dCTP, dGTP and dTTP
10 x cutsmart buffer	50 mM potassium acetate, 20 mM Tris-acetate, 10 mM magnesium acetate, 100 µg/ml BSA, pH 7.9
	***E. coli* cell growth medium**
LB medium	10 g/l tryptone, 5 g/l yeast extract, 10 g/l NaCl
LB agar plate	1% (w:v) agar added to LB medium before autoclaving and supplementing with ampicillin (100 µg/ml) before setting in 100 mm dishes
	Cell growth medium

HEK293 cell culture medium	DMEM supplemented with 10% fetal bovine serum (FBS)
Dulbecco's phosphate-buffered saline (dPBS)	2.7 mM KCl, 1.5 mM KH_2PO_4, 136.9 mM NaCl, 8.9 mM Na_2HPO_4
10 x Trypsin-EDTA	5 g/l trypsin, 2 g/l EDTA●4Na, 8.5 g/l NaCl resolved in phosphate buffered saline (PBS)
	Antibiotics
Ampicillin	Ampicillin (50 mg/ml) dissolved in water and sterilised with a 0.22 µl filter
G418	G418 (20 mg/ml) dissolved in water and sterilised with a 0.22 µl filter
	Immunocytochemistry
PBS	10 mM Na_2HPO_4, 2 mM KH_2PO_4, 2.7 mM KCl and 137 mM NaCl, pH 7.4
Zamboni's fixative	15% (v/v) picric acid and 5.5% (v/v) formaldehyde in PBS
PBS-T	0.4% (v/v) Triton X-100 dissolved in PBS
Blocking solution	10% (v/v) goat serum in PBS-T
Antibody dilution buffer	Blocking solution with the indicated concentration of antibody
	Calcium imaging
Standard buffer solution (SBS)	134 mM NaCl, 5 mM KCl, 1.2 mM $MgCl_2$ and 1.5 mM $CaCl_2$, 8 mM glucose, 2.4 mM HEPES, pH 7.4
Loading buffer	SBS containing 1 µM Fura2-AM and 0.01% (v:v) pluronic acid
	YOPRO1 uptake assay

Assay buffer	147 mM NaCl, 2 mM KCl, 0.3 mM $CaCl_2$, 10 mM HEPES, 22 mM glucose, pH 7.3
YOPRO1 buffer	Assay buffer containing 1 μM YO-PRO-1 and either dimethyl sulfoxide (DMSO) or the test compound
	Patch-clamp recording
Standard extracellular solution	147 mM NaCl, 10 mM HEPES, 13 mM glucose, 2 mM KCl, 1 mM $MgCl_2$ and 2 mM $CaCl_2$, pH 7.3
Low divalent solution	147 mM NaCl, 10 mM HEPES, 23 mM glucose, 2 mM KCl and 0.3 mM $CaCl_2$, pH 7.3
Intracellular solution	145 mM NaCl, 10 mM HEPES and 10 mM EDTA, pH 7.3

Table 2.2 Conditions and buffers for digestions

Restriction enzyme	**Buffer for digestion**	**Restriction reaction (for 20 μl reaction system)**
EcoRI	NEBuffer 1	10 U enzyme
HindIII	NEBuffer 2	10 U enzyme
PmeI	NEBuffer 4	10 U enzyme

Table 2.3 Dilutions of antibodies

Primary antibody		
Antibody	**Source**	**Concentration**
Mouse anti-EE	Covance	1:1000
Secondary antibody		
Goat anti-mouse FITC	Sigma	1:2000

residues in allowed regions of the Ramachandran plot were selected for use in further investigations. The non-conserved loop region between the β2 and β3 strands was modelled *de novo* using the ModLoop server (Fiser et al., 2000).

2.2.2 Molecular docking simulations

Prior to docking studies, the structures of ligands to be docked were produced in Maestro. Energy minimisation of each ligand structure was carried out in Maestro as a pre-set function of the program. Docking studies were carried out in AutoDock version 4.2 (Morris et al., 2009). The target cavity file for each docking simulation consisted of a 50 Å sphere surrounding a central point in the extracellular domain. Affinity grid files were generated using the auxiliary program AutoGrid. The ATP molecule bound within the binding site in the crystal structure was used as the centre of these grids. One starting conformation was used of each small molecule docked, as determined by the energy minimisation in Maestro. The 'detect root' function in AutoDock was used to automatically select the central 'fixed portion' around which the small molecule was given flexibility with no constraints. 100 docking conformations were produced during each run.

2.2.3 Virtual screening of compounds

eHiTS version 12 (Zsoldos et al., 2007) software was used for virtual screening. The cavity file, in which the screening was carried out, was produced in SPROUT (Gillet et al., 1995) and consisted of a 10 Å sphere using the ATP molecule bound within the binding site as the centre of the sphere. The ZINC Omega database (Irwin et al., 2012), a free database containing ~100,000 structurally diverse compounds, was docked to the active site. 500 of the best eHiTS scoring compounds were further scored in SPROUT and assessed for suitability as potential inhibitors. PyMOL (DeLano, 2002) was used for the visual inspection of results and later graphical representations.

2.3 Molecular biology methods

2.3.1 Bacterial cell heat shock transformation

20-50 µl aliquots of competent cells (plasmid DNA amplification using α-select bronze efficiency from Bioline or XL10-Gold ultracompetent cells from Agilent, or PCR and ligation products using XL1-Blue Supercompetent cells from Agilent) were thawed on ice and 0.5-1 µl of 100 ng/µl plasmid DNA, or 2-5 µl PCR product added. Cells were incubated on ice for 30 min, then heat shocked at 42°C for 45 s and incubated on ice for 2 min. 1 ml of pre-warmed LB media was added and the mixture incubated at 37°C with shaking at 200 revolutions per minute (rpm) for 60 min. Cells were collected by brief centrifugation and the cell pellet resuspended in 100 µl LB media. The cell suspension was spread on an agar plate containing 100 µg/ml ampicillin and incubated at 37°C overnight. Plates were subsequently stored at 4°C.

2.3.2 Preparation of plasmid DNA

2.3.2.1 Small scale isolation of plasmid DNA

For small scale preparation of plasmid DNA (up to 20 µg), the QIAprep spin Miniprep kit was used (Table 2.1) following the suggested protocol as described below. LB growth media (5 ml) containing 100 µg/ml ampicillin was inoculated with a single colony of transformed *E. coli* cells and incubated overnight at 37°C with shaking (250 rpm). Cells were collected by centrifugation using a bench-top centrifuge at 13,000 rpm (~17,900 g) for 3 min at room temperature (RT) and the pellet resuspended in 250 µl of chilled buffer P1 by pipetting. Cells were lysed by addition of 250 µl of buffer P2 followed by gentle inversion of the tube. 350 µl of buffer N3 was added and the resulting cell debris cleared by centrifugation (13,000 rpm/~17,900 x g for 10 min at RT). The supernatant was applied to a QIAprep spin column by pipetting, which was centrifuged (13,000 rpm/~17,900 x g for 1 min at RT). The flow-through was discarded and the column washed by addition of 750 µl of buffer PE followed by centrifugation (13,000 rpm/~17,900

x g for 1 min at RT). The flow-through was discarded and the DNA eluted by the addition of 50 µl of buffer EB (elution buffer). The column was incubated for 1 min at RT, and then centrifuged (13,000 rpm/~17,900 x g for 1 min at RT). This final step was repeated to ensure complete elution of DNA. Plasmid DNA was stored at -20°C.

2.3.2.2 Large scale isolation of plasmid DNA

For large scale DNA preparation (up to 100 µg), the Qiagen Midiprep kit was used (Table 2.1) following the suggested protocol as described below. LB growth media (10 ml) containing 100 µg/ml ampicillin was inoculated with a single colony of transformed *E. coli* cells and incubated for 8 hours (hrs) at 37°C with shaking (250 rpm). This culture was diluted in 90 ml of LB growth media containing 100 µg/ml ampicillin and cultured overnight at 37°C with shaking (250 rpm). Cells were harvested by centrifugation (13,000 rpm/6000 x g for 15 min at 4°C). The supernatant was removed and the pellet resuspended in 4 ml of buffer P1 by pipetting, then lysed by the addition of 4 ml of buffer P2 followed by gentle inversion of the tube. This mixture was incubated at RT for 5 min. 4 ml of chilled buffer P3 was added to the tube, which was then incubated on ice for 15 min. The cell debris was cleared by two separate centrifugation steps; 30,000 rpm/≥20,000 x g (for 30 min at 4°C followed by 30,000 rpm/≥20,000 x g for 15 min at 4°C. The supernatant was removed and applied to the QIAGEN-tip 100, which had been pre-equilibrated by the addition of 4 ml buffer QBT, and allowed to enter by gravity flow. The tip was washed with 2 x 10 ml of buffer QC. The DNA was eluted with 5 ml of buffer QF and then precipitated by the addition of 3.5 ml of RT ispopropanol. The precipitated DNA was collected by centrifugation (30,000 rpm/≥20,000 x g for 30 min at 4°C) and the supernatant removed. The DNA pellet was washed with 2 ml of RT 70% ethanol, then centrifuged (20,000 rpm/≥20,000 x g for 10 min at 4°C). The supernatant was removed and the pellet air-dried for 5-10 min, then redissolved in in 500 µl EB buffer. The plasmid DNA was stored at -20°C.

2.3.3 Site-directed mutagenesis

Primers were designed to introduce point mutations into the P2X7R (Table 2.4). Primers were between 25-46 bases with 10-15 bases either side of the mutation. The PCR mix contained 1.5 µl of each primer (10 µM), 5 µl of 10x PfuUltra DNA polymerase buffer, 1 µl dNTP mix (10 mM), 1 µl of P2X7 DNA (100 ng/µl), 1 µl PfuUltra DNA polymerase, and was adjusted to a final volume of 50 µl using water. PCR was carried out in an Eppendorf thermocycler. The PCR runs consisted of the following steps; 96°C for 60 s, then 18 cycles consisting of 96°C for 50 s, 60°C for 50 s, 68°C for 14 min, a final step of 68°C for 30 min. A mixture consisting of 15 µl PCR product, 4 µl 10 x cutsmart buffer (Table 2.1), 0.5 µl DpnI digestion enzyme (10 U) (Table 2.2) with the final volume adjusted to 40 µl with water. The mixture was incubated at 37°C for 60 min. 2-5 µl of the digested PCR product was transformed into competent *E. coli* cells (section 2.3.1) and small-scale isolation of plasmid DNA performed (section 2.3.2.1). The mutation was confirmed by commercial sequencing (Beckman Coulter Genomics).

2.3.4 Generation of a C-terminal His-tagged human P2X7 receptor construct

In order to add a His-tag to hP2X7, a 100 µl PCR reaction was set up containing 10 µl of each of the hP2X7-His primers (Table 2.4) (10 µM), 10 µl of 10x PfuUltra DNA polymerase buffer, 4 µl dNTP mix (10 mM), 2 µl of human P2X7R cDNA in pcDNA3.1 (100 ng/µl), 1 µl PfuUltra DNA polymerase, and was adjusted to a final volume using water. PCR was carried out in an Eppendorf thermocycler. A program was run consisting of the following steps; 30 cycles consisting of 94°C for 40 s, 65°C for 1 min, 72°C for 1 min/0.5 kb followed by a final step at 72°C for 10 min. Phosphate groups were added at the 5' end of the DNA products to allow them to join with other DNA sequences by ligation using T4 polynucleotide kinase (PNK) (New England Biolabs). A reaction with a total volume of 20 µl was set up consisting of 0.5-1 µl of 10 U/µl T4 PNK, 2 µl of 10 x PNK

Table 2.4 Sequences of the primers used in this study

Name	5’ to 3’ sequence
A44C forward	CTTTTCCTACGTTTGCTTTTGTCTGGTGAGTGACAAGCTG
A44C reverse	CAGCTTGTCACTCACCAGACAAAAGCAAACGTAGGAAAAG
D48C forward	CTTTGCTCTGGTGAGTTGCAAGCTGTACCAGCGG
D48C reverse	CTTTGCTCTGGTGAGTTGCAAGCTGTACCAGCGG
I58C forward	CGGAAAGAGCCTGTCTGCAGTTCTGTGCACACC
I58C reverse	GGTGTGCACAGAACTGCAGACAGGCTCTTTCCG
S60C forward	GAGCCTGTCATCAGTTGTGTGCACACCAAGGTG
S60C reverse	CACCTTGGTGTGCACACAACTGATGACAGGCTC
I75C forward	CAGAGGTGAAAGAGGAGTGCGTGGAGAATGGAGTG
I75C reverse	CACTCCATTCTCCACGCACTCCTCTTTCACCTCTG
K81C forward	GATCGTGGAGAATGGAGTGTGCAAGTTGGTGCACAGTGTC
K81C reverse	GACACTGTGCACCAACTTGCACACTCCATTCTCCACGATC
I87V forward	GTTAGTACACGGCGTCTTCGACACGGCCG
I87V reverse	CGGCCGTGTCGAAGACGCCGTGTACTAAC
R125A forward	CCGAGTATCCCACCGCCAGGACGCTCTGTTC
R125A reverse	GAACAGAGCGTCCTGGCGGTGGGATACTCGG
R125Q forward	CGAGTATCCCACCCAAAGGACGCTCTGTTC
R125Q reverse	GAACAGAGCGTCCTTTGGGTGGGATACTCG
R126A forward	GAGTATCCCACCCGCGCGACGCTCTGTTCCTC
R126A reverse	GAGGAACAGAGCGTCGCGCGGGTGGGATACTC

R126N forward	GAGTATCCCACCCGCCAGACGCTCTGTTCCTC
R126N reverse	GAGGAACAGAGCGTCTGGCGGGTGGGATACTC
R126Q forward	GTATCCCACCCGCCAGACGCTCTGTTC
R126Q reverse	GAACAGAGCGTCTGGCGGGTGGGATAC
I331C forward	CGGAGGAAAATTTGACATTTGCCAGCTGGTTGTGTACATC
I331C reverse	CGGAGGAAAATTTGACATTTGCCAGCTGGTTGTGTACATC
W139S forward	GTTGTAAAAAGGGATCGATGGACCCGCAGAG
W139S reverse	CTCTGCGGGTCCATCGATCCCTTTTTACAAC
Q143H forward	GATGGATGGACCCGCATAGCAAAGGAATTCAGAC
Q143H reverse	GTCTGAATTCCTTTGCTATGCGGGTCCATCCATC
Q143R forward	GATGGATGGACCCGCGGAGCAAAGGAATTC
Q143R reverse	GAATTCCTTTGCTCCGCGGGTCCATCCATC
P177C forward	GAGGCAGTGGAAGAGGCCTGTCGGCCTGCTCTCTTGAAC
P177C reverse	GTTCAAGAGAGCAGGCCGACAGGCCTCTTCCACTGCCTC
Y288A forward	CACCAACGTGTCCTTGGCCCCTGGCTACAACTTC
Y288A reverse	GAAGTTGTAGCCAGGGGCCAAGGACACGTTGGTG
Y288E forward	CCACCAACGTGTCCTTGGAGCCTGGCTACAACTTCAG
Y288E reverse	CTGAAGTTGTAGCCAGGCTCCAAGGACACGTTGGTGG
Y288F forward	CCACCAACGTGTCCTTGTTCCCTGGCTACAAC
Y288F reverse	GTTGTAGCCAGGGAACAAGGACACGTTGGTGG
Y288S forward	CACCAACGTGTCCTTGAGCCCTGGCTACAACTTC
Y288S reverse	GAAGTTGTAGCCAGGGCTCAAGGACACGTTGGTG

Y288V forward	CACCAACGTGTCCTTGGTCCCTGGCTACAACTTC
Y288V reverse	GAAGTTGTAGCCAGGGACCAAGGACACGTTGGTG
V304C forward	CAGATACGCCAAGTACTACAAGGAAAACAATTGTGAGAAACG GAC
V304C reverse	GTCCGTTTCTCACAATTGTTTTCCTTGTAGTACTTGGCGTATC TG
F313C forward	CGTTTTGACATCCTGGTTTGTGGCACCGGAGGAAAATTTG
F313C reverse	CAAATTTTCCTCCGGTGCCACAAACCAGGATGTCAAAACG
L320C forward	GGGATCCGTTTTGACATCTGCGTTTTTGGCACCGGAGG
L320C reverse	CCTCCGGTGCCAAAAACGCAGATGTCAAAACGGATCCC
hP2X7-His1	GCTAGCCGCTGTGTTCATCG
hP2X7-His2	CAACCAGAGGAGATACAGC
hP2X7-His3	GGAAAATTTGACATTATCCAGC

buffer, 2.5 mM ATP (final concentration), 1-2 µg of DNA and water to adjust the final volume. The reaction was incubated at 37°C for 1 hr and the DNA subsequently cleaned using a QIAquick PCR purification kit.

DNA was then digested with HindIII (Table 2.2) to produce sticky ends to ensure insertion of the P2X7 cDNA/PCR product in the correct orientation. DNA was digested in a 10-100 µl volume containing DNA, 10 x restriction buffer, 1 µl HindIII (10 U), and water to adjust the final volume. Digestion was carried out at 37°C for 1 hr. After agarose gel electrophoresis (as described below), DNA was extracted using the QIAquick gel extraction kit according to the suggested protocol. T4 DNA ligase (New England Biolabs) was used to carry out ligation of hP2X7-His cDNA and the pcDNA3.1 vector, which was also digested with HindIII as described above, in order to produce the hP2X7-His plasmid. A reaction with total volume 20 µl was set up with 2 µl DNA ligase (10 U), 2 µl 10 x T4 DNA ligase buffer and 1-2 µg of DNA product in a molar ratio of 1:3. The reaction was incubated at 16°C overnight, and 5 µl of ligation product was used for transformation as described above (section 2.3.1).

2.3.5 Gel electrophoresis

DNA samples were analysed using agarose gel electrophoresis. A 1% agarose gel solution (Table 2.1) was produced by heating in a microwave. When the gel had cooled to approximately 60°C, EtBr was added to a final concentration of 0.5 µg/ml. The solution was poured into gel cast with a comb inserted and left to cool. A 6 µl DNA sample was prepared (1 µl of plasmid, 1 µl 6 x DNA loading buffer and 4 µl water). Samples were loaded into wells alongside a well containing either a 1 kb or 100 bp DNA ladder depending on the sample. Gel electrophoresis was carried out at 70 V for 90 min and visualised by fluorescence under UV light in a gel doc XR quantity system (Biorad, UK). To quantify the DNA yield, a 2 µl sample of plasmid DNA was measured using the Nanodrop 2000 (ThermoFisher Scientific).

2.3.6 Mammalian HEK293 cell culture and transfection

2.3.6.1 Preparation of frozen cell stocks

Frozen cells were kept in liquid nitrogen and, when required, upon thawing quickly at 37°C, added to a T25 culture flask containing 5 ml of culture medium. The cells were incubated overnight, the DMSO-containing media replaced and the cells grown to confluency and maintained as described below. In order to replace used cell stocks, cells with a low passage number were frozen in liquid nitrogen. Cells were grown in a T75 flask and grown to confluence then collected by trypsinisation as described below. The cell media was removed and the cell pellet resuspended in 1 ml FBS containing 10% DMSO (v/v) and pipetted into a vial. The vial was placed into a box containing isopropanol, and frozen at -80°C overnight before being transferred into liquid nitrogen.

2.3.6.2 Maintenance of HEK293 cells

Native HEK293 cells and HEK293 cells stably expressing the hP2X7R or rP2X7R, rP2X3R or hP2X4R were cultured in DMEM supplemented with 10% FBS at 37°C and 5% CO_2, under humidified conditions. Cells were cultured in T25 flasks and passaged once confluent. To passage cells, media was removed and the cells washed with 3 ml PBS. The PBS was removed and 1 ml of trypsin added and the cells incubated at 37°C for 2 min. 2 ml of culture media was added and the cells collected by centrifugation at 1000 rpm for 5 min. 10-20% of cells were added to a new T25 flask depending on the frequency of use.

2.3.6.3 Transient transfection of HEK293 cells

WT and mutant P2X7Rs were heterologously expressed in HEK293 cells by transient transfection with Lipofectamine™ 2000. Cells were transfected in 6-well plates at 70-80% confluency (~10^6 cells). For each transfection, 0.1 µg of GFP plasmid and 1 µg of plasmid for P2X7 were diluted in 100 µl of transfection medium in one 1.5 ml eppendorf and 3 µl of Lipofectamine-2000 into 100 µl of transfection medium in a second eppendorf. These tubes were incubated for 5 min at room temperature. The contents of the two

tubes were combined and incubated at room temperature for 20 minutes. 800 µl of culture medium was added and the entire mixture transferred to the cells.

2.3.6.4 Generation of a hP2X7-His stable cell line

HEK293 cells were transiently transfected with the hP2X7-His plasmid (generation described in section 2.3.4) in 6-well plates as described above in DMEM supplemented with 10% FBS. The transfected cells were cultured for two days and the media was changed to DMEM supplemented with 10% FBS and 400 µg/ml G418. Cells were cultured in the presence of G418 for 1-2 weeks, with G418 being replaced every 2-3 days, following which cells were trypsinised and individual islands of cells plated in 96-well plates and grown until confluent. Cells were trypsinised and plated in a T25 flask and grown until confluent.

2.3.7 Calcium imaging

Compounds identified by virtual screening were tested for activity at P2XRs using a FlexStation II (Marshall et al., 2005). Human or rat P2X3R, P2X4R or P2X7R stably expressing HEK293 cells were prepared in a poly-D-lysine-coated 96-well plate, with 50,000 cells per well, 24 hrs prior to use. The cell plate was prepared for use in the FlexStation by removing the media and rinsing the cells once with SBS (Table 2.1). 100 µl of loading buffer made of SBS containing 1 µM Fura2-AM and 0.01% (v:v) pluronic acid was added to each well. The plate was incubated at 37°C for 45 min, rinsed once with SBS, after which 160 µl of SBS containing either control DMSO or a compound were added to each well. The plate was incubated at 37°C for a further 30 min. Cells were excited at 340 nm and 380 nm alternatively and the emission at 510 nm recorded using the FlexStation. The ratio of fluorescence intensity (F_{340}/F_{380}) was used to indicate the intracellular Ca^{2+} concentration. Basal Ca^{2+} level was recorded for 60 seconds prior to exposure of cells to 100 or 300 µM BzATP or 100 mM ATP as specified and recording was continued for a further 120 seconds.

2.3.8 YOPRO1 uptake

YO-PRO-1 uptake was mainly recorded using the FlexStation as described in a previous study (Cankurtaran-Sayar et al., 2009). HEK293 cells expressing the hP2X7R were plated in poly-D-lysine coated 96-well plates, with 50,000 cells per well 24 hrs prior to use. Cells were rinsed with assay buffer (Table 2.1). 80 µl of assay buffer containing 1 µM YO-PRO-1 and either DMSO or the test compound was added to each well and the plate was incubated at 37°C for 20 min. Cells were excited at 485 nm and the emission at 530 nm recorded using the FlexStation. Recordings lasted 120 s and BzATP was added at 20 s to a final concentration of 300 µM. The maximal changes in F530 were used for quantitative analysis.

YO-PRO uptake was also examined using single cell imaging. Cells were plated in 24-well plates, with 20,000 cells per well 24 hrs prior to use. 1 mM ATP alone or with the indicated antagonists in addition to YOPRO1 at a final concentration of 1 µM and DAPI to 1 µg/ml were added into the cell culture media. The plate was incubated at 37°C for 30 min. Cells were imaged using an EVOS FL cell imaging system (Life Technologies). Cells stained with YOPRO1 were counted in one randomly selected field for each well, and this value was presented as the percentage of the total number of cells as identified by DAPI staining in the same field. ImageJ was used for cell counting.

2.3.9 PI cell death assay

Cells were plated in six well-plates, with 40,000 cells per well 24 hrs prior to use. ATP at a final concentration of 3 mM, by itself or with the test compounds indicated at the concentrations shown, were added to the culture media in each well. The plate was incubated at 37°C and 5% CO_2 for 6 hrs. PI was added to a final concentration of 5 µg/ml in addition to 1 µg/ml DAPI 30 min prior to imaging and the plate was incubated for a further 30 min. Cells were imaged using an EVOS FL cell imaging system (Life Technologies). For each well, PI-stained cells were counted in one randomly selected

field and presented as the percentage of the total number of cells identified by DAPI staining in the same field. Cell counting was carried out using ImageJ.

2.3.10 Immunostaining

HEK293 cells transfected in 35 mm dishes as described above were seeded onto 13 mm cover slips with 20,000 cells per slip and incubated overnight. Cells were gently rinsed with 500 µl PBS, left for 5 min before being briefly incubated with a mixture of 500 µl PBS and 500 µl Zamboni's fixative solution (15% (v/v) picric acid and 5.5% (v/v) formaldehyde in PBS). This mixture was immediately removed before cells were fixed with 500 µl Zamboni's fixative solution alone at RT for 1 hr. Cells were washed 3 times with 500 µl PBS which was added, left for 5 min, removed and the subsequent wash added immediately. Following this cells were incubated with blocking solution (10% (v/v) goat serum in PBST (0.4% (v/v) Triton X-100 dissolved in PBS)) for 1 hr at RT. Mouse anti-EE primary antibody was added into the blocking solution at a dilution of 1:1000 and cells were incubated at 4°C overnight. Cells were washed in PBS 3 times as described above, then incubated in blocking solution containing goat anti-mouse fluorescein isothiocyanate (FITC) IgG secondary antibody at 1:5000 for 1 hr at RT. The cells were washed once in PBS and twice in water, then cover slips were mounted onto microscope slides with SlowFadeGold Antifade mountant with DAPI (Invitrogen) and stored at 4°C. Images were captured using a Zeiss LSM 880 upright microscope ZEN imaging software.

2.4 Electrophysiology

2.4.1 Solutions used for agonist-induced current recordings

Standard extracellular solution was used during recordings (Table 2.1). P2X7Rs are strongly inhibited by divalent cations (Surprenant et al., 1996; Virginio et al., 1997). This, in addition to their low sensitivity to ATP, means that it is often necessary to make electrophysiological recordings in extracellular solutions containing low concentrations

of divalent cations in order to elicit a greater current response. Therefore, unless otherwise stated, electrophysiological recordings were carried out in low divalent extracellular solution (Table 2.1). Intracellular solution was included in the pipette (Table 2.1). ATP stock solution (100 mM) was prepared in extracellular solution and adjusted to pH 7.3 with 4 M NaOH, and BzATP stock solution (100 mM) was prepared in water. Stock solutions of antagonists (AZ11645373 to 10 mM and all custom compounds to 100 mM) were prepared in DMSO.

2.4.2 Preparation of cells for patch-clamp recording

HEK293 cells prepared in 35 mm petri dishes were co-transfected with both the plasmid containing the P2X7R and eGFP as described in section 2.3.6, or HEK293 cells stably expressing EE- or His-tagged P2X7Rs were used. Cells were plated onto glass coverslips 24 hrs following transfection, and used 12-24 hrs later.

2.4.3 Preparation of recording and reference electrodes

Pipettes used for recording were made from borosilicate glass capillaries with an outer diameter of 1.5 mm and an inner diameter of 1.12 mm (World Precision Instruments). Pipettes were pulled in two stages by a vertical puller (PP-830, Narishige Scientific Instruments) to produce a tip of approximately 1 µm, which had a resistance of 3-5 MΩ when placed in recording solutions. When used for recordings, pipettes were filled with intracellular solution (Table 2.1) and mounted onto a headstage (CV203BU, Axon instruments) via an AgCl coated Ag wire, which was in turn connected to a Axopatch 200B amplifier (Molecular Devices). The reference electrode was an AgCl pellet, which was immersed in the extracellular solution and connected to the ground via the headstage.

2.4.4 Patch-clamp recording

For transiently transfected HEK293 cells, single cells identified under UV light to be eGFP positive were used. The micropipette was lowered into the bath solution and manoeuvred using the head stage until it was seen through the microscope to have come into contact with the surface of the cell. Suction was applied to the cell membrane through a syringe connected via a tube to the pipette until a seal was formed, and additional suction applied until the membrane was broken and the whole-cell configuration was achieved. Cells were kept at a holding potential of -80 mV. During recordings a rapid solution changer (RSC-160, Biologic Sciences Instruments) was used in order to apply the agonists or antagonists indicated during recordings for the time shown in individual experiments. The recording chamber was connected to a solution drain driven by a gravity feed at a rate of 5 ml min^{-1}.

Prior to carrying out experiments, it was necessary to ensure that current facilitation as seen in the P2X7R did not affect the results obtained through patch-clamp recording. In order to avoid this, a low concentration of agonist was applied for 4 s at 2 min intervals until the current amplitude remained consistent. Following this, dose-response (DR) curves of agonists were obtained by applying increasing concentrations of the agonist for 4 s at a time with 2 min intervals in between. When constructing dose-inhibition curves of antagonists, the same protocol was used with the exception that during the 2 min interval the cell was bathed in extracellular solution containing the antagonist. For the novel antagonists in this study, the antagonist was also included in the agonist-containing solution applied for 4 s due to their fast washout. When producing DR curves, membrane currents were analysed with pClamp 10.3 software (Axon instruments) and the peak current subsequently used to produce DR curves.

The agonist concentrations evoking half activation (EC_{50}) were derived by using Origin to fit the data from each independent experiment to the Hill equation:

$$R = R_{max}/[1 + (EC_{50}/[A])^{n}]$$

where R_{max} is the maximal response (ionic currents or dye uptake) for each case, *R* is the response induced by given agonist concentrations ([A]) and *n* is the Hill coefficient. The antagonist concentrations evoking half inhibition (IC_{50}) were derived by using Origin to fit the data from each independent experiment (Ca^{2+} response and YOPRO1 uptake) or cells (current) to the Hill equation:

$$I = 100/(1+([B]/IC_{50})^{n})$$

where *I* is the agonist-induced current following exposure to identified concentrations of antagonist ([B]) and expressed as the percentage of the control responses and *n* is the Hill coefficient. The solid line shown in the figures represent the fitting of mean data.

2.4.5 Statistical analysis

All data are presented as mean ± standard error of the mean (SEM). The number of independent experiments is indicated by 'n'. Student's t-test was used for two groups and one-way analysis of variance test and Tukey's *post hoc* test for more than two groups, and a probability (p) value of <0.05 was considered significant. Data was analysed and figures were prepared in Origin (version 9.1).

Chapter 3

Homology Modelling of the Human P2X7 Receptor

3.1 Introduction

Understanding the structure of proteins is often a vital step in underpinning structure-function relationships. Initially, understanding of the P2XR family structure was gained by computer analysis of their primary sequences which predicted the largely extracellular nature of the protein, in addition to the TM domains and intracellular N- and C- termini (Valera et al., 1994; Brake et al., 1994). This, as well as later studies which utilised experimental methods to investigate the accuracy of these conclusions (Torres et al., 1998a; Newbolt et al., 1998; Jiang et al., 2000b) clarified the distinctive structure of the P2XRs which was unlike any other ligand-gated ion channel studied at the time. A significant shift in the field of P2XR structure followed the publication of the zfP2X4R crystal structure to 3.1 Å, showing that these receptors were trimeric with subunits resembling the shape of a dolphin (Figure 1.4) (Kawate et al., 2009). A second publication by the same group in 2012 detailed the structure of the ATP-bound open state at 2.8 Å, as well as a higher resolution structure in the closed state at 2.9 Å (Hattori and Gouaux, 2012).

There is a considerable degree of sequence identity between the zfP2X4R and the mammalian P2X7Rs, therefore the former could be used to produce P2X7R homology models (the hP2X3R structure was published after the completion of this study and therefore was not used in homology modelling). Indeed, there are numerous examples of this structure guiding in-depth structure-based studies of P2XRs based on homology models which have been used to shed light on previous experimental evidence (Browne et al., 2010), form the basis of disulfide locking experiments to probe the movements of these proteins (Jiang et al., 2003; Marquez-Klaka et al., 2009; Stelmashenko et al., 2014) and aid the engineering of light-activated P2X2Rs (Browne et al., 2014). However, before designing further experiments using these models it is vital to ensure that they are representative of the protein in its native state. This chapter details the production of P2X7R models based on the zfP2X4R structures and the tests carried out to validate these models. A combination of *in silico* and *in vitro* experiments is described.

3.2 Results

3.2.1 Production of homology models based on the crystal structure

In order to provide a structural basis for designing further experiments to better understand ligand-receptor interactions and receptor activation at the P2X7R, the first step was to construct P2X7R homology models. Fortunately, the closed and ATP-bound open state zfP2X4R structures published in the last decade (Kawate et al., 2009; Hattori and Gouaux, 2012) mean it is possible to produce P2X7R models using the zfP2X4R sequence as the basis. The human and rat isoforms of the P2X7R have 80% sequence identity with each other and 50-56% sequence identity with the zfP2X4R (Bradley et al., 2011b). The sequence alignment used to produce the P2X7R models in this study is shown in Figure 3.1A. Models in the closed and open states (Protein Data Bank codes 4DW0 and 4DW1, respectively) were made using Modeller version 9.12 (Figure 3.1B and C). One hundred models were generated for each state and those with the greatest percentage of residues in allowed regions of the Ramachandran plot selected from the five with the lowest energy. Analysis with MolProbity showed these models to have 98.8-99.6% of residues in allowed regions.

These homology models show distinct differences between the closed and open states (Figures 3.1B and C, 3.2). The upper body domain (Figure 1.4) remains relatively rigid between the closed and open states (Figure 3.2A). In contrast, there is considerable conformational change in the lower body domain of the receptor. When this receptor is activated, the rotation of the lower body domain leads to a considerable movement of the TM domains and the subsequent dilation of the central ion-permeating pathway (Figure 3.2B). In addition to this central pore, the lateral fenestrations through which ions have been predicted to move through the receptor (Samways et al., 2011; Kawate et al., 2011; Hattori and Gouaux, 2012; Mansoor et al., 2016) widen markedly (Figure 3.2C).

Further to these obvious larger movements, the models illustrated some of the more subtle rearrangements of the subunits, assuming the P2X7R has the same approximate

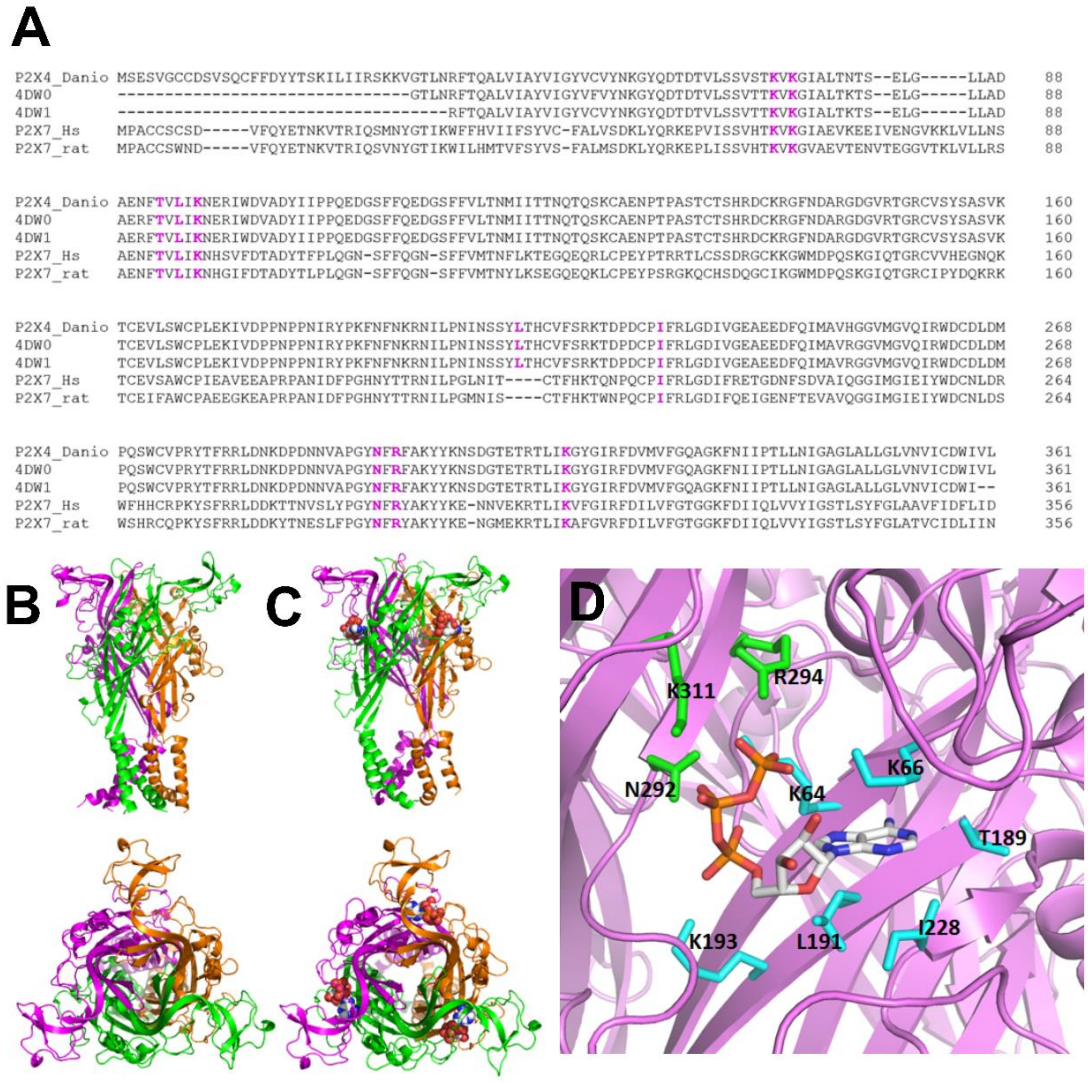

Figure 3.1 Homology models of the hP2X7 receptor and ATP binding

(A) Sequence alignment of the zfP2X4 sequence (P2X4_Danio), the sequence of the zfP2X4R protein used to determine the closed (4DW0) and open (4DW1) state structures and the human (P2X7_Hs) and rat (P2X7_rat) P2X7R. Residues involved in ATP binding are shown in magenta. (B) The trimeric hP2X7R structure with the receptor shown in the closed state, showing the whole receptor (top) and the extracellular view (bottom). (C) As in (*B*) for the ATP-bound hP2X7R. Bound ATP molecules are depicted as spheres. (D) Zoomed in view of the ATP binding site in the hP2X7R with ATP bound, showing the interactions of ATP with the nine vital amino acids highlighted in magenta in (A), three of which are from one subunit (in green) and six from the adjacent subunit (cyan).

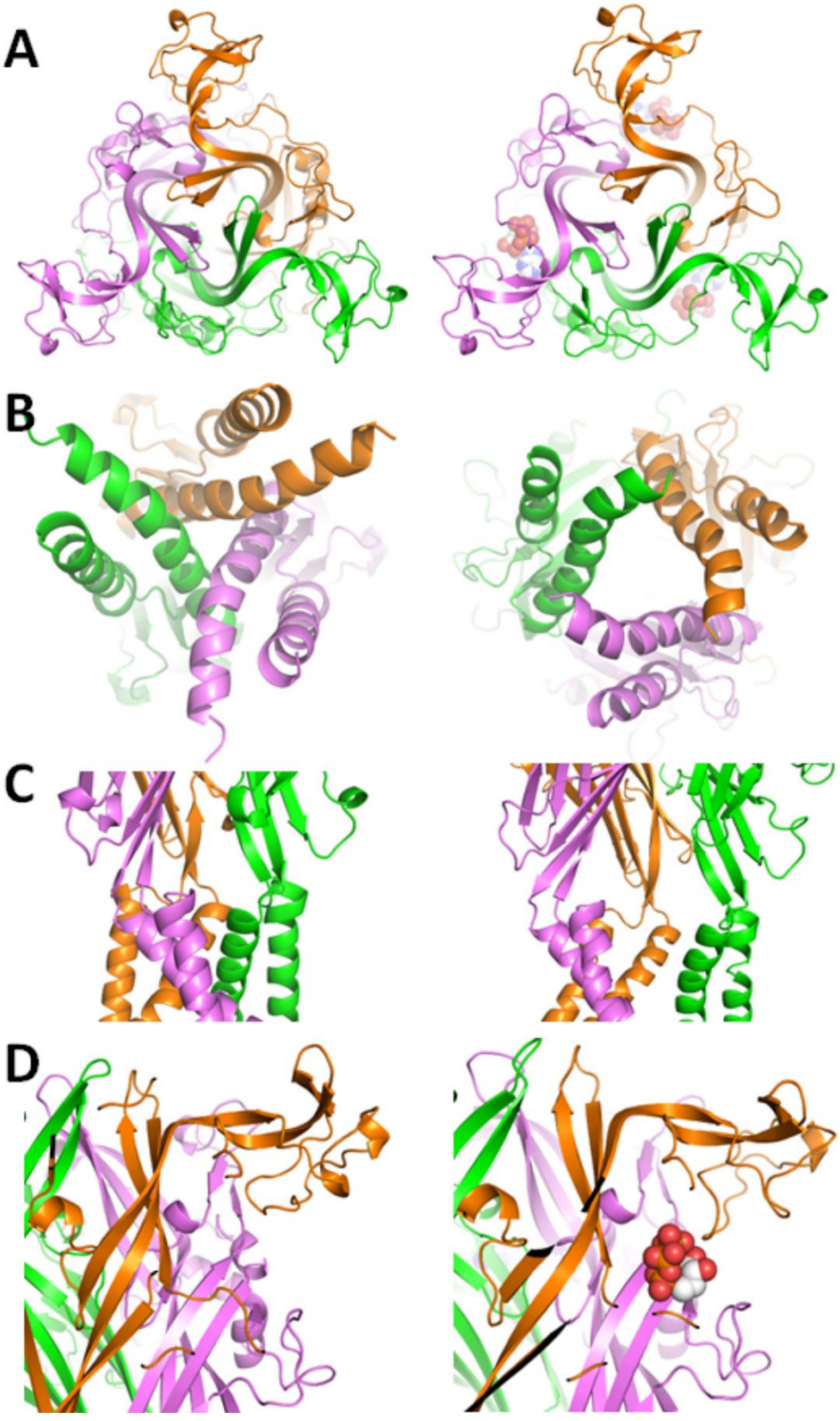

Figure 3.2 Differences between closed and open models of the hP2X7R

The hP2X7R in the closed state is shown on the left and in the open state on the right. (A) Extracellular view of the hP2X7R. (B) Intracellular view of the hP2X7R. (C) Side view of the lower body β-sheet and TM domains. (D) Side view of the head domain.

conformational shifts as the P2X4R. For example, the slight ‘jaw tightening’ in the head domain is important in receptor activation (Jiang et al., 2012) and the end states of this movement can be discerned in the P2X7R homology models (Figure 3.2D). These distinct differences between the closed and ATP-bound P2X7R models reflect the large number of conformational changes in the receptor accompanying its activation.

3.2.2 Model validation by ATP docking

One method of determining the accuracy of homology models was to evaluate them with respect to existing experimental evidence. The ATP binding site of the P2XR family was previously unknown, even after receptors were sequenced, due to the lack of a conventional ATP binding sequence such as the Walker motif. The zfP2X4R structure solved in the open, ATP-bound state definitively revealed the ATP binding site (Hattori and Gouaux, 2012). Consequently, comparing the results from molecular docking of ATP to the homology model with the known mechanism of ATP binding in the crystal structure can be used to test the validity of docking experiments in the P2XR.

This was firstly used to investigate the accuracy of the molecular docking approach in the zfP2X4R. ATP was docked to the extracellular region of the open state zfP2X4R model using AutoDock, a widely used and highly refined commercial software package (Morris et al., 2009). When docking experiments are carried out, the results are often analysed by considering both the docking conformation which has the lowest predicted binding energy and the one with the highest number of molecules in a very similar conformation (the highest populated). Each of these populations was identified from the output histogram from AutoDock (Figure 3.3A). In the case of ATP docking these were two separate populations. Despite the size of the protein, molecular docking accurately identified the ATP binding site as being within the binding pocket as shown in the crystal structure for both the lowest energy and highest populated conformations (Figure 3.3B and C). Moreover, the conformation of the ATP molecule predicted by these experiments

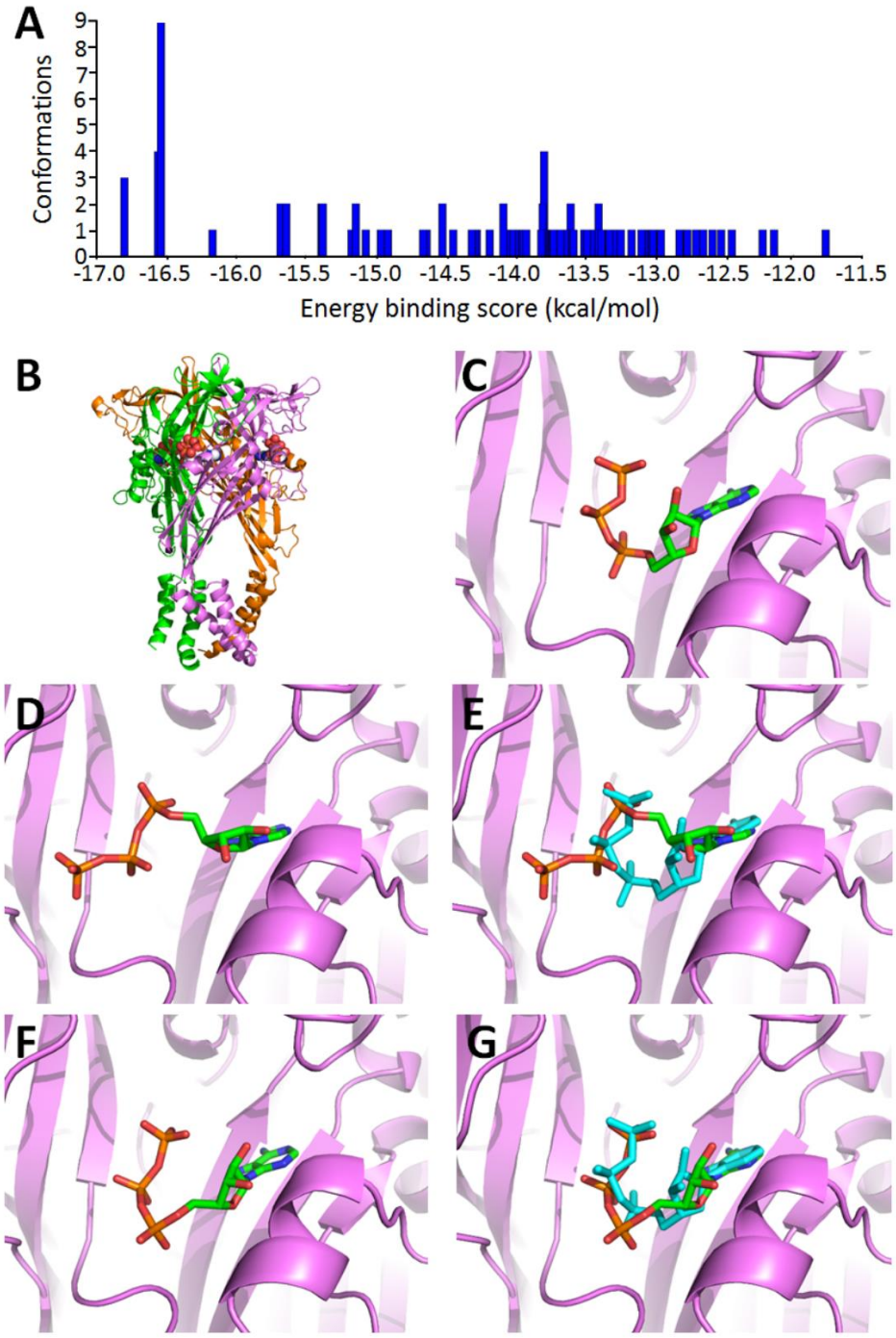

Figure 3.3 Predicted ATP binding in the open state zfP2X4R model

(A) Molecular docking output histogram showing the predicted energy binding scores of each docking conformation. (B) The trimeric zfP2X4R structure in the open state with ATP molecules shown as spheres. (C) Binding conformation of ATP in the zfP2X4R as determined by crystallography. (D and E) The ATP binding conformation with the lowest predicted binding energy expected in the open state zfP2X4R model (D) and the overlay with the zfP2X4R crystal structure ATP (cyan) (E). (F and G) The ATP binding conformation from the highest populated result expected in the open state zfP2X4R model (F) and the overlay with the zfP2X4R crystal structure ATP (cyan) (G).

showed remarkable similarity. The ATP docking predicted to have the lowest binding energy was in a similar conformation to that seen in the crystal structure (Figure 3.3D and E). Whilst the lowest binding energy ATP pose was bent in the opposite direction as in the zfP2X4R structure, the overall orientation of the ATP was essentially the same. The triphosphate chain protruded further into the binding pocket than in the crystal structure but two of the three phosphate groups aligned in the same region, and the ribose and adenine groups matched closely (Figure 3.3E). The ATP pose from the highest populated group showed greater similarities to the ATP as determined in the zfP2X4R crystal structure compared to the lowest energy conformation (Figure 3.3F and G). The adenine and ribose groups aligned almost exactly, as did two of the three phosphate groups. Overall the form of the ATP was very similar, bent in a very distinctive 'U' shape (Figure 3.3F), which due to the constraints of this unnatural position seems to be an unlikely prediction to make were it not in the context of this binding site. Taken as a whole, these predictions provide compelling evidence for the effectiveness of the molecular docking approach when used in P2XR models. This was a good indication that experiments carried out in AutoDock would be potentially useful in further tests involving hP2X7R homology models.

Further evidence for the usefulness of the molecular docking method, as well as the first indication for the validity of the homology model, was provided by ATP docking to the hP2X7R model. The ATP binding site in the hP2X7R model was accurately determined by molecular docking (Figure 3.4). As with the docking in the zfP2X4R model, the binding poses predicted to have the lowest binding energy (-14.6 kcal/mol) and the highest populated (-13.4 kcal/mol) were two distinct populations. Each shared characteristics with the ATP binding position as determined by the zfP2X4R crystal structure. The pose with the lowest predicted binding energy (Figure 3.4A) had an orientation slightly different to that of the crystal structure with the ATP molecule bent in a less constrained 'U' shape and the ribose and adenine groups protruded in a different direction. However, there was considerable overlap between the triphosphate chains (Figure 3.4B). Similarly, the ATP

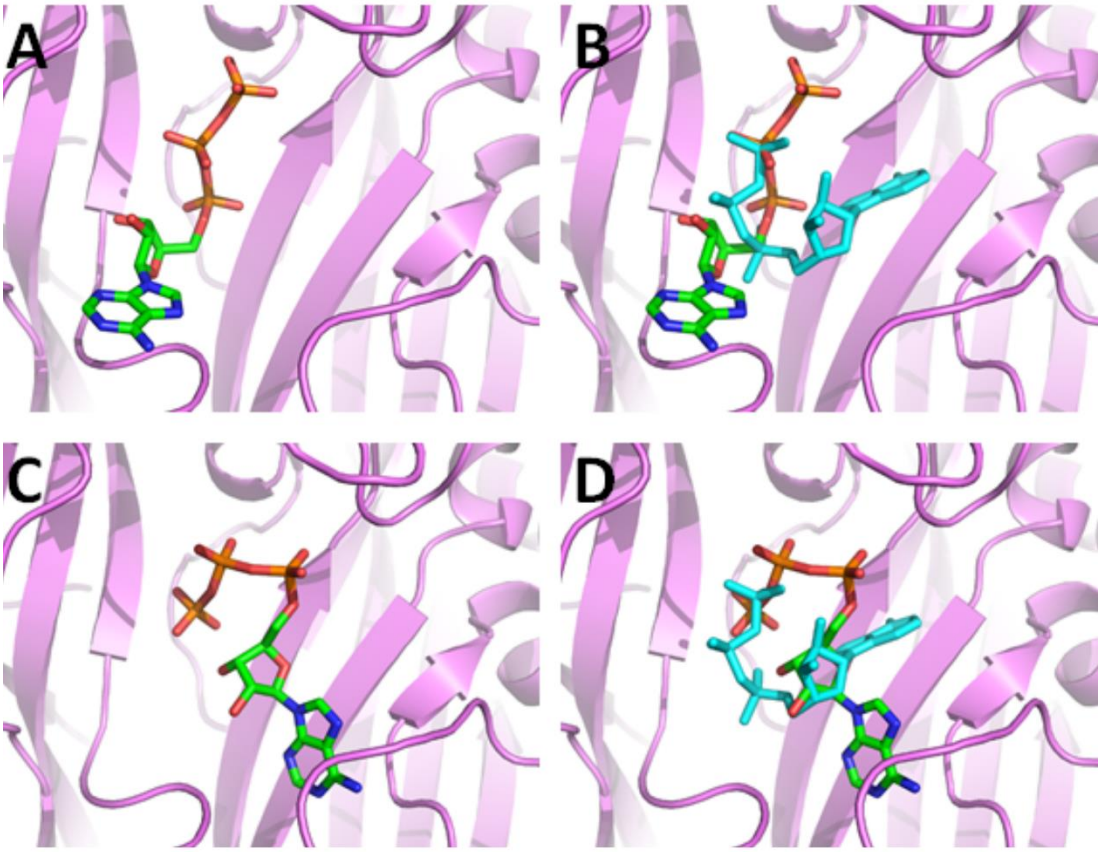

Figure 3.4 Predicted ATP binding in the open state human P2X7R model

(A and B) The ATP binding conformation with the lowest predicted binding energy expected in the open state hP2X7R model (B) and the overlay with the zfP2X4R crystal structure ATP (cyan). (C and D) The ATP binding conformation from the highest populated result expected in the open state hP2X7R model (C) and the overlay with the zfP2X4R crystal structure ATP (cyan) (D).

pose from the highest populated group (Figure 3.4C) had a third phosphate which overlapped with its counterpart in the crystal structure. The ribose group also displayed similarity to the crystal structure, although the adenine was oriented in the opposite direction (Figure 3.4D). Whilst there were numerous differences between the binding poses of the docked ATP in the hP2X7R and the ATP seen in the zfP2X4R crystal structure, there were also similarities. This, along with AutoDock's ability to identify the ATP binding site within the large extracellular domain, provides a level of validation for both the docking approach and the hP2X7R model.

3.2.3 Model validation by antagonist docking

As further validation of the homology models, three P2X7-specific antagonists were docked to the P2X7R models. These were AZ11645373, KN62 and SB203580, which all display species specificity by acting as strong hP2X7R inhibitors but lacking activity at the rP2X7R (Michel et al., 2006; Humphreys et al., 1998; Stokes et al., 2006). Previous studies have shown that this species specificity is largely due to the Phe residue at position 95 (Phe95) in the hP2X7R. This residue is a leucine in the rP2X7R and affects the efficacy of all three of these antagonists at the hP2X7R. This has been shown experimentally; mutating Phe95 in the hP2X7R to Leu greatly reduces their inhibitory activity, and introducing the reciprocal mutation into the rP2X7R variably affects their inhibition but generally improves the ability of these compounds to block rP2X7R function (Michel et al., 2008; Michel et al., 2009).

SB203580, AZ11645373 and KN62 were docked to homology models of the human and rat P2X7Rs using a sphere centred on the ATP binding site containing all the residues within 30 Å of ATP. Docking to the hP2X7R revealed a common binding region for the antagonists proximal to the ATP binding site (Figure 3.5A). Residues in this region which come into immediate contact with the docked inhibitors include the hydrophobic Phe95, Tyr295, Tyr299 and Tyr300 as well as the positively charged Lys297, which likely play a

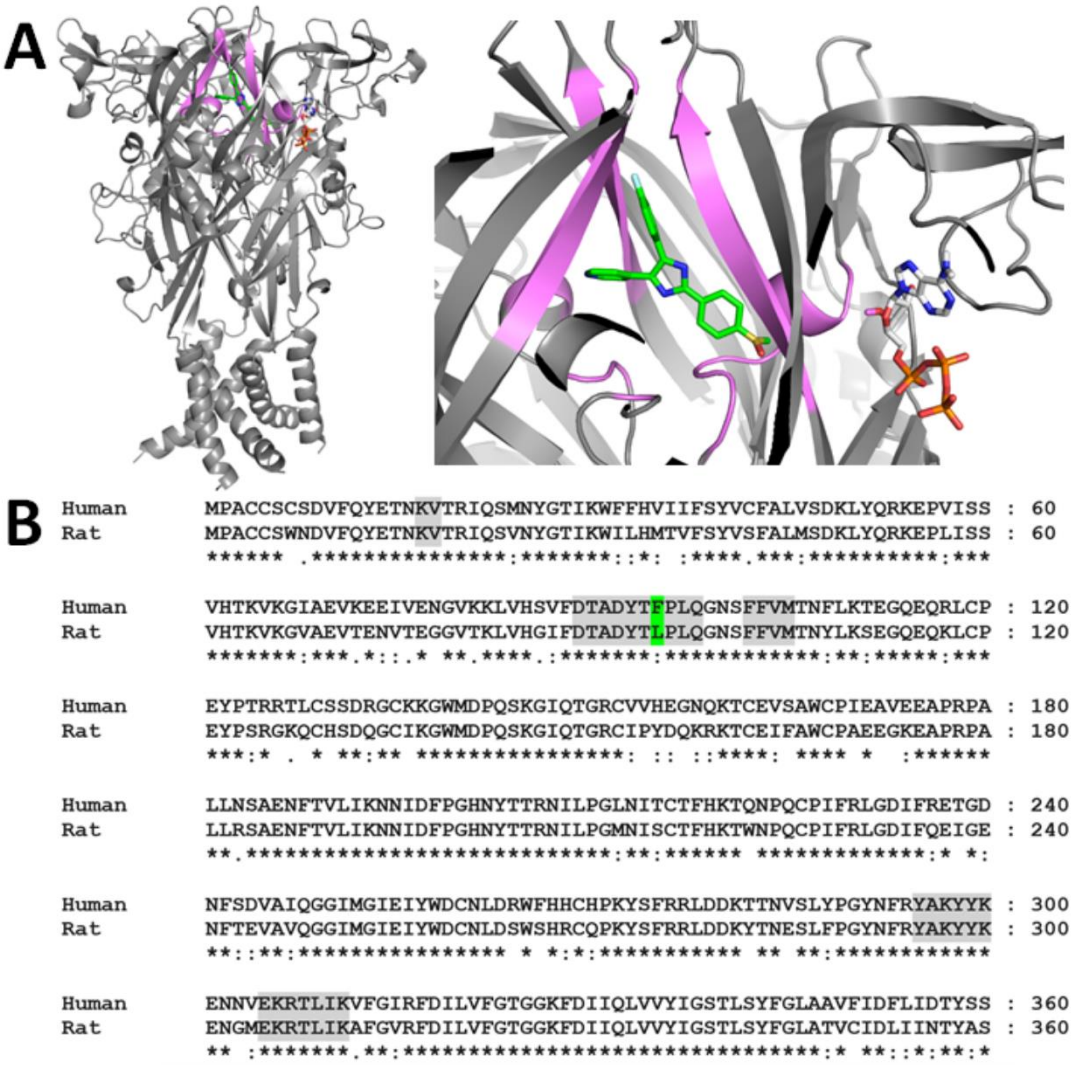

Figure 3.5 Predicted antagonist binding in human and rat P2X7Rs

(A) Predicted SB203580 binding site in relation to the known ATP binding site shown in the whole hP2X7R receptor (left) and in the ATP binding pocket (right). Residues proximal to the antagonist binding site are shown in purple. (B) Sequence alignment of the first 360 amino acids of the rat and human P2X7Rs. Residues within 8 Å of the ligand binding site are highlighted in grey and non-conserved residues in green.

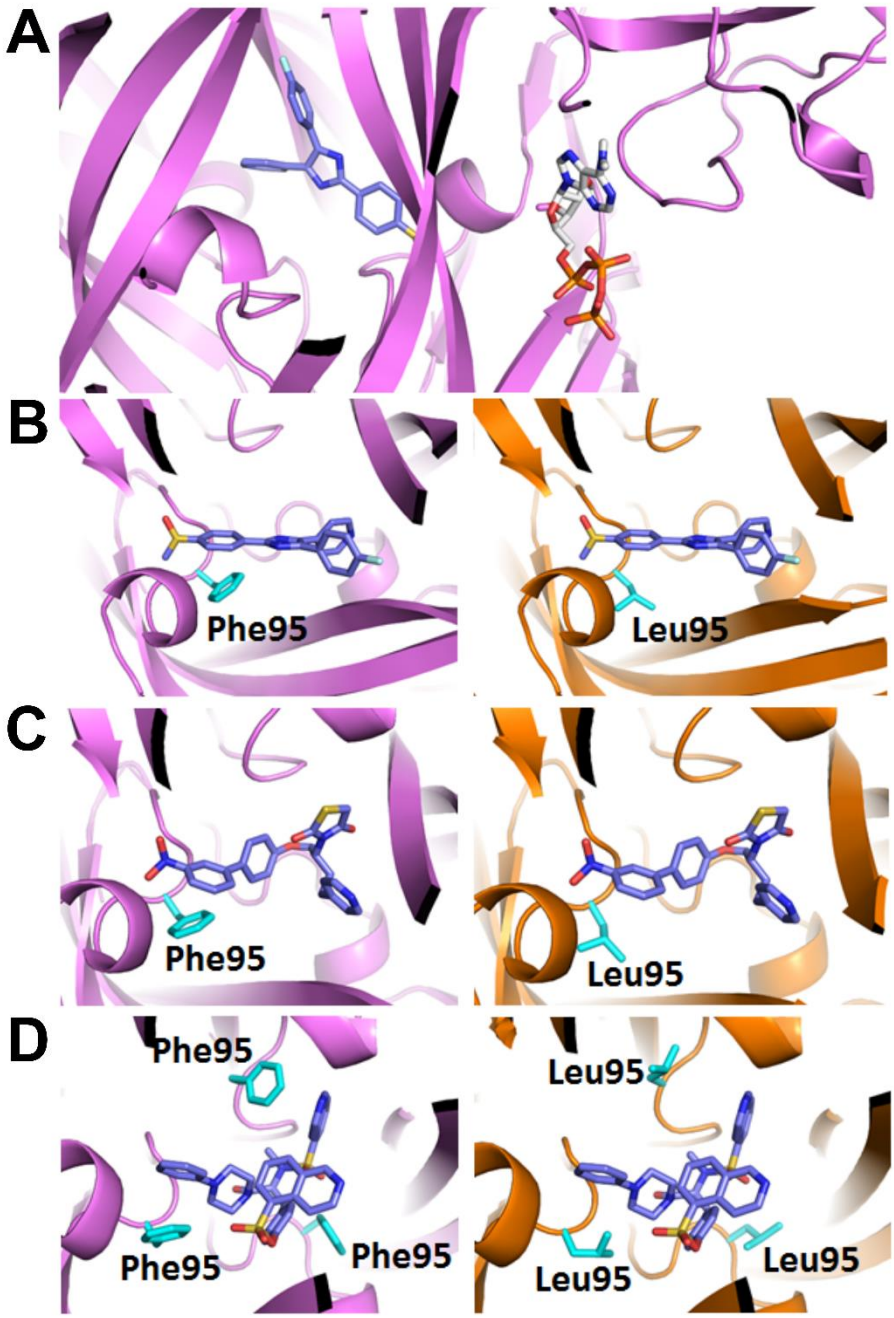

Figure 3.6 Residues predicted to contribute to antagonist species specificity

(A) Predicted binding site of SB203580 in relation to the known ATP binding site shown in the ATP binding pocket. (B-D) Docking of SB203580 (B), AZ11645373 (C) and KN62 (D) in the human (purple) and rat (orange) P2X7 receptors, respectively. Residues Phe95 and Leu95 as well as docked inhibitors are depicted in stick format. Each Phe95 or Leu95 residue shown is contributed by a separate P2X7R monomer.

role in determining the orientation of bound antagonists such as those docked in this study. However, sequence alignment of the residues within 8 Å of the predicted binding site demonstrates that Phe95 is the only non-conserved residue between the human and rat isoforms which could interact with the antagonists (Figure 3.5B). As such, Phe95 appears of the most interest with respect to the species-specific activity of these antagonists. In the human isoform, Phe95 is predicted to form pi-stacking interactions with the aromatic rings in the compounds (Figure 3.6). However, the rat isoform of the receptor has Leu95 which lacks an aromatic side chain and is therefore unable to form this stacking interaction with the compounds. As a result, docking of these molecules onto the rP2X7R model displays lower binding affinities as well as notably different binding poses within this site, suggesting that the change from Phe95 to Leu95 lowers the affinity of these antagonists for the rP2X7R due to the lack of stacking interactions rather than affecting binding.

In addition to carrying out molecular docking with non-competitive antagonists, further evidence for the accuracy of the P2X7R homology models was provided via the docking of the competitive antagonist A740003 which acts at the ATP binding site (Honore et al., 2006). Docking this compound to the hP2X7R homology model predicted its binding site to overlap with that of ATP (Figure 3.7). Whilst the binding site of this compound (Figure 3.7A) is predicted to be somewhat closer to the α5 alpha helix than the ATP molecule (Figure 3.7B), there is still an overlap between A740003 and the phosphate groups of ATP and this inhibitor is predicted to interact very much within the ATP binding site. This docking also gives some indication of residues which may contribute towards the P2X7R specificity of this antagonist (Figure 3.7). These include E173, Q248 and Y288. In the case of E173 and Y288, the other P2XR subtypes either have no equivalent or have residues which are small and uncharged (Figure 1.3), which could be a vital difference in the binding pocket when coordinating the interaction of A740003 with the P2X7R. In addition, Q248 may have an influence as the homology model predicts it to be in close proximity with the bound antagonist (Figure 3.7). The other P2XR subtypes largely have

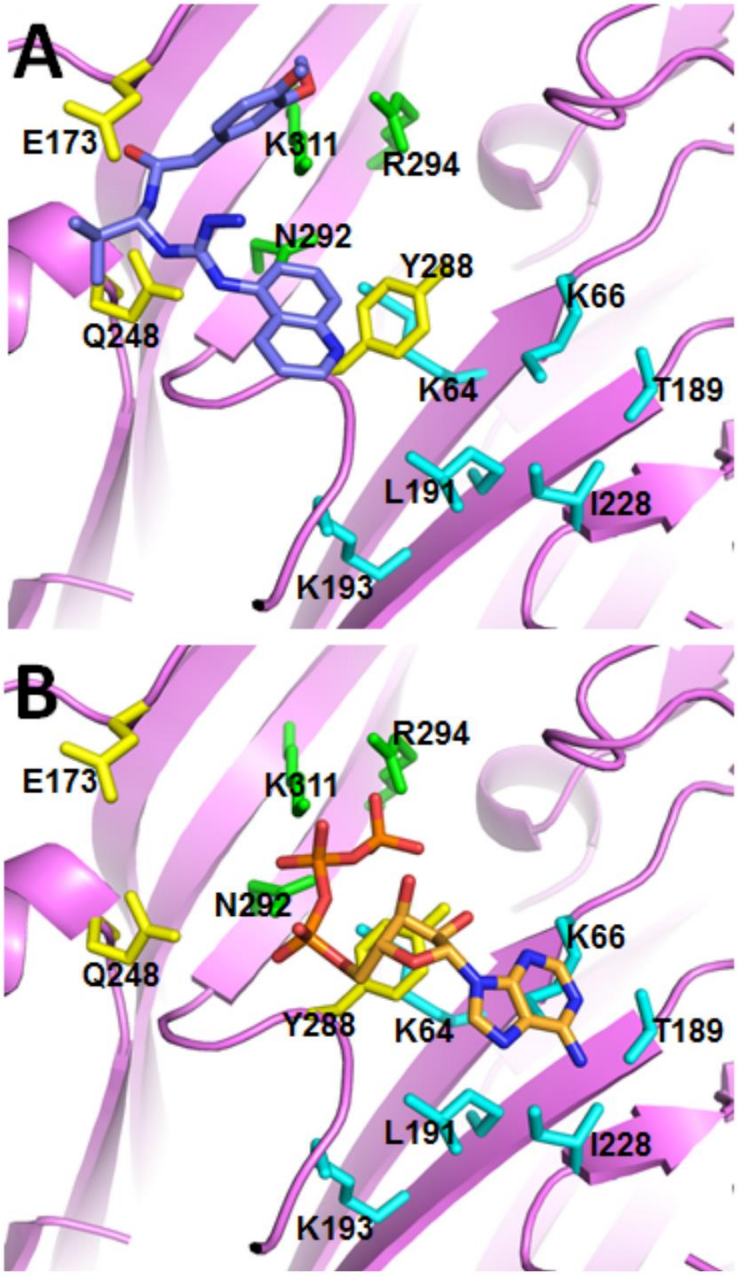

Figure 3.7 Predicted A740003 binding site in relation to the ATP binding site

(A) Predicted antagonist binding site showing A740003 in relation to the known ATP binding site shown in the closed state hP2X7R ATP binding pocket. (B) ATP binding within the ATP binding site in the hP2X7R as determined by ATP docking to the closed-state model. Conserved ATP binding residues from one subunit are shown in green and those from the other in cyan, and potential residues contributing to P2X7R specificity shown in yellow.

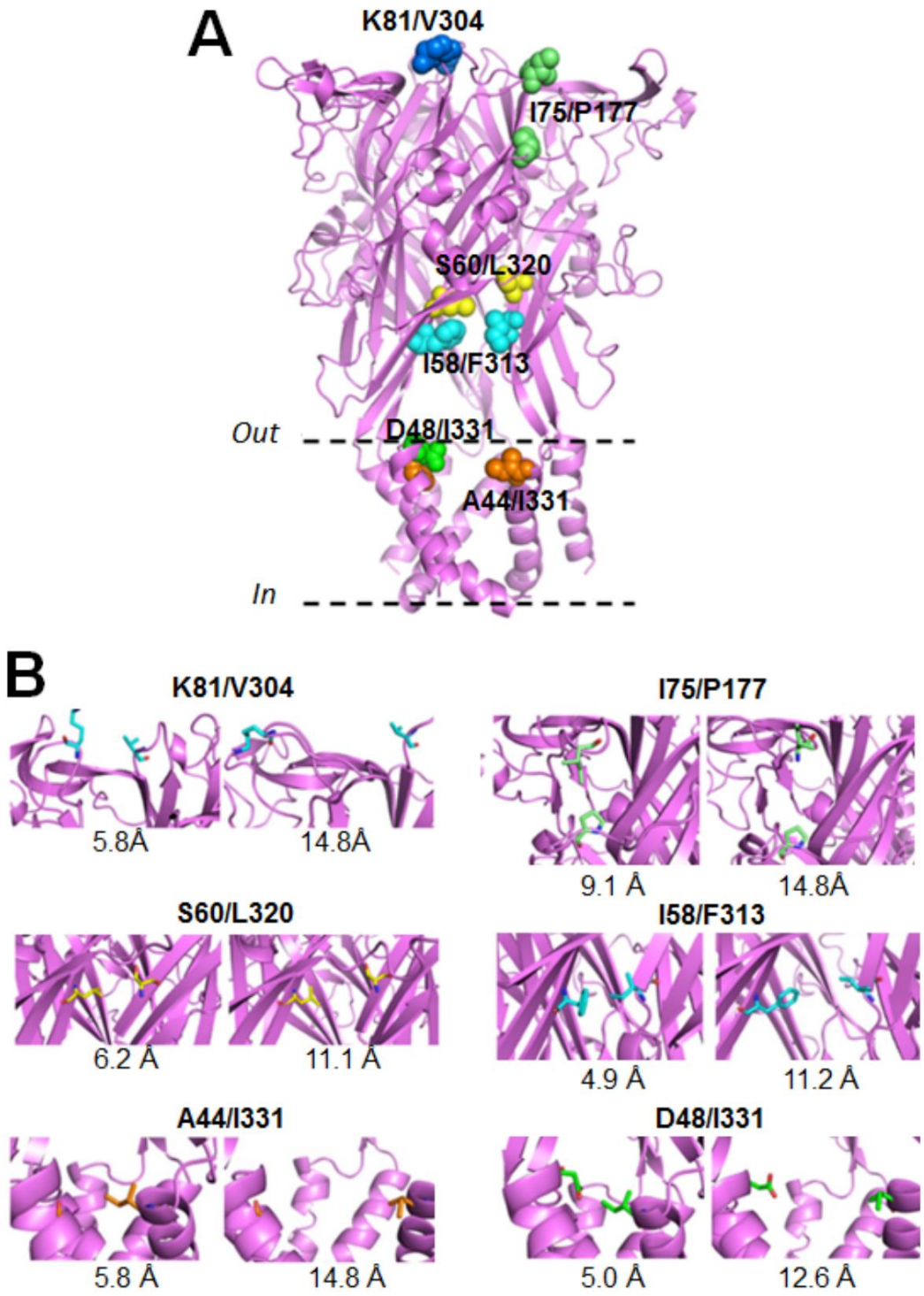

Figure 3.8 Location of pairs of residues for disulfide locking experiments

(A) Homology model of the hP2X7R with pairs of residues which were mutated in this study coloured to correspond with (B) and the names of the residues labelled. (B) Expanded views of the pairs of amino acids indicated in (A) with sidechains indicated and distances between the Cβ atoms in both the closed (left) and open (right) states detailed.

arginine or lysine residues at this position (Figure 1.3), which could interfere with antagonist binding due to their positive charge. Overall, docking known antagonists to the hP2X7R model provides a further indication that this model is a valid and useful tool.

3.2.4 Validation by disulfide linking

Cysteine-based cross-linking is a commonly employed technique and is highly valuable when investigating the movements of proteins and their interactions, either between adjacent regions of the same protein or between two proteins in close proximity. It is also valuable when validating protein models, as this method can be used to show regions which are in close proximity to each other as predicted by homology models. Mutating residues to cysteine has been utilised in the study of ion channel gating (for example the P2X2R (Jiang et al., 2001), the $GABA_AR$ (Kash et al., 2003) and K_v channels (Elliott et al., 2004), subunit stoichiometry of the P2X2/3R (Jiang et al., 2003), the inter-subunit ATP-binding site in the P2XR (Marquez-Klaka et al., 2009; Marquez-Klaka et al., 2007) and in studies of agonist-induced conformational changes in the P2X1R (Roberts et al., 2012), P2X2R (Stelmashenko et al., 2014) and P2X3R (Stephan et al., 2016). The same approach was enlisted to identify pairs of residues which would lock the hP2X7R into a closed conformation and be later sensitive to oxidative release, to provide validation of our homology model.

Structural models of the hP2X7R in both the closed and open states showed conformational changes that occur during receptor activation across various regions; the head, upper and lower body of the extracellular domain in addition to the TM α-helices (Figure 3.8A and B). Several pairs of residues which are predicted to migrate from being in close proximity to being distant from each other when changing from the closed to the open state illustrate these conformational changes. Pymol was used to calculate the distances between the Cβ atoms of these residues in the closed and open states (Figure 3.8B). The Cβ-Cβ distance in the closed state is predicted to be 5-7 Å, whereas the

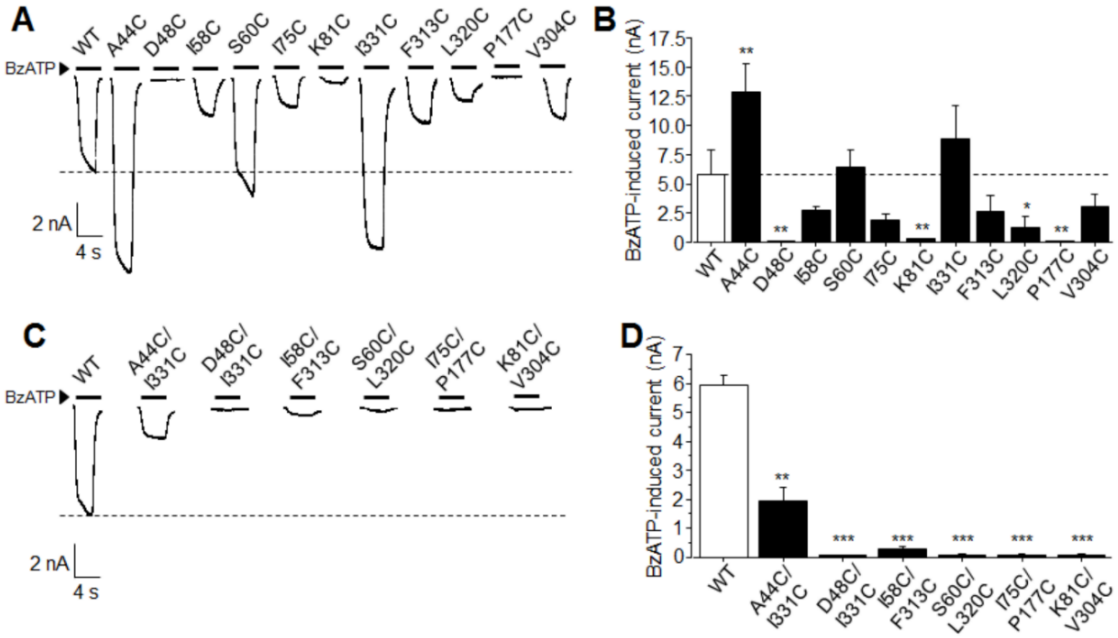

Figure 3.9 Functional assays characterising cysteine single mutants

(A) Representative patch-clamp recording traces of whole-cell currents evoked by 300 µM BzATP from HEK293 cells expressing the wild-type (WT) or indicated single mutant receptors. (B) Bar chart summary of current amplitude from HEK293 cells transfected with the WT hP2X7R or single mutants. (C) Representative patch-clamp recording traces of whole-cell currents evoked by 300 µM BzATP from HEK293 cells expressing the WT or indicated double mutant receptors. (D) Summary of BzATP-induced currents for WT or double mutant receptors. *, $p < 0.05$; **, $p < 0.01$; ***, $p < 0.005$ compared to the WT hP2X7R. 3-6 cells were recorded for each condition.

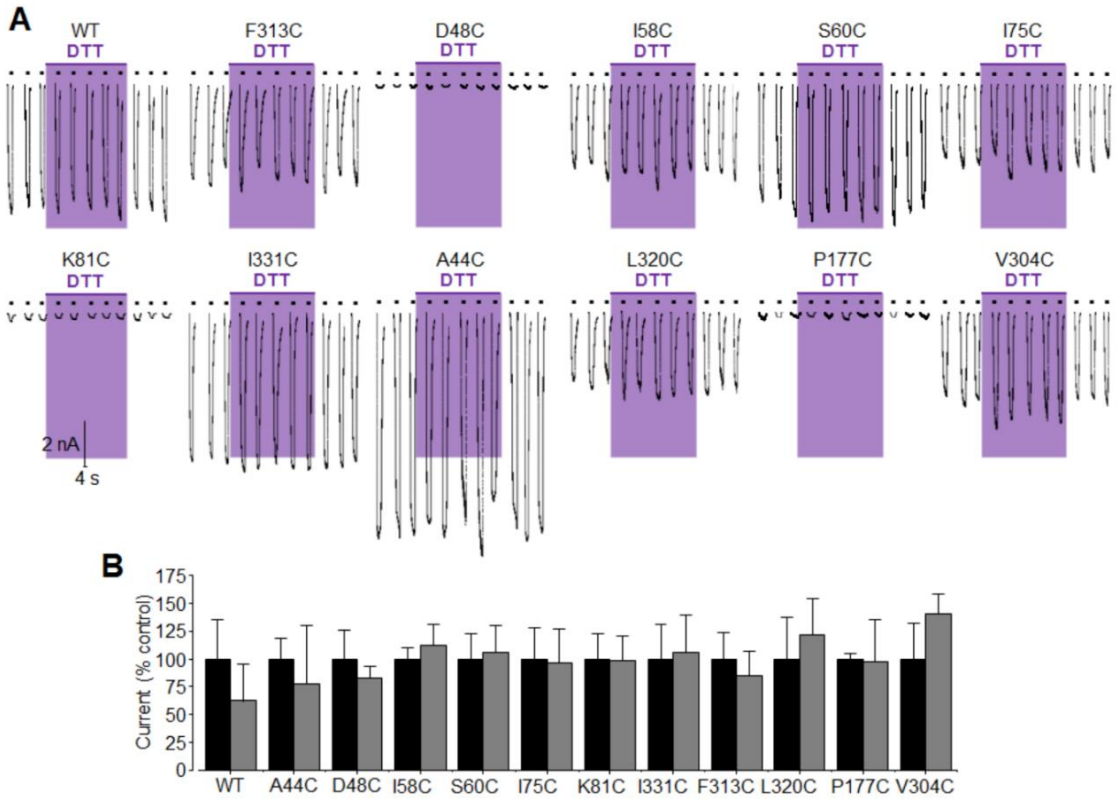

Figure 3.10 Functional assays characterising single cysteine mutants

(A) Representative traces of whole-cell recordings showing BzATP-induced currents evoked from HEK293 cells expressing the WT or indicated single mutant receptors prior to and during exposure to 10 mM DTT. (B) Bar chart summary of the effects of DTT exposure on WT or mutant hP2X7Rs. BzATP-induced currents after 10 min exposure to DTT (grey bar) are expressed as a percentage of the current induced immediately prior to DTT treatment (black bar).

Cβ-Cβ distance is predicted to increase to 11-15 Å during the transition from the closed to open state (Figure 3.8B). Specifically these pairs consisted of the Lys81 and Val304 (K81/V304) residues in the upper body, I58/F311 and S60/L320 in the lower body, and A44/I331 and D48/I331 at the outer ends of the TM1 and TM2 domains (Figure 3.8A), half of each pair being contributed by a different subunit. In addition, I75/P177 in the head are predicted to move from 9 Å in the closed state to 14 Å in the open state within the same subunit (Figure 3.8B). Single and double cysteine mutations were introduced into the hP2X7R at these positions and whole-cell patch-clamp recording used to assess the functionality of cells expressing both the single and double mutants compared to the WT receptor (Figure 3.9). Cells expressing these mutants were exposed to 300 µM BzATP, a super-maximal concentration at the WT receptor (Liu et al., 2008). The current amplitude elicited by the single mutants varied greatly. Cells expressing D48C and P177C single mutants displayed no current, indicating that these single mutants were non-functional (Figure 3.9A and B). The following nine single mutants had wide-ranging responses; A44C significantly increased the current amplitude, with an average current of 12.8 ± 2.4 nA compared to 5.8 ± 2.1 nA in the WT, whereas K81C and L320C significantly decreased it in comparison to the WT hP2X7R (Figure 3.9A and B). This is interesting in terms of indicating which residues which may be critical in receptor function. In the case of the six double mutants, only A44C/I331C gave rise to sizeable BzATP-induced currents. I58C/F313C elicited noticeable, but very small, currents (Figure 3.9C and D). The lack of response from several double mutants could be attributed to the lack of, or drastically reduced functionality displayed by many of the single mutants, in particular K81C, P313C and P177C (Figure 3.9A and B).

Subsequently, cells expressing the WT receptor or the single or double mutants were exposed to 300 µM BzATP before and after incubation with 10 mM DTT, which can reduce disulfide bonds introduced into P2XRs (Stelmashenko et al., 2014; Jiang et al., 2003; Marquez-Klaka et al., 2009), and the BzATP-induced currents evoked from patch-clamped cells were compared. Whilst the current amplitude differed between the single

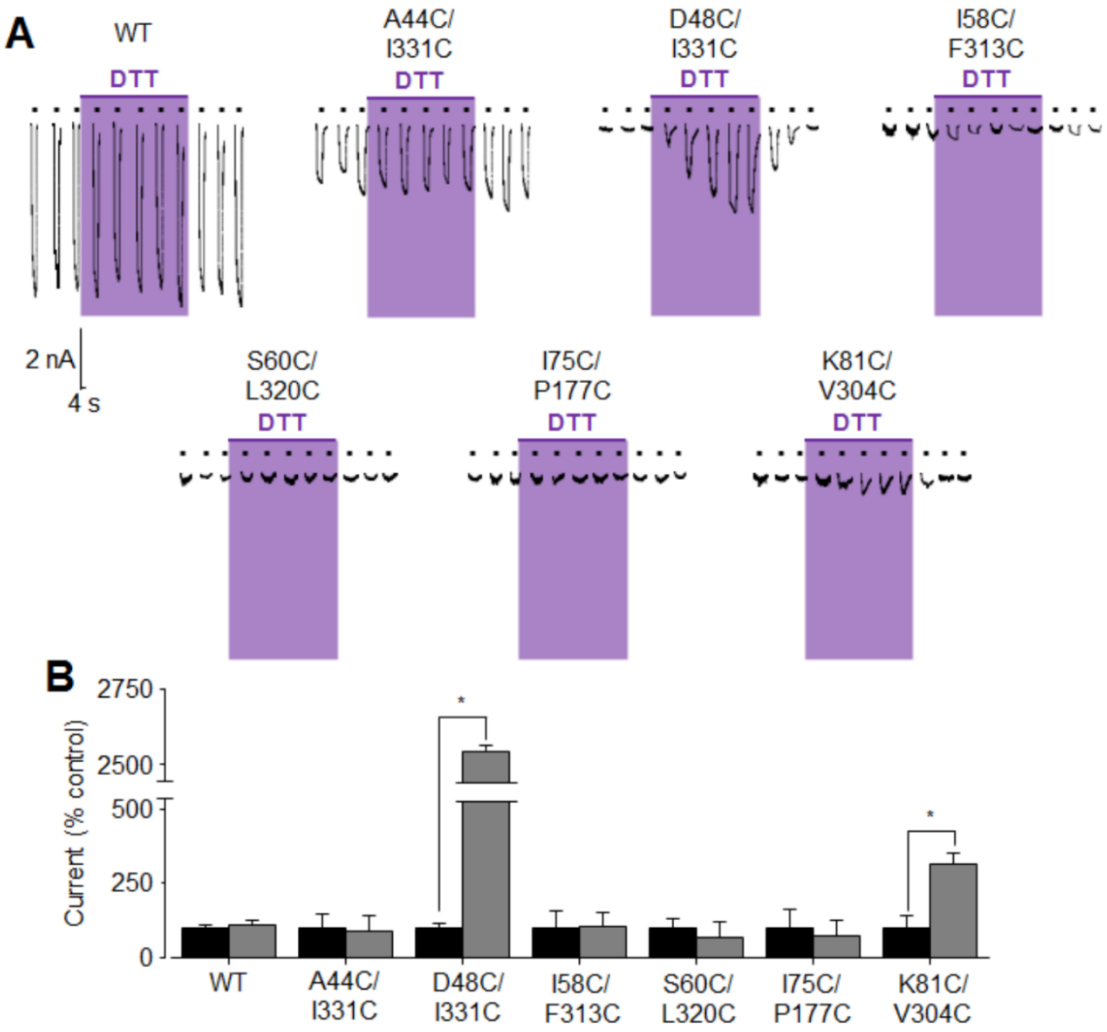

Figure 3.11 Functional assays characterising double cysteine mutants

(A) Representative traces of whole-cell recordings showing BzATP-induced currents evoked from HEK293 cells expressing the WT or indicated double mutant receptors prior to and during exposure to 10 mM DTT. (B) Bar chart summary of the effects of DTT exposure on WT or mutant hP2X7Rs. BzATP-induced currents after 10 min exposure to DTT (grey bar) are expressed as a percentage of the current induced immediately prior to DTT treatment (black bar). *, $p < 0.05$. 3-6 cells were recorded in each case.

mutants, the WT receptor and single mutants did not exhibit a significant difference in current amplitude prior to and post-DTT application (Figure 3.10). This reducing agent did not affect functional single mutants such as I331C, nor did it mediate a current increase in cells expressing non-functional single mutants such as D48C (Figure 3.10A). However, patch-clamped cells expressing the double mutants treated with 10 mM DTT showed a range of responses (Figure 3.11). No effect was seen in cells expressing the A44C/I331C, I58C/F313C, S60C/L320C and I75C/P177C double mutants (Figure 3.11). However, the application of DTT to cells transfected with the D48C/I331C mutant led to a considerable progressive increase in current amplitude (Figure 3.11A). D48 and I331 are predicted in the model to have Cβ atoms which are 5.0 Å apart in the closed state and 12.6 Å in the open state and are located at the outermost point of the TM domains at the point closest to the extracellular domain of TM1 and TM2, respectively (Figure 3.8). After 8 minutes of DTT treatment the current amplitude reached a steady state which was 64 ± 12% of that mediated by the WT receptor (Figure 3.11A), an increase of 2556 ± 19 % compared to before DTT addition which rapidly reversed following 6 minutes of washout (Figure 3.11). DTT treatment of cells expressing the K81C/V304C double mutant also led to a significant increase in current amplitude compared to that elicited prior to BzATP treatment. However, the current amplitude was still much smaller than that seen in the WT receptor even following DTT exposure (Figure 3.11A). The currents from these functional double mutants displayed similar features to those from the WT receptor despite being of smaller amplitude. Together these results provide further evidence for the importance of the movement of the TM regions during activation in the functioning of the P2X7R ion channel, as well as providing some validation for the homology models used in this study.

3.3 Discussion

In this chapter, the production and validation of hP2X7R homology models was described. Models of the trimeric hP2X7R and rP2X7R in the closed (Figure 3.1B) and ATP-bound open states (Figure 3.1C) were produced and the residues involved in ATP binding in the P2X7R were found to be in the expected regions (Figure 3.1D).

Two *in silico* methods were used to test the validity of the P2XR homology models and whether they reflect the protein in its native state in addition to testing the molecular docking approach. The first was docking ATP to the zfP2X4R homology model, which accurately pinpointed the position of the agonist binding site within the large extracellular domain (Figure 3.3A). Both the lowest predicted binding energy (Figure 3.3C and D) and highest populated binding modes (Figure 3.3E and F) showed considerable similarity to the ATP binding determined in the zfP2X4R crystal structure (Figure 3.3B), particularly the highest populated binding mode which overlapped well with the crystal structure (Figure 3.3F). This is a valuable indication that molecular docking in the model is able to accurately represent known binding modes of ATP. Moreover, the ability of the virtual docking method to accurately place the ATP molecule in the ATP binding site in the hP2X7R (Figure 3.4) provides further validation for both the docking approach and for the hP2X7R homology model.

In addition to agonists, docking of P2X7R antagonists was used to show how valuable the P2X7R models can be in the design of future experiments. The first group examined was a trio of non-competitive antagonists, SB203580, AZ11645373 and KN62, which are active against the human isoform of the P2X7R but not the rat (Michel et al., 2006; Humphreys et al., 1998; Stokes et al., 2006). Docking revealed a common binding site, proximal to the ATP binding site and buried within the receptor (Figure 3.5A and Figure 3.6A). This docking, as well as giving new insights into the binding mode of these antagonists, provides validation of the hP2X7R model and the molecular docking techniques due to the predicted interactions involving Phe95 (Figure 3.6A-D). Phe95 has

been shown to be pivotal in determining the ability of these compounds to inhibit the hP2X7R, as substituting this residue in the hP2X7R for the Leu found in the rP2X7R greatly reduces the efficacy of these inhibitors (Michel et al., 2008; Michel et al., 2009) whereas introducing the L95F mutation into the rP2X7R allows SB203580 and KN62 to inhibit rP2X7R-mediated responses (Michel et al., 2008). The pi-stacking interactions predicted by this experiment between the ring structures in the inhibitors and the aromatic side chain in Phe95 provide an explanation for the species-specific activity of these antagonists (Figure 3.6B-D). Furthermore, the agreement between the docking carried out here and previous experimental evidence indicates that a combining the P2X7R homology model with AutoDock is a useful approach for further tests.

As well as the non-competitive antagonists, further authentication of the hP2X7R model was provided by docking the competitive antagonist A740003 (Honore et al., 2006). This inhibitor was predicted to bind within the ATP binding pocket, overlapping considerably with the established ATP binding site (Figure 3.7). This further shows that molecular docking in the homology model corresponds nicely with prior experimental evidence.

In addition to *in silico* methods, an approach was adopted in which a combination of cysteine-based cross-linking and patch-clamp recording was used to probe conformational changes in the receptor. Disulfide locking is useful for bridging the gap between the snapshots seen in protein structures and their behaviours in native environments. Six pairs of residues located across the head, upper and lower body and outer ends of the TM domains predicted to undergo considerable movement when transitioning between the closed and open states were mutated to cysteine (Figure 3.8). Several of the single and double mutants were non-functional or exhibited largely impaired responses (Figure 3.9). DTT treatment did not restore the function of any of the single mutants which had impaired function, nor did it restore the function of the non-functional double mutants I58C/F313C, S60C/L320C and I75C/P177C (Figure 3.10 and 11). It is possible that these mutations affect the receptor in ways which lead to

deficiencies in protein synthesis, membrane trafficking, activation or several of these simultaneously.

Of the double mutants, A44C/I331C displayed the largest currents, although these were still much smaller than those seen in the WT hP2X7R (Figure 3.9C and D). The A44C/I331C mutant was unaffected by DTT treatment (Figure 3.11), suggesting that it is unlikely that disulfide bond formation impedes the ion channel from opening. In contrast to A44C/I331C, the D48C/I331C mutant was almost non-functional in the presence of a disulfide bond (Figure 3.9C and D) but had a progressive increase in BzATP-induced current amplitude during DTT treatment (Figure 3.11A). In the steady state the current amplitude reached more than half of that seen in the WT receptor, which was rapidly reversed upon washout (Figure 3.11A). This suggests that Asp48 and Ile331 form an inter-subunit disulfide bond in the closed state which 'locks' the receptor in place to the extent that it does not allow the opening of the channel until this bond is reduced, as described in previous studies for the rP2X2R, rP2X2/3R and hP2X3R (Jiang et al., 2001; Jiang et al., 2003; Stelmashenko et al., 2014; Stephan et al., 2016). The disparity between A44C/I331C and D48C/I331C is interesting because of their shared I331C residue. As the distances between these residues in the closed and open states are comparable in magnitude (Figure 3.8B), the likely lack of A44C/I331C disulfide bond may reflect the accessibility of the Ala44 compared to Asp48; in the hP2X7R model Ala44 is predicted to be nestled more deeply in the TM1 alpha helix which might prevent its ability to form disulfide bonds as effectively (Figure 3.8A).

In addition to these mutants, Lys81 and Val304 in the upper body of the hP2X7R were mutated to produce K81C/V304C. DTT significantly enhanced BzATP-induced currents in cells expressing K81C/V304C, although the current remained very small (Figure 3.11). This suggests the formation of a disulfide bond between K81C and V304C in the receptors that were trafficked to the cell surface, which agrees with the predicted movement of these residues further away from each other when transitioning from the closed to the open ion channel states (Figure 3.8B). The results of these disulfide linking

experiments provide evidence to support the notion that conformational changes in the upper part of the extracellular and the outer ends of the TM domains are crucial for hP2X7R activation, as well as proposing that these models may be representative of the receptor within the membrane.

Overall, the various validation studies carried out on the hP2X7R model in this chapter suggest that this model is a good approximation of the protein in its native state. As a result, further experiments based around in silico antagonist design were performed and are described in the following chapters.

Chapter 4

Identification of Novel Human P2X7 Receptor Antagonists Using a Structure-Based Approach

4.1 Introduction

The ability to specifically block the activity of the protein of interest is a vital component of ion channel investigation. As such, having a large arsenal of tools with which to study hP2X7R function, in particular potent and specific antagonists, is fundamental. Whilst huge strides have been made in the discovery of P2X7R-specific antagonists (Guile et al., 2009; Lambertucci et al., 2015; Subramanyam et al., 2011), increasing the range of structures available by introducing novel compounds with diverse characteristics is one particular way to aid in the study of the P2X7R. In addition to being important in P2X7R research, widening the pool of compounds that can block this receptor is important in a therapeutic context as these inhibitors can form the basis for novel drugs.

The P2X7R is implicated in a large number of diseases, and the large pore forming function of this receptor is of particular relevance with respect to human disease (Sorge et al., 2012; Fowler et al., 2014). As a result the P2X7R is a desirable drug target and P2X7R-specific antagonists have been taken to clinical trials. After many years of disappointment following antagonists proving ineffective in clinical trials, promising progress has been made recently with the orally active P2X7R inhibitor AZD9056. In a phase 2a trial this antagonist has shown promise in treating moderately to severely active Crohn's disease (Eser et al., 2015). As such, increasing the diversity of structures available for the development of therapeutic compounds has been shown to be increasingly valuable.

Considering the importance of identifying novel P2X7R-specific blockers, exploring different methods of antagonist discovery is a valuable area of investigation. Previously, P2X7R-specific antagonists have predominantly been discovered using high throughput methods involving screening large libraries of compounds against the receptor. Whilst this technique has been successful thus far, it is still both time consuming and expensive. Therefore, exploring methods to make this process more efficient can prove to be massively beneficial. Utilising a structure-based approach can potentially provide an

alternative and cost effective approach, which will be useful particularly when researchers do not have access to the large resources available to pharmaceutical companies. Fortunately, the crystal structure of the zfP2X4R (Hattori and Gouaux, 2012; Kawate et al., 2009) means that a rational approach can now be used to discover novel inhibitors through the use of homology modelling and virtual screening.

In this chapter, the pharmacological characteristics of a series of novel hP2X7R antagonists identified using a structure-based approach were investigated. The ability of these compounds to inhibit P2X7R functions and the structural basis of the antagonistic effects of these compounds is described.

4.2 Results

4.2.1 Compound identification by structure-based virtual screening

In order to explore the potential of a structure-based approach in the identification of P2X7R antagonists, homology models produced as described in chapter 3 were used as a template. These homology models included the ATP binding site as determined by the zfP2X4R, and the main residues identified as playing a role in ATP binding were almost completely conserved in the hP2X7R models. The bound ATP molecule in the structure was used as the centre of a 10 Å sphere in which virtual screening was carried out (Figure 4.1A). Comparison of the zfP2X4R and the hP2X7R sequences (Figure 4.1B) showed a 62% amino acid sequence identity between these receptors within the 10 Å sphere. The atypical nature of this ATP binding pocket in the hP2X7R made it an ideal target to perform virtual screening experiments, whereby toxicity through promiscuous binding to more typical ATP binding pockets is reduced. The ZINC12 chemical library of approximately 100,000 commercially available, structurally diverse compounds (Irwin et al., 2012) were screened against the ATP binding site-containing sphere (Figure 4.1A) in eHits (eg. Figure 4.1C) and a corresponding energy binding score was predicted for each. For the 50 compounds with the highest scores, 42 that could be sourced

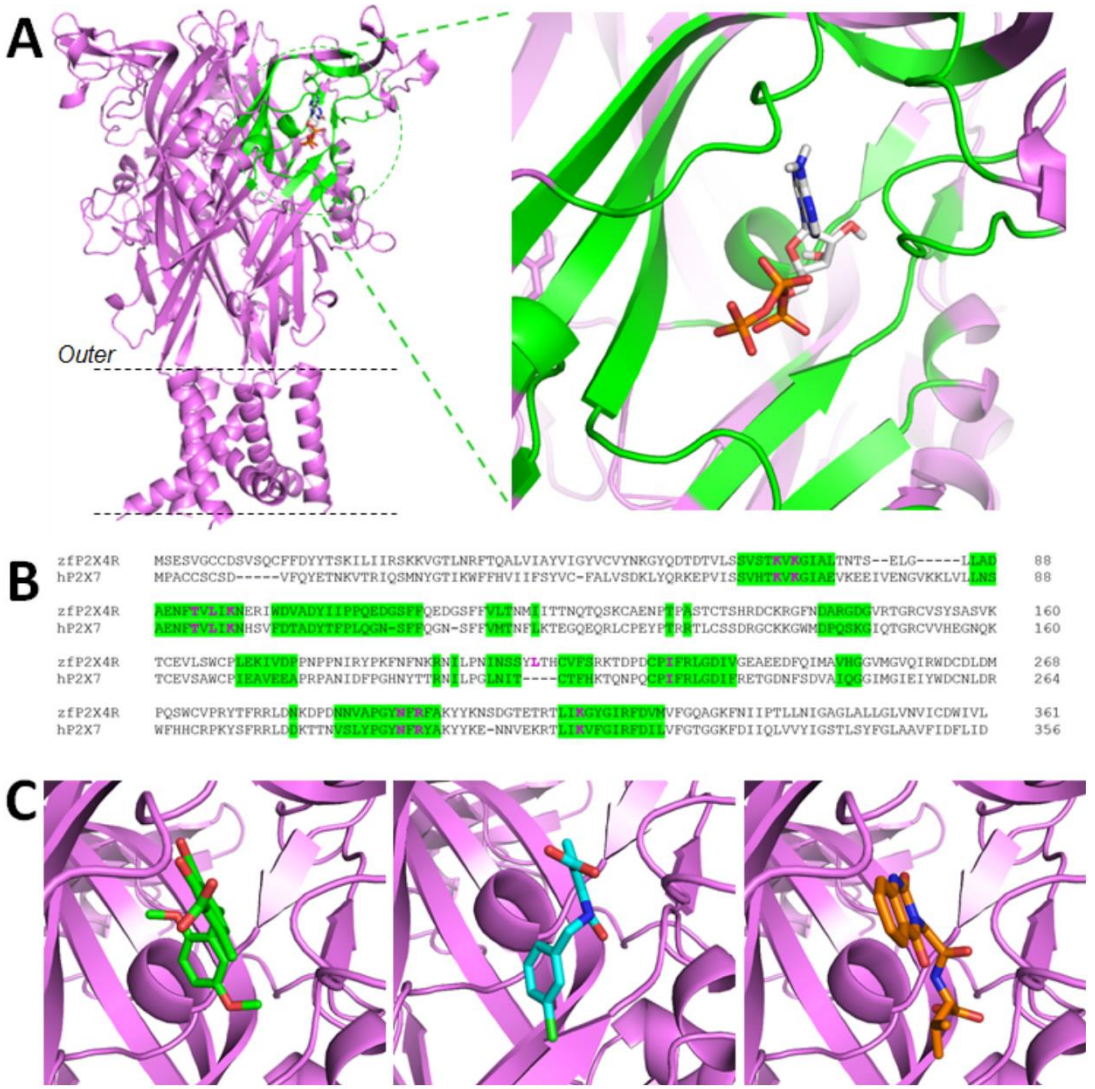

Figure 4.1 Homology models of the hP2X7R and ATP binding

(A) Homology model of the hP2X7R in the apo state, lacking the intracellular domains, with an ATP molecule bound to one of the three inter-subunit binding pockets as determined by molecular docking. The 10 Å sphere that formed the basis of virtual screening is highlighted in green. An expanded view of ATP bound as predicted by molecular docking experiments within the hP2X7R binding pocket is shown. (B) Sequence alignment of the zfP2X4R and hP2X7R, with the 10 Å sphere highlighted in green and core ATP binding residues in magenta. (C) The three top-ranked compounds from the ZINC12 database predicted to bind most favourably to the hP2X7R ATP binding site and their anticipated conformations.

commercially had predicted energy binding scores ranging from -4 to -10.5 kcal/mol. These values are comparable to those predicted for known hP2X7R antagonists including AZ11645373 (-10.8 kcal/mol), SB203580 (-8.75 kcal/mol) and KN-62 (-5.2 kcal/mol) as reported in our recent study (Caseley et al., 2015). These top 42 compounds were assessed experimentally against the P2X7R.

Chemicals were screened in the first instance by calcium measurement using the FlexStation carried out in HEK293 cells stably expressing the human and rat P2X7R. These compounds were applied at 10 μM and initially none showed agonist activity at the P2X7R. However, two compounds were capable of blocking P2X7R-mediated calcium responses induced by 300 μM BzATP. These compounds were C23 and C40 (ZINC12 database numbers ZINC67825876 and ZINC58368839, respectively), which had an initial predicted docking score of -7.1 kcal/mol and -5.5 kcal/mol, respectively. Both compounds exhibited strong inhibition of the hP2X7R and reduced BzATP-induced calcium responses by 73.2 ± 2% and 84.3 ± 7%, respectively (Figure 4.2). This is in contrast to all the other compounds which had no or minimal effect, as illustrated by C10 (ZINC19868610) (Figure 4.2). This inhibition by C23 and C40 was slightly greater than the 28.5 ± 5% hP2X7R inhibition by BBG and the 81.9 ± 5% inhibition by AZ11645373 (Stokes et al., 2006).

In addition to the human isoform, assessment of these 42 compounds against HEK293 cells stably expressing the rP2X7R showed that, whilst some of these 42 compounds had minimal effects on BzATP-induced calcium responses, none had a significant effect on rP2X7R activity (Figure 4.2). BBG was used as a positive control and strongly inhibited BzATP-induced Ca^{2+} responses, whereas AZ11645373 was much less effective (Figure 4.2). C23 and C40 had no significant effect at the rP2X7R. The BzATP-induced calcium responses observed in rP2X7R-expressing cells were 100.2 ± 21% and 88.2 ± 2% of the untreated control response when cells were incubated with C23 and C40, respectively.

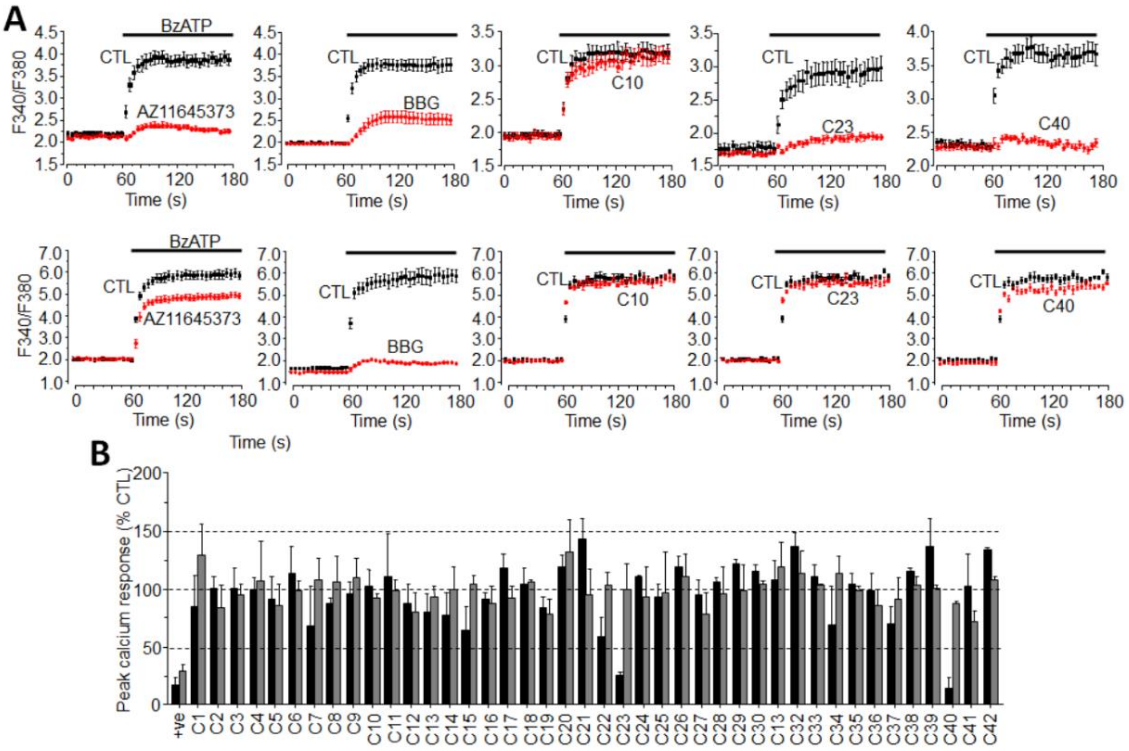

Figure 4.2 Effects of 42 compounds on calcium responses

(A) Representative FlexStation recording traces from HEK293 cells expressing the hP2X7R (top) and the rP2X7R (bottom) indicating calcium responses following the application of 300 µM BzATP after 60 s. The control response is shown in black and the response following incubation with the indicated compounds in red, with AZ11645373 and BBG used at 200 nM and C10, C23 and C40 used at 10 µM as indicated above. (B) Summary of the initial screen of 42 compounds and their effects on calcium responses mediated by the hP2X7R (black) and the rP2X7R (grey). Results are presented as the mean ± SEM, from 8-12 wells of cells from 3 independent experiments.

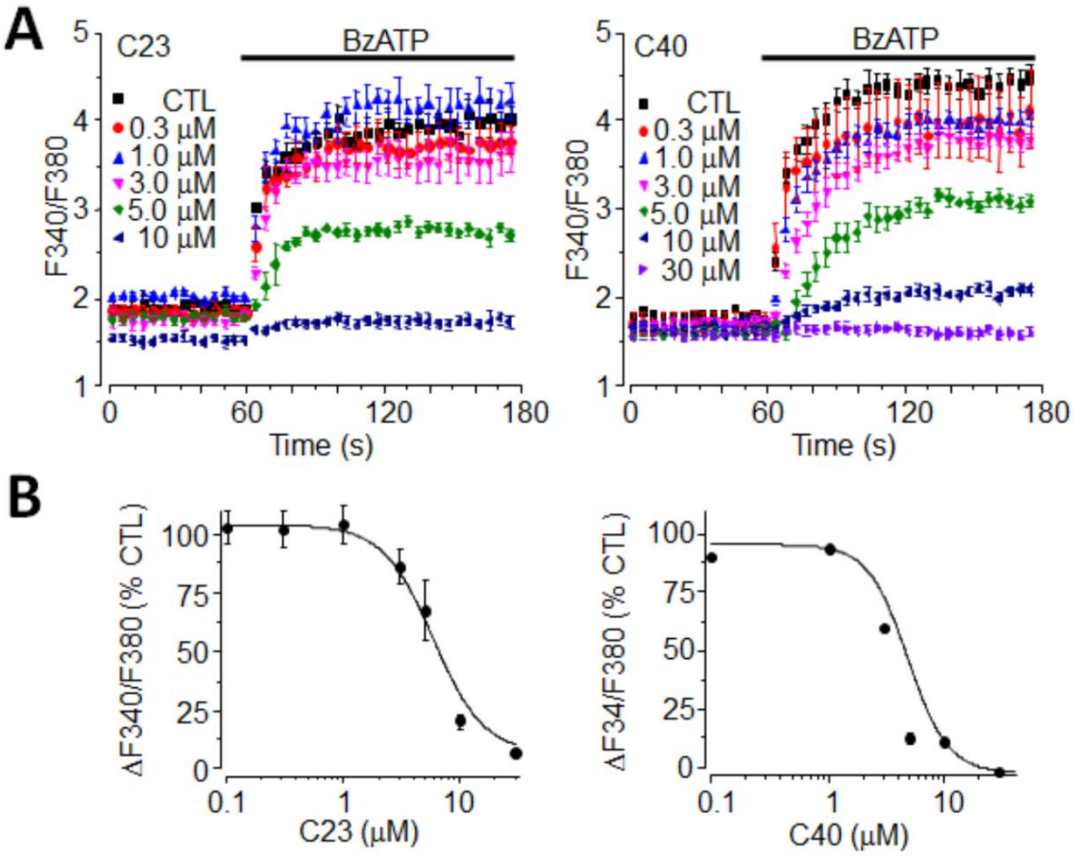

Figure 4.3 Effects of C23 and C40 on hP2X7R-mediated calcium responses

(A) Representative BzATP-induced calcium responses from HEK293 cells stably expressing the hP2X7R treated with either C23 (left) or C40 (right) at the indicated concentrations. (B) DR relationship curves for hP2X7R currents following exposure to C23 (left) and C40 (right). Each data point represents mean ± SEM from 4 cells from 3-4 independent experiments. The solid lines in B and D are fits of the data to the Hill equation. The IC_{50} for C23 and C40 is 5.1 µM ± 0.3 µM and 4.8 ± 0.8 µM, respectively.

4.2.2 Effects of C23 and C40 on the human and rat P2X7R

The properties of the initial hits, C23 and C40, were characterised in greater depth using both calcium measurement and patch-clamp recording. Measurement of BzATP-induced calcium responses from cells stably expressing the hP2X7R was carried out using a FlexStation. Figure 4.3A shows examples of BzATP-induced calcium responses from cells incubated with increasing concentrations of C23 and C40, from 0.1 to 10 μM. The corresponding DR curves (Figure 4.3B) produced by fitting the accumulated FlexStation data to the Hill equation indicates that C23 inhibits calcium responses with an IC_{50} of 5.1 ± 0.3 μM, whilst C40 inhibits this same response with an IC_{50} of 4.8 ± 0.8 μM.

Whole-cell patch-clamp recordings of BzATP-induced currents from HEK293 cells stably expressing the hP2X7R revealed that the blocking by C23 and C40 at the receptor was reversible upon washout, with maximal currents elicited following a three minute washout period (Figure 4.4A). The fit of data to the Hill equation showed that C23 and C40 inhibits hP2X7R currents with an IC_{50} of 0.35 ± 0.3 μM and 1.2 ± 0.1 μM, respectively (Figure 4.4B). The small differences in potency may be due to the methods used to apply the compounds and to measure the P2X7R mediated responses as the two assays inspect different effects of the compounds. Calcium response measurement examines the addition of inhibitors to the receptor in the closed state, whereas patch-clamp recording investigates the effect of applying the compounds to the channel in the open state and is accumulative.

4.2.3 Identification and characterisation of structurally similar compounds

Compounds sharing common structural features with C23 and C40 were identified through the ZINC12 database. 31 compounds with ≥ 80% structural similarity as determined by the ZINC website were tested against the human and rat P2X7R at 10 μM using the FlexStation as described above. Of the 31 compounds screened, C60

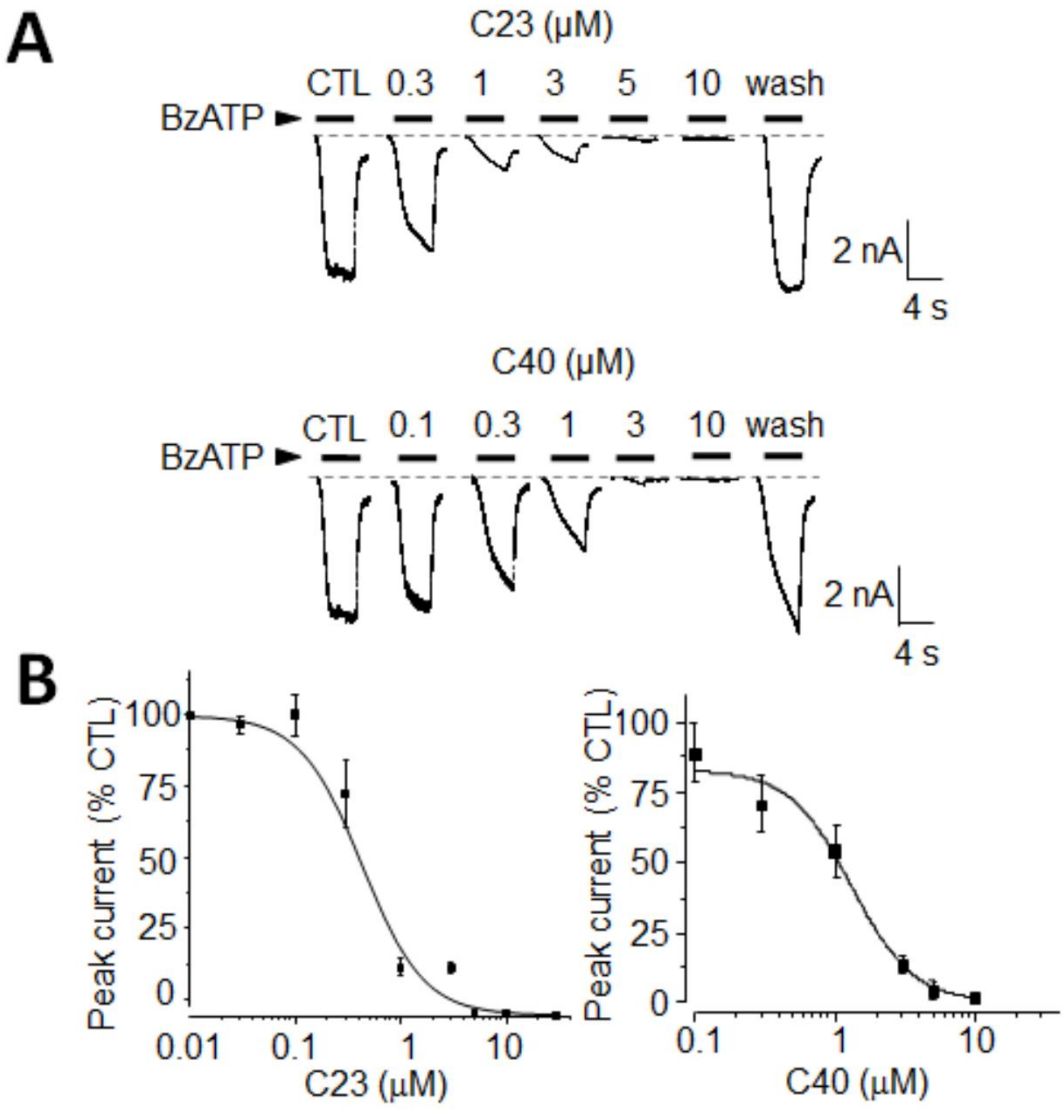

Figure 4.4 Effects of C23 and C40 on hP2X7R-mediated currents

(A) Representative BzATP-induced currents from HEK293 cells stably expressing the hP2X7R treated with either C23 (top) or C40 (bottom) at the indicated concentrations. (B) DR relationship curves for hP2X7R currents following exposure to C23 (left) and C40 (right). Each data point represents mean ± SEM from 4 cells from 3-4 independent experiments. The solid lines in B and D are fits of the data to the Hill equation. The IC_{50} for C23 and C40 is 0.35 ± 0.3 μM and 1.2 ± 0.1 μM, respectively.

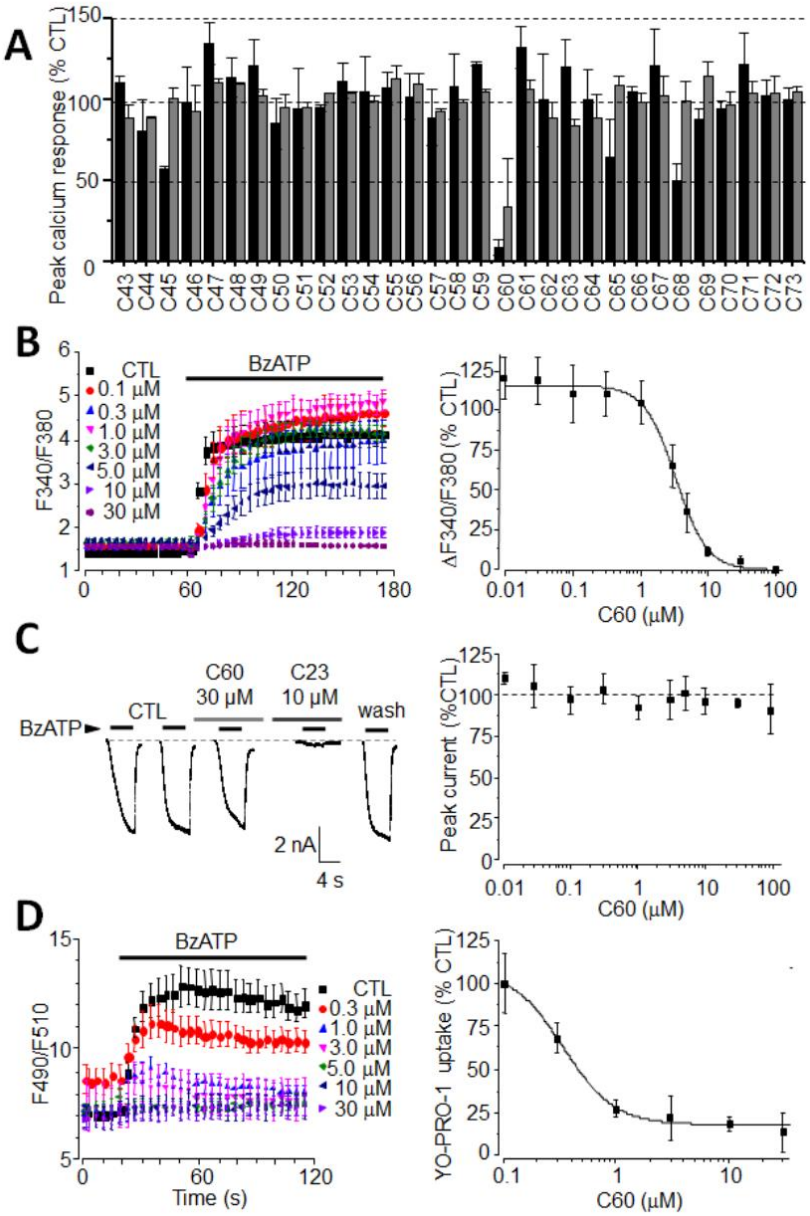

Figure 4.5 Effects of C60 on BzATP-induced P2X7R responses

(A) Summary of the effects of 31 C23 analogues on hP2X7R (black) and rP2X7R (grey) calcium responses. (B) Example traces of BzATP-induced calcium responses at the concentrations of C60 indicated and the corresponding DR curve. (C) Example traces of BzATP-induced currents at the concentrations of C60 indicated and the corresponding DR curve. (D) Representative recordings of YO-PRO-1 uptake in the presence of the indicated concentrations of C60 and the corresponding DR relationship curve. Each data point represents the mean ± SEM from 8-12 wells of cells from 3-5 independent experiments (calcium response and YO-PRO-1 dye uptake) and 4 cells from 3-4 experiments (currents). The solid lines in B, C and D are fits to the Hill equation. The IC_{50} for (B) and (D) is 3.2 ± 0.2 µM and 0.3 ± 0.04 µM, respectively.

(ZINC12 database number ZINC09315614) showed antagonistic activity by blocking the calcium response elicited by 300 µM BzATP by 91 ± 4% in hP2X7R-expressing cells and 66 ± 22% in rP2X7R-expressing cells (Figure 4.5A). Determination of a concentration-response relationship curve of the BzATP-induced calcium response showed C60 to have an IC_{50} of 3.2 ± 0.2 µM at the hP2X7R (Figure 4.5B). However, when whole-cell patch-clamp recordings were carried out, C60 had no inhibitory effect (Figure 4.5C). Even when applied at concentrations of 30 µM, which almost completely abolished BzATP-induced calcium responses (Figure 4.5B), no antagonism was seen and yet the hP2X7R current was almost completely inhibited by subsequent application of C23 (Figure 4.5C).

Prolonged P2X7R activation leads to large pore formation (Surprenant et al., 1996, Yan et al., 2008). This is an alternative route for P2X7R-mediated calcium entry, and as such C60 was tested for its effects on the pore rather than the ion channel opened during short term activation. HEK293 cells stably expressing the hP2X7R were stimulated with BzATP for 120 s and the intracellular accumulation of the 629 Da cationic fluorescent dye YO-PRO-1 was measured, as this dye is only able to enter the cell when the large pore is open. C60 potently blocked this dye uptake in a dose-dependent manner with an IC_{50} of 0.3 ± 0.04 µM (Figure 4.5D). Investigation of YO-PRO-1 uptake into single cells showed C60 to significantly inhibit this uptake. 62 ± 12% of cells exposed to ATP alone exhibited YO-PRO-1 fluorescence, whereas only 33 ± 6% of cells co-incubated with 5 µM C60 did (Figure 4.6). This near halving of individual cells exhibiting YO-PRO-1 uptake provides further evidence for the specific inhibition of the hP2X7R-dependent large pore by C60.

4.2.4 Effects of C23, C40 and C60 on P2X7R mediated cell death

The three hits C23, C40 and C60 are potent antagonists of the hP2X7R. Previously established P2X7R antagonists have been shown to protect cells including macrophages

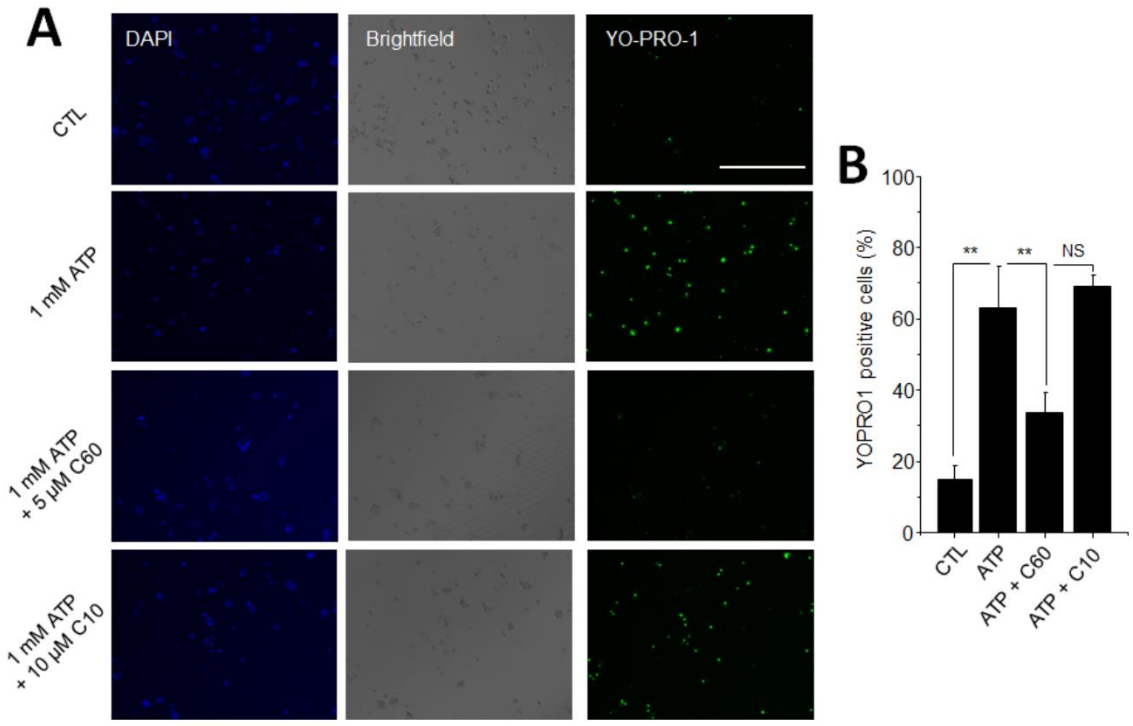

Figure 4.6 Inhibition of YO-PRO-1 uptake in single cells by C60

(A) Representative bright field and fluorescent images showing all cells, DAPI stained cells and YO-PRO-1 stained cells, respectively, under the indicated conditions. Scale bar is 400 µM. (B) Summary of YO-PRO-1 staining under the indicated conditions. Results are presented as mean ± SEM from 4 independent experiments. ** P< 0.01 significantly different from control.

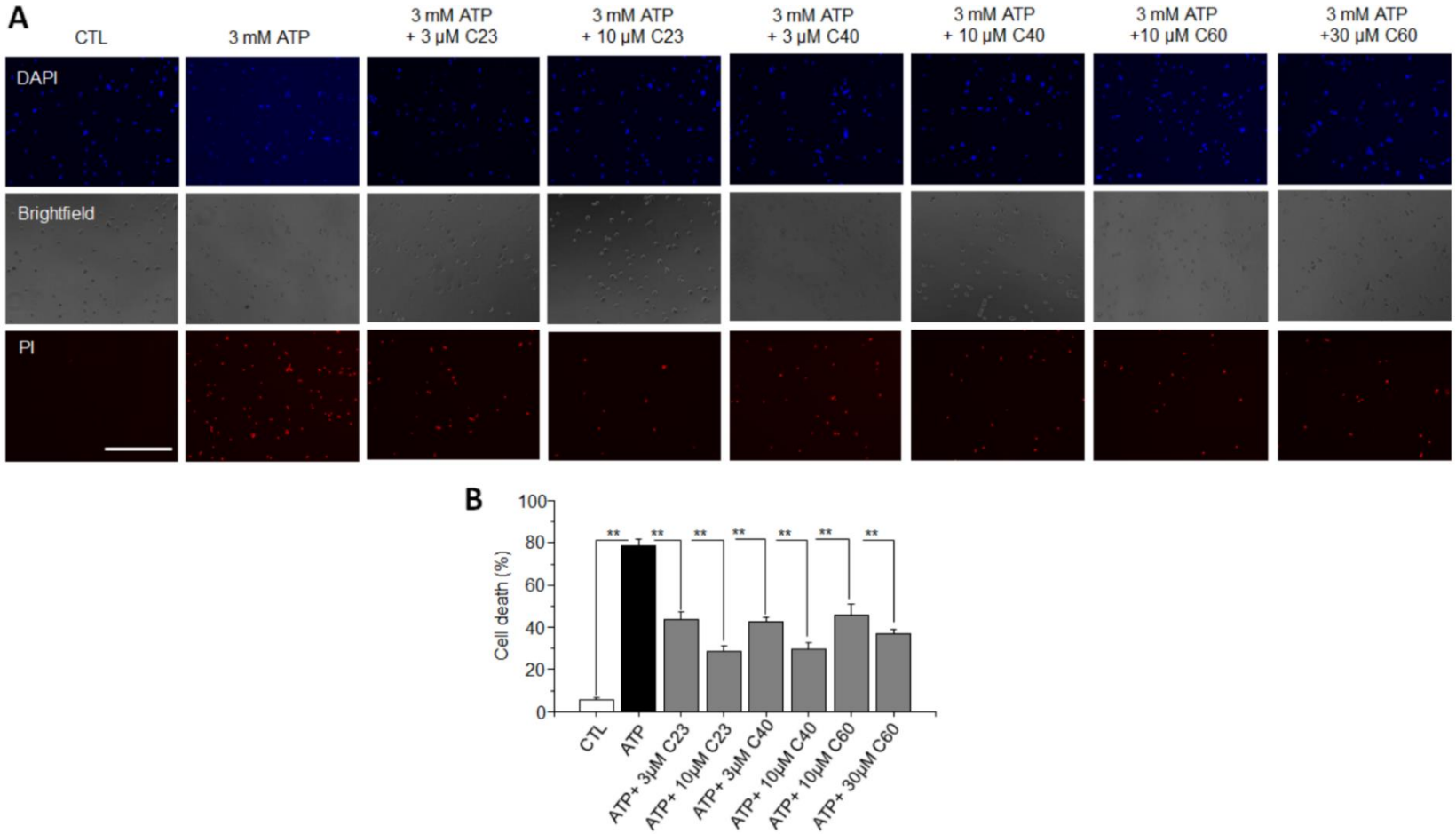

Figure 4.7 Effects of C23, C40 and C60 on hP2X7-mediated cell death

(A) Representative bright field and fluorescent images showing all cells, DAPI stained cells and PI stained dead cells respectively under the conditions indicated. Scale bar is 100 μM. (B) Summary of cell death under the conditions indicated. Results are presented as mean ± SEM from 4 independent experiments. ** P< 0.01 significantly different from control.

(Le Feuvre et al., 2002), astrocytes (Salas et al., 2013) and microglia (Eyo et al., 2013) against ATP-mediated cell death, as prolonged P2X7R activation causes membrane blebbing and subsequent cell death (Chow et al., 1997; Di Virgilio et al., 1998). HEK293 cells stably expressing the hP2X7R were exposed to millimolar concentrations of ATP for extended periods in order to determine whether C23, C40 and C60 could protect cells following pre-treatment with these compounds (Figure 4.7). PI staining assays showed that incubation of cells with ATP for 6 hrs led to a significant degree of cell death, with 78 ± 3% of cells stained by PI compared to 5 ± 1% of untreated control cells. Cells pre-treated with C23 at 3 μM and 10 μM reduced the percentage of cell death to 44 ± 3% and 29 ± 3%, respectively. Similarly, pre-treatment of cells with C40 at 3 μM and 10 μM reduced the percentage of PI stained cells to 43 ± 2% and 30 ± 3%, respectively. C60 was shown to be less effective at preventing cell death; at 10 μM 45 ± 5% of cells were PI stained, whereas incubation with 30 μM C60 only reduced this to 37 ± 2%. The reduction under all these conditions reached statistical significance (Figure 4.7). These results provide evidence supporting the ability of the novel antagonists identified in this study to inhibit ATP-induced cell death as previously described for P2X7R antagonists such as A438079 (Haanes et al., 2012) and BBG (Notomi et al., 2011). The compounds vary in their ability to affect this function of the P2X7R; C23 and C40 seem to be the most effective, whereas C60 is less so. All three compounds appear to act in a dose-dependent manner in order to act protectively at hP2X7R-expressing cells.

4.2.5 P2X subtype selectivity of C23, C40 and C60

Whilst there are a number of general P2XR antagonists, studies often preferentially utilise those with specificity for a particular subtype. The P2X4R has the highest degree of sequence identity with the P2X7R (~40%) and the two are co-expressed in numerous cell types (Xiang and Burnstock, 2005; Ma et al., 2006; Guo et al., 2007), which suggests that this receptor is the most likely candidate to also be inhibited by C23, C40 and C60.

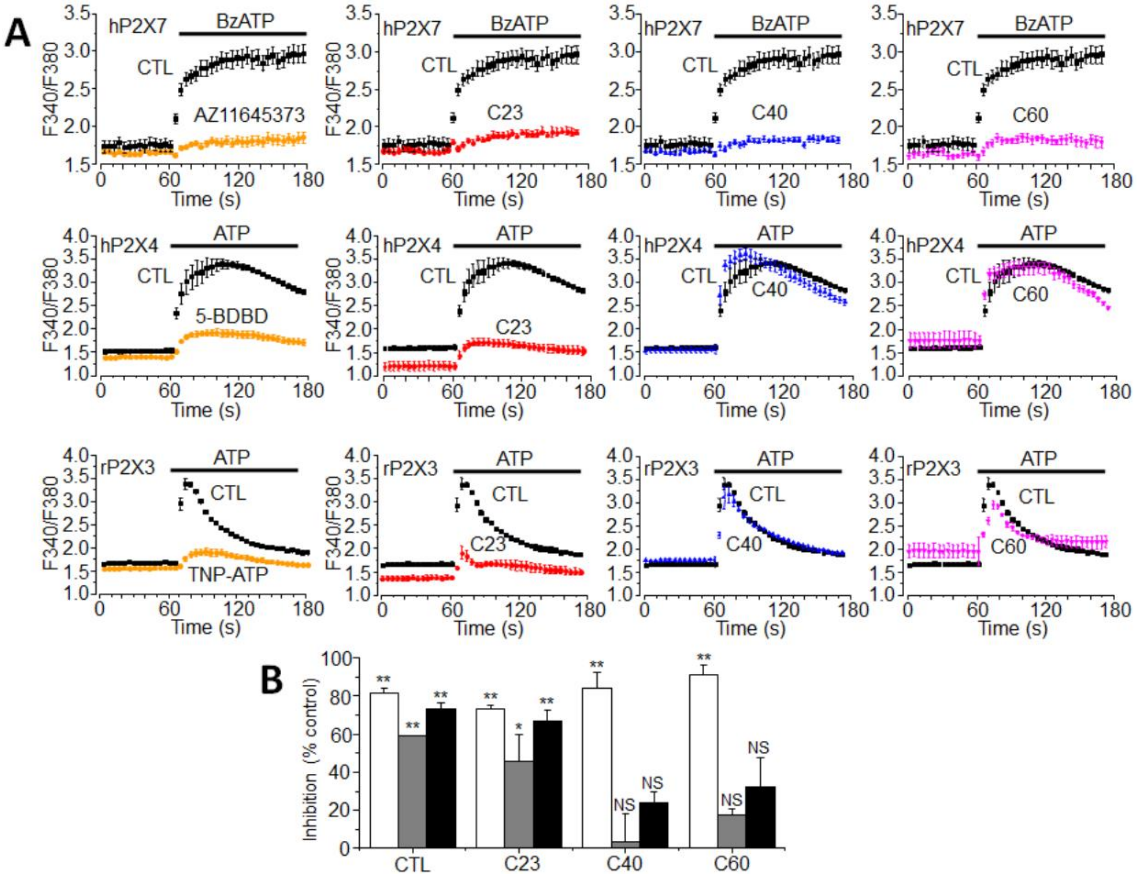

Figure 4.8 Influence of novel antagonists on different P2XRs

(A) Representative traces of calcium responses in HEK293 cells stably expressing the hP2X7R, hP2X4R and rP2X3R in response to 100 µM BzATP, 100 µM ATP and 100 µM ATP respectively in the absence or presence of 10 µM C23, C40 and C60 as indicated. (B) Summary of inhibition of the hPX7R (white bar), hP2X4R (grey bar) and rP2X3R (black bar). Results are presented as mean ± SEM from 8-12 wells of cells from 3-5 independent experiments. * $p<0.05$, ** $p<0.01$, NS, not significant compared no antagonist.

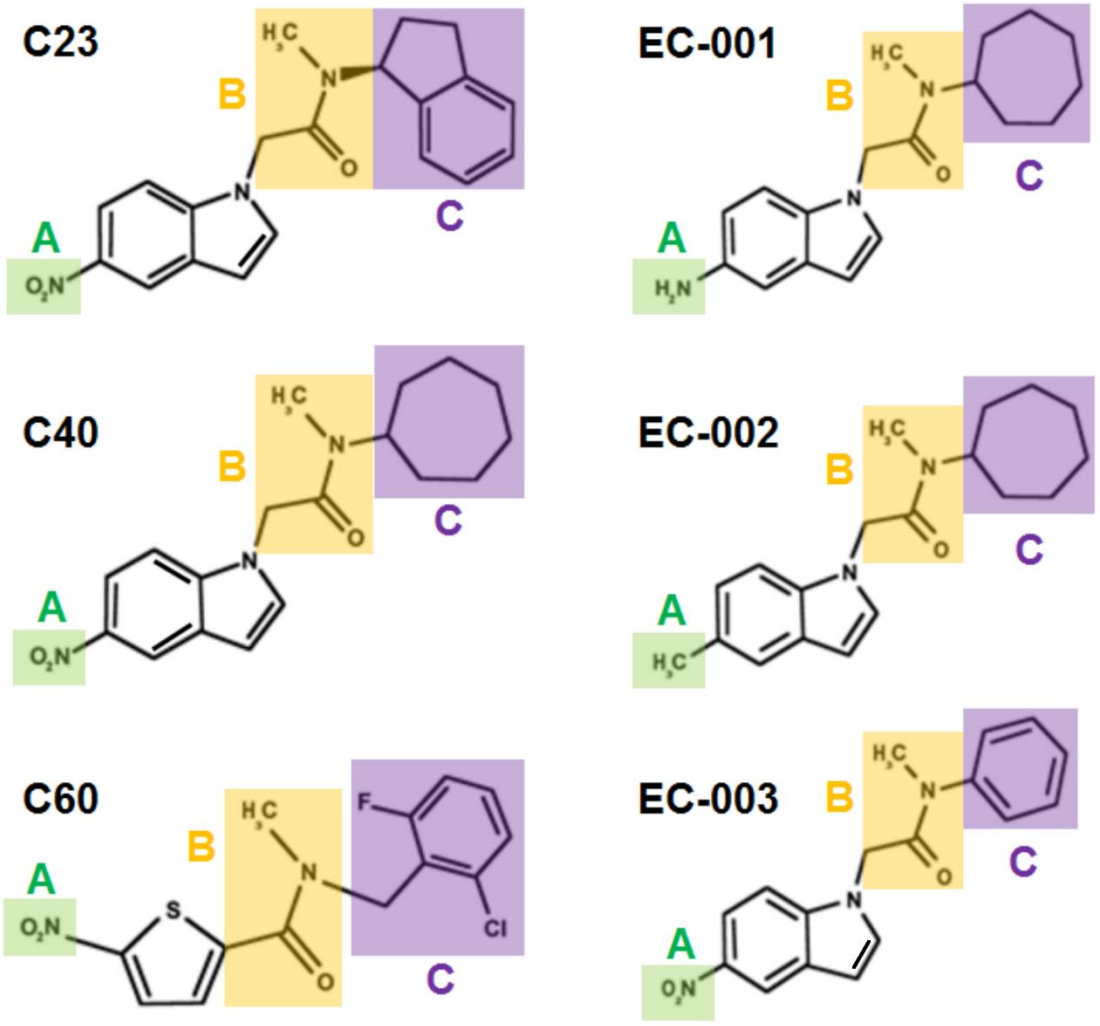

Figure 4.9 Notable structural features of novel antagonists

Structures of the three novel hP2X7R antagonists and the EC-001, EC-002 and EC-003 compounds described in this study. The common structural elements between C23, C40 and C60 are highlighted; A, an NO_2 group, B, an N-methyl amide group and C, a bulky ring structure. The structural modifications made in EC-001, EC-002 and EC-003 are also shown.

Compound activity was assessed against HEK293 cells stably expressing the hP2X4R as well as the rP2X3R (Figure 4.8). C40 and C60 showed little to no block of agonist-induced calcium responses mediated by both the hP2X4R and rP2X3R. C40 reduced hP2X7R-mediated calcium response by 84 ± 8% compared to 24 ± 6% and 4 ± 14% in the rP2X3R and hP2X4R respectively, whereas C60 reduced calcium response in the hP2X7R by 91 ± 5% compared to 33 ± 15% and 17 ± 4% in the rP2X3R and hP2X4R. These antagonists show a clear selectivity for inhibition of the hP2X7R (Figure 4.8A). In comparison, C23 significantly blocks all three P2XRs tested, decreasing calcium responses in cells expressing the hP2X7R, rP2X3R and hP2X4R by 73 ± 2%, 66 ± 6% and 46 ± 14% at 10 μM (Figure 4.8B). As such, C23 appears to act as a less selective antagonist, although inhibition caused by C40 and C60 is much more selective and acts primarily on the P2X7R. This suggests that C40 and C60 are of greater use in terms of study of the P2X7R specifically.

4.2.6 Structure-activity relationship studies of the novel antagonists

C23, C40 and C60 demonstrate some common structural features. Each compound features an NO_2 group (A), a central moiety consisting of an N-methyl amide group (B) and a large ring structure (C) (Figure 4.9). These aspects of the compound structures may be important in antagonist binding to the hP2X7R extracellular domain. A further three compounds were designed based around the common scaffold of the novel antagonists in order to investigate the importance of particular pharmacophore elements of the three structures (Figure 4.9). These compounds were bought from Enamine.

From these new structures, it is apparent that the NO_2 group (A, Figure 4.9) is not vital for the inhibitory activity of these compounds. EC-001, in which the NO_2 group in the C40 structure was replaced with NH_2, blocks 91 ± 1% of hP2X7R-mediated calcium response compared to C40 which blocked 71 ± 9% (Figure 4.10). EC-001 was a more effective antagonist than all three of the initial hits. However, the replacement of this group with

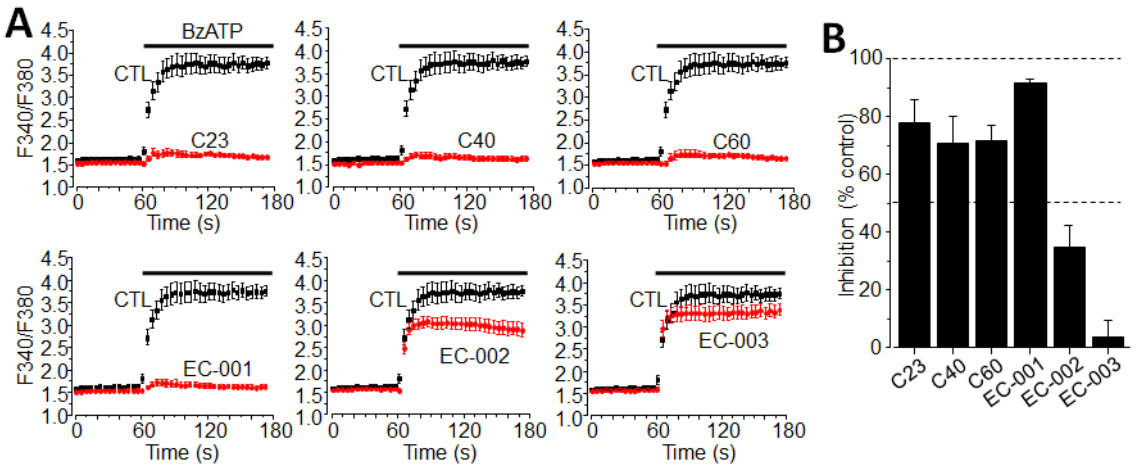

Figure 4.10 Effects of structurally altering the novel antagonists

(A) Representative FlexStation recording traces from HEK293 cells expressing the hP2X7R indicating calcium responses in response to the application of 300 µM BzATP after 60 s, with the control response shown in black and the compound response shown in red. The compounds indicated were applied at 10 µM. (B) Summary of inhibition resulting from application of 10 µM EC-001, EC-002 and EC-003 compared to C23, C40 and C60. Results are presented as mean ± SEM. from 8-12 wells of cells from 3-5 independent experiments.

CH_3 as in EC-002 greatly reduced the block of the BzATP-induced calcium response by approximately half that of C40, 35 ± 7% (Figure 4.10). This suggests that the ability to hydrogen bond in this group may play an important role in compound binding to the P2X7R.

Further to this, the size of the ring structures (C, Figure 4.9) was altered in order to determine whether the bulk in this region of the compound contributes to interactions between the antagonist and the receptor. EC-003 is a similar structure to C23 and C40 except for the ring structure (C) being replaced by an alternative ring moiety, in this instance a benzene ring. EC-003 reduced calcium responses in hP2X7R-expressing cells by 4 ± 6%, exhibiting no significant antagonism of the receptor and supporting the idea that a hydrophobic group of a size larger, or possibly less flat, than a benzene ring is critical in the interaction of these inhibitors with the hP2X7R (Figure 4.10).

4.3 Discussion

The information presented in this chapter shows the application of a structure-driven approach to identify four novel antagonists of the hP2X7R; C23, C40, C60 and EC-001 (Figure 4.1 to 4.5, 4.9 and 4.10). These compounds are able to inhibit physiological functions of the P2X7R such as agonist-induced large pore formation and cell death (Figure 4.6 and 4.7), although interestingly C60 specifically affects large pore formation (Figure 4.5). This study is the first to date to make use of the structural information available from the previously published crystal structure of the zfP2X4R in order to make selective P2XR antagonists.

The compound database in this study was screened against the hP2X7R ATP binding site, and as such it is highly likely that the antagonists discovered are competitive and interact with the orthosteric binding site. This could be considered a disadvantage due to the fact that competitive antagonism is surmountable and, if high enough levels of agonist are present, a higher concentration of antagonist must be applied to compensate.

In a therapeutic context this could be dangerous as administering higher concentrations of drug can lead to adverse side effects. However, the identification of competitive P2X7R antagonists means that a structure-based approach can be applied in order to reduce both the time and resources used. Such as approach means that antagonist discovery is much more efficient.

Two of the antagonists identified in this study showed subtype specificity for the P2X7R over other receptors including the P2X3R and the P2X4R (Figure 4.8). This specificity is vital for the development of therapeutic compounds, as P2XRs are expressed widely throughout the body (North, 2002). Whilst it would be advantageous to test these antagonists on additional members of the P2XR family, C40 and C60 did not inhibit the hP2X4R which shares the highest degree of sequence identity with the hP2X7R, suggesting that it is unlikely that these inhibitors strongly block other P2XR subtypes (although this is speculative and further experimentation would be beneficial). In contrast, C23 significantly inhibits both the hP2X4R and the rP2X3R in addition to the hP2X7R, indicating that this compound may interact with further members of the P2XR family and lacks selectivity.

The P2X7R has the ability to form large pores following sustained stimulation with an agonist. This pore allows permeability to large cations and fluorescent dyes of sizes up to 900 Da (Surprenant et al., 1996) and is crucial for the release of the inflammatory cytokine IL-1β, linking the P2X7R with the pathogenesis of diseases including chronic inflammatory and neuropathic pain and the aged-related macular degeneration responsible for loss of vision in the elderly. As such, the ability of C60 to preferentially block large pore formation as opposed to the small ion-conducting channel in hP2X7R-expressing cells is potentially exciting in terms of future drug development (Figure 4.5). The ~630 Da fluorescent dye YO-PRO-1 is unable to pass through the P2X7R when it is acting as an ion channel, which means the prevention of YO-PRO-1 entry by C60 provides evidence for the inhibition of large pore formation in the hP2X7R by this compound. However, there are some aspects of C60 activity which mean that it is not

entirely clear whether this compound acts exclusively at the large pore and as such alternative explanations must be considered. Inhibition of calcium responses occurs rapidly after addition of the agonist (Figure 4.5), which complicates this explanation since large pore formation is known to occur after prolonged stimulation of the P2X7R. It may be that other factors influence the ability of C60 to inhibit the receptor. One possibility is that the different assays used in this study show some variation in the concentration of calcium in their buffers; patch clamping was carried out in low divalent solution with calcium concentrations of 0.3 mM compared to the 1.5 mM calcium used when measuring calcium responses. From this it could be suggested that calcium may act as a co-factor for high affinity C60 binding to the protein. On the other hand, YO-PRO-1 uptake was measured in a buffer containing 0.3 mM calcium which complicates this explanation. Further investigation of the effect of the calcium content of assay buffers to C60 would be hugely beneficial in this regard, as would conducting the experiments shown in this chapter using P2X7R mutants which lack large pore forming activity. If C60 does indeed preferentially block the large pore, it may prove valuable in further mechanistic investigation of the P2X7R. It is a widely debated issue whether the large pore is mediated by the receptor itself or if activation of the receptor causes the large pore to open via a separate protein (Wei et al., 2016; Alberto et al., 2013). The ability of C60 to specifically block this large pore formation provides a further facet of evidence to suggest a distinct mechanism for large pore formation in the P2X7R from its ion channel function.

As well as its subtype specificity, C23, C40 and C60 show species specificity in that they inhibit the human but not rat P2X7R. This is a common pattern within P2X7R-specific antagonists and includes inhibitors including KN62 (Humphreys et al., 1998), AZ11645373 (Stokes et al., 2006) and SB203580 (Michel et al., 2006). These compounds were screened against the ATP binding region and as such it is likely that they act as competitive antagonists, with the difference between binding in the human and rat receptors possibly being caused by a variation in residues localised to the ATP

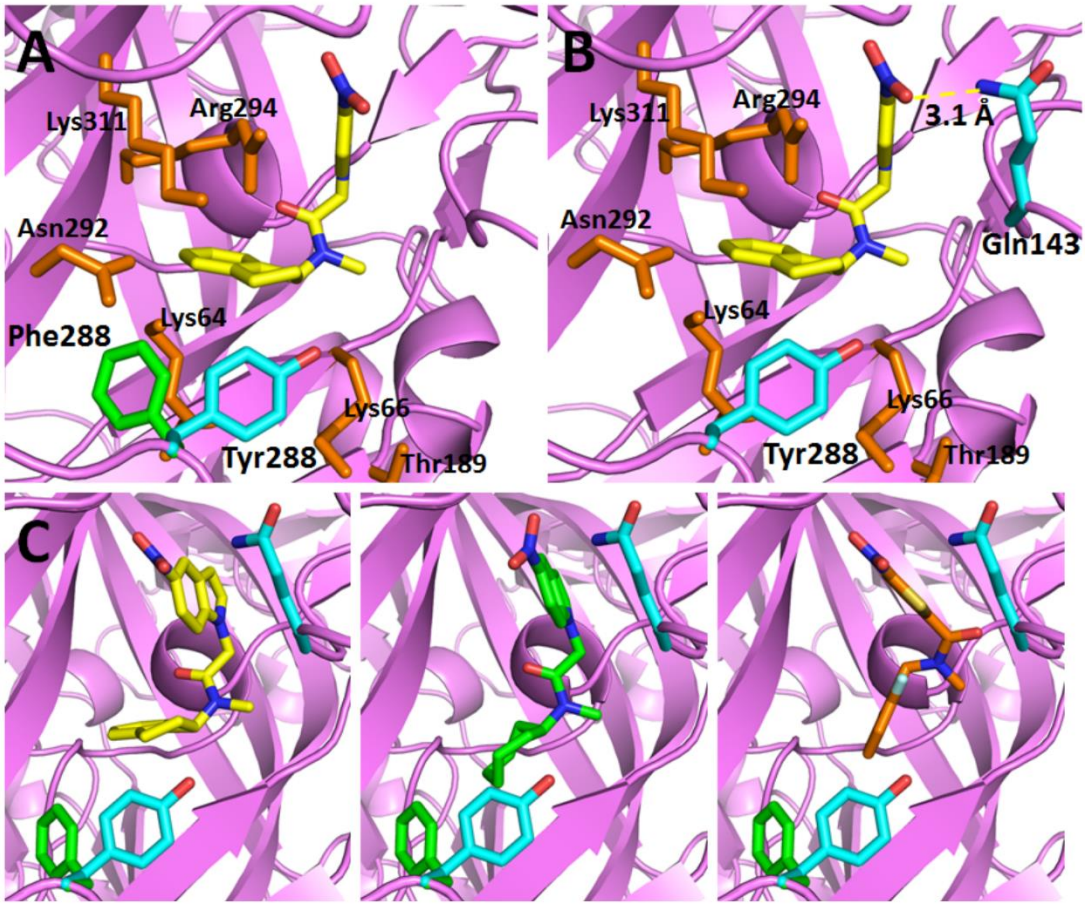

Figure 4.11 Residues which may influence compound-receptor interactions

(A) C23 docked to the P2X7R showing Tyr288 from the human receptor in cyan and Phe288 from the rat receptor in green. Conserved ATP binding residues are shown in orange. (B) C23 docked to the receptor with residues thought to interact with the antagonists shown in cyan. Conserved ATP binding residues are shown in orange. (C) The novel compounds C23, C40 and C60 (from left to right) shown docked as predicted by eHits to the hP2X7R, with potentially influential residues highlighted as sticks.

binding region. For example, the residue at position 288 is a Tyr in the hP2X7R but Phe in the rP2X7R. The homology model of the P2X7R on which this study is based predicts the Tyr residue to be flipped further out into the ATP binding pocket in the hP2X7R (Figure 4.11A) which may be caused by its OH group, which would clash with other residues in the receptor if it were to be in the same orientation as Phe in the rP2X7R. The size of the area of the binding pocket with which the antagonists can interact appears to be increased by the additional protrusion introduced by this particular conformation of the side chain of Tyr288. Such structural differences provide a potential explanation for why these compounds interact preferentially with the hP2X7R. Position 288 is occupied by Ser in all other P2XR subtypes except for the P2X6R, which has no equivalent residue (Figure 1.3). This may provide some explanation for the specificity of these compounds for the P2X7R subtype.

The three antagonists are structurally similar in several ways. They have a common central moiety consisting of an N-methyl amide group (B, Figure 4.9) in addition to a prominent NO_2 group at one end of the molecule (A, Figure 4.9) and bulky ring structures at the other (C, Figure 4.9). The recurrence of these common elements suggest that these components form the basis of this group of antagonists. When the NO_2 group in C40 is replaced with NH_2, the inhibitory activity of the resulting compound is greatly increased, as seen in EC-001 (Figure 4.9 and 4.10). Conversely, replacing this group to CH_3 as in EC-002 rendered the resulting compound much less effective (Figure 4.9 and 4.10), signifying that the ability to hydrogen bond is an important component of these inhibitors. This may be due to its ability to interact with residues in the receptor, for example Gln143 in the ATP binding pocket which appears ideally situated to form a hydrogen bond with this group (Figure 4.11B). In addition to this nitrogen-containing group, the size of the ring structures (C, Figure 4.9) may be important in mediating ligand-receptor interactions. Replacement of the cycloheptane group or the benzo-fused five membered heterocyclic group, found in C23 and C40 structures respectively, with a benzene ring produced a compound with no hP2X7R antagonistic activity (Figure 4.10).

This clearly signifies that the bulk of these groups relative to the benzene ring may be important in allowing these compounds to interact with the receptor. In addition, Tyr288 in the hP2X7R could be important in forming the pocket in which the ring structures from C23, C40 and C60 (C, Figure 4.9) nestle. In addition, visual assessment of the structures in this study suggests that the central common moiety is important. This may be due to the flexibility of the central linker, which would allow the antagonists to adopt the bent conformation predicted to be necessary for ligand binding (Figure 4.11). Further analysis of antagonist binding using the homology model in this way has provided suggestions for important aspects of the compound structures described in this study which could aid the future development of even more effective antagonists. As such, these antagonists form the basis of a potentially exciting novel group of hP2X7R antagonists.

Taken as a whole, the results discussed here detail the discovery of several novel hP2X7R antagonists by a structure-based approach. Interestingly, it describes the first P2X7R inhibitor to preferentially inhibit large pore formation mediated by this receptor without having an effect on the ion channel function.

Chapter 5

Identification of Residues Influencing P2X7-ligand Interactions

5.1 Introduction

The P2X7R is a prominent mediator of purinergic signalling, being activated by ATP within the body (Surprenant et al., 1996), and a promising drug target with involvement in a number of disorders (North and Jarvis, 2013). Having a thorough understanding of ligand binding to the P2X7R is a subject of great interest. Agonist binding to the P2XR family was first determined with any level of certainty when the ATP-bound zfP2X4R crystal structure was solved (Hattori and Gouaux, 2012). However, prior to this a number of mutagenesis studies provided valuable insights into gross regions, as well as individual residues, which are important in ligand binding to the P2X7R. In the P2X7R there are nine core residues identified in playing a direct role in ATP binding which are contributed from two adjacent subunits. The first subunit provides four hydrophillic residues, Lys64, Lys66, Thr189 and Lys193, and two hydrophobic residues, Leu191 and Ile228 (the P2X7R does not possess an equivalent residue to Leu217 in the zfP2X4R structure at this subunit). The second subunit contributes three hydrophilic residues, Asn292, Arg294, and Lys311 (Figure 5.1). These residues have been shown to be fundamental in the stimulation of P2X7R activity by ATP (Worthington et al., 2002; Schwarz et al., 2009; Browne et al., 2010; Jiang et al., 2013). In addition to the essential residues, there are further sections of the P2X7R surrounding the ATP binding site which have an influence on receptor activation. For example, Asn284 in the rP2X7R has been shown to account for the higher sensitivity of this receptor to ATP and Asn284 in combination with Lys127 governs its higher sensitivity to BzATP (Young et al., 2007).

In order to investigate additional, previously unexplored residues which may play a role in agonist interactions with the P2X7R, potentially influential amino acids were identified using the P2X7R homology models and these residues were subjected to site-directed mutagenesis. Patch-clamp recording was subsequently used to analyse the function of these mutants. This chapter details three residues which were identified to have separate, distinct effects on the hP2X7R. The effects of these mutations on receptor function and expression are described.

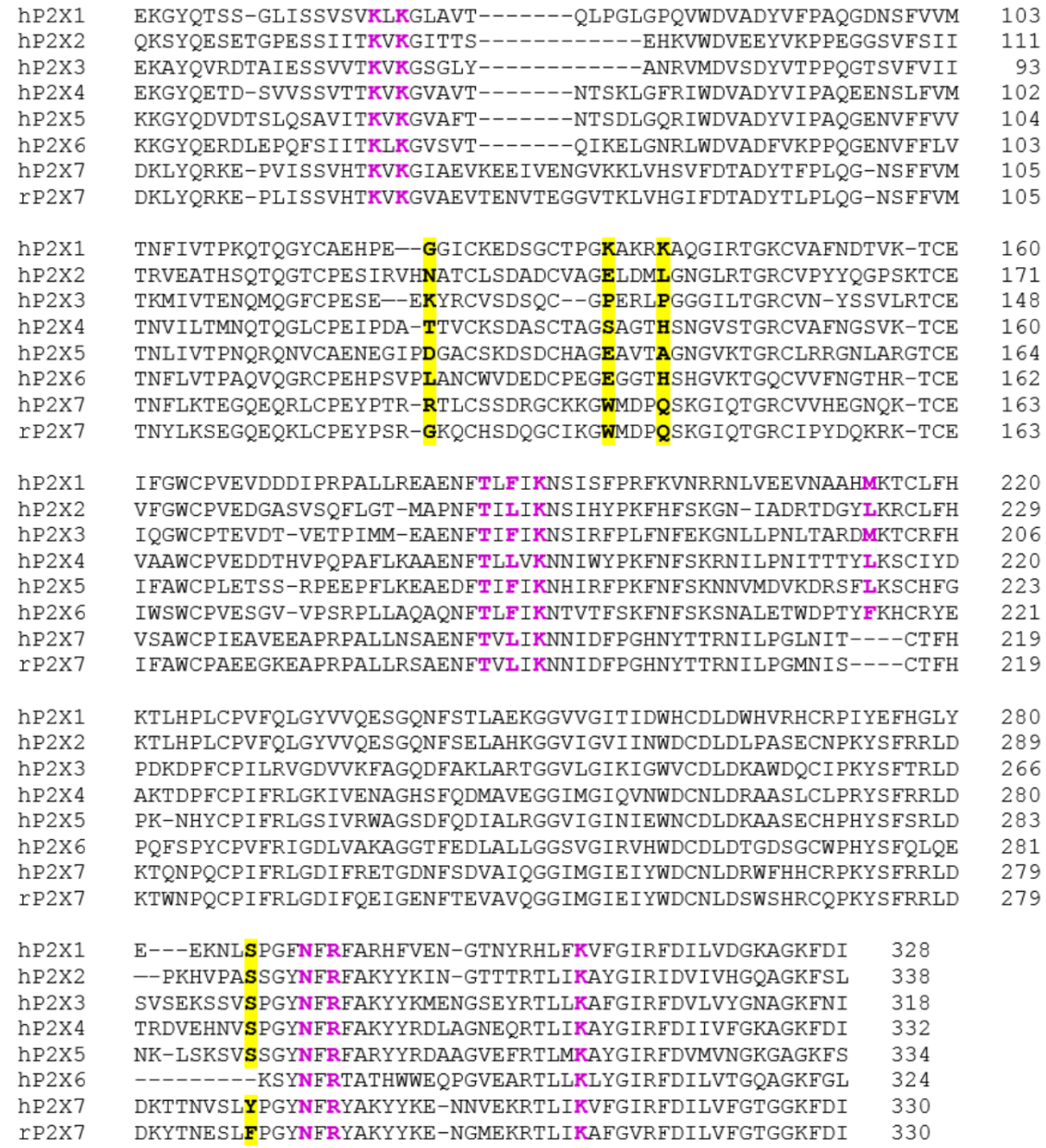

Figure 5.1 Sequence alignment of the human P2XRs and the rat P2X7R

Alignment of P2XR subunit sequences relevant to this study as determined by Clustal Omega. The ATP binding residues are shown in pink and the residues investigated in this chapter are highlighted in yellow.

5.2 Results

5.2.1 Effect of Arg126 mutation on hP2X7R-mediated currents

As outlined in chapter 3, homology models of the P2X7R can be used as a tool to make predictions about the location of different residues and the movement of the protein. Therefore, as a first approach, hP2X7R models were used to identify amino acids that may influence receptor-agonist interactions. These residues were identified by examining the ATP binding pocket in both the agonist-free closed states and the ATP or BzATP-bound open states, where docking experiments identified the likely binding sites of these two agonists. The first of these residues was an arginine at position 126 in the hP2X7R (Arg126). Arg126 is adjacent to Arg125, which plays a vital role in the gating of the P2X7R by ADP ribosylation (Adriouch et al., 2008) and Lys127, which when paired with Asn284 partly determines the sensitivity of the rP2X7R to ATP and BzATP (Young et al., 2007) (Figure 5.1). This amino acid overhangs the ‘entrance’ to the ATP binding pocket (Figure 5.2A). The large, positively charged side chain of Arg126 may aid binding due to its potential to attract the phosphate group of both ATP and BzATP. As such, Arg126 was substituted by site-directed mutagenesis for the uncharged residue alanine to determine whether this may be the case.

Patch-clamp recording of cells transfected with the R126A hP2X7R mutant was used to investigate the effects of this mutation on receptor currents (Figure 5.2B and C). These recordings showed BzATP-evoked currents to be similar in the WT and R126A mutant receptor; both the maximal current (7268 ± 744 pA and 6242 ± 1244 pA for the WT and R126A receptors, respectively) and EC_{50} values (39 ± 2 µM and 45 ± 6 µM for the WT and R126A receptors, respectively) were not significantly different (Figure 5.2D). Because of this lack of effect, there was no further investigation of this residue.

5.2.2 Effect of mutating Trp139 on hP2X7R-mediated currents

The second residue to be mutated was the Trp residue at position 139 (Trp139) (Figure

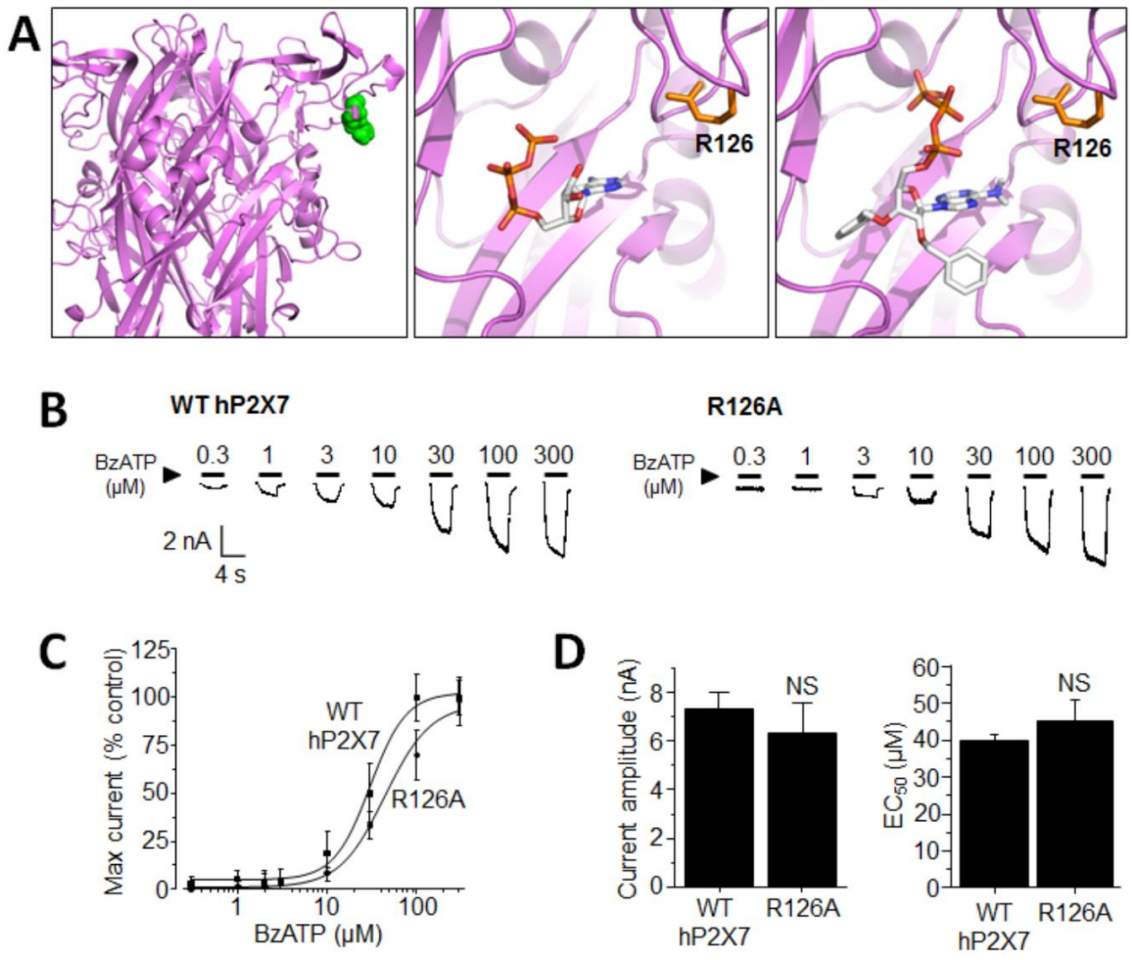

Figure 5.2 Summary of the effect of mutating Arg126 on hP2X7R function

(A) Location of Arg126 in the hP2X7R shown in green (left) and expanded views showing its location in relation to the predicted binding site of ATP (middle) and BzATP (right). (B) Representative traces of BzATP-evoked currents from cells transfected with the WT or R126A hP2X7R. (C) Mean BzATP dose-response (DR) relationship curves of currents from cells expressing the WT or R126A hP2X7R. The solid lines are fits of the data to the Hill equation. (D) Bar chart summary of the mean current amplitudes evoked from cells transfected with the WT or R126A hP2X7R by 300 μM BzATP and the mean EC_{50} for BzATP. NS, not significant compared to WT hP2X7R.

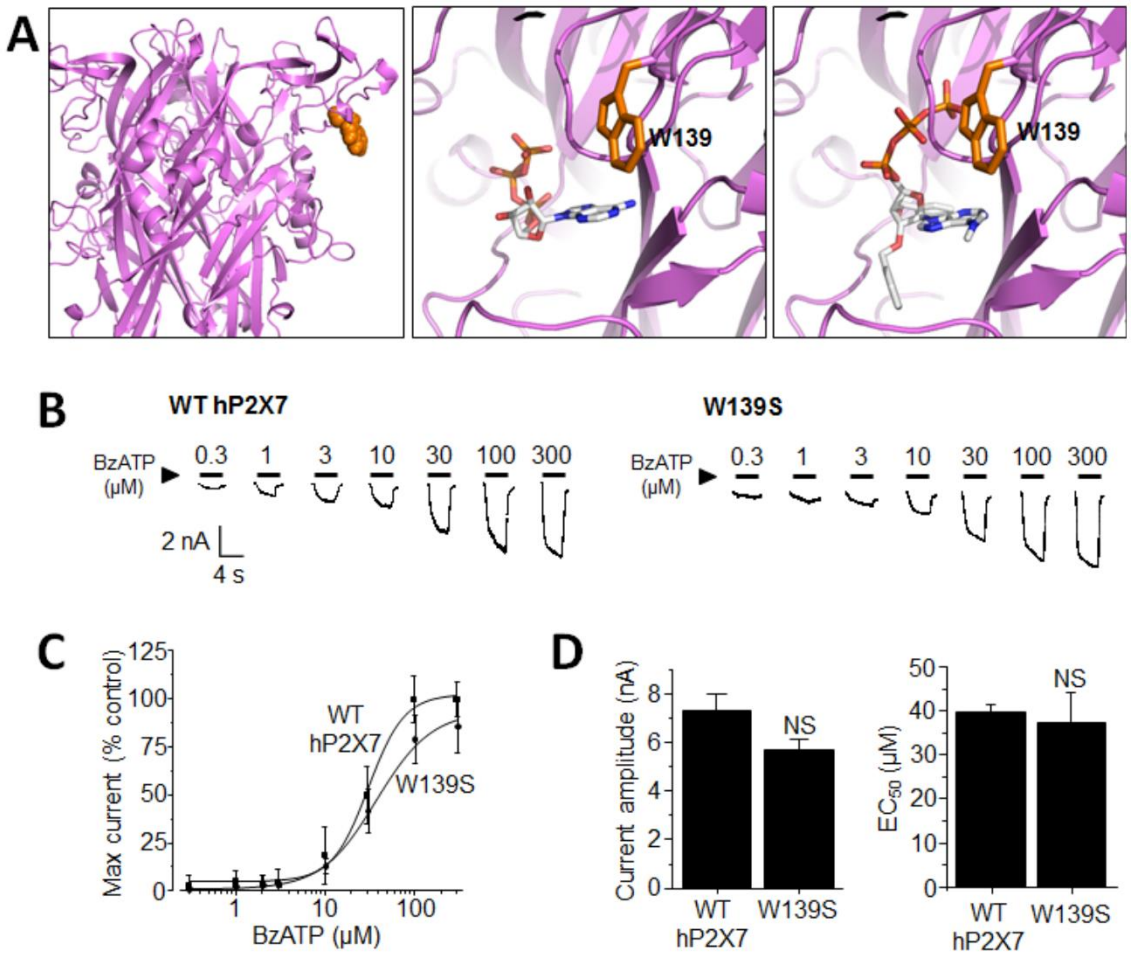

Figure 5.3 Summary of the effect of mutating Trp139 on hP2X7R function

(A) Location of Trp139 in the hP2X7R shown in orange (left) and expanded views showing its location in relation to the predicted binding site of ATP (middle) and BzATP (right). (B) Representative traces of BzATP-evoked currents from cells transfected with the WT or W139S hP2X7R. (C) Mean BzATP DR relationship curves of currents from cells expressing the WT or W139S hP2X7R. The solid lines are fits of the data to the Hill equation. (D) Bar chart summary of the mean current amplitudes evoked from cells transfected with the WT or W139S hP2X7R by 300 μM BzATP and the mean EC_{50} for BzATP. NS, not significant compared to WT hP2X7R.

5.1). As with Arg126, Trp139 is located at the ‘entrance’ to the ATP binding pocket (Figure 5.3A). This amino acid was mutated in order to determine whether it could influence the access of agonists to the binding pocket. This residue is fully conserved across the P2X7Rs from different species but in other subtypes varies greatly, consisting of Glu, Ser, Pro, or Lys (Figure 5.1). Trp139 was mutated to the smaller serine to establish whether the large bulk of the Trp residue influences ligand binding. Evaluation using patch-clamp recording also showed the BzATP-evoked currents from the W139S hP2X7R mutant to be similar to the WT (Figure 5.3B and C). The maximal current (7268 ± 744 pA and 5857 ± 429 pA for the WT and R126A receptors, respectively) and EC_{50} values (39 ± 2 μM and 37 ± 7 μM for the WT and R126A receptors, respectively) were not significantly different (Figure 5.2D). This residue was also not studied further.

5.2.3 Effect of mutating Gln143 on hP2X7R-mediated currents

Gln143 is found in close proximity to Trp139 and is present in P2X7Rs from all species except for the guinea pig, where it is Lys. Gln143 is located more centrally in the ATP binding pocket, close to the area where the adenine ring is predicted to bind by docking experiments (Figure 5.4A). The orientation of this residue in the P2X7R is indicated in the model to be angled in such a way that it leads to a sizeable ‘dip’ in the available ATP binding pocket, reducing the potential interaction between the agonist and the receptor surface. Site-directed mutagenesis was used to mutate Gln143 to two different residues; His as seen in the hP2X4R and hP2X6R (Q143H) (Figure 5.1), and Arg (Q143R) which was used to test whether introducing a consistent positive charge at this position would affect receptor activation.

Q143R and Q143H hP2X7R mutant function was characterised by patch-clamp recording. Figures 5.4 and 5.5 show the response of each of these mutants to BzATP and ATP, respectively. The Q143H current response to BzATP and ATP was comparable

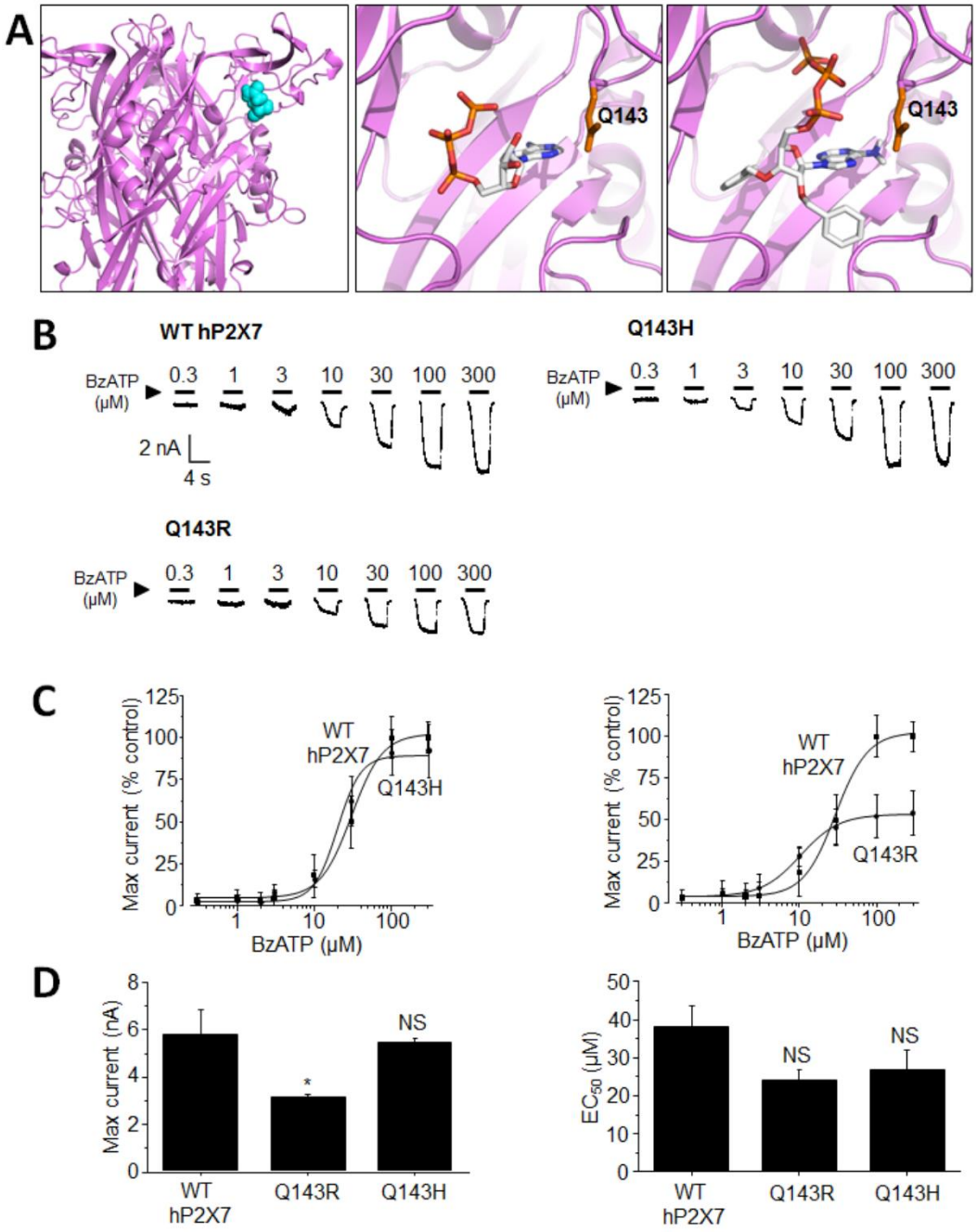

Figure 5.4 Effect of mutating Gln143 on BzATP-evoked currents

(A) Location of Gln143 in the hP2X7R shown in cyan (left) and expanded views showing its location in relation to the predicted binding site of ATP (middle) and BzATP (right). (B) Representative traces of BzATP-evoked currents from cells transfected with the WT, Q143H or Q143R hP2X7R. (C) Mean BzATP DR relationship curves of currents from cells expressing the WT or W139S hP2X7R. The solid lines are fits of the data to the Hill equation. (D) Bar chart summary of the mean current amplitudes evoked from cells transfected with the WT, Q143H or Q143R hP2X7R by 300 μM BzATP and the mean EC_{50} for BzATP. * $p<0.05$, NS, not significant compared to the WT hP2X7R.

to the WT receptor (Figure 5.4B and C and 5.5A and B, respectively). The maximal mutant current was 5382 ± 243 pA in response to BzATP and 4821 ± 853 pA to ATP, showing no significant difference from the WT (Figure 5.4D and 5.5C). However, the maximal currents elicited by BzATP and ATP from the Q143R mutant were 3108 ± 165 pA for BzATP and 3021 ± 570 pA for BzATP, 54% and 53% of the WT hP2X7R current respectively ($p<0.05$). From this it appears that the introduction of a histidine residue does not affect the receptor response, whereas Q143R reduces the receptor function by approximately half.

In addition, the DR data was analysed to determine the EC_{50} for BzATP and ATP. The EC_{50} for the WT hP2X7R was 37.8 ± 5.8 μM for BzATP and 0.9 ± 0.3 mM for ATP. These values for both the Q143R and Q143H mutants were very similar, indicating no statistically significant different in sensitivity to these two ligands (Figure 5.4D and 5.5C). Together, this data indicates that the introduction of an Arg residue at position 143 resulted in a loss of hP2X7R function which did not occur when this residue was replaced with His, although neither of these mutations had an impact on the agonist sensitivity of the receptor.

5.2.4 Effect of mutating Tyr288 on hP2X7R-mediated currents

The residue at position 288 is a Tyr in the hP2X7R. The predicted binding modes of ATP and BzATP appear to require these agonists to bend around this residue, as the bulk of the aromatic side chain protrudes into the binding pocket (Figure 5.6A). It is therefore possible that Tyr288 plays a role in facilitating the agonist binding position in the hP2X7R. In other subtypes of the P2XR, this position is occupied by Ser, which has a much smaller side chain (Figure 5.1). This may contribute in part to the difference in agonist affinity between the P2X7R and other P2XRs, allowing ATP or BzATP to adopt a conformation which is not constrained by the bulk of Tyr288. In order to test whether this is the case, this residue was mutated to several alternatives by site-directed mutagenesis. Ser, Gly,

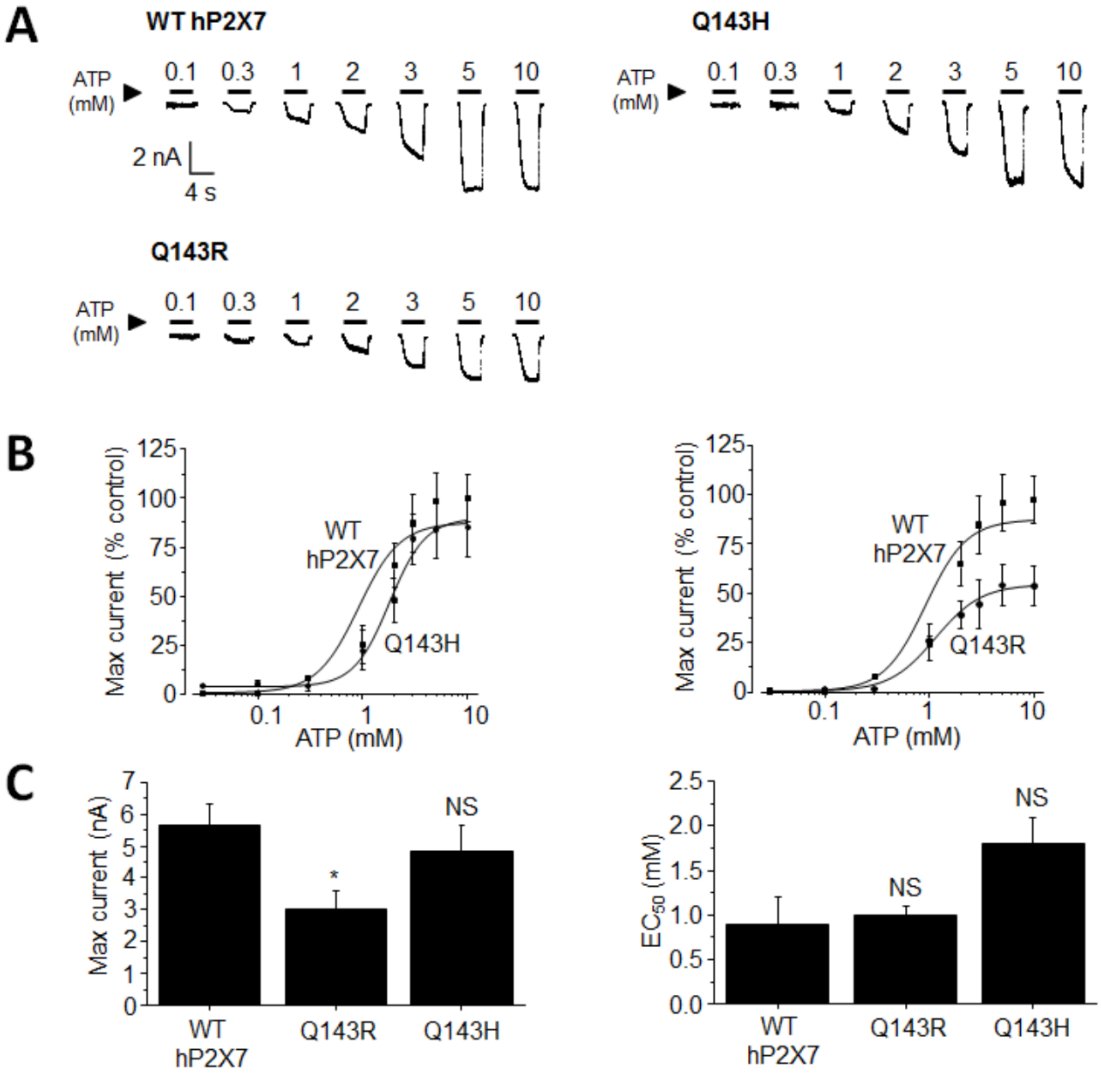

Figure 5.5 Effect of mutating Gln143 on ATP-evoked currents

(A) Representative traces of ATP-evoked currents from cells transfected with the WT, Q143H or Q143R hP2X7R. (B) Mean ATP DR relationship curves of currents from cells expressing the WT or W139S hP2X7R. The solid lines are fits of the data to the Hill equation. (C) Bar chart summary of the mean current amplitudes evoked from cells transfected with the WT, Q143H or Q143R hP2X7R by 10 mM ATP and the mean EC_{50} for ATP. * $p<0.05$, NS, not significant compared to the WT hP2X7R.

Phe and Val (Y288S, Y288G, Y288F and Y288V) were introduced to study the effect of introducing amino acids with side chains of varying sizes.

The effect of mutating Tyr288 on the hP2X7R response to both ATP and BzATP was tested, and substitution of this residue for alternative amino acids with smaller side chains showed a similar response for both of these agonists. Each had extremely small responses which could only be seen in response to high concentrations of these agonists (300 µM BzATP or 10 mM ATP) (Figure 5.6 and 5.7) and as such mutating Tyr288 to Gly, Ser or Val essentially abolished the current response in the hP2X7R. The Y288G, Y288S and Y288V mutants elicited currents of 120 ± 41, 115 ± 53 and 101 ± 22 pA in response to 300 µM BzATP, respectively (Figure 5.6B-D) and 75 ± 25, 115 ± 53 and 111 ± 24 pA in response to 10 mM ATP, respectively (Figure 5.7A-C).

The influence of the Y288F mutation on receptor activity was investigated by a combination of patch-clamp recording and immunofluorescent staining. The size of the side chain of the Tyr residue makes it appear in the homology model of the hP2X7R that this bulk may play a role in determining the conformation that agonists adopt when binding to the ATP binding site (Figure 5.6A). As such Tyr288 was mutated to Phe which has a side chain of comparable bulk to that of Tyr in order to determine whether the Y288F substitution could recover some, or all, of the lost hP2X7R activity. This would be expected, as in the rat isoform of the P2X7R residue 288 is a Phe (Figure 5.1). In response to ATP, the current elicited from the Y288F hP2X7R receptor was comparable to that of the other mutants with a maximal current of 140 ± 61 pA (Figure 5.7C). This is an indication that Phe does not help to restore receptor function in this instance. In contrast, when exposed to high concentrations of BzATP the Y288F hP2X7R mutant exhibited a noticeable, though not statistically significant, current. In response to 300 µM BzATP an average current amplitude of 294 ± 48 pA was observed (Figure 5.6D) which, whilst being almost 3 times the size of the largest current induced from the other mutants, was still less than 10% of the control WT hP2X7R-expressing cells.

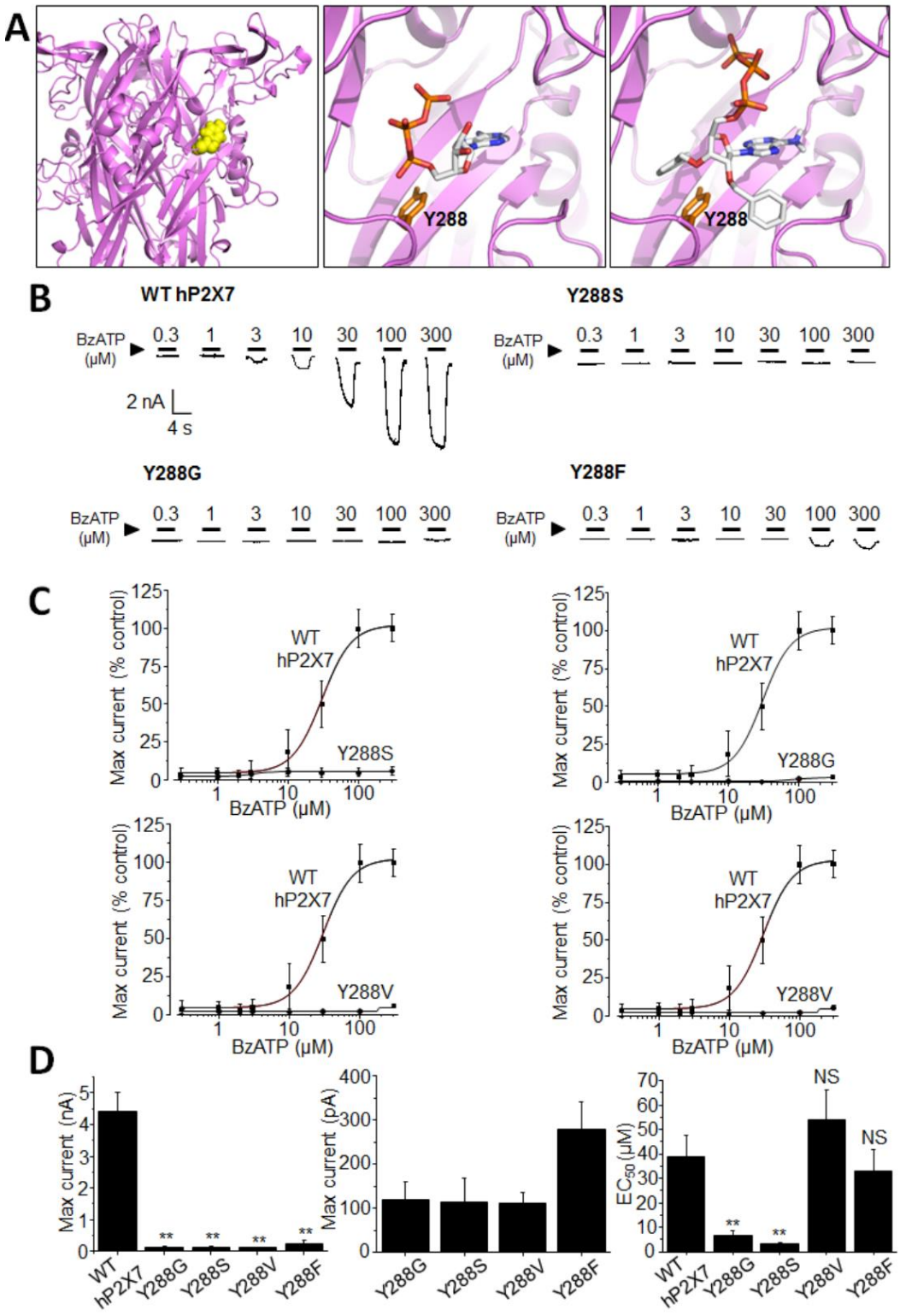

Figure 5.6 Effect of mutating Tyr288 on BzATP-evoked currents

(A) Location of Tyr288 in the hP2X7R shown in yellow (left) and expanded views showing its location relative to the predicted binding site of ATP (middle) and BzATP (right). (B) Representative traces of BzATP-evoked currents from cells transfected with the WT or mutant hP2X7R. (C) Mean BzATP DR curves of currents from the WT or mutant hP2X7R. Solid lines are fits of the data to the Hill equation. (D) Bar chart summary of the mean current from cells transfected with the WT or mutant hP2X7R by 300 μM BzATP and the mean EC_{50} for BzATP. ** $p<0.01$, NS, not significant compared to WT hP2X7R.

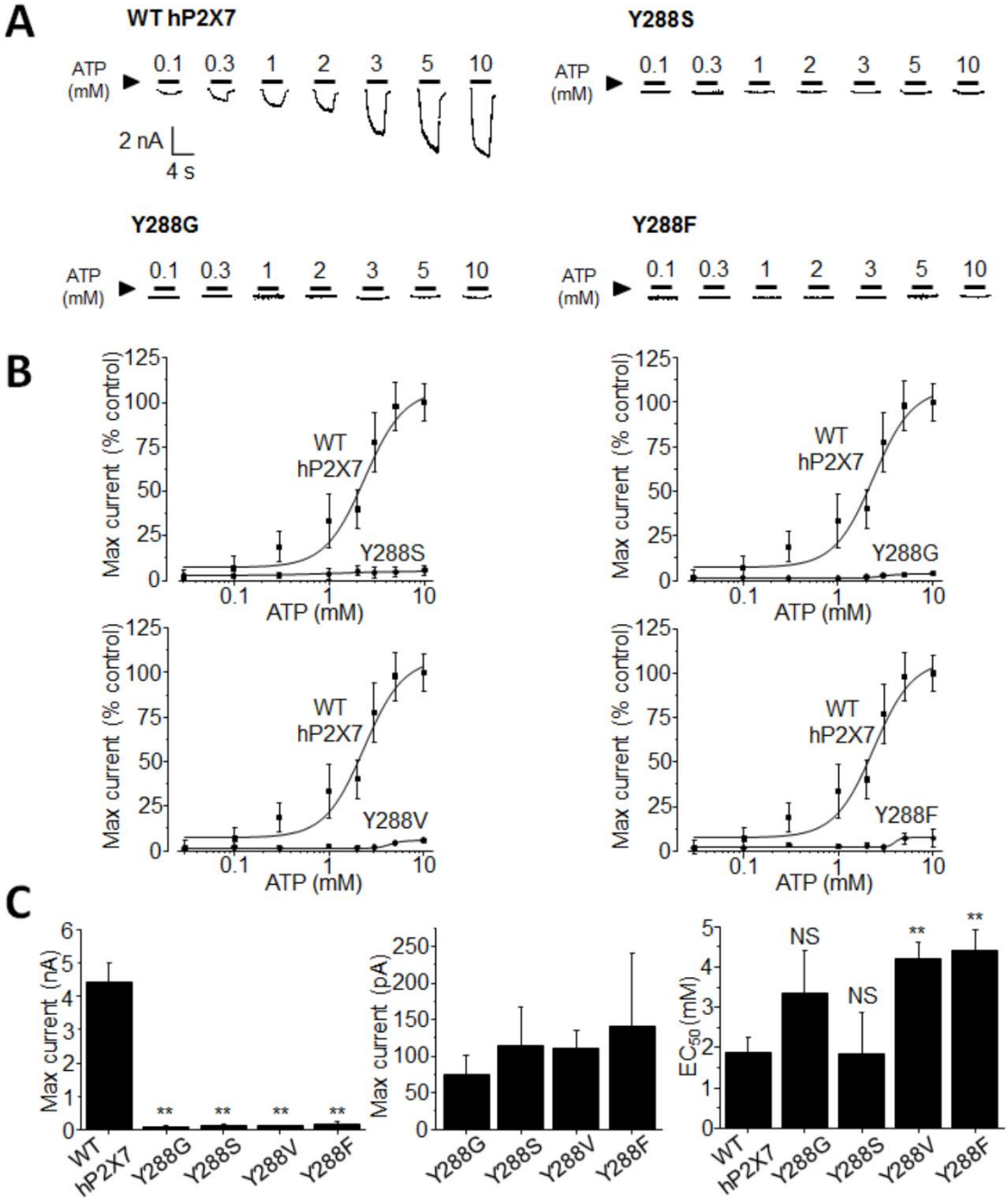

Figure 5.7 Effect of mutating Tyr288 on ATP-evoked currents

(A) Representative traces of ATP-evoked currents from cells transfected with the WT or indicated mutant hP2X7R. (B) Mean ATP DR relationship curves of currents from cells expressing the WT or indicated mutant hP2X7R. The solid lines are fits of the data to the Hill equation. (D) Bar chart summary of the mean current amplitudes evoked from cells transfected with the WT or indicated mutant hP2X7R by 10 mM ATP and the mean EC_{50} for ATP. ** $p<0.01$, NS, not significant compared to WT hP2X7R.

Further to this, the DR data was assessed to determine whether these mutations influenced the EC_{50} of ATP and BzATP. The ATP EC_{50} value was 1.9 ± 0.4 mM for hP2X7 WT, 3.4 ± 1.0 mM for Y288G and 1.8 ± 1.1 mM for Y288S respectively ($p<0.01$), and 4.2 ± 0.4 mM for Y288V and 4.4 ± 0.5 mM for Y288F (not significant) (Figure 5.7C).

Conversely the BzATP EC_{50} value was 38.6 ± 9.1 µM for hP2X7 WT, 6.6 ± 1.9 µM for Y288G and 3.0 ± 0.7 µM for Y288S respectively (not significant), and 54.1 ± 12.2 µM for Y288V and 33.1 ± 8.8 µM for Y288F which were different from the WT ($p<0.01$) (Figure 5.6D). Mutating Tyr288 seems to have a varying effect on agonist sensitivity depending on the agonist and the residue that Tyr is substituted for; there appears to be an inverse effect on the sensitivity of each mutant depending on whether it is exposed to ATP or BzATP. This may be due to the maximal current being so small for the mutants, meaning that the EC_{50} calculations could be skewed. It is also possible that there are different molecular interactions occurring not obvious when exploring the homology model.

5.2.5 Effect of mutating Y288 on P2XR expression

In order to explore potential reasons for the loss of function seen in Y288V and Y288F hP2X7R mutants, cells were stained by immunocytochemistry to examine the subcellular distribution of the protein in P2X7R-transfected HEK293 cells. Due to the unreliable nature of anti-P2X7 antibodies in identifying different isoforms of the receptor (Anderson and Nedergaard, 2006), an alternative antibody was used for the staining. Both the WT and mutant receptors in this study possessed a C-terminal EYMPME (EE) tag, and as such an anti-EE antibody which has previously been shown to be effective in the identification of EE-tagged P2X7R proteins (Bradley et al., 2011a; Roger et al., 2010a) was used to explore the location of WT and mutants P2X7Rs. Figure 5.8 shows representative images illustrating the effect of introducing the Y288V or Y288F mutation into the hP2X7R on subcellular localisation.

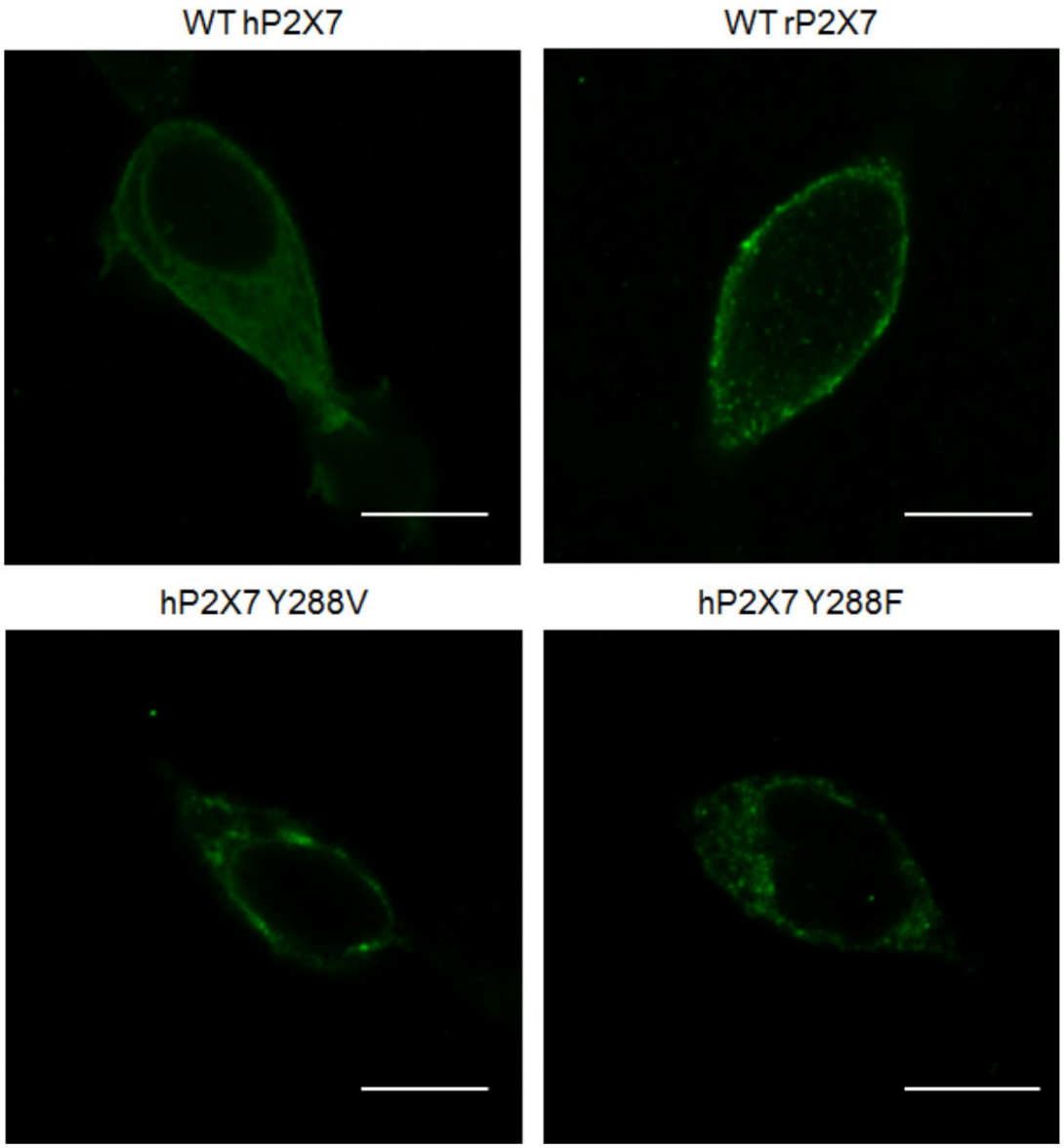

Figure 5.8 Effect of mutating Y288 on receptor expression

Representative confocal images of fluorescently stained HEK293 cells transfected with either the WT or mutant P2X7R as indicated, determined using an anti-EE antibody. The scale bar is 10 μm.

Immunostaining of the WT rP2X7R was shown to be localised primarily to the cell membrane, with minimal fluorescence throughout the rest of the cell compared to the WT hP2X7R which was much more widely distributed throughout the whole of the cell. In comparison to these WT receptors, introduction of the Y288V mutation into the hP2X7R appears to lead to reduced levels of the protein at the cell surface and cause brighter focal points. It is possible that mutating the Tyr288 residue has an impact on the trafficking of the receptor to the cell surface, which would provide an explanation for why these mutant receptors show only a minimal current even when high concentrations of agonists were applied.

5.2.6 Impact of introducing reciprocal mutations from the human to rat receptor on BzATP-induced currents

Further to the residues which were designed above based on the P2X7R homology model, additional residues were investigated based on the difference in sequence between the human and rat isoforms of the receptor (Figure 5.1). As introduced above, the rP2X7R is significantly more sensitive to activation by ATP and BzATP compared to the hP2X7R. Previously residues have been identified which are pivotal for mediating this difference in sensitivity but it is possible that there are additional ones which have an influence on this aspect of P2X7R activation. As such, a series of mutants were produced throughout the hP2X7R which substituted residues found in the human isoform of the receptor with that in the rat. These plasmids were kindly provided by Helen Bradley who previously worked in the Jiang group. As with the previous batch of mutants, an initial screen was carried out in order to determine which of the mutations may make the hP2X7R more sensitive to activation by BzATP.

Patch-clamp recording of HEK293 cells expressing the 13 mutants available revealed a range of responses (Figure 5.9A), a large number of which were reduced, whilst only one mutant appeared to result in a significant increase in BzATP-induced hP2X7R-

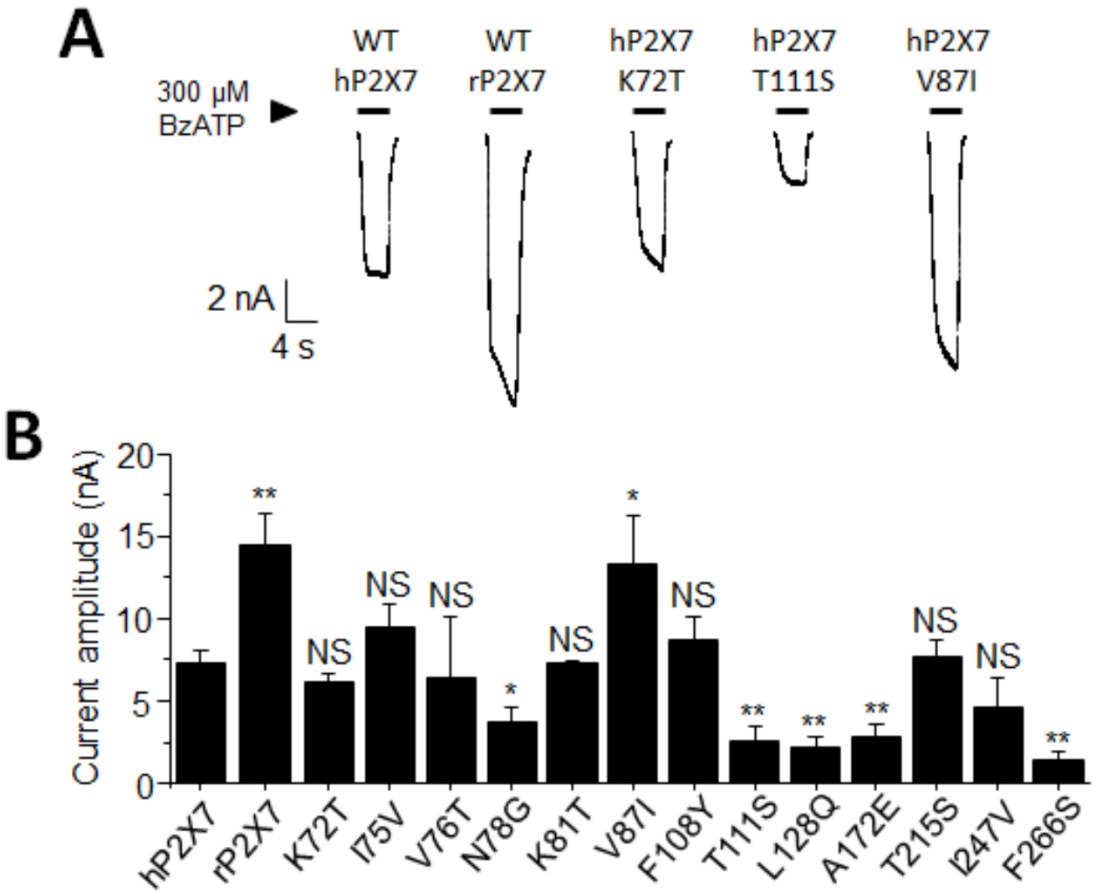

Figure 5.9 Electrophysiological screen of reciprocal human-to-rat mutations

(A) Representative current traces of BzATP-evoked currents from HEK293 cells expressing the WT hP2X7R, the WT rP2X7R or mutant hP2X7Rs as indicated. (B) Bar chart summary of the mean current amplitudes evoked from cells transfected with the WT hP2X7R, the WT rP2X7R or the indicated mutant by 300 µM BzATP. Values are taken from 6 recordings from 3-4 individual cells. * $p<0.05$, ** $p<0.01$, NS, not significant * compared to WT hP2X7R.

mediated currents (Figure 5.9B). This was V87I, which displayed a mean maximal current of 15021 ± 3371 pA in contrast to 7268 ± 744 pA displayed by the WT hP2X7R ($p<0.05$). The degree to which the V87I hP2X7R response was increased in this initial screen was comparable to the WT rP2X7R, so to further investigate this further in-depth functional studies were carried out as described below.

5.2.7 Effect of mutating residue 87 on hP2X7R-mediated currents

From the initial screen of residues which may have an effect on the species-specific response of the human and rat P2X7Rs, the V87I mutation in the hP2X7R was particularly interesting. The introduction of this mutation into the human receptor significantly increased the average maximal current response to 300 μM BzATP compared to the WT hP2X7R (Figure 5.9). The contribution of this residue to species-mediated differences in P2X7R response to BzATP was further investigated by both patch-clamp recording (Figure 5.10 and 5.11) and immunofluorescent staining (Figure 5.12) of both human and rat mutant P2X7Rs. Application of BzATP to the V87I hP2X7R mutant elicited a current which was significantly larger than the WT hP2X7R at all concentrations, whilst being smaller than that seen at the WT rP2X7R. Conversely, the I87V rP2X7R mutant displayed a current that was smaller than the WT rP2X7R whilst being larger than the WT hP2X7R at all concentrations (Figure 5.10A and B), indicating that this residue may play a partial role in determining the response of the receptor to BzATP.

The BzATP DR data from these electrophysiological tests was further analysed in order to determine the average maximal responses and EC_{50} of each of these receptors. Figure 5.10A-C shows, the maximal currents mediated by WT and mutant P2X7Rs; 3712 ± 430 pA for WT hP2X7R and 5761 ± 846 pA for V87I hP2X7R, which was significantly larger ($p<0.05$), whilst these values were 9828 ± 1576 pA for the WT rP2X7R, and 8007 ± 976 pA for I87V rP2X7R. Whilst the current response for the WT rP2X7R was larger

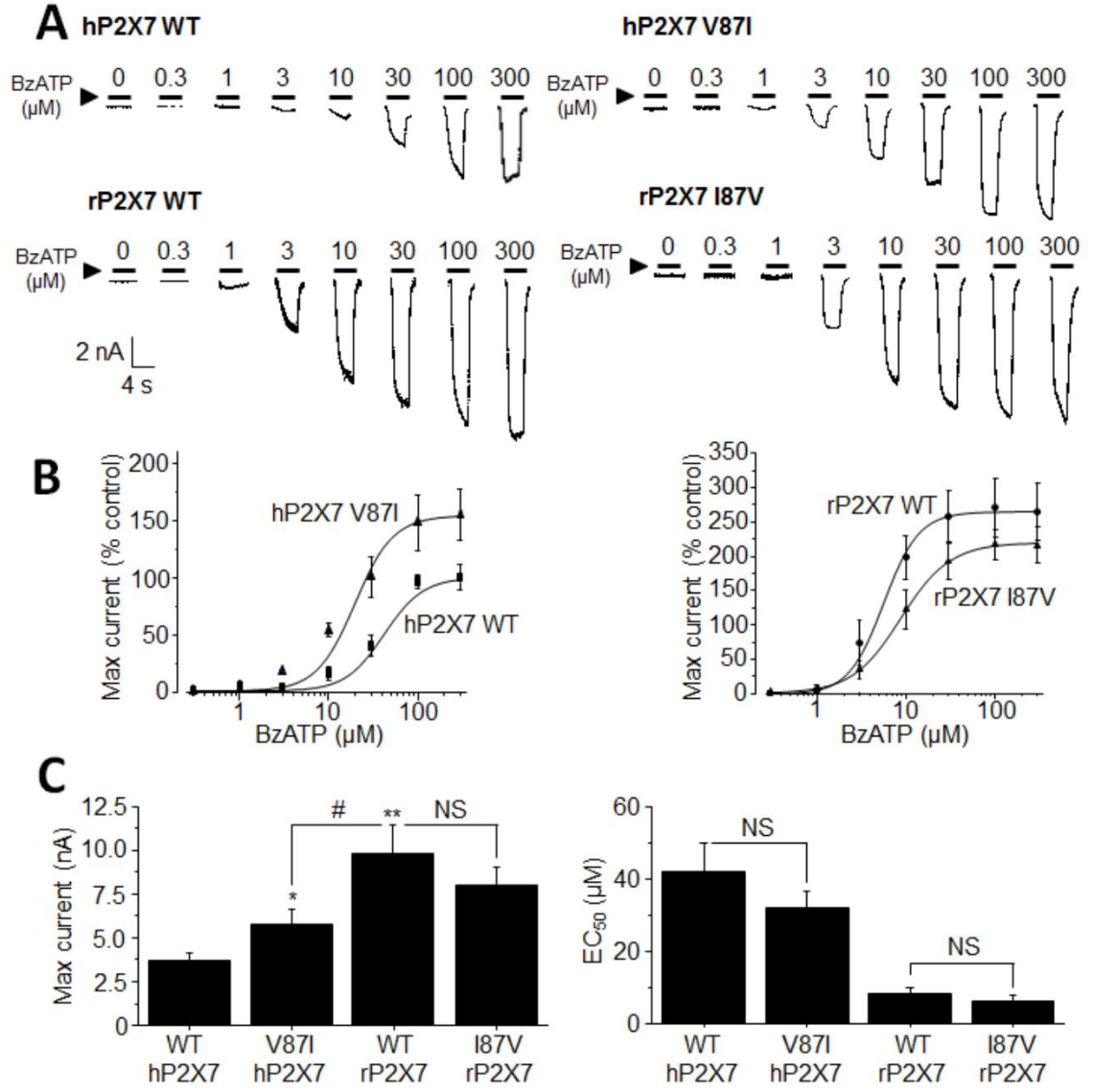

Figure 5.10 Effect of V87I and I87V on BzATP-evoked currents

(A) Representative traces of BzATP-evoked currents from HEK293 cells expressing the WT receptor or mutant indicated. (B) Mean BzATP DR relationship curves of currents from cells expressing the WT P2X7R compared with the indicated mutant. The solid lines are fits of the data to the Hill equation. (C) Bar chart summary of the mean current amplitudes evoked from cells transfected with the WT hP2X7R or the indicated mutant by 300 μM BzATP and the mean EC_{50} for BzATP. * and # $p<0.05$, ** $p<0.01$, NS, not significant, * is compared to WT hP2X7R and # to the WT rP2X7R.

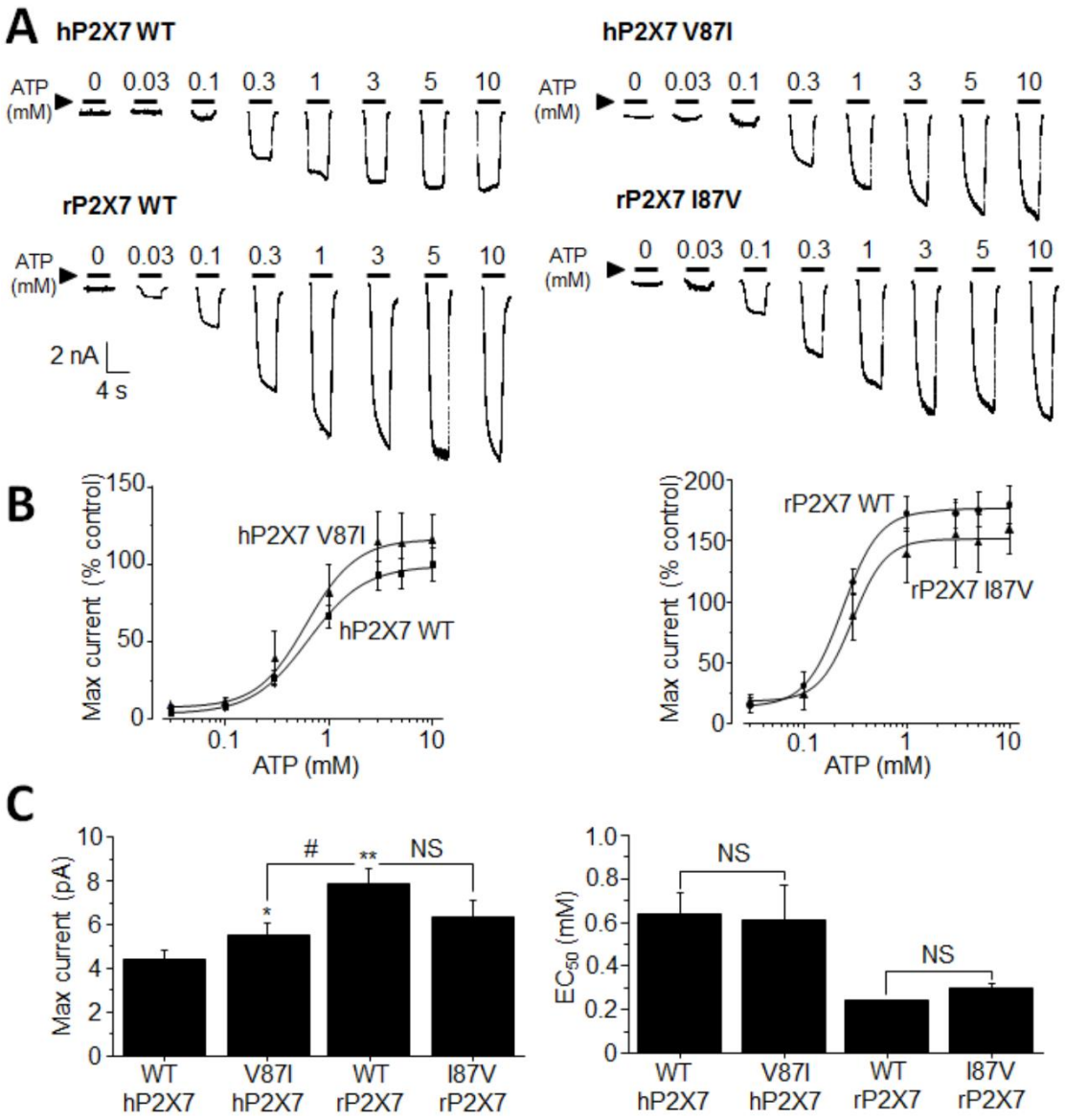

Figure 5.11 Effects of V87I and I87V on ATP-evoked currents

(A) Representative traces of ATP-evoked currents from HEK293 cells expressing the WT receptor or mutant indicated. (B) Mean ATP DR relationship curves of currents from cells expressing the WT P2X7R compared with the indicated mutant. The solid lines are fits of the data to the Hill equation. (C) Bar chart summary of the mean current amplitudes evoked from cells transfected with the WT hP2X7R or the indicated mutant by 10 mM ATP and the mean EC_{50} for BzATP. * and # $p<0.05$, NS, not significant, * is compared to WT hP2X7R and # to the WT rP2X7R.

compared to the I87V rP2X7R, this difference was not significant (Figure 5.10C). This indicates a considerable effect of introducing the human residue into the rat receptor and vice versa on BzATP-evoked responses, although this difference is primarily seen in the human-to-rat mutation.

Similarly, the EC_{50} value for each receptor varied. For BzATP these values were 42.1 ± 7.6 µM for WT hP2X7R, 31.8 ± 4.8 µM for V87I hP2X7R, 8.1 ± 1.8 µM for WT rP2X7R and 6.2 ± 1.7 µM for I87V rP2X7R (Figure 5.10C). It has been previously shown that the hP2X7R is less sensitive to activation by BzATP when compared to the rP2X7R (Rassendren et al., 1997). However, in the case of these mutants the substitution of the residue at position 87 for the reciprocal amino acid did not seem to have a significant effect on the EC_{50} of BzATP. The EC_{50} from the WT hP2X7R and the V87I hP2X7R are comparable, as are those from the WT rP2X7R and the I87V rP2X7R. It is interesting that the V87I mutation in the hP2X7R can increase the maximal response without affecting the sensitivity to BzATP (Figure 5.10B and C).

In order to determine whether this was a BzATP-specific effect, these same tests were carried out with ATP as the agonist. DR curves produced from patch-clamp recording data (Figure 5.11A and B) gave an initial indication that this mutation had an effect on the receptor response to ATP as well as BzATP; the maximal response of the V87I hP2X7R mutant to ATP was slightly increased compared to the WT hP2X7R (5524 ± 523 pA and 4386 ± 455 pA, respectively), and although this was to a lesser degree to that seen with BzATP-evoked responses it was significant ($p<0.05$). Similarly, the I87V rP2X7R mutant led to a decrease in the maximal response to ATP compared to the WT rP2X7R (6346 ± 767 pA and 7901 ± 682 pA, respectively), although again this difference was not as prominent as when cells were exposed to BzATP and was not significant (Figure 5.11C). As such these mutations appear to have an effect on the P2X7R response to ATP, though this is less prominent than the effect on the response to BzATP. As described for BzATP, the EC_{50} values for each receptor in response to ATP were analysed. For ATP these values were 0.6 ± 0.09 mM for WT hP2X7R, 0.6 ± 0.2 mM for

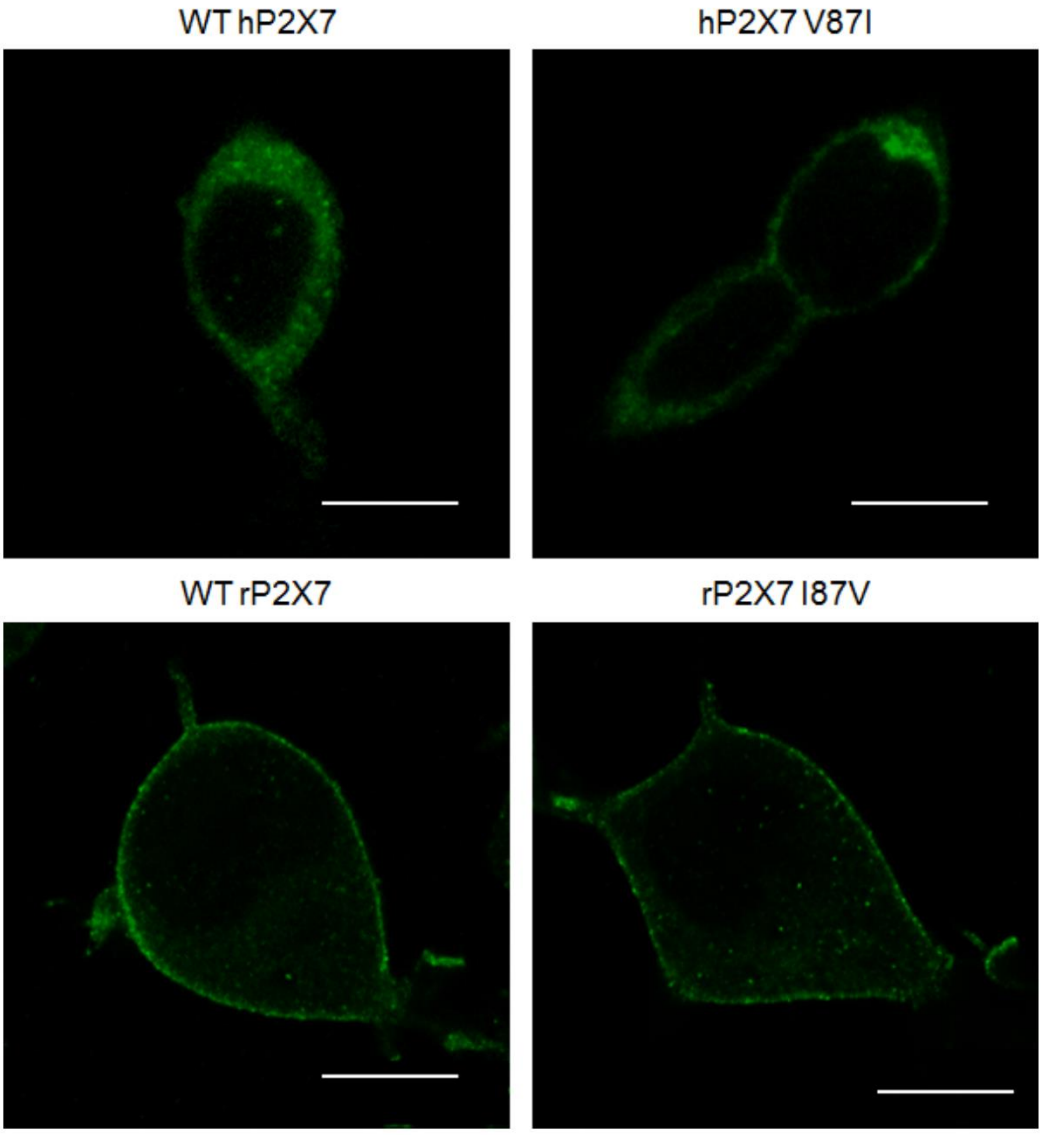

Figure 5.12 Effect of mutating residue 87 on P2X7R expression

Representative confocal images of fluorescently stained HEK293 cells transfected with either the WT or mutant P2X7R as indicated, determined using an anti-EE antibody. The scale bar is 10 μM.

V87I hP2X7R, 0.2 ± 0.01 mM for WT rP2X7R and 0.3 ± 0.02 mM for I87V rP2X7R (Figure 5.11C). Again, the human isoform of this receptor has been previously shown to be less sensitive to activation by ATP compared to the rat (Rassendren et al., 1997), but as shown above for BzATP the EC_{50} from the WT and mutant receptors for each species showed no significant difference. The value for the WT hP2X7R and the V87I hP2X7R are alike, as are those from the WT rP2X7R and the I87V rP2X7R, even more so than in the case of the BzATP values (Figure 5.11C). This lack of effect on the sensitivity of the P2X7R to both agonists indicates that the effect that results from this mutation is not a BzATP-specific effect, but it does seem to influence the change in response to BzATP more prominently compared to ATP.

5.2.8 Effect of introducing V87I and I87V on P2X7R expression

As for the Y288 hP2X7R mutants above, cells transfected with either the human or rat WT P2X7R or the V87I hP2X7R or I87V rP2X7R were investigated by immunostaining using an anti-EE antibody. This was done to determine whether the increased current response seen in the V87I mutation-containing hP2X7R or the rP2X7R containing the inverse mutation was due to an alteration in the level of receptor expression at the cell surface. The subcellular localisation of each of these receptors as determined by these tests is shown in figure 5.12. The WT hP2X7R fluorescence was diffuse and distributed throughout the cell, compared to the fluorescence from the WT rP2X7R which was mainly restricted to the cell membrane. Both the V87I hP2X7R and the I87V rP2X7R did not show any particular deviation from the pattern of membrane decoration seen in their WT counterparts. In the case of the I87V rP2X7R staining it could be argued that a small amount of additional fluorescence is visible surrounding the nucleus which may suggest that this mutation has some small influence on the levels of this protein seen at the cell membrane, however it appears that mutating the residue at position 87 overall does not have a particular effect on the cell membrane levels of the P2X7R.

5.3 Discussion

In this chapter, several residues are described that influence the activation of the hP2X7R by ATP and/or BzATP, in particular those at positions 143, 288 and 87 (Figure 5.3). Mutating Gln143 or Tyr288 mutation drastically reduced hP2X7R-mediated currents in response to both ATP and BzATP (Figure 5.4-7). In contrast, the V87I mutation in the hP2X7R and the reciprocal I87V mutation in the rP2X7R was demonstrated to partially contribute to the species-specific reaction of these receptors to agonists (Figure 5.10 and 5.11). The introduction of the Q143R mutation into the hP2X7R led to an approximately half reduction in both ATP and BzATP-evoked current amplitude (Figure 5.4 and 5.5). This suggests a common mechanism underlying this reduction in current in response to both agonists. However, interestingly the Q143H hP2X7R mutant had similar current characteristics to the WT. His is present at this position in a number of receptor subtypes (Figure 5.1), and the similar level of functionality between the Q143H and the WT hP2X7R suggests that the NH_2 group in the side chain of these residues may interact with the agonist in a manner which can be disrupted by the introduction of a positive charge at this position.

Mutation of Tyr288 in the human P2X7R receptor almost abolished the currents elicited from the receptor (Figure 5.6 and 5.7). This was true of both ATP and BzATP, similarly suggesting a common mechanism causing this insensitivity. This mechanism appears to be a disruption of receptor trafficking to the cell surface as, compared to the WT human and rat receptors, the hP2X7R mutant fluorescence was seen in the cytosol rather than localising to the cell membrane. It is also possible that this protein was unfolded, causing it to become stuck in inclusion bodies (Figure 5.8). However, this explanation is complicated due to the fact that the rat isoform of the P2X7R possesses a Phe at this position (Figure 5.1). As such this raises the question as to how the rP2X7R is so highly expressed at the cell membrane despite its Phe288 residue, which is possibly due to complementary mutations elsewhere in the structure. Further investigation of protein expression would be required to answer this question, ideally with Phe288 rP2X7R

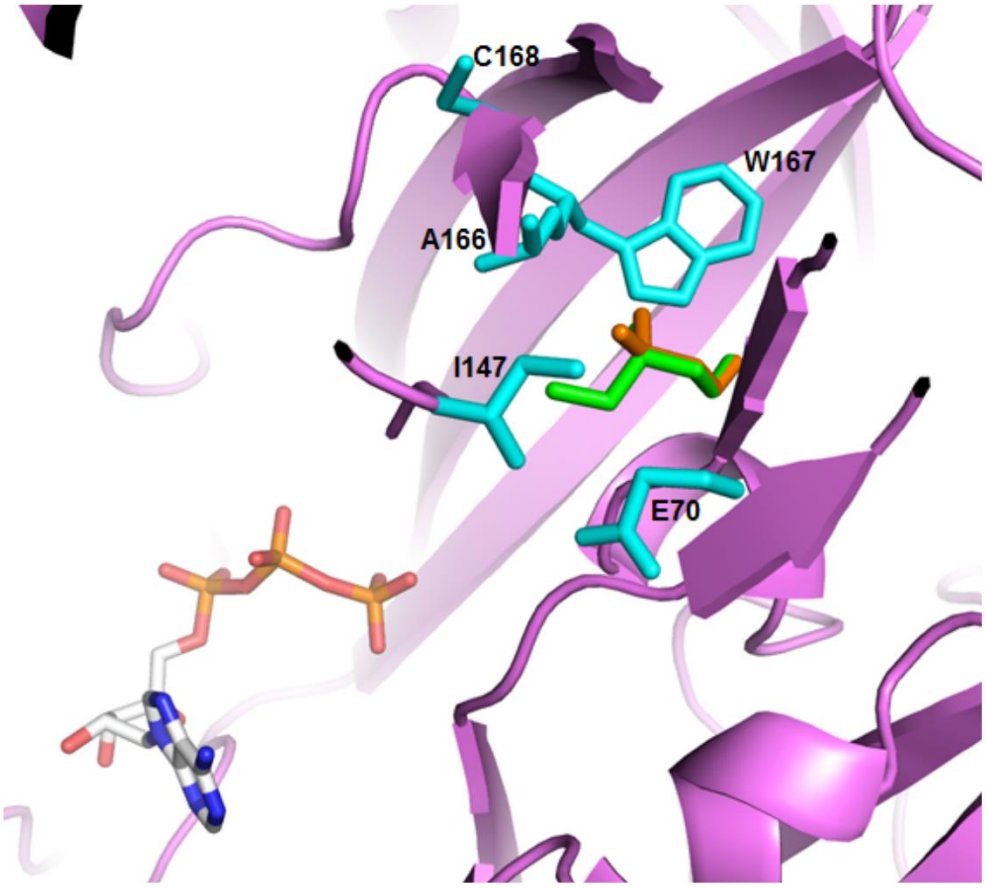

Figure 5.13 Location of residue 87 in the hP2X7R and rP2X7R

Homology model of the hP2X7R showing the location of V87 (orange) and I87 (green) as located in the rP2X7R and position in relation to the ATP binding site. Residues in close proximity to V87 are shown in cyan.

mutants in addition to the Tyr288 hP2X7R mutants examined above. For the time being, it could be speculated that the residue at this position has a different impact on the human and rat isoforms of the P2X7R, possibly due to the different combinations of residues in these receptors with the rat receptor compensating for this change through other complementary mutations. Furthermore, inspection of residues surrounding Tyr288 in the hP2X7R suggests that the OH group in the side chain may be important due to its ability to H-bond. The region of the receptor in which this residue is located is a relatively unstructured, unformed area which could be stabilised by H-bonds formed between Tyr288 and surrounding residues such as nearby lysines; there is a possibility that this interaction in the hP2X7R could be important for the formation of this particular ATP binding site.

Further to these two residues, Val87 in the hP2X7R was determined to have an important role in the species-specific response of P2X7Rs to agonists, though not solely to BzATP. The hP2X7R is significantly less responsive to both ATP and BzATP than the rP2X7R (Rassendren et al., 1997). When Ile from the rP2X7R was introduced at position 87 in the hP2X7R, the current elicited by both agonists was significantly larger than in the WT receptor. Conversely, introducing Val at position 87 in the rP2X7R reduced the agonist-induced current (Figure 5.10 and 5.11). This did not appear to be due to an effect on surface expression (Figure 5.12), although study of the P2X7R homology models did not immediately suggest a reason for why these small, hydrophobic residues would have such a remarkable impact on protein function. Val87 and Ile87 are located behind the ATP binding site, towards the top of the 'head' region of the subunit (Figure 5.13). Whilst this region does not move much during receptor activation, the 'jaw closing' motion of the head has been shown to be an important factor in the initiation of P2X7R function (Jiang et al., 2012). The location of residue 87 in the receptor suggests that this mutation could influence this aspect of receptor activation, although this is speculative and would require substantial further investigation.

Overall this chapter further establishes the value of a structure-based investigation of the P2X7R enabled by homology models, as highlighted in previous chapters, as well as providing a valuable insight into the structural basis of receptor function.

Chapter 6

General Discussion and Conclusions

6.1 General discussion and conclusions

The data presented in this thesis has provided valuable insights into the molecular basis of ligand binding in the P2X7R, as well as demonstrating the value of structure-based methods in identifying new ligands. In this chapter, the conclusions gained from these experiments will be summarised and the future direction of these studies introduced.

The high sequence similarity and identity with the zfP2X4R has allowed the production of homology models of the mammalian P2XRs. Such models have been used as a basis for structural investigations of P2XRs by providing more definitive insights into structure-function relationships inferred from site-directed mutagenesis (Marquez-Klaka et al., 2009; Stelmashenko et al., 2014; Browne et al., 2010; Browne et al., 2014). Homology models of the P2X7R were produced as described in chapter 3, and experiments have provided validation of these models as well as further insights into P2X7R function. The first of these experiments was molecular docking using P2X7R agonists. Docking ATP to the open state zfP2X4R crystal structure showed considerable similarity between the conformation of the docked molecule and that in the crystal structure. The same docking in the open state hP2X7R model identified the ATP binding site with slightly less accuracy, but with considerable similarities between the docked conformation and that of the zfP2X4R structure. Validation was additionally achieved by docking non-competitive P2X7R antagonists with species specific activity, in particular AZ11645373, KN-62 and SB203580 for which there was little understanding of the molecular mechanism of their action. However, in chapter 3 the binding site was shown to be proximal to the ATP binding site and this importantly involves the Phe95 which determines the species-specific inhibition of the compounds tested (Michel et al., 2008; Michel et al., 2009). Docking showed Phe95 in the hP2X7R to form pi-stacking interactions between the Phe side chain and the ring structures in the inhibitors which are lost when this residue is replaced with Leu as in the rP2X7R (Figure 1.3). This is supported by the fact that AZ11645373 potently inhibits the human, rhesus monkey and dog P2X7Rs, which have Phe95, but acts weakly or not at all at the mouse, guinea-pig

and rat P2X7Rs, which have Leu95. This provides a valuable insight into the molecular mechanism of action for these P2X7R antagonists as well as validating the model and docking approach. This part of the work has been published in Bioorganic and Medicinal Chemistry Letters (Caseley et al., 2015).

Disulfide locking of residues identified using the hP2X7R homology models identified two interacting pairs from the six studied across various domains. Several of the single and double mutants had impaired receptor function, though two pairs displayed BzATP-induced currents that were restored by DTT application. These were K81C/V304C and D48C/I331C, although the current from the K81C/V304C double mutant remained very small even after DTT treatment. Currents from the D48C/I331C mutant reached more than half the amplitude of that from the WT hP2X7R after incubation with DTT and rapidly reduced during DTT washout. This is comparable to a previous study, which similarly found disulfide bonds formed between pairs of amino acids in the TM domains to inhibit agonist-evoked currents prior to DTT reduction (Stelmashenko et al., 2014). In addition to the snapshots provided by the closed and open state zfP2X4R crystal structures, these experiments demonstrate the importance of relative movement between the first and second TM domains for receptor activation in the dynamic protein. As such the models in chapter 3 have been shown to be effective in experimental design as well as reflecting the protein in its native state, although they are by no means perfect and would stand to benefit from additional refinement.

The model validation carried out in chapter 3 gave confidence that *in silico* docking could be used to identify potential antagonists. Virtual screening of ~100,000 compounds with varied chemical structures initially identified three novel antagonists; C23, C40 and C60 (chapter 4). These all act with micromolar potency at the hP2X7R but not the rP2X7R, as determined by calcium imaging, patch-clamp recording, cell death and YO-PRO-1 uptake assays. They also variably antagonise different subtypes in that C40 and C60 exhibit preferential inhibition of the hP2X7R over the rP2X3R and hP2X4R. Structural modification of these initial hits not only provided valuable insights into the molecular

basis of their binding to the receptor but also identified two further antagonists. Of these, EC-001 was potent and proved more effective than the initial three. It is therefore evident that further structure-activity relationship studies are necessary to optimise these compounds and improve their potency and specificity (and possibly their metabolic stability for in vivo studies). However, despite this, it is clear that the compounds identified here are valuable novel antagonists of the hP2X7R. Interestingly, these were the first to be identified by a structure-based approach rather than functionally screening large compound libraries, which is often inefficient and costly. This ground-breaking implementation of structure-based ligand discovery in P2XRs has demonstrated the importance of such an approach for this family of receptors. These results have been published in Biochemical Pharmacology (Caseley et al., 2016).

Arguably the most interesting of the novel antagonists is C60. This compound has no inhibitory effect on the hP2X7 ion channel but selectively blocks hP2X7R-mediated large pore formation. The large pore is a key mediator of conditions including osteoporosis (Syberg et al., 2012b), chronic pain (Sorge et al., 2012) and age-related macular degeneration (Fowler et al., 2014) and thus selectively targeting this receptor function is desirable in the treatment of such diseases. Until this study, none of the published antagonists have been capable of specifically blocking large pore formation whilst sparing the ion channel function. As such, this compound will be advantageous in studying this function as well as possibly forming the basis of future therapeutic compounds.

Residue Tyr288 in the hP2X7R has been of particular interest throughout the course of this study. Its mutation has a marked impact on receptor function in response to both ATP and BzATP (chapter 5). This is most likely due to an effect on receptor trafficking to the cell surface, as its expression appeared to be located in the cytosol rather than in the plasma membrane as seen in the WT. Tyr288 was initially chosen for investigation due to its close proximity to the ATP binding site, which made it appear that it may directly influence agonist binding. Despite the fact that the side chain properties of Tyr and Phe

are very similar, when Tyr288 was mutated to Phe the resultant Y288F mutant was shown to exhibit reduced membrane expression levels. This is interesting due to the fact that there is a Phe at this position in the rP2X7R. Why this residue does not affect the expression of the rat subtype, and why the Y288F mutation uniquely affects the human receptor is intriguing. As it stands, if Tyr288 is indeed important in ensuring normal hP2X7R trafficking to the cell surface, it may achieve this by interacting with adjacent residues to maintain a conformation which facilitates trafficking. It is possible that Tyr288 could stabilise the area it is in by forming H-bonds between the OH group of this residue and nearby residues such as lysines, thereby influencing the structure.

Tyr288 was also implicated as being the most likely residue to affect the species-specific activity of the novel antagonists in chapter 4. The P2X7R homology models show the Tyr288 side chain to protrude further into the ATP binding pocket than the equivalent Phe288 in the rP2X7R, which could increase the area of interaction available between the compounds and the binding pocket. This residue is likely to affect species specificity, as there are few residues close to the predicted antagonist binding site which differ between the human and rat isoforms. However, although the homology models used in this study were demonstrated in chapter 3 to be valid representations of the protein in its native state, the side chains of individual residues may not be entirely accurate. As such, conclusions such as these are speculative and require further investigation, for example by additional site-directed mutagenesis.

Amino acids in the hP2X7R, which is less sensitive to ATP and BzATP compared to the rP2X7R (Rassendren et al., 1997), have previously been identified as determining this species-specific agonist response. Val87 (Ile87 in the rP2X7R) appears to be one such residue, which like Tyr288 has an intriguing impact on hP2X7R function in that introducing the reciprocal mutation between the human and rat isoforms increased the maximal current response in the human and conversely decreased it in the rat. Some residues influence P2X7R-mediated responses by affecting surface expression. For example, substituting His155 in the hP2X7R for Tyr in the rP2X7R causes an increase

in surface expression and subsequently higher ATP-induced currents, and vice versa in the rP2X7R (Bradley et al., 2011a). However, immunofluorescence imaging suggests that this was not the case with Val87. It is more likely that mutation of Val87 affects the single-channel function of the hP2X7R. This is similar to residue 348 which increases hP2X7R-mediated response when the equivalent rP2X7R amino acid is introduced, by affecting the conductance and opening probability of the receptor (Bradley et al., 2011a). Whilst this appears the most likely explanation for the effect of the V87I mutation, the exact mechanism underlying this change is unclear. The position of V87 at the top of the 'head' region of the receptor suggests that it may be involved in the vital 'jaw closing' motion of the head during receptor activation (Jiang et al., 2012). However, both Val and Ile are similar small, uncharged residues makes it difficult to predict, without further experimental work, why this residue has such an effect.

In conclusion, the study presented in this thesis demonstrates that homology models of the P2X7R are hugely beneficial in the targeted design of experiments for investigating the molecular basis for ligand-receptor interactions.

6.2 Future work

This study has provided substantial information concerning ligand binding in the P2X7R, and has built a platform from which future experiments could be designed. These are described below in addition to further avenues which would be potentially beneficial to investigate.

6.2.1 Subtype specificity of novel antagonists

The novel antagonists described in chapter 4 have varying degrees of subtype specificity. However, testing of these compounds against the human P2X1R, P2X2R, P2X3R, P2X5R or P2X6R is highly desirable as such information would allow a more comprehensive conclusion to be drawn with regards to their specificity. Additionally, it

would be interesting to determine whether the novel antagonists have any activity at the P2YRs.

6.2.2 Molecular basis of novel antagonist binding

As part of this study, EC-001, EC-002 and EC-003 were designed, custom synthesised by Enamine and tested. Further structure-activity relationship studies would provide a more comprehensive view of the molecular basis of their specific binding to the hP2X7R as well as identification of more potent and selective antagonists. In addition, further EC-compounds (as well as EC-001, -002 and -003) were designed. Testing further structural analogues of the identified antagonists would provide a more comprehensive view of the molecular basis of their binding to the hP2X7R as well as potentially providing more understanding of their species specificity. In addition to producing compounds with modified structures, the basis of antagonist binding to the P2X7R could be probed by site-directed mutagenesis. Residues implicated in affecting the subtype or species specifity of the novel antagonists were Tyr288 and Gln143 in the hP2X7R. Patch-clamp recording and calcium imaging of cells heterologously expressing mutations of these residues would provide the molecular mechanisms of antagonism.

6.2.3 Novel antagonist effects on P2X7R physiological function

As introduced in chapter 1, the P2X7R is crucial in mediating ATP-induced production of IL-1β from immune cells. Therefore, experiments to explore the effectiveness of the novel antagonists in suppressing ATP-induced IL-1β production would be valuable. Moreover, the P2X7R has been implicated in a diversity of disease conditions. In particular, as described above, several conditions are related to P2X7R-dependent large pore formation. Experiments using these novel antagonists, particularly C60, may inform the significance of P2X7-dependent ion channel and large pore in pathogenesis.

6.2.4 Developing further P2X7R antagonists

The structure-based approach described in chapter 4 proved very effective in discovering a series of novel P2X7R-specific antagonists. These had several common structural

elements, and as such have the potential to form the basis of a new family of structurally similar antagonists. However, buying custom compounds such as those used in this study can prove to be expensive and this is a limiting factor. Ideally, researchers specialising in chemistry would be able to explore a wider range of structural modifications of this family of compounds. The testing of a larger number of compounds containing the common central moiety highlighted in this study may reveal a plethora of effective P2X7R antagonists. Additional antagonists may possess more drug-like characteristics and, as a result, be candidates for future development into therapeutic compounds for the treatment of diseases such as Crohn's disease.

6.2.5 Mechanism of P2X7R large pore inhibition by C60

As described in chapter 4, C60 was able to specifically inhibit the large pore that forms upon prolonged P2X7R stimulation. However, there is some ambiguity surrounding this conclusion, in particular the fact that the inhibition of calcium responses occurred rapidly after agonist addition even though large pore formation follows prolonged P2X7R stimulation. Further study of this phenomenon would be beneficial, for example using a P2X7R variant such as that containing the R307Q mutation which lacks the ability to form large pores to determine whether calcium responses were still inhibited by C60. Varying the extracellular concentration of calcium in experiments would also answer whether calcium acts as a co-factor for binding of this compound to the protein.

6.2.4 Tyr288 in surface expression

The subcellular localisation of the mutants in chapter 5 with the largest impact on hP2X7R function (Tyr288 and Val87) was tested by confocal microscopy. It would be beneficial to assess their surface expression by further techniques to draw a more definitive conclusion due to limitations in using immunocytochemistry to assess surface expression. These include the rapid photobleaching seen in such experiments, especially when taking multiple images of the same cell, in addition to the potential for artefacts that may be introduced by the process of chemically fixing the cells. Combining

biotin labelling and Western blotting would give a more quantifiable indication of the expression levels of these proteins. Furthermore, as mutating Tyr288 in the hP2X7R appears disrupt either receptor trafficking or folding, determining which of these is the case would be useful.

6.2.5 V87 effect on receptor function

Of the P2X7R residues mutated in chapter 5, the effect at position 87 is the most difficult to explain. Study by confocal microscopy suggested that the receptor surface expression is not affected by mutating this residue, and the similarity in side chain characteristics between Val in the hP2X7R and Ile in the rP2X7R do not suggest an obvious explanation for their influence on agonist sensitivity. These residues may affect 'jaw closing' in the head during P2X7R activation, and as such it could prove beneficial to mutate these residues to others with differing characteristics as well as those in surrounding regions with which they may interact.

6.2.6 hP2X7R structure determination

The HEK293 cell line stably expressing the His-tagged hP2X7R used in this study was initially produced for another distinct purpose. The His tag was introduced to facilitate the purification of hP2X7R protein using nickel column purification for the structural biology study of the hP2X7R using cryo-electron microscopy (cryo-EM) as carried out for other membrane proteins (Liao et al., 2013; Twomey et al., 2016; Wu et al., 2016). However, this particular aspect of the project was more time consuming than initially anticipated. Experiments that would be the most beneficial to carry out with the HEK293 hP2X7-His stable cell line produced during this study would be to explore further methods of membrane protein purification. Previously, cell preparation has been carried out through cell sonication in both RIPA buffer and a NaCl-containing buffer made in-house. The detergent present was DDM and, as the detergent used in such experiments is known to be an integral factor on the success of membrane protein purification, further detergents such as sodium dodecyl sulfate could be explored. An alternative method

such as the use of SMA lipid particles (SMALPs), which act as ‘cookie cutters’ in the lipid membrane and have been shown to be effective as a tool for isolating proteins in a near-native lipid environment (Postis et al., 2015) may also be fruitful. Additionally, only very small-scale protein purification using Talon resin was attempted. Possibly more favourable results would be achieved if this purification was scaled up to avoid the loss of the already low levels of protein gained in smaller samples. Nonetheless, generation of the His-tagged hP2X7 receptor would be very useful for further structural investigation as well as functional studies of the receptor.

The P2X family of receptors are involved in diverse vital functions mediated by extracellular ATP. This project to set out to specifically target the P2X7R for inhibitor design and to this end a homology model has been created and validated by functional and *in silico* studies. This has resulted in a number of novel antagonists being developed with specific activity at the hP2X7R. These antagonists may be useful in developing therapeutic compounds. As described above, the P2X7R is a desirable drug target, particularly with respect to its large pore forming function which is related to pathologies. C60 in particular therefore has the potential to treat conditions due to its ability to specifically inhibit this large pore formation. Further development of these compounds with the aim of producing drugs capable of treating human conditions is an obvious next step for these novel antagonists. In the long term it is hoped that this will work will underpin future inhibitor design programs against the P2X7R and the wider P2XR family, potentially even further membrane proteins.

List of References

Abbracchio, M.P., Burnstock, G., Boeynaems, J.-M., Barnard, E.A., Boyer, J.L., Kennedy, C., Knight, G.E., Fumagalli, M., Gachet, C. and Jacobson, K.A. 2006. International Union of Pharmacology LVIII: update on the P2Y G protein-coupled nucleotide receptors: from molecular mechanisms and pathophysiology to therapy. *Pharmacological reviews.* **58**(3), pp.281-341.

Adinolfi, E., Callegari, M.G., Ferrari, D., Bolognesi, C., Minelli, M., Wieckowski, M.R., Pinton, P., Rizzuto, R. and Di Virgilio, F. 2005. Basal activation of the P2X7 ATP receptor elevates mitochondrial calcium and potential, increases cellular ATP levels, and promotes serum-independent growth. *Molecular biology of the cell.* **16**(7), pp.3260-3272.

Adinolfi, E., Cirillo, M., Woltersdorf, R., Falzoni, S., Chiozzi, P., Pellegatti, P., Callegari, M.G., Sandonà, D., Markwardt, F. and Schmalzing, G. 2010. Trophic activity of a naturally occurring truncated isoform of the P2X7 receptor. *The FASEB journal.* **24**(9), pp.3393-3404.

Adinolfi, E., Melchiorri, L., Falzoni, S., Chiozzi, P., Morelli, A., Tieghi, A., Cuneo, A., Castoldi, G., Di Virgilio, F. and Baricordi, O.R. 2002. P2X7 receptor expression in evolutive and indolent forms of chronic B lymphocytic leukemia. *Blood.* **99**(2), pp.706-708.

Adriouch, S., Bannas, P., Schwarz, N., Fliegert, R., Guse, A.H., Seman, M., Haag, F. and Koch-Nolte, F. 2008. ADP-ribosylation at R125 gates the P2X7 ion channel by presenting a covalent ligand to its nucleotide binding site. *The FASEB journal.* **22**(3), pp.861-869.

Aguirre, A., Shoji, K.F., Sáez, J.C., Henríquez, M. and Quest, A.F. 2013. FasL-triggered death of Jurkat cells requires caspase 8-induced, ATP-dependent cross-talk between fas and the purinergic receptor P2X7. *Journal of cellular physiology.* **228**(2), pp.485-493.

Alberto, A.V.P., Faria, R., Couto, C., Ferreira, L., Souza, C., Teixeira, P., Fróes, M. and Alves, L. 2013. Is pannexin the pore associated with the P2X7 receptor? *Naunyn-Schmiedeberg's archives of pharmacology.* **386**(9), pp.775-787.

Ali, Z., Laurijssens, B., Ostenfeld, T., McHugh, S., Stylianou, A., Scott-Stevens, P., Hosking, L., Dewit, O., Richardson, J.C. and Chen, C. 2013. Pharmacokinetic and pharmacodynamic profiling of a P2X7 receptor allosteric modulator GSK1482160 in healthy human subjects. *British journal of clinical pharmacology.* **75**(1), pp.197-207.

Allsopp, R.C. and Evans, R.J. 2011. The intracellular amino terminus plays a dominant role in desensitization of ATP-gated P2X receptor ion channels. *Journal of biological chemistry.* **286**(52), pp.44691-44701.

Anderson, C.M., Bergher, J.P. and Swanson, R.A. 2004. ATP-induced ATP release from astrocytes. *Journal of neurochemistry.* **88**(1), pp.246-256.

Anderson, C.M. and Nedergaard, M. 2006. Emerging challenges of assigning P2X 7 receptor function and immunoreactivity in neurons. *Trends in neurosciences.* **29**(5), pp.257-262.

Andreopoulos, S., Wasserman, M., Woo, K., Li, P. and Warsh, J. 2004. Chronic lithium treatment of B lymphoblasts from bipolar disorder patients reduces transient receptor potential channel 3 levels. *The pharmacogenomics journal.* **4**(6), pp.365-373.

Antico Arciuch, V.G., Elguero, M.E., Poderoso, J.J. and Carreras, M.C. 2012. Mitochondrial regulation of cell cycle and proliferation. *Antioxidants & redox signaling.* **16**(10), pp.1150-1180.

Armstrong, J.N., Brust, T.B., Lewis, R.G. and MacVicar, B.A. 2002. Activation of presynaptic P2X7-like receptors depresses mossy fiber–CA3 synaptic

transmission through p38 mitogen-activated protein kinase. *The Journal of neuroscience.* **22**(14), pp.5938-5945.

Arnett, F.C., Edworthy, S.M., Bloch, D.A., McShane, D.J., Fries, J.F., Cooper, N.S., Healey, L.A., Kaplan, S.R., Liang, M.H. and Luthra, H.S. 1988. The American Rheumatism Association 1987 revised criteria for the classification of rheumatoid arthritis. *Arthritis & rheumatism.* **31**(3), pp.315-324.

Arulkumaran, N., Unwin, R.J. and Tam, F.W. 2011. A potential therapeutic role for P2X7 receptor (P2X7R) antagonists in the treatment of inflammatory diseases. *Expert opinion on investigational drugs.* **20**(7), pp.897-915.

Aschrafi, A., Sadtler, S., Niculescu, C., Rettinger, J. and Schmalzing, G. 2004. Trimeric architecture of homomeric P2X 2 and heteromeric P2X 1+ 2 receptor subtypes. *Journal of molecular biology.* **342**(1), pp.333-343.

Balázs, B., Dankó, T., Kovacs, G., Köles, L., Hediger, M.A. and Zsembery, Á. 2013. Investigation of the inhibitory effects of the benzodiazepine derivative, 5-BDBD on P2X4 purinergic receptors by two complementary methods. *Cellular physiology and biochemistry.* **32**(1), pp.11-24.

Banfi, C., Ferrario, S., De Vincenti, O., Ceruti, S., Fumagalli, M., Mazzola, A., D'Ambrosi, N., Volontè, C., Fratto, P. and Vitali, E. 2005. P2 receptors in human heart: upregulation of P2X 6 in patients undergoing heart transplantation, interaction with TNFα and potential role in myocardial cell death. *Journal of molecular and cellular cardiology.* **39**(6), pp.929-939.

Baqi, Y., Hausmann, R., Rosefort, C., Rettinger, J.r., Schmalzing, G.n. and Müller, C.E. 2011. Discovery of potent competitive antagonists and positive modulators of the P2X2 receptor. *Journal of medicinal chemistry.* **54**(3), pp.817-830.

Baraldi, P.G., del Carmen Nuñez, M., Morelli, A., Falzoni, S., Di Virgilio, F. and Romagnoli, R. 2003. Synthesis and biological activity of N-arylpiperazine-modified analogues of KN-62, a potent antagonist of the purinergic P2X7 receptor. *Journal of medicinal chemistry.* **46**(8), pp.1318-1329.

Baraldi, P.G., Makaeva, R., Pavani, M.G., del Carmen Nuñez, M., Spalluto, G., Moro, S., Falzoni, S., Di Virgilio, F. and Romagnoli, R. 2002. Synthesis, biological activity and molecular modeling studies of 1, 2, 3, 4-tetrahydroiso-quinoline derivatives as conformationally constrained analogues of KN62, a potent antagonist of the P2X7-receptor containing a tyrosine moiety. *Arzneimittelforschung.* **52**(04), pp.273-285.

Baraldi, P.G., Romagnoli, R., Tabrizi, M.A., Falzoni, S. and Di Virgilio, F. 2000. Synthesis of conformationally constrained analogues of KN62, a potent antagonist of the P2X 7-receptor. *Bioorganic & medicinal chemistry letters.* **10**(7), pp.681-684.

Barclay, J., Patel, S., Dorn, G., Wotherspoon, G., Moffatt, S., Eunson, L., Abdel'al, S., Natt, F., Hall, J. and Winter, J. 2002. Functional downregulation of P2X3 receptor subunit in rat sensory neurons reveals a significant role in chronic neuropathic and inflammatory pain. *The Journal of neuroscience.* **22**(18), pp.8139-8147.

Barden, N., Harvey, M., Gagné, B., Shink, E., Tremblay, M., Raymond, C., Labbé, M., Villeneuve, A., Rochette, D. and Bordeleau, L. 2006. Analysis of single nucleotide polymorphisms in genes in the chromosome 12Q24. 31 region points to P2RX7 as a susceptibility gene to bipolar affective disorder. *American journal of medical genetics part B: neuropsychiatric genetics.* **141**(4), pp.374-382.

Baricordi, O., Ferrari, D., Melchiorri, L., Chiozzi, P., Hanau, S., Chiari, E., Rubini, M. and Di Virgilio, F. 1996. An ATP-activated channel is involved in mitogenic stimulation of. *Blood.* **87**(2), pp.682-690.

Baricordi, O.R., Melchiorri, L., Adinolfi, E., Falzoni, S., Chiozzi, P., Buell, G. and Di Virgilio, F. 1999. Increased proliferation rate of lymphoid cells transfected with the P2X7 ATP receptor. *Journal of biological chemistry.* **274**(47), pp.33206-33208.

Barrera, N.P., Ormond, S.J., Henderson, R.M., Murrell-Lagnado, R.D. and Edwardson, J.M. 2005. Atomic force microscopy imaging demonstrates that P2X2 receptors

are trimers but that P2X6 receptor subunits do not oligomerize. *Journal of biological chemistry.* **280**(11), pp.10759-10765.

Bartlett, R., Stokes, L. and Sluyter, R. 2014. The P2X7 receptor channel: recent developments and the use of P2X7 antagonists in models of disease. *Pharmacological reviews.* **66**(3), pp.638-675.

Bean, B.P. 1990. ATP-activated channels in rat and bullfrog sensory neurons: concentration dependence and kinetics. *The journal of neuroscience.* **10**(1), pp.1-10.

Berghe, T.V., Linkermann, A., Jouan-Lanhouet, S., Walczak, H. and Vandenabeele, P. 2014. Regulated necrosis: the expanding network of non-apoptotic cell death pathways. *Nature reviews Molecular cell biology.* **15**(2), pp.135-147.

Bhaskaracharya, A., Dao-Ung, P., Jalilian, I., Spildrejorde, M., Skarratt, K.K., Fuller, S.J., Sluyter, R. and Stokes, L. 2014. Probenecid blocks human P2X7 receptor-induced dye uptake via a pannexin-1 independent mechanism. *PloS one.* **9**(3), pe93058.

Bhattacharya, A., Wang, Q., Ao, H., Shoblock, J.R., Lord, B., Aluisio, L., Fraser, I., Nepomuceno, D., Neff, R.A. and Welty, N. 2013. Pharmacological characterization of a novel centrally permeable P2X7 receptor antagonist: JNJ-47965567. *British journal of pharmacology.* **170**(3), pp.624-640.

Bian, X., Ren, J., Vries, M., Schnegelsberg, B., Cockayne, D.A., Ford, A.P. and Galligan, J.J. 2003. Peristalsis is impaired in the small intestine of mice lacking the P2X3 subunit. *The journal of physiology.* **551**(1), pp.309-322.

Bianchi, B.R., Lynch, K.J., Touma, E., Niforatos, W., Burgard, E.C., Alexander, K.M., Park, H.S., Yu, H., Metzger, R. and Kowaluk, E. 1999. Pharmacological characterization of recombinant human and rat P2X receptor subtypes. *European journal of pharmacology.* **376**(1), pp.127-138.

Bianco, F., Ceruti, S., Colombo, A., Fumagalli, M., Ferrari, D., Pizzirani, C., Matteoli, M., Di Virgilio, F., Abbracchio, M.P. and Verderio, C. 2006. A role for P2X7 in microglial proliferation. *Journal of neurochemistry.* **99**(3), pp.745-758.

Blanton, S.H., Liang, C., Cai, M., Pandya, A., Du, L., Landa, B., Mummalanni, S., Li, K., Chen, Z. and Qin, X. 2002. A novel locus for autosomal dominant non-syndromic deafness (DFNA41) maps to chromosome 12q24-qter. *Journal of medical genetics.* **39**(8), pp.567-570.

Bo, X., Jiang, L.-H., Wilson, H.L., Kim, M., Burnstock, G., Surprenant, A. and North, R.A. 2003a. Pharmacological and biophysical properties of the human P2X5 receptor. *Molecular pharmacology.* **63**(6), pp.1407-1416.

Bo, X., Kim, M., Nori, S.L., Schoepfer, R., Burnstock, G. and North, R.A. 2003b. Tissue distribution of P2X4 receptors studied with an ectodomain antibody. *Cell and tissue research.* **313**(2), pp.159-165.

Boué-Grabot, E., Archambault, V. and Séguéla, P. 2000. A protein kinase C site highly conserved in P2X subunits controls the desensitization kinetics of P2X2 ATP-gated channels. *Journal of Biological Chemistry.* **275**(14), pp.10190-10195.

Boumechache, M., Masin, M., Edwardson, J.M., Górecki, D.C. and Murrell-Lagnado, R. 2009. Analysis of assembly and trafficking of native P2X4 and P2X7 receptor complexes in rodent immune cells. *Journal of biological chemistry.* **284**(20), pp.13446-13454.

Bradley, H.J., Baldwin, J.M., Goli, G.R., Johnson, B., Zou, J., Sivaprasadarao, A., Baldwin, S.A. and Jiang, L.-H. 2011a. Residues 155 and 348 contribute to the determination of P2X7 receptor function via distinct mechanisms revealed by single-nucleotide polymorphisms. *Journal of biological chemistry.* **286**(10), pp.8176-8187.

Bradley, H.J., Browne, L.E., Yang, W. and Jiang, L.H. 2011b. Pharmacological properties of the rhesus macaque monkey P2X7 receptor. *British journal of pharmacology.* **164**(2b), pp.743-754.

Brake, A.J., Wagenbach, M.J. and Julius, D. 1994. New structural motif for ligand-gated ion channels defined by an ionotropic ATP receptor.

Brough, D. and Rothwell, N.J. 2007. Caspase-1-dependent processing of pro-interleukin-1β is cytosolic and precedes cell death. *Journal of cell science.* **120**(5), pp.772-781.

Brown, S.G., Townsend-Nicholson, A., Jacobson, K.A., Burnstock, G. and King, B.F. 2002. Heteromultimeric P2X1/2 receptors show a novel sensitivity to extracellular pH. *Journal of pharmacology and experimental therapeutics.* **300**(2), pp.673-680.

Browne, L.E., Compan, V., Bragg, L. and North, R.A. 2013. P2X7 receptor channels allow direct permeation of nanometer-sized dyes. *The journal of neuroscience.* **33**(8), pp.3557-3566.

Browne, L.E., Jiang, L.-H. and North, R.A. 2010. New structure enlivens interest in P2X receptors. *Trends in pharmacological sciences.* **31**(5), pp.229-237.

Browne, L.E., Nunes, J.P., Sim, J.A., Chudasama, V., Bragg, L., Caddick, S. and North, R.A. 2014. Optical control of trimeric P2X receptors and acid-sensing ion channels. *Proceedings of the national academy of sciences.* **111**(1), pp.521-526.

Burnstock, G. 1972. Purinergic nerves. *Pharmacological reviews.* **24**(3), pp.509-581.

Burnstock, G. 2002. Purinergic signaling and vascular cell proliferation and death. *Arteriosclerosis, thrombosis, and vascular biology.* **22**(3), pp.364-373.

Burnstock, G. 2007. Purine and pyrimidine receptors. *Cellular and molecular life sciences.* **64**(12), pp.1471-1483.

Burnstock, G. 2008. Dual control of vascular tone and remodelling by ATP released from nerves and endothelial cells. *Pharmacological reports.* **60**(1), pp.12-20.

Burnstock, G. 2013. Introduction and perspective, historical note. *Frontiers in cellular neuroscience.* **7**, p227.

Burnstock, G. 2014. The Concept of Cotransmission: Focus on ATP as a Cotransmitter and its Significance in Health and Disease. *European review.* **22**(01), pp.1-17.

Cabrini, G., Falzoni, S., Forchap, S.L., Pellegatti, P., Balboni, A., Agostini, P., Cuneo, A., Castoldi, G., Baricordi, O.R. and Di Virgilio, F. 2005. A His-155 to Tyr polymorphism confers gain-of-function to the human P2X7 receptor of human leukemic lymphocytes. *The journal of immunology.* **175**(1), pp.82-89.

Cankurtaran-Sayar, S., Sayar, K. and Ugur, M. 2009. P2X7 receptor activates multiple selective dye-permeation pathways in RAW 264.7 and human embryonic kidney 293 cells. *Molecular pharmacology.* **76**(6), pp.1323-1332.

Cao, L., Broomhead, H.E., Young, M.T. and North, R.A. 2009. Polar residues in the second transmembrane domain of the rat P2X2 receptor that affect spontaneous gating, unitary conductance, and rectification. *The journal of neuroscience.* **29**(45), pp.14257-14264.

Cao, L., Young, M.T., Broomhead, H.E., Fountain, S.J. and North, R.A. 2007. Thr339-to-serine substitution in rat P2X2 receptor second transmembrane domain causes constitutive opening and indicates a gating role for Lys308. *The journal of neuroscience.* **27**(47), pp.12916-12923.

Caseley, E.A., Muench, S.P., Baldwin, S.A., Simmons, K., Fishwick, C.W. and Jiang, L.-H. 2015. Docking of competitive inhibitors to the P2X7 receptor family reveals key differences responsible for changes in response between rat and human. *Bioorganic & medicinal chemistry letters.* **25**(16), pp.3164-3167.

Caseley, E.A., Muench, S.P., Fishwick, C.W. and Jiang, L.-H. 2016. Structure-based identification and characterisation of structurally novel human P2X7 receptor antagonists. *Biochemical Pharmacology.* **116**, pp.130-139.

Caseley, E.A., Muench, S.P., Roger, S., Mao, H.-J., Baldwin, S.A. and Jiang, L.-H. 2014. Non-synonymous single nucleotide polymorphisms in the P2X receptor genes: association with diseases, impact on receptor functions and potential use as diagnosis biomarkers. *International journal of molecular sciences.* **15**(8), pp.13344-13371.

Chan, J., Xing, Y., Magliozzo, R. and Bloom, B. 1992. Killing of virulent Mycobacterium tuberculosis by reactive nitrogen intermediates produced by activated murine macrophages. *The journal of experimental medicine.* **175**(4), pp.1111-1122.

Charlton, S.J., Brown, C.A., Weisman, G.A., Turner, J.T., Erb, L. and Boarder, M.R. 1996. PPADS and suramin as antagonists at cloned P2Y-and P2U-purinoceptors. *British journal of pharmacology.* **118**(3), pp.704-710.

Cheewatrakoolpong, B., Gilchrest, H., Anthes, J.C. and Greenfeder, S. 2005. Identification and characterization of splice variants of the human P2X 7 ATP channel. *Biochemical and biophysical research communications.* **332**(1), pp.17-27.

Chen, C.-C., Akopian, A.N., Sivilottit, L., Colquhoun, D., Burnstock, G. and Wood, J.N. 1995. A P2X purinoceptor expressed by a subset of sensory neurons. *Nature.* **377**(6548), pp.428-431.

Chen, L. and Brosnan, C.F. 2006. Exacerbation of experimental autoimmune encephalomyelitis in P2X7R−/− mice: evidence for loss of apoptotic activity in lymphocytes. *The journal of immunology.* **176**(5), pp.3115-3126.

Chen, M.-L., Cao, H., Chu, Y.-X., Cheng, L.-Z., Liang, L.-L., Zhang, Y.-Q. and Zhao, Z.-Q. 2012a. Role of P2X7 receptor-mediated IL-18/IL-18R signaling in morphine tolerance: multiple glial-neuronal dialogues in the rat spinal cord. *The journal of pain.* **13**(10), pp.945-958.

Chen, Y., Li, G. and Huang, L.-Y.M. 2012b. P2X7 receptors in satellite glial cells mediate high functional expression of P2X3 receptors in immature dorsal root ganglion neurons. *Molecular pain.* **8**(1), p1.

Chen, Y., Zhang, X., Wang, C., Li, G., Gu, Y. and Huang, L.-Y.M. 2008. Activation of P2X7 receptors in glial satellite cells reduces pain through downregulation of P2X3 receptors in nociceptive neurons. *Proceedings of the national academy of sciences.* **105**(43), pp.16773-16778.

Chessell, I., Simon, J., Hibell, A., Michel, A., Barnard, E. and Humphrey, P. 1998. Cloning and functional characterisation of the mouse P2X7 receptor. *FEBS letters.* **439**(1-2), pp.26-30.

Chessell, I.P., Hatcher, J.P., Bountra, C., Michel, A.D., Hughes, J.P., Green, P., Egerton, J., Murfin, M., Richardson, J. and Peck, W.L. 2005. Disruption of the P2X7 purinoceptor gene abolishes chronic inflammatory and neuropathic pain. *Pain.* **114**(3), pp.386-396.

Chow, S.C., Kass, G.E. and Orrenius, S. 1997. Purines and their roles in apoptosis. *Neuropharmacology.* **36**(9), pp.1149-1156.

Cockayne, D.A., Hamilton, S.G., Zhu, Q.-M., Dunn, P.M., Zhong, Y., Novakovic, S., Malmberg, A.B., Cain, G., Berson, A. and Kassotakis, L. 2000. Urinary bladder hyporeflexia and reduced pain-related behaviour in P2X 3-deficient mice. *Nature.* **407**(6807), pp.1011-1015.

Coleman, M.L., Sahai, E.A., Yeo, M., Bosch, M., Dewar, A. and Olson, M.F. 2001. Membrane blebbing during apoptosis results from caspase-mediated activation of ROCK I. *Nature cell biology.* **3**(4), pp.339-345.

Collo, G., North, R.A., Kawashima, E., Merlo-Pich, E., Neidhart, S., Surprenant, A. and Buell, G. 1996. Cloning of P2X5 and P2X6 receptors and the distribution and properties of an extended family of ATP-gated ion channels. *The journal of neuroscience.* **16**(8), pp.2495-2507.

Compan, V., Ulmann, L., Stelmashenko, O., Chemin, J., Chaumont, S. and Rassendren, F. 2012. P2X2 and P2X5 subunits define a new heteromeric receptor with P2X7-like properties. *The journal of neuroscience.* **32**(12), pp.4284-4296.

Corrêa, G., da Silva, C.M., de Abreu Moreira-Souza, A.C., Vommaro, R.C. and Coutinho-Silva, R. 2010. Activation of the P2X 7 receptor triggers the elimination of Toxoplasma gondii tachyzoites from infected macrophages. *Microbes and infection.* **12**(6), pp.497-504.

Coutinho-Silva, R., Persechini, P.M., Bisaggio, R.D.C., Perfettini, J.-L., Neto, A.C.T.D.S., Kanellopoulos, J.M., Motta-Ly, I., Dautry-Varsat, A. and Ojcius, D.M. 1999. P2Z/P2X7receptor-dependent apoptosis of dendritic cells. *American journal of physiology-cell physiology.* **276**(5), pp.C1139-C1147.

Creed, K.E., Loxley, R.A. and Phillips, J.K. 2010. Functional expression of muscarinic and purinoceptors in the urinary bladder of male and female rats and guinea pigs. *Journal of Smooth Muscle Research.* **46**(4), pp.201-215.

da Silva, R.C. and Langoni, H. 2009. Toxoplasma gondii: host–parasite interaction and behavior manipulation. *Parasitology research.* **105**(4), pp.893-898.

Dahl, G. 2015. ATP release through pannexon channels. *Phil. Trans. R. Soc. B.* **370**(1672), p20140191.

Dahl, G. and Locovei, S. 2006. Pannexin: to gap or not to gap, is that a question? *IUBMB life.* **58**(7), pp.409-419.

Damer, S., Niebel, B., Czeche, S., Nickel, P., Ardanuy, U., Schmalzing, G., Rettinger, J., Mutschler, E. and Lambrecht, G. 1998. NF279: a novel potent and selective antagonist of P2X receptor-mediated responses. *European journal of pharmacology.* **350**(1), pp.R5-R6.

Dao-Ung, L.P., Fuller, S.J., Sluyter, R., SkarRatt, K.K., Thunberg, U., Tobin, G., Byth, K., Ban, M., Rosenquist, R. and Stewart, G.J. 2004. Association of the 1513C polymorphism in the P2X7 gene with familial forms of chronic lymphocytic leukaemia. *British journal of haematology.* **125**(6), pp.815-817.

Darbousset, R., Delierneux, C., Mezouar, S., Hego, A., Lecut, C., Guillaumat, I., Riederer, M.A., Evans, R.J., Dignat-George, F. and Panicot-Dubois, L. 2014. P2X1 expressed on polymorphonuclear neutrophils and platelets is required for thrombosis in mice. *Blood.* **124**(16), pp.2575-2585.

Davis, I.W., Leaver-Fay, A., Chen, V.B., Block, J.N., Kapral, G.J., Wang, X., Murray, L.W., Arendall, W.B., Snoeyink, J. and Richardson, J.S. 2007. MolProbity: all-atom contacts and structure validation for proteins and nucleic acids. *Nucleic acids research.* **35**(suppl 2), pp.W375-W383.

de Baaij, J.H., Blanchard, M.G., Lavrijsen, M., Leipziger, J., Bindels, R.J. and Hoenderop, J.G. 2014. P2X4 receptor regulation of transient receptor potential melastatin type 6 (TRPM6) Mg2+ channels. *Pflügers archiv-european journal of physiology.* **466**(10), pp.1941-1952.

de Baaij, J.H., Kompatscher, A., Viering, D.H., Bos, C., Bindels, R.J. and Hoenderop, J.G. 2016. P2X6 Knockout Mice Exhibit Normal Electrolyte Homeostasis. *PloS one.* **11**(6), pe0156803.

Deiteren, A., van der Linden, L., de Wit, A., Ceuleers, H., Buckinx, R., Timmermans, J.-P., Moreels, T.G., Pelckmans, P.A., Joris, G. and De Winter, B.Y. 2015. P2X 3 Receptors Mediate Visceral Hypersensitivity during Acute Chemically-Induced Colitis and in the Post-Inflammatory Phase via Different Mechanisms of Sensitization. *PloS one.* **10**(4), pe0123810.

DeLano, W.L. 2002. The PyMOL molecular graphics system.

Dell'Antonio, G., Quattrini, A., Cin, E.D., Fulgenzi, A. and Ferrero, M.E. 2002. Relief of inflammatory pain in rats by local use of the selective P2X7 ATP receptor inhibitor, oxidized ATP. *Arthritis & rheumatism.* **46**(12), pp.3378-3385.

Deuchars, S.A., Atkinson, L., Brooke, R.E., Musa, H., Milligan, C.J., Batten, T.F., Buckley, N.J., Parson, S.H. and Deuchars, J. 2001. Neuronal P2X7 receptors are targeted to presynaptic terminals in the central and peripheral nervous systems. *The journal of neuroscience.* **21**(18), pp.7143-7152.

DeVries, M., Vessalo, M. and Galligan, J.J. 2010. Deletion of P2X2 and P2X3 receptor subunits does not alter motility of the mouse colon. *Frontiers in neuroscience.* **4**, p1.

Di Virgilio, F., Chiozzi, P., Falzoni, S., Ferrari, D., Sanz, J.M., Venketaraman, V. and Baricordi, O.R. 1998. Cytolytic P2X purinoceptors. *Cell death and differentiation.* **5**, pp.191-199.

Diaz-Hernandez, J.I., Gomez-Villafuertes, R., León-Otegui, M., Hontecillas-Prieto, L., del Puerto, A., Trejo, J.L., Lucas, J.J., Garrido, J.J., Gualix, J. and Miras-Portugal, M.T. 2012. In vivo P2X7 inhibition reduces amyloid plaques in Alzheimer's disease through GSK3β and secretases. *Neurobiology of aging.* **33**(8), pp.1816-1828.

Donnelly-Roberts, D., McGaraughty, S., Shieh, C.-C., Honore, P. and Jarvis, M.F. 2008. Painful purinergic receptors. *Journal of pharmacology and experimental therapeutics.* **324**(2), pp.409-415.

Donnelly-Roberts, D. and Jarvis, M. 2007. Discovery of P2X7 receptor-selective antagonists offers new insights into P2X7 receptor function and indicates a role in chronic pain states. *British journal of pharmacology.* **151**(5), pp.571-579.

Donnelly-Roberts, D.L., Namovic, M.T., Han, P. and Jarvis, M.F. 2009. Mammalian P2X7 receptor pharmacology: comparison of recombinant mouse, rat and human P2X7 receptors. *British journal of pharmacology.* **157**(7), pp.1203-1214.

Dorn, G., Patel, S., Wotherspoon, G., Hemmings-Mieszczak, M., Barclay, J., Natt, F.J., Martin, P., Bevan, S., Fox, A. and Ganju, P. 2004. siRNA relieves chronic neuropathic pain. *Nucleic acids research.* **32**(5), pp.e49-e49.

Duan, S., Anderson, C.M., Keung, E.C., Chen, Y., Chen, Y. and Swanson, R.A. 2003. P2X7 receptor-mediated release of excitatory amino acids from astrocytes. *The Journal of neuroscience.* **23**(4), pp.1320-1328.

Dunn, P. and Blakeley, A. 1988. Suramin: a reversible P2-purinoceptor antagonist in the mouse vas deferens. *British journal of pharmacology.* **93**(2), pp.243-245.

Eddy, M.C., Eschle, B.K., Barrows, J., Hallock, R.M., Finger, T.E. and Delay, E.R. 2009. Double P2X2/P2X3 purinergic receptor knockout mice do not taste NaCl or the artificial sweetener SC45647. *Chemical senses.* **34**(9), pp.789-797.

Elliott, D.J., Neale, E.J., Aziz, Q., Dunham, J.P., Munsey, T.S., Hunter, M. and Sivaprasadarao, A. 2004. Molecular mechanism of voltage sensor movements in a potassium channel. *The EMBO journal.* **23**(24), pp.4717-4726.

Elneil, S., Skepper, J.N., Kidd, E.J., Williamson, J.G. and Ferguson, D.R. 2001. Distribution of P2X1 and P2X3 receptors in the rat and human urinary bladder. *Pharmacology.* **63**(2), pp.120-128.

Eltzschig, H.K., Eckle, T., Mager, A., Küper, N., Karcher, C., Weissmüller, T., Boengler, K., Schulz, R., Robson, S.C. and Colgan, S.P. 2006. ATP release from activated neutrophils occurs via connexin 43 and modulates adenosine-dependent endothelial cell function. *Circulation research.* **99**(10), pp.1100-1108.

Emsley, H.C., Appleton, R.E., Whitmore, C.L., Jury, F., Lamb, J.A., Martin, J.E., Ollier, W.E., de la Morandière, K.P., Southern, K.W. and Allan, S.M. 2014. Variations in inflammation-related genes may be associated with childhood febrile seizure susceptibility. *Seizure.* **23**(6), pp.457-461.

Ennion, S. and Evans, R. 2001. The role of cysteine residues and disulphide bonds in P2X 1 receptor function. In: *Proceedings of the physiological society*: the physiological society.

Ennion, S., Hagan, S. and Evans, R.J. 2000. The role of positively charged amino acids in ATP recognition by human P2X1 receptors. *Journal of biological chemistry.* **275**(38), pp.29361-29367.

Ennion, S.J. and Evans, R.J. 2002. Conserved cysteine residues in the extracellular loop of the human P2X1 receptor form disulfide bonds and are involved in receptor trafficking to the cell surface. *Molecular pharmacology.* **61**(2), pp.303-311.

Erhardt, A., Lucae, S., Unschuld, P.G., Ising, M., Kern, N., Salyakina, D., Lieb, R., Uhr, M., Binder, E.B. and Keck, M.E. 2007. Association of polymorphisms in P2RX7 and CaMKKb with anxiety disorders. *Journal of affective disorders.* **101**(1), pp.159-168.

Eser, A., Colombel, J.-F., Rutgeerts, P., Vermeire, S., Vogelsang, H., Braddock, M., Persson, T. and Reinisch, W. 2015. Safety and Efficacy of an Oral Inhibitor of the Purinergic Receptor P2X7 in Adult Patients with Moderately to Severely Active Crohn's Disease: A Randomized Placebo-controlled, Double-blind, Phase IIa Study. *Inflammatory bowel diseases.* **21**(10), pp.2247-2253.

Eswar, N., Webb, B., Marti-Renom, M.A., Madhusudhan, M., Eramian, D., Shen, M.y., Pieper, U. and Sali, A. 2006. Comparative protein structure modeling using Modeller. *Current protocols in bioinformatics.* pp.5.6. 1-5.6. 30.

Evans, R., Lewis, C., Buell, G., Valera, S., North, R. and Surprenant, A. 1995. Pharmacological characterization of heterologously expressed ATP-gated cation channels (P2x purinoceptors). *Molecular pharmacology.* **48**(2), pp.178-183.

Eyo, U.B., Miner, S.A., Ahlers, K.E., Wu, L.-J. and Dailey, M.E. 2013. P2X7 receptor activation regulates microglial cell death during oxygen-glucose deprivation. *Neuropharmacology.* **73**, pp.311-319.

Faletra, F., Girotto, G., D'Adamo, A.P., Vozzi, D., Morgan, A. and Gasparini, P. 2014. A novel P2RX2 mutation in an Italian family affected by autosomal dominant nonsyndromic hearing loss. *Gene.* **534**(2), pp.236-239.

Falzoni, S., Munerati, M., Ferrari, D., Spisani, S., Moretti, S. and Di Virgilio, F. 1995. The purinergic P2Z receptor of human macrophage cells. Characterization and possible physiological role. *Journal of clinical investigation.* **95**(3), p1207.

Feng, Y.-H., Li, X., Wang, L., Zhou, L. and Gorodeski, G.I. 2006. A truncated P2X7 receptor variant (P2X7-j) endogenously expressed in cervical cancer cells antagonizes the full-length P2X7 receptor through hetero-oligomerization. *Journal of biological chemistry.* **281**(25), pp.17228-17237.

Fernando, S.L., Saunders, B.M., Sluyter, R., Skarratt, K.K., Goldberg, H., Marks, G.B., Wiley, J.S. and Britton, W.J. 2007. A polymorphism in the P2X7 gene increases susceptibility to extrapulmonary tuberculosis. *American journal of respiratory and critical care medicine.* **175**(4), pp.360-366.

Ferrari, D., Chiozzi, P., Falzoni, S., Hanau, S. and Di Virgilio, F. 1997. Purinergic modulation of interleukin-1β release from microglial cells stimulated with bacterial endotoxin. *The journal of experimental medicine.* **185**(3), pp.579-582.

Ferrari, D., La Sala, A., Chiozzi, P., Morelli, A., Falzoni, S., Girolomoni, G., Idzko, M., Dichmann, S., Norgauer, J. and Di Virgilio, F. 2000. The P2 purinergic receptors of human dendritic cells: identification and coupling to cytokine release. *The FASEB journal.* **14**(15), pp.2466-2476.

Ferrari, D., Los, M., Bauer, M.K., Vandenabeele, P., Wesselborg, S. and Schulze-Osthoff, K. 1999. P2Z purinoreceptor ligation induces activation of caspases with distinct roles in apoptotic and necrotic alterations of cell death. *FEBS letters.* **447**(1), pp.71-75.

Ferrari, D., Pizzirani, C., Adinolfi, E., Lemoli, R.M., Curti, A., Idzko, M., Panther, E. and Di Virgilio, F. 2006. The P2X7 receptor: a key player in IL-1 processing and release. *The journal of immunology.* **176**(7), pp.3877-3883.

Finger, T.E., Danilova, V., Barrows, J., Bartel, D.L., Vigers, A.J., Stone, L., Hellekant, G. and Kinnamon, S.C. 2005. ATP signaling is crucial for communication from taste buds to gustatory nerves. *Science.* **310**(5753), pp.1495-1499.

Fischer, R., Kalthof, B., Rank, E., Stelte-Ludwig, B. and Wuttke, M. 2004. Preparation of benzofuro-1, 4-diazepin-2-ones as P2X 4 receptor antagonists for the treatment of arteriosclerosis and restenosis. *DE 10312969A1.* pp.1-14.

Fiser, A., Do, R.K.G. and Šali, A. 2000. Modeling of loops in protein structures. *Protein science.* **9**(9), pp.1753-1773.

Fonfria, E., Clay, W., Levy, D., Goodwin, J., Roman, S., Smith, G., Condreay, J. and Michel, A. 2008. Cloning and pharmacological characterization of the guinea pig P2X7 receptor orthologue. *British journal of pharmacology.* **153**(3), pp.544-556.

Ford, A.P., Gever, J.R., Nunn, P.A., Zhong, Y., Cefalu, J.S., Dillon, M.P. and Cockayne, D.A. 2006. Purinoceptors as therapeutic targets for lower urinary tract dysfunction. *British journal of pharmacology.* **147**(S2), pp.S132-S143.

Fowler, B.J., Gelfand, B.D., Kim, Y., Kerur, N., Tarallo, V., Hirano, Y., Amarnath, S., Fowler, D.H., Radwan, M. and Young, M.T. 2014. Nucleoside reverse transcriptase inhibitors possess intrinsic anti-inflammatory activity. *Science.* **346**(6212), pp.1000-1003.

Franceschini, A., Capece, M., Chiozzi, P., Falzoni, S., Sanz, J.M., Sarti, A.C., Bonora, M., Pinton, P. and Di Virgilio, F. 2015. The P2X7 receptor directly interacts with the NLRP3 inflammasome scaffold protein. *The FASEB journal.* **29**(6), pp.2450-2461.

Fredholm, B.B., Arslan, G., Halldner, L., Kull, B., Schulte, G. and Wasserman, W. 2000. Structure and function of adenosine receptors and their genes. *Naunyn-Schmiedeberg's archives of pharmacology.* **362**(4-5), pp.364-374.

Gachet, C. 2008. P2 receptors, platelet function and pharmacological implications. *Thrombosis and haemostasis-Stuttgart.* **99**(3), p466.

Garcia-Guzman, M., Soto, F., Gomez-Hernandez, J.M., Lund, P.-E. and Stühmer, W. 1997. Characterization of recombinant human P2X4 receptor reveals pharmacological differences to the rat homologue. *Molecular pharmacology.* **51**(1), pp.109-118.

Gargett, C.E. and Wiley, J.S. 1997. The isoquinoline derivative KN-62 a potent antagonist of the P2Z-receptor of human lymphocytes. *British journal of pharmacology.* **120**(8), pp.1483-1490.

Gartland, A., Buckley, K., Bowler, W. and Gallagher, J. 2003a. Blockade of the pore-forming P2X7 receptor inhibits formation of multinucleated human osteoclasts in vitro. *Calcified tissue international.* **73**(4), pp.361-369.

Gartland, A., Buckley, K.A., Hipskind, R.A., Perry, M., Tobias, J., Buell, G., Chessell, I., Bowler, W.B. and Gallagher, J.A. 2003b. Multinucleated osteoclast formation in vivo and in vitro by P2X 7 receptor-deficient mice. *Critical reviews™ in eukaryotic gene expression.* **13**(2-4).

Gartland, A., Skarratt, K.K., Hocking, L.J., Parsons, C., Stokes, L., Jørgensen, N.R., Fraser, W.D., Reid, D.M., Gallagher, J.A. and Wiley, J.S. 2012. Polymorphisms in the P2X7 receptor gene are associated with low lumbar spine bone mineral density and accelerated bone loss in post-menopausal women. *European journal of human genetics.* **20**(5), pp.559-564.

Gavrieli, Y., Sherman, Y. and Ben-Sasson, S.A. 1992. Identification of programmed cell death in situ via specific labeling of nuclear DNA fragmentation. *The journal of cell biology.* **119**(3), pp.493-501.

Geistlinger, J., Du, W., Groll, J., Liu, F., Hoegel, J., Foehr, K., Pasquarelli, A. and Schneider, E. 2012. P2RX7 genotype association in severe sepsis identified by a novel Multi-Individual Array for rapid screening and replication of risk SNPs. *Clinica chimica acta.* **413**(1), pp.39-47.

Gever, J.R., Cockayne, D.A., Dillon, M.P., Burnstock, G. and Ford, A.P. 2006. Pharmacology of P2X channels. *Pflügers Archiv.* **452**(5), pp.513-537.

Gever, J.R., Soto, R., Henningsen, R.A., Martin, R.S., Hackos, D.H., Panicker, S., Rubas, W., Oglesby, I.B., Dillon, M.P. and Milla, M.E. 2010. AF-353, a novel, potent and orally bioavailable P2X3/P2X2/3 receptor antagonist. *British journal of pharmacology.* **160**(6), pp.1387-1398.

Gidlöf, O., Smith, J.G., Melander, O., Lövkvist, H., Hedblad, B., Engström, G., Nilsson, P., Carlson, J., Berglund, G. and Olsson, S. 2012. A common missense variant in the ATP receptor P2X7 is associated with reduced risk of cardiovascular events. *PLoS one.* **7**(5), pe37491.

Gillet, V.J., Myatt, G., Zsoldos, Z. and Johnson, A.P. 1995. SPROUT, HIPPO and CAESA: Tools for de novo structure generation and estimation of synthetic accessibility. *Perspectives in drug discovery and design.* **3**(1), pp.34-50.

Glass, R., Townsend-Nicholson, A. and Burnstock, G. 2000. P2 receptors in the thymus: expression of P2X and P2Y receptors in adult rats, an immunohistochemical and in situ hybridisation study. *Cell and tissue research.* **300**(2), pp.295-306.

Gong, Q.J., Li, Y.Y., Xin, W.J., Zang, Y., Ren, W.J., Wei, X.H., Li, Y.Y., Zhang, T. and Liu, X.G. 2009. ATP induces long-term potentiation of C-fiber-evoked field potentials in spinal dorsal horn: the roles of P2X4 receptors and p38 MAPK in microglia. *Glia.* **57**(6), pp.583-591.

Gonnord, P., Delarasse, C., Auger, R., Benihoud, K., Prigent, M., Cuif, M., Lamaze, C. and Kanellopoulos, J. 2009. Palmitoylation of the P2X7 receptor, an ATP-gated channel, controls its expression and association with lipid rafts. *The FASEB journal.* **23**(3), pp.795-805.

Gonzales, E., Julien, B., Serrière-Lanneau, V., Nicou, A., Doignon, I., Lagoudakis, L., Garcin, I., Azoulay, D., Duclos-Vallée, J.-C. and Castaing, D. 2010. ATP release after partial hepatectomy regulates liver regeneration in the rat. *Journal of hepatology.* **52**(1), pp.54-62.

Gordon, J.L. 1986. Extracellular ATP: effects, sources and fate. *Biochemical journal.* **233**(2), p309.

Green, E.K., Grozeva, D., Raybould, R., Elvidge, G., Macgregor, S., Craig, I., Farmer, A., McGuffin, P., Forty, L. and Jones, L. 2009. P2RX7: a bipolar and unipolar disorder candidate susceptibility gene? *American journal of medical genetics part B: neuropsychiatric genetics.* **150**(8), pp.1063-1069.

Greenberg, S., Di Virgilio, F., Steinberg, T. and Silverstein, S. 1988. Extracellular nucleotides mediate Ca2+ fluxes in J774 macrophages by two distinct mechanisms. *Journal of biological chemistry.* **263**(21), pp.10337-10343.

Greenwood, D., Yao, W.P. and Housley, G.D. 1997. Expression of the P2X2 receptor subunit of the ATP-gated ion channel in the retina. *Neuroreport.* **8**(5), pp.1083-1088.

Grigoroiu-Serbanescu, M., Herms, S., Mühleisen, T.W., Georgi, A., Diaconu, C.C., Strohmaier, J., Czerski, P., Hauser, J., Leszczynska-Rodziewicz, A. and Jamra, R.A. 2009. Variation in P2RX7 candidate gene (rs2230912) is not associated with bipolar I disorder and unipolar major depression in four European samples. *American journal of medical genetics part B: neuropsychiatric genetics.* **150**(7), pp.1017-1021.

Grol, M.W., Panupinthu, N., Korcok, J., Sims, S.M. and Dixon, S.J. 2009. Expression, signaling, and function of P2X7 receptors in bone. *Purinergic signalling.* **5**(2), pp.205-221.

Gröschel-Stewart, U., Bardini, M., Robson, T. and Burnstock, G. 1999. Localisation of P2X5 and P2X7 receptors by immunohistochemistry in rat stratified squamous epithelia. *Cell and tissue research.* **296**(3), pp.599-605.

Gu, B.J., Baird, P.N., Vessey, K.A., Skarratt, K.K., Fletcher, E.L., Fuller, S.J., Richardson, A.J., Guymer, R.H. and Wiley, J.S. 2013. A rare functional haplotype of the P2RX4 and P2RX7 genes leads to loss of innate phagocytosis and confers increased risk of age-related macular degeneration. *The FASEB journal.* **27**(4), pp.1479-1487.

Gu, B.J., Field, J., Dutertre, S., Ou, A., Kilpatrick, T.J., Lechner-Scott, J., Scott, R., Lea, R., Taylor, B.V. and Stankovich, J. 2015. A rare P2X7 variant Arg307Gln with absent pore formation function protects against neuroinflammation in multiple sclerosis. *Human molecular genetics.* pddv278.

Gu, B.J., Rathsam, C., Stokes, L., McGeachie, A.B. and Wiley, J.S. 2009. Extracellular ATP dissociates nonmuscle myosin from P2X7 complex: this dissociation regulates P2X7 pore formation. *American journal of physiology-cell physiology.* **297**(2), pp.C430-C439.

Guile, S.D., Alcaraz, L., Birkinshaw, T.N., Bowers, K.C., Ebden, M.R., Furber, M. and Stocks, M.J. 2009. Antagonists of the P2X7 receptor. From lead identification to drug development. *Journal of medicinal chemistry.* **52**(10), pp.3123-3141.

Gum, R.J., Wakefield, B. and Jarvis, M.F. 2012. P2X receptor antagonists for pain management: examination of binding and physicochemical properties. *Purinergic signalling.* **8**(1), pp.41-56.

Guo, C., Masin, M., Qureshi, O.S. and Murrell-Lagnado, R.D. 2007. Evidence for functional P2X4/P2X7 heteromeric receptors. *Molecular pharmacology.* **72**(6), pp.1447-1456.

Guo, H., Callaway, J.B. and Ting, J.P. 2015. Inflammasomes: mechanism of action, role in disease, and therapeutics. *Nature medicine.* **21**(7), pp.677-687.

Haanes, K.A., Schwab, A. and Novak, I. 2012. The P2X7 receptor supports both life and death in fibrogenic pancreatic stellate cells. *PloS one.* **7**(12), pe51164.

Hamilton, S.G., McMahon, S.B. and Lewin, G.R. 2001. Selective activation of nociceptors by P2X receptor agonists in normal and inflamed rat skin. *The journal of physiology.* **534**(2), pp.437-445.

Hansen, R.R., Nasser, A., Falk, S., Baldvinsson, S.B., Ohlsson, P.H., Bahl, J.M., Jarvis, M.F., Ding, M. and Heegaard, A.-M. 2012. Chronic administration of the selective P2X3, P2X2/3 receptor antagonist, A-317491, transiently attenuates cancer-induced bone pain in mice. *European journal of pharmacology.* **688**(1), pp.27-34.

Hattori, M. and Gouaux, E. 2012. Molecular mechanism of ATP binding and ion channel activation in P2X receptors. *Nature.* **485**(7397), pp.207-212.

Hausmann, R., Rettinger, J., Gerevich, Z., Meis, S., Kassack, M.U., Illes, P., Lambrecht, G. and Schmalzing, G. 2006. The suramin analog 4, 4′, 4 ″, 4 ‴-(carbonylbis (imino-5, 1, 3-benzenetriylbis (carbonylimino))) tetra-kis-benzenesulfonic acid (NF110) potently blocks P2X3 receptors: subtype selectivity is determined by location of sulfonic acid groups. *Molecular pharmacology.* **69**(6), pp.2058-2067.

Hausmann, R. and Schmalzing, G. 2012. P2X1 and P2X2 receptors in the central nervous system as possible drug targets. *CNS & neurological disorders-drug targets (formerly current drug targets-CNS & neurological disorders).* **11**(6), pp.675-686.

Hechler, B., Lenain, N., Marchese, P., Vial, C., Heim, V., Freund, M., Cazenave, J.-P., Cattaneo, M., Ruggeri, Z.M. and Evans, R. 2003. A role of the fast ATP-gated P2X1 cation channel in thrombosis of small arteries in vivo. *The journal of experimental medicine.* **198**(4), pp.661-667.

Hejjas, K., Szekely, A., Domotor, E., Halmai, Z., Balogh, G., Schilling, B., Sarosi, A., Faludi, G., Sasvari-Szekely, M. and Nemoda, Z. 2009. Association between depression and the Gln460Arg polymorphism of P2RX7 gene: a dimensional approach. *American journal of medical genetics part B: neuropsychiatric genetics.* **150**(2), pp.295-299.

Hiasa, M., Togawa, N., Miyaji, T., Omote, H., Yamamoto, A. and Moriyama, Y. 2014. Essential role of vesicular nucleotide transporter in vesicular storage and release of nucleotides in platelets. *Physiological reports.* **2**(6), pe12034.

Hickman, S.E., El Khoury, J., Greenberg, S., Schieren, I. and Silverstein, S.C. 1994. P2Z adenosine triphosphate receptor activity in cultured human monocyte-derived macrophages. *Blood.* **84**(8), pp.2452-2456.

Hidaka, H. and Yokokura, H. 1996. Molecular and cellular pharmacology of a calcium/calmodulin-dependent protein kinase II (CaM kinase II) inhibitor, KN-62, and proposal of CaM kinase phosphorylation cascades. *Advances in pharmacology (San Diego, Calif.).* **36**, p193.

Ho, T., Vessey, K. and Fletcher, E. 2014. Immunolocalization of the P2X4 receptor on neurons and glia in the mammalian retina. *Neuroscience.* **277**, pp.55-71.

Holton, F. and Holton, P. 1954. The capillary dilator substances in dry powders of spinal roots; a possible role of adenosine triphosphate in chemical transmission from nerve endings. *The journal of physiology.* **126**(1), pp.124-140.

Honore, P., Donnelly-Roberts, D., Namovic, M.T., Hsieh, G., Zhu, C.Z., Mikusa, J.P., Hernandez, G., Zhong, C., Gauvin, D.M. and Chandran, P. 2006. A-740003 [N-(1-{[(cyanoimino)(5-quinolinylamino) methyl] amino}-2, 2-dimethylpropyl)-2-(3, 4-dimethoxyphenyl) acetamide], a novel and selective P2X7 receptor antagonist, dose-dependently reduces neuropathic pain in the rat. *Journal of pharmacology and experimental therapeutics.* **319**(3), pp.1376-1385.

Honore, P., Mikusa, J., Bianchi, B., McDonald, H., Cartmell, J., Faltynek, C. and Jarvis, M.F. 2002. TNP-ATP, a potent P2X 3 receptor antagonist, blocks acetic acid-induced abdominal constriction in mice: comparison with reference analgesics. *Pain.* **96**(1), pp.99-105.

Housley, G.D., Kanjhan, R., Raybould, N.P., Greenwood, D., Salih, S.G., Järlebark, L., Burton, L.D., Setz, V.C., Cannell, M.B. and Soeller, C. 1999. Expression of the P2X2 receptor subunit of the ATP-gated ion channel in the cochlea: implications

for sound transduction and auditory neurotransmission. *The journal of neuroscience.* **19**(19), pp.8377-8388.

Housley, G.D., Morton-Jones, R., Vlajkovic, S.M., Telang, R.S., Paramananthasivam, V., Tadros, S.F., Wong, A.C.Y., Froud, K.E., Cederholm, J.M. and Sivakumaran, Y. 2013. ATP-gated ion channels mediate adaptation to elevated sound levels. *Proceedings of the national academy of sciences.* **110**(18), pp.7494-7499.

Hoyle, C.H., Pintor, J., Gualix, J. and Miras-Portugal, M.T. 1997. Antagonism of P2X receptors in guinea-pig vas deferens by diinosine pentaphosphate. *European journal of pharmacology.* **333**(2), pp.R1-R2.

Hughes, J.P., Hatcher, J.P. and Chessell, I.P. 2007. The role of P2X7 in pain and inflammation. *Purinergic signalling.* **3**(1-2), pp.163-169.

Hülsmann, M., Nickel, P., Kassack, M., Schmalzing, G., Lambrecht, G. and Markwardt, F. 2003. NF449, a novel picomolar potency antagonist at human P2X 1 receptors. *European journal of pharmacology.* **470**(1), pp.1-7.

Humphreys, B.D., Virginio, C., Surprenant, A., Rice, J. and Dubyak, G.R. 1998. Isoquinolines as antagonists of the P2X7 nucleotide receptor: high selectivity for the human versus rat receptor homologues. *Molecular pharmacology.* **54**(1), pp.22-32.

Husted, L., Harsløf, T., Stenkjær, L., Carstens, M., Jørgensen, N. and Langdahl, B.L. 2013. Functional polymorphisms in the P2X7 receptor gene are associated with osteoporosis. *Osteoporosis international.* **24**(3), pp.949-959.

Inoue, K., Tsuda, M. and Koizumi, S. 2004. ATP-and adenosine-mediated signaling in the central nervous system: chronic pain and microglia: involvement of the ATP receptor P2X4. *Journal of pharmacological sciences.* **94**(2), pp.112-114.

Inscho, E.W., Cook, A.K., Imig, J.D., Vial, C. and Evans, R.J. 2003. Physiological role for P2X 1 receptors in renal microvascular autoregulatory behavior. *The journal of clinical investigation.* **112**(12), pp.1895-1905.

Ireland, M., Noakes, P. and Bellingham, M. 2004. P2X 7-like receptor subunits enhance excitatory synaptic transmission at central synapses by presynaptic mechanisms. *Neuroscience.* **128**(2), pp.269-280.

Irwin, J.J., Sterling, T., Mysinger, M.M., Bolstad, E.S. and Coleman, R.G. 2012. ZINC: a free tool to discover chemistry for biology. *Journal of chemical information and modeling.* **52**(7), pp.1757-1768.

Jacobson, K.A., Kim, Y.-C., Wildman, S.S., Mohanram, A., Harden, T.K., Boyer, J.L., King, B.F. and Burnstock, G. 1998. A pyridoxine cyclic phosphate and its 6-azoaryl derivative selectively potentiate and antagonize activation of P2X1 receptors. *Journal of medicinal chemistry.* **41**(13), pp.2201-2206.

Jacobson, K.A., Paoletta, S., Katritch, V., Wu, B., Gao, Z.-G., Zhao, Q., Stevens, R.C. and Kiselev, E. 2015. Nucleotides acting at P2Y receptors: connecting structure and function. *Molecular pharmacology.* **88**(2), pp.220-230.

Jamieson, S.E., Peixoto-Rangel, A.L., Hargrave, A.C., de Roubaix, L.-A., Mui, E.J., Boulter, N.R., Miller, E.N., Fuller, S.J., Wiley, J.S. and Castellucci, L. 2010. Evidence for associations between the purinergic receptor P2X7 (P2RX7) and toxoplasmosis. *Genes and immunity.* **11**(5), pp.374-383.

Janssen, B., Vugts, D.J., Funke, U., Spaans, A., Schuit, R.C., Kooijman, E., Rongen, M., Perk, L.R., Lammertsma, A.A. and Windhorst, A.D. 2014. Synthesis and initial preclinical evaluation of the P2X7 receptor antagonist [11C] A-740003 as a novel tracer of neuroinflammation. *Journal of labelled compounds and radiopharmaceuticals.* **57**(8), pp.509-516.

Järlebark, L.E., Housley, G.D. and Thorne, P.R. 2000. Immunohistochemical localization of adenosine 5-triphosphate-gated ion channel P2X2 receptor subunits in adult and developing rat cochlea. *Journal of comparative neurology.* **421**(3), pp.289-301.

Jarvis, M.F., Burgard, E.C., McGaraughty, S., Honore, P., Lynch, K., Brennan, T.J., Subieta, A., van Biesen, T., Cartmell, J. and Bianchi, B. 2002. A-317491, a novel potent and selective non-nucleotide antagonist of P2X3 and P2X2/3 receptors,

reduces chronic inflammatory and neuropathic pain in the rat. *Proceedings of the national academy of sciences.* **99**(26), pp.17179-17184.

Jelassi, B., Anchelin, M., Chamouton, J., Cayuela, M.L., Clarysse, L., Li, J., Goré, J., Jiang, L.-H. and Roger, S. 2013. Anthraquinone emodin inhibits human cancer cell invasiveness by antagonizing P2X7 receptors. *Carcinogenesis.* pbgt099.

Jelassi, B., Chantome, A., Alcaraz-Perez, F., Baroja-Mazo, A., Cayuela, M., Pelegrin, P., Surprenant, A. and Roger, S. 2011. P2X7 receptor activation enhances SK3 channels-and cystein cathepsin-dependent cancer cells invasiveness. *Oncogene.* **30**(18), pp.2108-2122.

Jiang, L.-H. 2012. P2X receptor-mediated ATP purinergic signalling in health and disease. *Cell health cytoskeleton.* **4**, pp.83-101.

Jiang, L.-H. 2015. HIV drug nucleoside reverse transcriptase inhibitors as promising anti-inflammation therapeutics by targeting P2X7-dependent large pore formation: one stone for two birds? *Frontiers in pharmacology.* **6**, p38.

Jiang, L.-H., Baldwin, J.M., Roger, S. and Baldwin, S.A. 2013. Insights into the molecular mechanisms underlying mammalian P2X7 receptor functions and contributions in diseases, revealed by structural modeling and single nucleotide polymorphisms. *Frontiers in pharmacology.* **4**.

Jiang, L.-H., Kim, M., Spelta, V., Bo, X., Surprenant, A. and North, R.A. 2003. Subunit arrangement in P2X receptors. *The journal of neuroscience.* **23**(26), pp.8903-8910.

Jiang, L.-H., Mackenzie, A.B., North, R.A. and Surprenant, A. 2000a. Brilliant blue G selectively blocks ATP-gated rat P2X7 receptors. *Molecular pharmacology.* **58**(1), pp.82-88.

Jiang, L.-H., Rassendren, F., Mackenzie, A., Zhang, Y.-H., Surprenant, A. and North, R.A. 2005. N-methyl-D-glucamine and propidium dyes utilize different permeation pathways at rat P2X7 receptors. *American journal of physiology-cell physiology.* **289**(5), pp.C1295-C1302.

Jiang, L.-H., Rassendren, F., Spelta, V., Surprenant, A. and North, R.A. 2001. Amino acid residues involved in gating identified in the first membrane-spanning domain of the rat P2X2 receptor. *Journal of biological chemistry.* **276**(18), pp.14902-14908.

Jiang, L.-H., Rassendren, F., Surprenant, A. and North, R.A. 2000b. Identification of amino acid residues contributing to the ATP-binding site of a purinergic P2X receptor. *Journal of biological chemistry.* **275**(44), pp.34190-34196.

Jiang, R., Taly, A., Lemoine, D., Martz, A., Cunrath, O. and Grutter, T. 2012. Tightening of the ATP-binding sites induces the opening of P2X receptor channels. *The EMBO journal.* **31**(9), pp.2134-2143.

Jimenez-Mateos, E.M., Arribas-Blazquez, M., Sanz-Rodriguez, A., Concannon, C., Olivos-Ore, L.A., Reschke, C.R., Mooney, C.M., Mooney, C., Lugara, E. and Morgan, J. 2015. microRNA targeting of the P2X7 purinoceptor opposes a contralateral epileptogenic focus in the hippocampus. *Scientific reports.* **5**.

Jimenez-Pacheco, A., Diaz-Hernandez, M., Arribas-Blázquez, M., Sanz-Rodriguez, A., Olivos-Oré, L.A., Artalejo, A.R., Alves, M., Letavic, M., Miras-Portugal, M.T. and Conroy, R.M. 2016. Transient P2X7 Receptor Antagonism Produces Lasting Reductions in Spontaneous Seizures and Gliosis in Experimental Temporal Lobe Epilepsy. *The journal of neuroscience.* **36**(22), pp.5920-5932.

Jones, C., Chessell, I., Simon, J., Barnard, E., Miller, K., Michel, A. and Humphrey, P. 2000. Functional characterization of the P2X4 receptor orthologues. *British journal of pharmacology.* **129**(2), pp.388-394.

Jones, C.A., Vial, C., Sellers, L.A., Humphrey, P.P., Evans, R.J. and Chessell, I.P. 2004. Functional regulation of P2X6 receptors by N-linked glycosylation: identification of a novel αβ-methylene ATP-sensitive phenotype. *Molecular pharmacology.* **65**(4), pp.979-985.

Jørgensen, N.R., Henriksen, Z., Sørensen, O.H., Eriksen, E.F., Civitelli, R. and Steinberg, T.H. 2002. Intercellular calcium signaling occurs between human

osteoblasts and osteoclasts and requires activation of osteoclast P2X7 receptors. *Journal of biological chemistry.* **277**(9), pp.7574-7580.

Jørgensen, N.R., Husted, L.B., Skarratt, K.K., Stokes, L., Tofteng, C.L., Kvist, T., Jensen, J.-E.B., Eiken, P., Brixen, K. and Fuller, S. 2012. Single-nucleotide polymorphisms in the P2X7 receptor gene are associated with post-menopausal bone loss and vertebral fractures. *European journal of human genetics.* **20**(6), pp.675-681.

Kaan, T.K., Yip, P.K., Patel, S., Davies, M., Marchand, F., Cockayne, D.A., Nunn, P.A., Dickenson, A.H., Ford, A.P. and Zhong, Y. 2010. Systemic blockade of P2X3 and P2X2/3 receptors attenuates bone cancer pain behaviour in rats. *Brain.* **133**(9), pp.2549-2564.

Kanis, J.A., Melton, L.J., Christiansen, C., Johnston, C.C. and Khaltaev, N. 1994. The diagnosis of osteoporosis. *Journal of bone and mineral research.* **9**(8), pp.1137-1141.

Karmakar, M., Katsnelson, M.A., Dubyak, G.R. and Pearlman, E. 2016. Neutrophil P2X7 receptors mediate NLRP3 inflammasome-dependent IL-1 [beta] secretion in response to ATP. *Nature communications.* **7**.

Kash, T.L., Jenkins, A., Kelley, J.C., Trudell, J.R. and Harrison, N.L. 2003. Coupling of agonist binding to channel gating in the GABAA receptor. *Nature.* **421**(6920), pp.272-275.

Kasuya, G., Fujiwara, Y., Takemoto, M., Dohmae, N., Nakada-Nakura, Y., Ishitani, R., Hattori, M. and Nureki, O. 2016. Structural insights into divalent cation modulations of ATP-gated P2X receptor channels. *Cell reports.* **14**(4), pp.932-944.

Kauffenstein, G., Pelletier, J., Lavoie, E.G., Kukulski, F., Martín-Satué, M., Dufresne, S.S., Frenette, J., Fürstenau, C.R., Sereda, M.J. and Toutain, B. 2014. Nucleoside triphosphate diphosphohydrolase-1 ectonucleotidase is required for normal vas deferens contraction and male fertility through maintaining P2X1 receptor function. *Journal of biological chemistry.* **289**(41), pp.28629-28639.

Kawate, T., Michel, J.C., Birdsong, W.T. and Gouaux, E. 2009. Crystal structure of the ATP-gated P2X4 ion channel in the closed state. *Nature.* **460**(7255), pp.592-598.

Kawate, T., Robertson, J.L., Li, M., Silberberg, S.D. and Swartz, K.J. 2011. Ion access pathway to the transmembrane pore in P2X receptor channels. *The journal of general physiology.* **137**(6), pp.579-590.

Ke, H.Z., Qi, H., Weidema, A.F., Zhang, Q., Panupinthu, N., Crawford, D.T., Grasser, W.A., Paralkar, V.M., Li, M. and Audoly, L.P. 2003. Deletion of the P2X7 nucleotide receptor reveals its regulatory roles in bone formation and resorption. *Molecular Endocrinology.* **17**(7), pp.1356-1367.

Keystone, E.C., Wang, M.M., Layton, M., Hollis, S. and McInnes, I.B. 2012. Clinical evaluation of the efficacy of the P2X7 purinergic receptor antagonist AZD9056 on the signs and symptoms of rheumatoid arthritis in patients with active disease despite treatment with methotrexate or sulphasalazine. *Annals of the rheumatic diseases.* **71**(10), pp.1630-1635.

Khadra, A., Tomić, M., Yan, Z., Zemkova, H., Sherman, A. and Stojilkovic, S.S. 2013. Dual gating mechanism and function of P2X7 receptor channels. *Biophysical journal.* **104**(12), pp.2612-2621.

Khakh, B.S., Bao, X.R., Labarca, C. and Lester, H.A. 1999. Neuronal P2X transmitter-gated cation channels change their ion selectivity in seconds. *Nature neuroscience.* **2**(4), pp.322-330.

Kim, M., Jiang, L.H., Wilson, H.L., North, R.A. and Surprenant, A. 2001a. Proteomic and functional evidence for a P2X7 receptor signalling complex. *The EMBO journal.* **20**(22), pp.6347-6358.

Kim, Y.-C., Brown, S.G., Harden, T.K., Boyer, J.L., Dubyak, G., King, B.F., Burnstock, G. and Jacobson, K.A. 2001b. Structure-activity relationships of pyridoxal phosphate derivatives as potent and selective antagonists of P2X1 receptors. *Journal of medicinal chemistry.* **44**(3), pp.340-349.

King, B., Liu, M., Pintor, J., Gualix, J., Miras-Portugal, M. and Burnstock, G. 1999. Diinosine pentaphosphate (IP5I) is a potent antagonist at recombinant rat P2X1 receptors. *British journal of pharmacology.* **128**(5), pp.981-988.

Klapperstück, M., Büttner, C., Nickel, P., Schmalzing, G., Lambrecht, G. and Markwardt, F. 2000. Antagonism by the suramin analogue NF279 on human P2X 1 and P2X 7 receptors. *European journal of pharmacology.* **387**(3), pp.245-252.

Kobayashi, K., Yamanaka, H. and Noguchi, K. 2013. Expression of ATP receptors in the rat dorsal root ganglion and spinal cord. *Anatomical science international.* **88**(1), pp.10-16.

Korcok, J., Raimundo, L.N., Ke, H.Z., Sims, S.M. and Dixon, S.J. 2004. Extracellular Nucleotides Act Through P2X7 Receptors to Activate NF-κB in Osteoclasts. *Journal of bone and mineral research.* **19**(4), pp.642-651.

Kukley, M., Barden, J.A., Steinhäuser, C. and Jabs, R. 2001. Distribution of P2X receptors on astrocytes in juvenile rat hippocampus. *Glia.* **36**(1), pp.11-21.

Kukley, M., Stausberg, P., Adelmann, G., Chessell, I.P. and Dietrich, D. 2004. Ecto-nucleotidases and nucleoside transporters mediate activation of adenosine receptors on hippocampal mossy fibers by P2X7 receptor agonist 2′-3′-O-(4-benzoylbenzoyl)-ATP. *The journal of neuroscience.* **24**(32), pp.7128-7139.

Kusner, D.J. and Adams, J. 2000. ATP-induced killing of virulent Mycobacterium tuberculosis within human macrophages requires phospholipase D. *The journal of immunology.* **164**(1), pp.379-388.

Kusner, D.J. and Barton, J.A. 2001. ATP stimulates human macrophages to kill intracellular virulent Mycobacterium tuberculosis via calcium-dependent phagosome-lysosome fusion. *The Journal of Immunology.* **167**(6), pp.3308-3315.

Kvist, T., Syberg, S., Petersen, S., Ding, M., Jørgensen, N. and Schwarz, P. 2015. The role of the P2X7 receptor on bone loss in a mouse model of inflammation-mediated osteoporosis. *Bone reports.*

Kwon, H.J. 2012. Extracellular ATP signaling via P2X4 receptor and cAMP/PKA signaling mediate ATP oscillations essential for prechondrogenic condensation. *Journal of endocrinology.* **214**(3), pp.337-348.

Labasi, J.M., Petrushova, N., Donovan, C., McCurdy, S., Lira, P., Payette, M.M., Brissette, W., Wicks, J.R., Audoly, L. and Gabel, C.A. 2002. Absence of the P2X7 receptor alters leukocyte function and attenuates an inflammatory response. *The journal of immunology.* **168**(12), pp.6436-6445.

Lambertucci, C., Dal Ben, D., Buccioni, M., Marucci, G., Thomas, A. and Volpini, R. 2015. Medicinal chemistry of P2X receptors: Agonists and orthosteric antagonists. *Current medicinal chemistry.* **22**(7), pp.915-928.

Lambrecht, G. 1996. Design and pharmacology of selective P2-purinoceptor antagonists. *Journal of autonomic pharmacology.* **16**(6), pp.341-344.

Lambrecht, G., Friebe, T., Grimm, U., Windscheif, U., Bungardt, E., Hildebrandt, C., Bäumert, H.G., Spatz-Kümbel, G. and Mutschler, E. 1992. PPADS, a novel functionally selective antagonist of P2 purinoceptor-mediated responses. *European journal of pharmacology.* **217**(2-3), pp.217-219.

Lambrecht, G., Rettinger, J., Bäumert, H.G., Czeche, S., Damer, S., Ganso, M., Hildebrandt, C., Niebel, B., Spatz-Kümbel, G. and Schmalzing, G. 2000. The novel pyridoxal-5′-phosphate derivative PPNDS potently antagonizes activation of P2X 1 receptors. *European journal of pharmacology.* **387**(3), pp.R19-R21.

Lammas, D., Stober, C., Harvey, C., Kendrick, N., Panchalingam, S. and Kumararatne, D. 1997. ATP-induced killing of mycobacteria by human macrophages is mediated by purinergic P2Z (P2X 7) receptors. *Immunity.* **7**(3), pp.433-444.

Le Feuvre, R.A., Brough, D., Iwakura, Y., Takeda, K. and Rothwell, N.J. 2002. Priming of macrophages with lipopolysaccharide potentiates P2X7-mediated cell death via a caspase-1-dependent mechanism, independently of cytokine production. *Journal of biological chemistry.* **277**(5), pp.3210-3218.

Lê, K.-T., Babinski, K. and Séguéla, P. 1998. Central P2X4 and P2X6 channel subunits coassemble into a novel heteromeric ATP receptor. *The journal of neuroscience.* **18**(18), pp.7152-7159.

Lê, K.-T., Boué-Grabot, E., Archambault, V. and Séguéla, P. 1999. Functional and biochemical evidence for heteromeric ATP-gated channels composed of P2X1 and P2X5subunits. *Journal of biological chemistry.* **274**(22), pp.15415-15419.

Le Stunff, H., Auger, R., Kanellopoulos, J. and Raymond, M.-N. 2004. The Pro-451 to Leu polymorphism within the C-terminal tail of P2X7 receptor impairs cell death but not phospholipase D activation in murine thymocytes. *Journal of biological chemistry.* **279**(17), pp.16918-16926.

Lecut, C., Faccinetto, C., Delierneux, C., van Oerle, R., Spronk, H., Evans, R.J., El Benna, J., Bours, V. and Oury, C. 2012. ATP-gated P2X1 ion channels protect against endotoxemia by dampening neutrophil activation. *Journal of thrombosis and haemostasis.* **10**(3), pp.453-465.

Lecut, C., Frederix, K., Johnson, D.M., Deroanne, C., Thiry, M., Faccinetto, C., Marée, R., Evans, R.J., Volders, P.G. and Bours, V. 2009. P2X1 ion channels promote neutrophil chemotaxis through Rho kinase activation. *The journal of immunology.* **183**(4), pp.2801-2809.

Lee, H.G., Won, S.M., Gwag, B.J. and Lee, Y.B. 2011. Microglial P2X7 receptor expression is accompanied by neuronal damage in the cerebral cortex of the APPswe/PS1dE9 mouse model of Alzheimer's disease. *Experimental & molecular medicine.* **43**(1), pp.7-14.

Lees, M.P., Fuller, S.J., McLeod, R., Boulter, N.R., Miller, C.M., Zakrzewski, A.M., Mui, E.J., Witola, W.H., Coyne, J.J. and Hargrave, A.C. 2010. P2X7 receptor-mediated killing of an intracellular parasite, Toxoplasma gondii, by human and murine macrophages. *The journal of immunology.* **184**(12), pp.7040-7046.

Lenertz, L.Y., Wang, Z., Guadarrama, A., Hill, L.M., Gavala, M.L. and Bertics, P.J. 2010. Mutation of putative N-linked glycosylation sites on the human nucleotide receptor P2X7 reveals a key residue important for receptor function. *Biochemistry.* **49**(22), pp.4611-4619.

Letavic, M.A., Lord, B., Bischoff, F., Hawryluk, N.A., Pieters, S., Rech, J.C., Sales, Z., Velter, A.I., Ao, H. and Bonaventure, P. 2013. Synthesis and pharmacological characterization of two novel, brain penetrating P2X7 antagonists. *ACS medicinal chemistry letters.* **4**(4), pp.419-422.

Lewis, C., Neidhart, S., Holy, C., North, R., Buell, G. and Surprenant, A. 1995. Coexpression of P2X2 and P2X3 receptor subunits can account for ATP-gated currents in sensory neurons.

Leybaert, L., Braet, K., Vandamme, W., Cabooter, L., Martin, P.E. and Evans, W.H. 2003. Connexin channels, connexin mimetic peptides and ATP release. *Cell communication & adhesion.* **10**(4-6), pp.251-257.

Li, C.M., Campbell, S.J., Kumararatne, D.S., Bellamy, R., Ruwende, C., McAdam, K.P., Hill, A.V. and Lammas, D.A. 2002. Association of a polymorphism in the P2X7 gene with tuberculosis in a Gambian population. *Journal of infectious diseases.* **186**(10), pp.1458-1462.

Li, J., Liu, D., Ke, H.Z., Duncan, R.L. and Turner, C.H. 2005. The P2X7 nucleotide receptor mediates skeletal mechanotransduction. *Journal of biological chemistry.* **280**(52), pp.42952-42959.

Li, M., Chang, T.-H., Silberberg, S.D. and Swartz, K.J. 2008. Gating the pore of P2X receptor channels. *Nature neuroscience.* **11**(8), pp.883-887.

Li, M., Kawate, T., Silberberg, S.D. and Swartz, K.J. 2010. Pore-opening mechanism in trimeric P2X receptor channels. *Nature communications.* **1**, p44.

Li, M., Toombes, G.E., Silberberg, S.D. and Swartz, K.J. 2015. Physical basis of apparent pore dilation of ATP-activated P2X receptor channels. *Nature neuroscience.*

Li, X., Zhou, L., Feng, Y.-H., Abdul-Karim, F.W. and Gorodeski, G.I. 2006. The P2X7 receptor: a novel biomarker of uterine epithelial cancers. *Cancer epidemiology biomarkers & prevention.* **15**(10), pp.1906-1913.

Liao, M., Cao, E., Julius, D. and Cheng, Y. 2013. Structure of the TRPV1 ion channel determined by electron cryo-microscopy. *Nature.* **504**(7478), pp.107-112.

Liu, L., Zou, J., Liu, X., Jiang, L.-H. and Li, J. 2010. Inhibition of ATP-induced macrophage death by emodin via antagonizing P2X 7 receptor. *European journal of pharmacology.* **640**(1), pp.15-19.

Liu, X., Surprenant, A., Mao, H.-J., Roger, S., Xia, R., Bradley, H. and Jiang, L.-H. 2008. Identification of key residues coordinating functional inhibition of P2X7 receptors by zinc and copper. *Molecular pharmacology.* **73**(1), pp.252-259.

Locovei, S., Bao, L. and Dahl, G. 2006. Pannexin 1 in erythrocytes: function without a gap. *Proceedings of the National Academy of Sciences.* **103**(20), pp.7655-7659.

Longhurst, P.A., Schwegel, T., Folander, K. and Swanson, R. 1996. The human P 2× 1 receptor: molecular cloning, tissue distribution, and localization to chromosome 17 1. *Biochimica et biophysica acta (BBA)-gene structure and expression.* **1308**(3), pp.185-188.

López-Castejón, G., Young, M.T., Meseguer, J., Surprenant, A. and Mulero, V. 2007. Characterization of ATP-gated P2X 7 receptors in fish provides new insights into the mechanism of release of the leaderless cytokine interleukin-1β. *Molecular immunology.* **44**(6), pp.1286-1299.

Lord, B., Aluisio, L., Shoblock, J.R., Neff, R.A., Varlinskaya, E.I., Ceusters, M., Lovenberg, T.W., Carruthers, N., Bonaventure, P. and Letavic, M.A. 2014. Pharmacology of a Novel Central Nervous System–Penetrant P2X7 Antagonist JNJ-42253432. *Journal of pharmacology and experimental therapeutics.* **351**(3), pp.628-641.

Lucae, S., Salyakina, D., Barden, N., Harvey, M., Gagné, B., Labbé, M., Binder, E.B., Uhr, M., Paez-Pereda, M. and Sillaber, I. 2006. P2RX7, a gene coding for a purinergic ligand-gated ion channel, is associated with major depressive disorder. *Human molecular genetics.* **15**(16), pp.2438-2445.

Luo, X., Zheng, W., Yan, M., Lee, M.G. and Muallem, S. 1999. Multiple functional P2X and P2Y receptors in the luminal and basolateral membranes of pancreatic duct cells. *American Journal of Physiology-Cell Physiology.* **277**(2), pp.C205-C215.

Lustig, K.D., Shiau, A.K., Brake, A.J. and Julius, D. 1993. Expression cloning of an ATP receptor from mouse neuroblastoma cells. *Proceedings of the national academy of sciences.* **90**(11), pp.5113-5117.

Ma, W., Korngreen, A., Weil, S., Cohen, E.B.T., Priel, A., Kuzin, L. and Silberberg, S.D. 2006. Pore properties and pharmacological features of the P2X receptor channel in airway ciliated cells. *The journal of physiology.* **571**(3), pp.503-517.

Mackenzie, A.B., Young, M.T., Adinolfi, E. and Surprenant, A. 2005. Pseudoapoptosis induced by brief activation of ATP-gated P2X7 receptors. *Journal of biological chemistry.* **280**(40), pp.33968-33976.

Malmsjö, M., Bergdahl, A., Möller, S., Zhao, X.-H., Sun, X.-Y., Hedner, T., Edvinsson, L. and Erlinge, D. 1999. Congestive heart failure induces downregulation of P2X1-receptors in resistance arteries. *Cardiovascular research.* **43**(1), pp.219-227.

Mansoor, S.E., Lu, W., Oosterheert, W., Shekhar, M., Tajkhorshid, E. and Gouaux, E. 2016. X-ray structures define human P2X3 receptor gating cycle and antagonist action. *Nature.*

Marcoli, M., Cervetto, C., Paluzzi, P., Guarnieri, S., Alloisio, S., Thellung, S., Nobile, M. and Maura, G. 2008. P2X7 pre-synaptic receptors in adult rat cerebrocortical nerve terminals: a role in ATP-induced glutamate release. *Journal of neurochemistry.* **105**(6), pp.2330-2342.

Marquez-Klaka, B., Rettinger, J., Bhargava, Y., Eisele, T. and Nicke, A. 2007. Identification of an intersubunit cross-link between substituted cysteine residues located in the putative ATP binding site of the P2X1 receptor. *The journal of neuroscience.* **27**(6), pp.1456-1466.

Marquez-Klaka, B., Rettinger, J. and Nicke, A. 2009. Inter-subunit disulfide cross-linking in homomeric and heteromeric P2X receptors. *European biophysics journal.* **38**(3), pp.329-338.

Marshall, I.C., Boyfield, I. and McNulty, S. 2005. Ratiometric Ca2+ Measurements Using the FlexStation® Scanning Fluorometer. *Calcium signaling protocols.* Springer, pp.119-124.

Masin, M., Young, C., Lim, K., Barnes, S.J., Xu, X.J., Marschall, V., Brutkowski, W., Mooney, E.R., Gorecki, D.C. and Murrell-Lagnado, R. 2012. Expression, assembly and function of novel C-terminal truncated variants of the mouse P2X7 receptor: re-evaluation of P2X7 knockouts. *British journal of pharmacology.* **165**(4), pp.978-993.

Matute, C., Torre, I., Pérez-Cerdá, F., Pérez-Samartín, A., Alberdi, E., Etxebarria, E., Arranz, A.M., Ravid, R., Rodríguez-Antigüedad, A. and Sánchez-Gómez, M. 2007. P2X7 receptor blockade prevents ATP excitotoxicity in oligodendrocytes and ameliorates experimental autoimmune encephalomyelitis. *The journal of neuroscience.* **27**(35), pp.9525-9533.

McGaraughty, S., Chu, K., Namovic, M., Donnelly-Roberts, D., Harris, R., Zhang, X.-F., Shieh, C.-C., Wismer, C., Zhu, C. and Gauvin, D. 2007. P2X 7-related modulation of pathological nociception in rats. *Neuroscience.* **146**(4), pp.1817-1828.

McGaraughty, S., Wismer, C.T., Zhu, C.Z., Mikusa, J., Honore, P., Chu, K.L., Lee, C.H., Faltynek, C.R. and Jarvis, M.F. 2003. Effects of A-317491, a novel and selective P2X3/P2X2/3 receptor antagonist, on neuropathic, inflammatory and chemogenic nociception following intrathecal and intraplantar administration. *British journal of pharmacology.* **140**(8), pp.1381-1388.

McLaren, G., Lambrecht, G., Mutschler, E., Bäumert, H., Sneddon, P. and Kennedy, C. 1994. Investigation of the actions of PPADS, a novel P2X-purinoceptor antagonist, in the guinea-pig isolated vas deferens. *British journal of pharmacology.* **111**(3), pp.913-917.

McLarnon, J.G., Ryu, J.K., Walker, D.G. and Choi, H.B. 2006. Upregulated expression of purinergic P2X7 receptor in Alzheimer disease and amyloid-β peptide-treated microglia and in peptide-injected rat hippocampus. *Journal of neuropathology & experimental neurology.* **65**(11), pp.1090-1097.

McQuillin, A., Bass, N., Choudhury, K., Puri, V., Kosmin, M., Lawrence, J., Curtis, D. and Gurling, H. 2008. Case–control studies show that a non-conservative amino-acid change from a glutamine to arginine in the P2RX7 purinergic receptor protein is associated with both bipolar-and unipolar-affective disorders. *Molecular psychiatry.* **14**(6), pp.614-620.

Meng, E., Chang, H.-Y., Chang, S.-Y., Sun, G.-H., Yu, D.-S. and Cha, T.-L. 2011. Involvement of purinergic neurotransmission in ketamine induced bladder dysfunction. *The journal of urology.* **186**(3), pp.1134-1141.

Michel, A., Clay, W., Ng, S., Roman, S., Thompson, K., Condreay, J., Hall, M., Holbrook, J., Livermore, D. and Senger, S. 2008. Identification of regions of the P2X7 receptor that contribute to human and rat species differences in antagonist effects. *British journal of pharmacology.* **155**(5), pp.738-751.

Michel, A., Thompson, K., Simon, J., Boyfield, I., Fonfria, E. and Humphrey, P. 2006. Species and response dependent differences in the effects of MAPK inhibitors on P2X7 receptor function. *British journal of pharmacology.* **149**(7), pp.948-957.

Michel, A.D., Ng, S.W., Roman, S., Clay, W.C., Dean, D.K. and Walter, D.S. 2009. Mechanism of action of species-selective P2X7 receptor antagonists. *British journal of pharmacology.* **156**(8), pp.1312-1325.

Miller, C.M., Zakrzewski, A.M., Robinson, D.P., Fuller, S.J., Walker, R.A., Ikin, R.J., Bao, S.J., Grigg, M.E., Wiley, J.S. and Smith, N.C. 2015. Lack of a Functioning P2X7 Receptor Leads to Increased Susceptibility to Toxoplasmic Ileitis. *PloS one.* **10**(6), pe0129048.

Mills, J.C., Stone, N.L., Erhardt, J. and Pittman, R.N. 1998. Apoptotic membrane blebbing is regulated by myosin light chain phosphorylation. *The journal of cell biology.* **140**(3), pp.627-636.

Minato, Y., Suzuki, S., Hara, T., Kofuku, Y., Kasuya, G., Fujiwara, Y., Igarashi, S., Suzuki, E.-i., Nureki, O. and Hattori, M. 2016. Conductance of P2X4 purinergic receptor is determined by conformational equilibrium in the transmembrane region. *Proceedings of the national academy of sciences.* p201600519.

Morris, G.M., Huey, R., Lindstrom, W., Sanner, M.F., Belew, R.K., Goodsell, D.S. and Olson, A.J. 2009. AutoDock4 and AutoDockTools4: Automated docking with selective receptor flexibility. *Journal of computational chemistry.* **30**(16), pp.2785-2791.

Morton-Jones, R.T., Vlajkovic, S.M., Thorne, P.R., Cockayne, D.A., Ryan, A.F. and Housley, G.D. 2015. Properties of ATP-gated ion channels assembled from P2X2 subunits in mouse cochlear Reissner's membrane epithelial cells. *Purinergic signalling.* **11**(4), pp.551-560.

Mulryan, K., Gitterman, D., Lewis, C., Vial, C., Leckie, B., Cobb, A., Brown, J., Conley, E., Buell, G. and Pritchard, C. 2000. Reduced vas deferens contraction and male infertility in mice lacking P2X1 receptors. *Nature.* **403**(6765), pp.86-89.

Murgia, M., Hanau, S., Pizzo, P., Rippa, M. and Di Virgilio, F. 1993. Oxidized ATP. An irreversible inhibitor of the macrophage purinergic P2Z receptor. *Journal of biological chemistry.* **268**(11), pp.8199-8203.

Musa, H., Tellez, J.O., Chandler, N.J., Greener, I.D., Mączewski, M., Mackiewicz, U., Beresewicz, A., Molenaar, P., Boyett, M.R. and Dobrzynski, H. 2009. P2 purinergic receptor mRNA in rat and human sinoatrial node and other heart regions. *Naunyn-Schmiedeberg's archives of pharmacology.* **379**(6), pp.541-549.

Nelson, D.W., Gregg, R.J., Kort, M.E., Perez-Medrano, A., Voight, E.A., Wang, Y., Grayson, G., Namovic, M.T., Donnelly-Roberts, D.L. and Niforatos, W. 2006. Structure-activity relationship studies on a series of novel, substituted 1-benzyl-5-phenyltetrazole P2X7 antagonists. *Journal of medicinal chemistry.* **49**(12), pp.3659-3666.

Netea, M.G., Simon, A., van de Veerdonk, F., Kullberg, B.-J., Van der Meer, J.W. and Joosten, L.A. 2010. IL-1β processing in host defense: beyond the inflammasomes. *PLoS pathology.* **6**(2), pe1000661.

Newbolt, A., Stoop, R., Virginio, C., Surprenant, A., North, R.A., Buell, G. and Rassendren, F. 1998. Membrane topology of an ATP-gated ion channel (P2X receptor). *Journal of biological chemistry.* **273**(24), pp.15177-15182.

Nicke, A. 2008. Homotrimeric complexes are the dominant assembly state of native P2X7 subunits. *Biochemical and biophysical research communications.* **377**(3), pp.803-808.

Nicke, A., Bäumert, H.G., Rettinger, J., Eichele, A., Lambrecht, G., Mutschler, E. and Schmalzing, G. 1998. P2X1 and P2X3 receptors form stable trimers: a novel structural motif of ligand-gated ion channels. *The EMBO journal.* **17**(11), pp.3016-3028.

Nicke, A., Kerschensteiner, D. and Soto, F. 2005. Biochemical and functional evidence for heteromeric assembly of P2X1 and P2X4 subunits. *Journal of neurochemistry.* **92**(4), pp.925-933.

Nicke, A., Kuan, Y.-H., Masin, M., Rettinger, J., Marquez-Klaka, B., Bender, O., Górecki, D.C., Murrell-Lagnado, R.D. and Soto, F. 2009. A functional P2X7 splice variant with an alternative transmembrane domain 1 escapes gene inactivation in P2X7 knock-out mice. *Journal of biological chemistry.* **284**(38), pp.25813-25822.

Niño-Moreno, P., Portales-Pérez, D., Hernández-Castro, B., Portales-Cervantes, L., Flores-Meraz, V., Baranda, L., Gómez-Gómez, A., Acuña-Alonzo, V., Granados, J. and González-Amaro, R. 2007. P2X7 and NRAMP1/SLC11 A1 gene polymorphisms in Mexican mestizo patients with pulmonary tuberculosis. *Clinical & experimental immunology.* **148**(3), pp.469-477.

Nori, S., Fumagalli, L., Bo, X., Bogdanov, Y. and Burnstock, G. 1998. Coexpression of mRNAs for P2X1, P2X2 and P2X4 receptors in rat vascular smooth muscle: an in situ hybridization and RT-PCR study. *Journal of vascular research.* **35**(3), pp.179-185.

North, R.A. 2002. Molecular physiology of P2X receptors. *Physiological reviews.* **82**(4), pp.1013-1067.

North, R.A. and Barnard, E.A. 1997. Nucleotide receptors. *Current opinion in neurobiology.* **7**(3), pp.346-357.

North, R.A. and Jarvis, M.F. 2013. P2X receptors as drug targets. *Molecular pharmacology.* **83**(4), pp.759-769.

North, R.A. and Surprenant, A. 2000. Pharmacology of cloned P2X receptors. *Annual review of pharmacology and toxicology.* **40**(1), pp.563-580.

Notomi, S., Hisatomi, T., Kanemaru, T., Takeda, A., Ikeda, Y., Enaida, H., Kroemer, G. and Ishibashi, T. 2011. Critical involvement of extracellular ATP acting on P2RX7 purinergic receptors in photoreceptor cell death. *The American journal of pathology.* **179**(6), pp.2798-2809.

Novak, I., Jans, I.M. and Wohlfahrt, L. 2010. Effect of P2X7 receptor knockout on exocrine secretion of pancreas, salivary glands and lacrimal glands. *The journal of physiology.* **588**(18), pp.3615-3627.

Nückel, H., Frey, U.H., Dürig, J., Dührsen, U. and Siffert, W. 2004. 1513A/C polymorphism in the P2X7 receptor gene in chronic lymphocytic leukemia: absence of correlation with clinical outcome. *European journal of haematology.* **72**(4), pp.259-263.

Ohlendorff, S.D., Tofteng, C.L., Jensen, J.-E.B., Petersen, S., Civitelli, R., Fenger, M., Abrahamsen, B., Hermann, A.P., Eiken, P. and Jørgensen, N.R. 2007. Single nucleotide polymorphisms in the P2X7 gene are associated to fracture risk and to effect of estrogen treatment. *Pharmacogenetics and genomics.* **17**(7), pp.555-567.

Okumura, H., Shiba, D., Kubo, T. and Yokoyama, T. 2008. P2X7 receptor as sensitive flow sensor for ERK activation in osteoblasts. *Biochemical and biophysical research communications.* **372**(3), pp.486-490.

Orriss, I., Syberg, S., Wang, N., Robaye, B., Gartland, A., Jorgensen, N., Arnett, T. and Boeynaems, J.-M. 2011. Bone phenotypes displayed by P2 receptor knockout mice. *Frontiers in bioscience. S.* **3**, pp.1038-1046.

Osmond, D.A. and Inscho, E.W. 2010. P2X1 receptor blockade inhibits whole kidney autoregulation of renal blood flow in vivo. *American journal of physiology-renal physiology.* **298**(6), pp.F1360-F1368.

Oury, C., Kuijpers, M.J., Toth-Zsamboki, E., Bonnefoy, A., Danloy, S., Vreys, I., Feijge, M.A., De Vos, R., Vermylen, J. and Heemskerk, J.W. 2003. Overexpression of the platelet P2X1 ion channel in transgenic mice generates a novel prothrombotic phenotype. *Blood.* **101**(10), pp.3969-3976.

Ouyang, L., Shi, Z., Zhao, S., Wang, F.T., Zhou, T.T., Liu, B. and Bao, J.K. 2012. Programmed cell death pathways in cancer: a review of apoptosis, autophagy and programmed necrosis. *Cell proliferation.* **45**(6), pp.487-498.

Oyanguren-Desez, O., Rodríguez-Antigüedad, A., Villoslada, P., Domercq, M., Alberdi, E. and Matute, C. 2011. Gain-of-function of P2X7 receptor gene variants in multiple sclerosis. *Cell calcium.* **50**(5), pp.468-472.

Panupinthu, N., Rogers, J.T., Zhao, L., Solano-Flores, L.P., Possmayer, F., Sims, S.M. and Dixon, S.J. 2008. P2X7 receptors on osteoblasts couple to production of lysophosphatidic acid: a signaling axis promoting osteogenesis. *The journal of cell biology.* **181**(5), pp.859-871.

Panupinthu, N., Zhao, L., Possmayer, F., Ke, H.Z., Sims, S.M. and Dixon, S.J. 2007. P2X7 nucleotide receptors mediate blebbing in osteoblasts through a pathway involving lysophosphatidic acid. *Journal of biological chemistry.* **282**(5), pp.3403-3412.

Papp, L., Vizi, E.S. and Sperlágh, B. 2004. Lack of ATP-evoked GABA and glutamate release in the hippocampus of P2X7 receptor−/− mice. *Neuroreport.* **15**(15), pp.2387-2391.

Parvathenani, L.K., Tertyshnikova, S., Greco, C.R., Roberts, S.B., Robertson, B. and Posmantur, R. 2003. P2X7 mediates superoxide production in primary microglia and is up-regulated in a transgenic mouse model of Alzheimer's disease. *Journal of biological chemistry.* **278**(15), pp.13309-13317.

Paukert, M., Hidayat, S. and Gründer, S. 2002. The P2X7 receptor from Xenopus laevis: formation of a large pore in Xenopus oocytes. *FEBS letters.* **513**(2-3), pp.253-258.

Pelegrin, P. and Surprenant, A. 2006. Pannexin-1 mediates large pore formation and interleukin-1β release by the ATP-gated P2X7 receptor. *The EMBO journal.* **25**(21), pp.5071-5082.

Peng, W., Cotrina, M.L., Han, X., Yu, H., Bekar, L., Blum, L., Takano, T., Tian, G.-F., Goldman, S.A. and Nedergaard, M. 2009. Systemic administration of an antagonist of the ATP-sensitive receptor P2X7 improves recovery after spinal cord injury. *Proceedings of the national academy of sciences.* **106**(30), pp.12489-12493.

Perregaux, D. and Gabel, C.A. 1994. Interleukin-1 beta maturation and release in response to ATP and nigericin. Evidence that potassium depletion mediated by these agents is a necessary and common feature of their activity. *Journal of biological chemistry.* **269**(21), pp.15195-15203.

Petruska, J.C., Mena, N., Nakatsuka, T., Cooper, B.Y., Johnson, R.D. and Gu, J.G. 2000. P2X1 receptor subunit immunoreactivity and ATP-evoked fast currents in adult rat dorsal root ganglion neurons. *Neuroreport.* **11**(16), pp.3589-3592.

Pfizer. 2008. *A study of the effect of CE-224535 on knee OA (osteoarthritis) pain.* [Online]. [Accessed 10 June].

Pintor, J., Diaz-Hernandez, M., Gualix, J., Gomez-Villafuertes, R. and Miras-Portugal, T. 1999. Diadenosine polyphosphate receptors: from rat and guinea-pig brain to human central nervous system. *Cellular and Molecular Biology Letters.* **4**(3).

Pintor, J., Gualix, J. and Miras-Portugal, M.T. 1997. Diinosine polyphosphates, a group of dinucleotides with antagonistic effects on diadenosine polyphosphate receptor. *Molecular pharmacology.* **51**(2), pp.277-284.

Portales-Cervantes, L., Niño-Moreno, P., Salgado-Bustamante, M., García-Hernández, M.H., Baranda-Candido, L., Reynaga-Hernández, E., Barajas-López, C., González-Amaro, R. and Portales-Pérez, D.P. 2012. The His155Tyr (489C> T) single nucleotide polymorphism of P2RX7 gene confers an enhanced function of P2X7 receptor in immune cells from patients with rheumatoid arthritis. *Cellular immunology.* **276**(1), pp.168-175.

Postis, V., Rawson, S., Mitchell, J.K., Lee, S.C., Parslow, R.A., Dafforn, T.R., Baldwin, S.A. and Muench, S.P. 2015. The use of SMALPs as a novel membrane protein scaffold for structure study by negative stain electron microscopy. *Biochimica et biophysica acta (BBA)-biomembranes.* **1848**(2), pp.496-501.

Prasad, M., Fearon, I.M., Zhang, M., Laing, M., Vollmer, C. and Nurse, C.A. 2001. Expression of P2X2 and P2X3 receptor subunits in rat carotid body afferent neurones: role in chemosensory signalling. *The journal of physiology.* **537**(3), pp.667-677.

Queiroz, G., Talaia, C. and Gonçalves, J. 2003. ATP modulates noradrenaline release by activation of inhibitory P2Y receptors and facilitatory P2X receptors in the rat vas deferens. *Journal of pharmacology and experimental therapeutics.* **307**(2), pp.809-815.

Raffaghello, L., Chiozzi, P., Falzoni, S., Di Virgilio, F. and Pistoia, V. 2006. The P2X7 Receptor Sustains the Growth of Human Neuroblastoma Cells through a Substance P–Dependent Mechanism. *Cancer research.* **66**(2), pp.907-914.

Ransford, G.A., Fregien, N., Qiu, F., Dahl, G., Conner, G.E. and Salathe, M. 2009. Pannexin 1 contributes to ATP release in airway epithelia. *American journal of respiratory cell and molecular biology.* **41**(5), pp.525-534.

Rappold, P., Lynd-Balta, E. and Joseph, S. 2006. P2X 7 receptor immunoreactive profile confined to resting and activated microglia in the epileptic brain. *Brain research.* **1089**(1), pp.171-178.

Rassendren, F., Buell, G.N., Virginio, C., Collo, G., North, R.A. and Surprenant, A. 1997. The permeabilizing ATP receptor, P2X7 cloning and expression of a human cDNA. *Journal of biological chemistry.* **272**(9), pp.5482-5486.

Ren, K. and Torres, R. 2009. Role of interleukin-1β during pain and inflammation. *Brain research reviews.* **60**(1), pp.57-64.

Rettinger, J., Braun, K., Hochmann, H., Kassack, M.U., Ullmann, H., Nickel, P., Schmalzing, G. and Lambrecht, G. 2005. Profiling at recombinant homomeric and heteromeric rat P2X receptors identifies the suramin analogue NF449 as a highly potent P2X 1 receptor antagonist. *Neuropharmacology.* **48**(3), pp.461-468.

Rettinger, J., Schmalzing, G., Damer, S., Müller, G., Nickel, P. and Lambrecht, G. 2000. The suramin analogue NF279 is a novel and potent antagonist selective for the P2X 1 receptor. *Neuropharmacology.* **39**(11), pp.2044-2053.

Riteau, N., Baron, L., Villeret, B., Guillou, N., Savigny, F., Ryffel, B., Rassendren, F., Le Bert, M., Gombault, A. and Couillin, I. 2012. ATP release and purinergic signaling: a common pathway for particle-mediated inflammasome activation. *Cell death & disease.* **3**(10), pe403.

Roberts, J.A., Allsopp, R.C., El Ajouz, S., Vial, C., Schmid, R., Young, M.T. and Evans, R.J. 2012. Agonist binding evokes extensive conformational changes in the extracellular domain of the ATP-gated human P2X1 receptor ion channel. *Proceedings of the national academy of sciences.* **109**(12), pp.4663-4667.

Robinson, L. and Murrell-Lagnado, R. 2013. Lipid rafts as regulators of P2X7 receptor and pannexin-1 signalling. In: *Proceedings of the physiological society*: the physiological society.

Robinson, L.E., Shridar, M., Smith, P. and Murrell-Lagnado, R.D. 2014. Plasma membrane cholesterol as a regulator of human and rodent P2X7 receptor activation and sensitization. *Journal of biological chemistry.* **289**(46), pp.31983-31994.

Roger, S., Gillet, L., Baroja-Mazo, A., Surprenant, A. and Pelegrin, P. 2010a. C-terminal calmodulin-binding motif differentially controls human and rat P2X7 receptor current facilitation. *Journal of Biological Chemistry.* **285**(23), pp.17514-17524.

Roger, S., Jelassi, B., Couillin, I., Pelegrin, P., Besson, P. and Jiang, L.-H. 2015. Understanding the roles of the P2X7 receptor in solid tumour progression and therapeutic perspectives. *Biochimica et biophysica acta (BBA)-biomembranes.* **1848**(10), pp.2584-2602.

Roger, S., Mei, Z.-Z., Baldwin, J.M., Dong, L., Bradley, H., Baldwin, S.A., Surprenant, A. and Jiang, L.-H. 2010b. Single nucleotide polymorphisms that were identified in affective mood disorders affect ATP-activated P2X 7 receptor functions. *Journal of psychiatric research.* **44**(6), pp.347-355.

Roger, S., Pelegrin, P. and Surprenant, A. 2008. Facilitation of P2X7 receptor currents and membrane blebbing via constitutive and dynamic calmodulin binding. *The journal of neuroscience.* **28**(25), pp.6393-6401.

Roman, S., Cusdin, F., Fonfria, E., Goodwin, J., Reeves, J., Lappin, S., Chambers, L., Walter, D., Clay, W. and Michel, A. 2009. Cloning and pharmacological characterization of the dog P2X7 receptor. *British journal of pharmacology.* **158**(6), pp.1513-1526.

Rong, W., Gourine, A.V., Cockayne, D.A., Xiang, Z., Ford, A.P., Spyer, K.M. and Burnstock, G. 2003. Pivotal role of nucleotide P2X2 receptor subunit of the ATP-gated ion channel mediating ventilatory responses to hypoxia. *The journal of neuroscience.* **23**(36), pp.11315-11321.

Rong, W., Keating, C., Sun, B., Dong, L. and Grundy, D. 2009. Purinergic contribution to small intestinal afferent hypersensitivity in a murine model of postinfectious bowel disease. *Neurogastroenterology & motility.* **21**(6), pp.665-e632.

Rozman, C. and Montserrat, E. 1995. Chronic lymphocytic leukemia. *New England journal of medicine.* **333**(16), pp.1052-1057.

Ryten, M., Dunn, P.M., Neary, J.T. and Burnstock, G. 2002. ATP regulates the differentiation of mammalian skeletal muscle by activation of a P2X5 receptor on satellite cells. *The journal of cell biology.* **158**(2), pp.345-355.

Ryu, J.K. and McLarnon, J.G. 2008. Block of purinergic P2X7 receptor is neuroprotective in an animal model of Alzheimer's disease. *Neuroreport.* **19**(17), pp.1715-1719.

Salas, E., Carrasquero, L.M.G., Olivos-Oré, L.A., Bustillo, D., Artalejo, A.R., Miras-Portugal, M.T. and Delicado, E.G. 2013. Purinergic P2X7 receptors mediate cell death in mouse cerebellar astrocytes in culture. *Journal of pharmacology and experimental therapeutics.* **347**(3), pp.802-815.

Sambasivan, V., Murthy, K.J.R., Reddy, R., Vijayalakshimi, V. and Hasan, Q. 2010. P2X7 gene polymorphisms and risk assessment for pulmonary tuberculosis in Asian Indians. *Disease markers.* **28**(1), pp.43-48.

Samways, D.S. and Egan, T.M. 2007. Acidic amino acids impart enhanced Ca2+ permeability and flux in two members of the ATP-gated P2X receptor family. *The journal of general physiology.* **129**(3), pp.245-256.

Samways, D.S., Khakh, B.S., Dutertre, S. and Egan, T.M. 2011. Preferential use of unobstructed lateral portals as the access route to the pore of human ATP-gated ion channels (P2X receptors). *Proceedings of the national academy of sciences.* **108**(33), pp.13800-13805.

Samways, D.S., Migita, K., Li, Z. and Egan, T.M. 2008. On the role of the first transmembrane domain in cation permeability and flux of the ATP-gated P2X2 receptor. *Journal of biological chemistry.* **283**(8), pp.5110-5117.

Schenk, U., Westendorf, A.M., Radaelli, E., Casati, A., Ferro, M., Fumagalli, M., Verderio, C., Buer, J., Scanziani, E. and Grassi, F. 2008. Purinergic control of T cell activation by ATP released through pannexin-1 hemichannels. *Scientific signalling.* **1**(39), pp.ra6-ra6.

Schulze-Lohoff, E., Hugo, C., Rost, S., Arnold, S., Gruber, A., Brüne, B. and Sterzel, R.B. 1998. Extracellular ATP causes apoptosis and necrosis of cultured mesangial cells via P2Z/P2X7receptors. *American journal of physiology-renal physiology.* **275**(6), pp.F962-F971.

Schwarz, N., Fliegert, R., Adriouch, S., Seman, M., Guse, A.H., Haag, F. and Koch-Nolte, F. 2009. Activation of the P2X7 ion channel by soluble and covalently bound ligands. *Purinergic signalling.* **5**(2), pp.139-149.

Sellick, G.S., Rudd, M., Eve, P., Allinson, R., Matutes, E., Catovsky, D. and Houlston, R.S. 2004. The P2X7 receptor gene A1513C polymorphism does not contribute to risk of familial or sporadic chronic lymphocytic leukemia. *Cancer epidemiology biomarkers & prevention.* **13**(6), pp.1065-1067.

Sharp, A.J., Polak, P.E., Simonini, V., Lin, S.X., Richardson, J.C., Bongarzone, E.R. and Feinstein, D.L. 2008. P2x7 deficiency suppresses development of experimental autoimmune encephalomyelitis. *Journal of neuroinflammation.* **5**(33.10), p1186.

Shink, E., Harvey, M., Tremblay, M., Gagné, B., Belleau, P., Raymond, C., Labbé, M., Dubé, M.P., Lafrenière, R.G. and Barden, N. 2005. Analysis of microsatellite markers and single nucleotide polymorphisms in candidate genes for susceptibility to bipolar affective disorder in the chromosome 12Q24. 31 region. *American journal of medical genetics part B: neuropsychiatric genetics.* **135**(1), pp.50-58.

Shinoda, M., Feng, B. and Gebhart, G. 2009. Peripheral and central P2X 3 receptor contributions to colon mechanosensitivity and hypersensitivity in the mouse. *Gastroenterology.* **137**(6), pp.2096-2104.

Sikora, J., Orlov, S.N., Furuya, K. and Grygorczyk, R. 2014. Hemolysis is a primary ATP-release mechanism in human erythrocytes. *Blood.* **124**(13), pp.2150-2157.

Sim, J.A., Chaumont, S., Jo, J., Ulmann, L., Young, M.T., Cho, K., Buell, G., North, R.A. and Rassendren, F. 2006. Altered hippocampal synaptic potentiation in P2X4 knock-out mice. *The Journal of neuroscience.* **26**(35), pp.9006-9009.

Sim, J.A., Young, M.T., Sung, H.-Y., North, R.A. and Surprenant, A. 2004. Reanalysis of P2X7 receptor expression in rodent brain. *The journal of neuroscience.* **24**(28), pp.6307-6314.

Skarratt, K.K., Fuller, S.J., Sluyter, R., Dao-Ung, L.-P., Gu, B.J. and Wiley, J.S. 2005. A 5′ intronic splice site polymorphism leads to a null allele of the P2X7 gene in 1–2% of the Caucasian population. *FEBS letters.* **579**(12), pp.2675-2678.

Sklar, P., Ripke, S., Scott, L.J., Andreassen, O.A., Cichon, S., Craddock, N., Edenberg, H.J., Nurnberger, J.I., Rietschel, M. and Blackwood, D. 2011. Large-scale genome-wide association analysis of bipolar disorder identifies a new susceptibility locus near ODZ4. *Nature genetics.* **43**(10), p977.

Sklar, P., Smoller, J., Fan, J., Ferreira, M., Perlis, R., Chambert, K., Nimgaonkar, V., McQueen, M., Faraone, S. and Kirby, A. 2008. Whole-genome association study of bipolar disorder. *Molecular psychiatry.* **13**(6), pp.558-569.

Slater, M., Danieletto, S., Gidley-Baird, A., Teh, L. and Barden, J. 2004a. Early prostate cancer detected using expression of non-functional cytolytic P2X7 receptors. *Histopathology.* **44**(3), pp.206-215.

Slater, M., Danieletto, S., Pooley, M., Teh, L.C., Gidley-Baird, A. and Barden, J.A. 2004b. Differentiation between cancerous and normal hyperplastic lobules in breast lesions. *Breast cancer research and treatment.* **83**(1), pp.1-10.

Sluyter, R., Dalitz, J. and Wiley, J. 2004a. P2X7 receptor polymorphism impairs extracellular adenosine 5′-triphosphate-induced interleukin-18 release from human monocytes. *Genes and immunity.* **5**(7), pp.588-591.

Sluyter, R., Shemon, A.N. and Wiley, J.S. 2004b. Glu496 to Ala polymorphism in the P2X7 receptor impairs ATP-induced IL-1β release from human monocytes. *The journal of immunology.* **172**(6), pp.3399-3405.

Smart, M.L., Gu, B., Panchal, R.G., Wiley, J., Cromer, B., Williams, D.A. and Petrou, S. 2003. P2X7 receptor cell surface expression and cytolytic pore formation are regulated by a distal C-terminal region. *Journal of biological chemistry.* **278**(10), pp.8853-8860.

Sobel, R.A. 2015. Greenfield's Neuropathology: 2-Volume Set. *Journal of neuropathology & experimental neurology.* **74**(12), pp.1185-1185.

Solini, A., Cuccato, S., Ferrari, D., Santini, E., Gulinelli, S., Callegari, M.G., Dardano, A., Faviana, P., Madec, S. and Di Virgilio, F. 2008. Increased P2X7 receptor expression and function in thyroid papillary cancer: a new potential marker of the disease? *Endocrinology.* **149**(1), pp.389-396.

Solle, M., Labasi, J., Perregaux, D.G., Stam, E., Petrushova, N., Koller, B.H., Griffiths, R.J. and Gabel, C.A. 2001. Altered cytokine production in mice lacking P2X7Receptors. *Journal of biological chemistry.* **276**(1), pp.125-132.

Song, X., Gao, X., Guo, D., Yu, Q., Guo, W., He, C., Burnstock, G. and Xiang, Z. 2012. Expression of P2X2 and P2X3 receptors in the rat carotid sinus, aortic arch, vena cava, and heart, as well as petrosal and nodose ganglia. *Purinergic signalling.* **8**(1), pp.15-22.

Sorge, R.E., Trang, T., Dorfman, R., Smith, S.B., Beggs, S., Ritchie, J., Austin, J.-S., Zaykin, D.V., Vander Meulen, H. and Costigan, M. 2012. Genetically determined P2X7 receptor pore formation regulates variability in chronic pain sensitivity. *Nature medicine.* **18**(4), pp.595-599.

Soto, F., Lambrecht, G., Nickel, P., Stühmer, W. and Busch, A.E. 1999. Antagonistic properties of the suramin analogue NF023 at heterologously expressed P2X receptors. *Neuropharmacology.* **38**(1), pp.141-149.

Souslova, V., Cesare, P., Ding, Y., Akopian, A.N., Stanfa, L., Suzuki, R., Carpenter, K., Dickenson, A., Boyce, S. and Hill, R. 2000. Warm-coding deficits and aberrant inflammatory pain in mice lacking P2X 3 receptors. *Nature.* **407**(6807), pp.1015-1017.

Sperlágh, B. and Illes, P. 2014. P2X7 receptor: an emerging target in central nervous system diseases. *Trends in pharmacological sciences.* **35**(10), pp.537-547.

Sperlágh, B., Köfalvi, A., Deuchars, J., Atkinson, L., J Milligan, C., Buckley, N.J. and Vizi, E.S. 2002. Involvement of P2X7 receptors in the regulation of neurotransmitter release in the rat hippocampus. *Journal of neurochemistry.* **81**(6), pp.1196-1211.

Sperlágh, B., Vizi, E.S., Wirkner, K. and Illes, P. 2006. P2X 7 receptors in the nervous system. *Progress in neurobiology.* **78**(6), pp.327-346.

Sperlágh, B. and Vizi, S.E. 1996. Neuronal synthesis, storage and release of ATP. In: *Seminars in Neuroscience*: Elsevier, pp.175-186.

Sridharan, M., Adderley, S.P., Bowles, E.A., Egan, T.M., Stephenson, A.H., Ellsworth, M.L. and Sprague, R.S. 2010. Pannexin 1 is the conduit for low oxygen tension-induced ATP release from human erythrocytes. *American journal of physiology-heart and circulatory physiology.* **299**(4), pp.H1146-H1152.

Starczynski, J., Pepper, C., Pratt, G., Hooper, L., Thomas, A., Hoy, T., Milligan, D., Bentley, P. and Fegan, C. 2003. The P2X7 receptor gene polymorphism 1513 A→ C has no effect on clinical prognostic markers, in vitro sensitivity to fludarabine, Bcl-2 family protein expression or survival in B-cell chronic lymphocytic leukaemia. *British journal of haematology.* **123**(1), pp.66-71.

Stehle, J., Rivkees, S., Lee, J., Weaver, D., Deeds, J. and Reppert, S. 1992. Molecular cloning and expression of the cDNA for a novel A2-adenosine receptor subtype. *Molecular endocrinology.* **6**(3), pp.384-393.

Steinberg, T.H., Newman, A.S., Swanson, J. and Silverstein, S.C. 1987. ATP4- permeabilizes the plasma membrane of mouse macrophages to fluorescent dyes. *Journal of biological chemistry.* **262**(18), pp.8884-8888.

Stelmashenko, O., Compan, V., Browne, L.E. and North, R.A. 2014. Ectodomain movements of an ATP-gated ion channel (P2X2 receptor) probed by disulfide locking. *Journal of biological chemistry.* **289**(14), pp.9909-9917.

Stelmashenko, O., Lalo, U., Yang, Y., Bragg, L., North, R.A. and Compan, V. 2012. Activation of trimeric P2X2 receptors by fewer than three ATP molecules. *Molecular pharmacology.* **82**(4), pp.760-766.

Stephan, G., Kowalski-Jahn, M., Zens, C., Schmalzing, G., Illes, P. and Hausmann, R. 2016. Inter-subunit disulfide locking of the human P2X3 receptor elucidates ectodomain movements associated with channel gating. *Purinergic signalling.* **12**(2), pp.221-233.

Stock, T.C., Bloom, B.J., Wei, N., Ishaq, S., Park, W., Wang, X., Gupta, P. and Mebus, C.A. 2012. Efficacy and safety of CE-224,535, an antagonist of P2X7 receptor, in treatment of patients with rheumatoid arthritis inadequately controlled by methotrexate. *The journal of rheumatology.* **39**(4), pp.720-727.

Stojilkovic, S.S., He, M.-L., Koshimizu, T.-a., Balik, A. and Zemkova, H. 2010. Signaling by purinergic receptors and channels in the pituitary gland. *Molecular and cellular endocrinology.* **314**(2), pp.184-191.

Stokes, L., Fuller, S.J., Sluyter, R., Skarratt, K.K., Gu, B.J. and Wiley, J.S. 2010. Two haplotypes of the P2X7 receptor containing the Ala-348 to Thr polymorphism exhibit a gain-of-function effect and enhanced interleukin-1β secretion. *The FASEB journal.* **24**(8), pp.2916-2927.

Stokes, L., Jiang, L.H., Alcaraz, L., Bent, J., Bowers, K., Fagura, M., Furber, M., Mortimore, M., Lawson, M. and Theaker, J. 2006. Characterization of a selective and potent antagonist of human P2X7 receptors, AZ11645373. *British journal of pharmacology.* **149**(7), pp.880-887.

Stokes, L., Scurrah, K., Ellis, J.A., Cromer, B.A., Skarratt, K.K., Gu, B.J., Harrap, S.B. and Wiley, J.S. 2011. A loss-of-function polymorphism in the human P2X4 receptor is associated with increased pulse pressure. *Hypertension.* **58**(6), pp.1086-1092.

Suadicani, S.O., Brosnan, C.F. and Scemes, E. 2006. P2X7 receptors mediate ATP release and amplification of astrocytic intercellular Ca2+ signaling. *The journal of neuroscience.* **26**(5), pp.1378-1385.

Subramanyam, C., Duplantier, A.J., Dombroski, M.A., Chang, S.-P., Gabel, C.A., Whitney-Pickett, C., Perregaux, D.G., Labasi, J.M., Yoon, K. and Shepard, R.M. 2011. Discovery, synthesis and SAR of azinyl-and azolylbenzamides antagonists of the P2X 7 receptor. *Bioorganic & medicinal chemistry letters.* **21**(18), pp.5475-5479.

Sun, C., Heid, M.E., Keyel, P.A. and Salter, R.D. 2013. The second transmembrane domain of P2X7 contributes to dilated pore formation. *PLoS One.* **8**(4), pe61886.

Surprenant, A., Rassendren, F., Kawashima, E., North, R. and Buell, G. 1996. The cytolytic P2Z receptor for extracellular ATP identified as a P2X receptor (P2X7). *Science.* **272**(5262), pp.735-738.

Syberg, S., Petersen, S., Beck Jensen, J.-E., Gartland, A., Teilmann, J., Chessell, I., Steinberg, T.H., Schwarz, P. and Jørgensen, N.R. 2012a. Genetic background strongly influences the bone phenotype of P2X7 receptor knockout mice. *Journal of osteoporosis.* **2012**.

Syberg, S., Schwarz, P., Petersen, S., Steinberg, T.H., Jensen, J.-E.B., Teilmann, J. and Jørgensen, N.R. 2012b. Association between P2X7 receptor polymorphisms and bone status in mice. *Journal of osteoporosis.* **2012**.

Tenneti, L., Gibbons, S.J. and Talamo, B.R. 1998. Expression and Trans-synaptic Regulation of P2x4 and P2z Receptors for Extracellular ATP in Parotid Acinar Cells effects of parasympathetic denervation. *Journal of biological chemistry.* **273**(41), pp.26799-26808.

Thomas, S., Virginio, C., North, R.A. and Surprenant, A. 1998. The antagonist trinitrophenyl-ATP reveals co-existence of distinct P2X receptor channels in rat nodose neurones. *The Journal of Physiology.* **509**(2), pp.411-417.

Thunberg, U., Tobin, G., Johnson, A., Söderberg, O., Padyukov, L., Hultdin, M., Klareskog, L., Enblad, G., Sundström, C. and Roos, G. 2002. Polymorphism in the P2X7 receptor gene and survival in chronic lymphocytic leukaemia. *The Lancet.* **360**(9349), pp.1935-1939.

Ting, A.Y., Lee, T.K. and MacDonald, I.M. 2009. Genetics of age-related macular degeneration. *Current opinion in ophthalmology.* **20**(5), pp.369-376.

Tokumitsu, H., Chijiwa, T., Hagiwara, M., Mizutani, A., Terasawa, M. and Hidaka, H. 1990. KN-62, 1-[N, O-bis (5-isoquinolinesulfonyl)-N-methyl-L-tyrosyl]-4-phenylpiperazi ne, a specific inhibitor of Ca2+/calmodulin-dependent protein kinase II. *Journal of biological chemistry.* **265**(8), pp.4315-4320.

Torres, G.E., Egan, T.M. and Voigt, M.M. 1998a. Topological analysis of the ATP-gated ionotrophic P2X2 receptor subunit. *FEBS letters.* **425**(1), pp.19-23.

Torres, G.E., Haines, W.R., Egan, T.M. and Voigt, M.M. 1998b. Co-expression of P2X1 and P2X5 receptor subunits reveals a novel ATP-gated ion channel. *Molecular pharmacology.* **54**(6), pp.989-993.

Tsuda, M., Shigemoto-Mogami, Y., Koizumi, S., Mizokoshi, A., Kohsaka, S., Salter, M.W. and Inoue, K. 2003. P2X4 receptors induced in spinal microglia gate tactile allodynia after nerve injury. *Nature.* **424**(6950), pp.778-783.

Twomey, E.C., Yelshanskaya, M.V., Grassucci, R.A., Frank, J. and Sobolevsky, A.I. 2016. Elucidation of AMPA receptor–stargazin complexes by cryo–electron microscopy. *Science.* **353**(6294), pp.83-86.

Usoskin, D., Furlan, A., Islam, S., Abdo, H., Lönnerberg, P., Lou, D., Hjerling-Leffler, J., Haeggström, J., Kharchenko, O. and Kharchenko, P.V. 2015. Unbiased classification of sensory neuron types by large-scale single-cell RNA sequencing. *Nature neuroscience.* **18**(1), pp.145-153.

Valera, S., Hussy, N., Evans, R.J., Adami, N., North, R.A., Surprenant, A. and Buell, G. 1994. A new class of ligand-gated ion channel defined by P2x receptor for extracellular ATP.

Verhoef, P.A., Estacion, M., Schilling, W. and Dubyak, G.R. 2003. P2X7 receptor-dependent blebbing and the activation of Rho-effector kinases, caspases, and IL-1β release. *The journal of immunology.* **170**(11), pp.5728-5738.

Vial, C. and Evans, R. 2000. P2X receptor expression in mouse urinary bladder and the requirement of P2X1 receptors for functional P2X receptor responses in the mouse urinary bladder smooth muscle. *British journal of pharmacology.* **131**(7), pp.1489-1495.

Virginio, C., Church, D., North, R.A. and Surprenant, A. 1997. Effects of divalent cations, protons and calmidazolium at the rat P2X 7 receptor. *Neuropharmacology.* **36**(9), pp.1285-1294.

Virginio, C., MacKenzie, A., North, R.A. and Surprenant, A. 1999a. Kinetics of cell lysis, dye uptake and permeability changes in cells expressing the rat P2X7 receptor. *The journal of physiology.* **519**(2), pp.335-346.

Virginio, C., MacKenzie, A., Rassendren, F., North, R. and Surprenant, A. 1999b. Pore dilation of neuronal P2X receptor channels. *Nature neuroscience.* **2**(4), pp.315-321.

Virginio, C., Robertson, G., Surprenant, A. and North, R.A. 1998. Trinitrophenyl-substituted nucleotides are potent antagonists selective for P2X1, P2X3, and heteromeric P2X2/3 receptors. *Molecular pharmacology.* **53**(6), pp.969-973.

von Kügelgen, I. and Hoffmann, K. 2016. Pharmacology and structure of P2Y receptors. *Neuropharmacology.* **104**, pp.50-61.

von Kügelgen, I. and Wetter, A. 2000. Molecular pharmacology of P2Y-receptors. *Naunyn-Schmiedeberg's archives of pharmacology.* **362**(4-5), pp.310-323.

Vulchanova, L., Riedl, M., Shuster, S., Buell, G., Surprenant, A., North, R. and Elde, R. 1997. Immunohistochemical study of the P2X 2 and P2X 3 receptor subunits in rat and monkey sensory neurons and their central terminals. *Neuropharmacology.* **36**(9), pp.1229-1242.

Wakx, A., Dutot, M., Massicot, F., Mascarelli, F., Limb, G.A. and Rat, P. 2016. Amyloid β Peptide Induces Apoptosis Through P2X7 Cell Death Receptor in Retinal Cells: Modulation by Marine Omega-3 Fatty Acid DHA and EPA. *Applied biochemistry and biotechnology.* **178**(2), pp.368-381.

Walker, J.E., Saraste, M., Runswick, M.J. and Gay, N.J. 1982. Distantly related sequences in the alpha-and beta-subunits of ATP synthase, myosin, kinases and other ATP-requiring enzymes and a common nucleotide binding fold. *The EMBO journal.* **1**(8), p945.

Wang, C.-Z., Namba, N., Gonoi, T., Inagaki, N. and Seino, S. 1996. Cloning and pharmacological characterization of a fourth P2X receptor subtype widely expressed in brain and peripheral tissues including various endocrine tissues. *Biochemical and biophysical research communications.* **220**(1), pp.196-202.

Wang, C.M., Chang, Y.Y., Kuo, J.S. and Sun, S.H. 2002. Activation of P2X7 receptors induced [3H] GABA release from the RBA-2 type-2 astrocyte cell line through a Cl−/HCO3−-dependent mechanism. *Glia.* **37**(1), pp.8-18.

Wang, J.C.-C., Raybould, N.P., Luo, L., Ryan, A.F., Cannell, M.B., Thorne, P.R. and Housley, G.D. 2003. Noise induces up-regulation of P2X2 receptor subunit of ATP-gated ion channels in the rat cochlea. *Neuroreport.* **14**(6), pp.817-823.

Wang, Q., Wang, L., Feng, Y.-H., Li, X., Zeng, R. and Gorodeski, G.I. 2004a. P2X7 receptor-mediated apoptosis of human cervical epithelial cells. *American journal of physiology-cell physiology.* **287**(5), pp.C1349-C1358.

Wang, X., Arcuino, G., Takano, T., Lin, J., Peng, W.G., Wan, P., Li, P., Xu, Q., Liu, Q.S. and Goldman, S.A. 2004b. P2X7 receptor inhibition improves recovery after spinal cord injury. *Nature medicine.* **10**(8), pp.821-827.

Webb, T.E., Simon, J., Krishek, B.J., Bateson, A.N., Smart, T.G., King, B.F., Burnstock, G. and Barnard, E.A. 1993. Cloning and functional expression of a brain G-protein-coupled ATP receptor. *FEBS letters.* **324**(2), pp.219-225.

Wei, L., Caseley, E., Li, D. and Jiang, L.-H. 2016. ATP-induced P2X Receptor-Dependent Large Pore Formation: How Much Do We Know? *Frontiers in pharmacology.* **7**.

Wesselius, A., Bours, M., Henriksen, Z., Syberg, S., Petersen, S., Schwarz, P., Jørgensen, N., van Helden, S. and Dagnelie, P. 2013. Association of P2X7

receptor polymorphisms with bone mineral density and osteoporosis risk in a cohort of Dutch fracture patients. *Osteoporosis international.* **24**(4), pp.1235-1246.

White, C.W., Choong, Y.-T., Short, J.L., Exintaris, B., Malone, D.T., Allen, A.M., Evans, R.J. and Ventura, S. 2013. Male contraception via simultaneous knockout of α1A-adrenoceptors and P2X1-purinoceptors in mice. *Proceedings of the national academy of sciences.* **110**(51), pp.20825-20830.

Wickert, L.E., Blanchette, J.B., Waldschmidt, N.V., Bertics, P.J., Denu, J.M., Denlinger, L.C. and Lenertz, L.Y. 2013. The C-terminus of human nucleotide receptor P2X7 is critical for receptor oligomerization and N-linked glycosylation. *PloS one.* **8**(5), pe63789.

Wiley, J.S., Dao-Ung, L.P., Gu, B.J., Sluyter, R., Shemon, A.N., Li, C., Taper, J., Gallo, J. and Manoharan, A. 2002. A loss-of-function polymorphic mutation in the cytolytic P2X7 receptor gene and chronic lymphocytic leukaemia: a molecular study. *The Lancet.* **359**(9312), pp.1114-1119.

Wilkinson, W.J., Jiang, L.-H., Surprenant, A. and North, R.A. 2006. Role of ectodomain lysines in the subunits of the heteromeric P2X2/3 receptor. *Molecular pharmacology.* **70**(4), pp.1159-1163.

Worthington, R., Smart, M., Gu, B., Williams, D., Petrou, S., Wiley, J. and Barden, J. 2002. Point mutations confer loss of ATP-induced human P2X7 receptor function. *FEBS letters.* **512**(1-3), pp.43-46.

Wu, G., Whiteside, G.T., Lee, G., Nolan, S., Niosi, M., Pearson, M.S. and Ilyin, V.I. 2004. A-317491, a selective P2X 3/P2X 2/3 receptor antagonist, reverses inflammatory mechanical hyperalgesia through action at peripheral receptors in rats. *European journal of pharmacology.* **504**(1), pp.45-53.

Wu, G., Zhao, M., Gu, X., Yao, Y., Liu, H. and Song, Y. 2014. The effect of P2X7 receptor 1513 polymorphism on susceptibility to tuberculosis: A meta-analysis. *Infection, genetics and evolution.* **24**, pp.82-91.

Wu, J., Xu, M., Miao, X., Lu, Z., Yuan, X., Li, X. and Yu, W. 2012. Functional up-regulation of P2X3 receptors in dorsal root ganglion in a rat model of bone cancer pain. *European journal of pain.* **16**(10), pp.1378-1388.

Wu, J., Yan, Z., Li, Z., Qian, X., Lu, S., Dong, M., Zhou, Q. and Yan, N. 2016. Structure of the voltage-gated calcium channel Cav1. 1 at 3.6 Å resolution. *Nature.*

Wu, T., Dai, M., Shi, X., Jiang, Z.-G. and Nuttall, A.L. 2011. Functional expression of P2X4 receptor in capillary endothelial cells of the cochlear spiral ligament and its role in regulating the capillary diameter. *American journal of physiology-heart and circulatory physiology.* **301**(1), pp.H69-H78.

Wynn, G., Ma, B., Ruan, H.Z. and Burnstock, G. 2004. Purinergic component of mechanosensory transduction is increased in a rat model of colitis. *American journal of physiology-gastrointestinal and liver physiology.* **287**(3), pp.G647-G657.

Xia, J., Yu, X., Tang, L., Li, G. and He, T. 2015. P2X7 receptor stimulates breast cancer cell invasion and migration via the AKT pathway. *Oncology reports.* **34**(1), pp.103-110.

Xiang, Z. and Burnstock, G. 2005. Expression of P2X receptors on rat microglial cells during early development. *Glia.* **52**(2), pp.119-126.

Xiao, J., Sun, L., Jiao, W., Li, Z., Zhao, S., Li, H., Jin, J., Jiao, A., Guo, Y. and Jiang, Z. 2009. Lack of association between polymorphisms in the P2X7gene and tuberculosis in a Chinese Han population. *FEMS immunology & medical microbiology.* **55**(1), pp.107-111.

Yamamoto, K., Korenaga, R., Kamiya, A. and Ando, J. 2000. Fluid shear stress activates Ca2+ influx into human endothelial cells via P2X4 purinoceptors. *Circulation research.* **87**(5), pp.385-391.

Yamamoto, K., Sokabe, T., Matsumoto, T., Yoshimura, K., Shibata, M., Ohura, N., Fukuda, T., Sato, T., Sekine, K. and Kato, S. 2006. Impaired flow-dependent

control of vascular tone and remodeling in P2X4-deficient mice. *Nature medicine.* **12**(1), pp.133-137.

Yan, D., Zhu, Y., Walsh, T., Xie, D., Yuan, H., Sirmaci, A., Fujikawa, T., Wong, A.C.Y., Loh, T.L. and Du, L. 2013. Mutation of the ATP-gated P2X2 receptor leads to progressive hearing loss and increased susceptibility to noise. *Proceedings of the national academy of sciences.* **110**(6), pp.2228-2233.

Yegutkin, G.G. 2008. Nucleotide-and nucleoside-converting ectoenzymes: important modulators of purinergic signalling cascade. *Biochimica et biophysica ACTA (BBA)-molecular cell research.* **1783**(5), pp.673-694.

Yiangou, Y., Facer, P., Baecker, P., Ford, A., Knowles, C., Chan, C., Williams, N. and Anand, P. 2001. ATP-gated ion channel P2X3 is increased in human inflammatory bowel disease. *Neurogastroenterology & motility.* **13**(4), pp.365-369.

Yilmaz, Ö., Yao, L., Maeda, K., Rose, T.M., Lewis, E.L., Duman, M., Lamont, R.J. and Ojcius, D.M. 2008. ATP scavenging by the intracellular pathogen Porphyromonas gingivalis inhibits P2X7-mediated host-cell apoptosis. *Cellular microbiology.* **10**(4), pp.863-875.

Young, M.T., Fisher, J.A., Fountain, S.J., Ford, R.C., North, R.A. and Khakh, B.S. 2008. Molecular shape, architecture, and size of P2X4 receptors determined using fluorescence resonance energy transfer and electron microscopy. *Journal of biological chemistry.* **283**(38), pp.26241-26251.

Young, M.T., Pelegrin, P. and Surprenant, A. 2007. Amino acid residues in the P2X7 receptor that mediate differential sensitivity to ATP and BzATP. *Molecular pharmacology.* **71**(1), pp.92-100.

Zhang, L., Ibbotson, R., Orchard, J., Gardiner, A., Seear, R., Chase, A., Oscier, D. and Cross, N. 2003. P2X7 polymorphism and chronic lymphocytic leukaemia: lack of correlation with incidence, survival and abnormalities of chromosome 12. *Leukemia.* **17**(11), pp.2097-2100.

Zhang, X., Chen, Y., Wang, C. and Huang, L.-Y. 2007. Neuronal somatic ATP release triggers neuron–satellite glial cell communication in dorsal root ganglia. *Proceedings of the national academy of sciences.* **104**(23), pp.9864-9869.

Zhong, Y., Dunn, P.M., Xiang, Z., Bo, X. and Burnstock, G. 1998. Pharmacological and molecular characterization of P2X receptors in rat pelvic ganglion neurons. *British journal of pharmacology.* **125**(4), pp.771-781.

Zhou, D., Chen, M.-L., Zhang, Y.-Q. and Zhao, Z.-Q. 2010. Involvement of spinal microglial P2X7 receptor in generation of tolerance to morphine analgesia in rats. *The journal of neuroscience.* **30**(23), pp.8042-8047.

Zhou, X. and Galligan, J.J. 1996. P2X purinoceptors in cultured myenteric neurons of guinea-pig small intestine. *The Journal of Physiology.* **496**(Pt 3), p719.

Zhu, S., Wang, Y., Wang, X., Li, J. and Hu, F. 2014. Emodin inhibits ATP-induced IL-1β secretion, ROS production and phagocytosis attenuation in rat peritoneal macrophages via antagonizing P2X7 receptor. *Pharmaceutical biology.* **52**(1), pp.51-57.

Zsoldos, Z., Reid, D., Simon, A., Sadjad, S.B. and Johnson, A.P. 2007. eHiTS: a new fast, exhaustive flexible ligand docking system. *Journal of molecular graphics and modelling.* **26**(1), pp.198-212.